

The multiformity of antennal chaetae in *Troglopedetes* Joseph, 1872 (Collembola, Paronellidae, Troglopedetinae), with descriptions of two new species from Thailand

Sopark Jantarit¹, Katthaleeya Surakhamhaeng², Louis Deharveng³

1 Excellence Center for Biodiversity of Peninsular Thailand, Faculty of Science, Prince of Songkla University, Hat Yai, Songkhla, 90110, Thailand **2** Division of Biological Science, Faculty of Science, Prince of Songkla University, Hat Yai, Songkhla, 90110, Thailand **3** Institut de Systématique, Évolution, Biodiversité (ISYEB) – UMR 7205 CNRS, MNHN, UPMC, EPHE, Museum national d'Histoire naturelle, Sorbonne Université, 45 rue Buffon, CP50, F-75005 Paris, France

Corresponding author: Sopark Jantarit (fugthong_dajj@yahoo.com)

Academic editor: W. M. Weiner | Received 15 May 2020 | Accepted 18 September 2020 | Published 6 November 2020

<http://zoobank.org/C46FAFC0-2322-47A6-8F5B-7DBC770C26EF>

Citation: Jantarit S, Surakhamhaeng K, Deharveng L (2020) The multiformity of antennal chaetae in *Troglopedetes* Joseph, 1872 (Collembola, Paronellidae, Troglopedetinae), with descriptions of two new species from Thailand. ZooKeys 987: 1–40. <https://doi.org/10.3897/zookeys.987.54234>

Abstract

Two new species of the genus *Troglopedetes* Joseph, 1872 (*T. meridionalis* **sp. nov.** and *T. kae* **sp. nov.**) are described from caves of the Thai peninsula. This is the first report of the genus south of the Kra Isthmus. The two new species have two rows of dental spines shared by all Thai *Troglopedetes*. They differ from other members of the genus mainly in the arrangement of dorsal chaetotaxy on head. The antennal chaetotaxy of the two species is analysed in detail in the second part of the paper. All types of antennal chaetae of both new species and their distribution patterns are described for each antennal segment: scales, ordinary chaetae, S-chaetae and subapical organite of Ant. IV. Twenty different types of chaetae are recognised and all except one are present in both species. The total numbers of ordinary chaetae and S-chaetae and their patterns of distribution on antenna are very similar between the two species (483 vs. 518 ordinary chaetae; 207 vs. 208 S-chaetae). Each type of chaetae has its own distribution pattern, markedly contrasted between dorsal and ventral side of antennae, and between antennal segments. This diversity of morphologies and distribution patterns and their similarity between the two species, as well as differences with other species of the same family, suggest that antennal chaetotaxy could provide powerful new characters for the taxonomy of *Troglopedetes* and related genera.

Keywords

Antennae, chaetotaxy, Entomobryoidea, Isthmus of Kra, phaneres, S-chaetae, subterranean habitat

Introduction

The genus *Troglopedetes* Joseph, 1872 is present in both edaphic and subterranean environments (Deharveng 1987) in three regions of the world: the Mediterranean basin, Africa and tropical continental Asia. The genus includes 31 species (Bellinger et al. 1996–2020), of which 12 are present and described from Thailand, all from caves of the northern and western part of the country (Deharveng 1988a, 1990; Deharveng and Gers 1993; Jantarit et al. 2016). Thailand is today the richest country of the world for *Troglopedetes*, which is diversified both in caves and in soils, with many undescribed species (Jantarit et al. 2016). The genus was only known from localities north of the Kra Isthmus, and replaced further south by the closely related genus *Cyphoderopsis* Carpenter, 1917, with most of its species still undescribed (Deharveng and Gers 1993; Jantarit et al. 2013, 2016).

The genus *Troglopedetes* was erected in 1872 by Joseph for *T. albus* Joseph, 1872 from caves in Slovenia. Later, Absolon (1907) also used the genus name *Troglopedetes* for his type *T. pallidus* Absolon, 1907 from a cave in Slovenia, without acknowledging Joseph's publication. This is currently accepted today, although in fact *T. albus* is not a *nomen nudum*, “however meager the description may be” according to Ellis and Bellinger (1973), who then placed *Troglopedetes* Absolon, 1907 as a junior homonym of *Troglopedetes* Joseph, 1872. Hence, *Troglopedetes* Joseph, 1872 is not a *nomen oblitum* and should be considered as the valid name for the genus in order of precedence.

The genus was subsequently recorded from Thailand by Deharveng (1988a) with *T. fredstonei*, a species from Chiang Dao cave in northern Thailand, and eleven species were later described from northern and western Thailand (Deharveng 1990; Deharveng and Gers 1993; Jantarit et al. 2016). The diagnostic characters for discriminating the different Thai species were primarily based on the dorsal chaetotaxy of head and on a set of adaptive (pigmentation, eye number, antenna length, claw complex) and non-adaptive (spines on dens) characters. Interspecific differences also exist for the length of chaetae of the labial basis and macrochaetotaxy.

Troglopedetes is one of the best-defined genera of Paronellidae by the subdivision of its 4th antennal segment, a feature unique in the family. However, other important taxonomic characters have not been described in detail in many species, like the dorsal chaetotaxy of head and body, S-chaetal pattern on antennae and tergites, trichobothria complex, arrangement of pseudopores, and furcal structure. Regarding the antennae, like for other Entomobryoidea, only a few chaetae have been considered in published descriptions, mostly those of the sensorial organ of the third antennal segment. The complexity of antennal chaetotaxy in Entomobryoidea, with its large number of chaetal types and strong polychaetosis, may explain why authors have been so reluctant to analyse these organs in great detail. Recent works, however, by Fanciulli

et al. (2003) and Soto-Adames et al. (2014) depicted more details of antennal chaetal patterns, focusing on a group of subcylindrical S-chaetae on antennal segments II and III of European species. Also, attempts to categorise antennal phaneres by Lukić et al. (2015, 2018) for *Heteromurus* (*Verhoeffiella*) and Jantarit and Sangsiri (2020) for *Alloscopus* point to the potential interest of more thoroughly investigating the antennal chaetotaxy of *Troglopedetes*.

In this study, we describe two new species, *T. meridionalis* sp. nov. and *T. kae* sp. nov., from caves of peninsular Thailand. These records are the first report of the genus south of the Kra Isthmus, considered so far as a probable biogeographical transition zone between the genus *Troglopedetes* and the closely related genus *Cyphoderopsis* (Deharveng and Gers 1993; Jantarit et al. 2013). In a second part of the paper, we describe in detail the morphological diversity of antennal chaetae of the two species as well as their arrangements. The objective is to provide a reference framework for homologising as far as possible chaetae and chaetal patterns across different genera of Entomobryodea, and for evaluating the importance of antennal chaetotaxy for the taxonomy of Entomobryodea.

Materials and methods

The specimens of the two *Troglopedetes* species described here were found in the dark zone of two caves, Tham Don Non, Lang Suan district, Chumphon Province and Tham Kae, La-ngu district, Satun Province (Fig. 1). Collembola were collected with aspirators and Berlese extractors. They were stored in 95% ethanol and were mounted on slides in Marc Andre II medium after clearing in lactic acid. Morphological characters were examined using Leica DMLB and Leica DM1000 LED microscope with phase-contrast. Photos of the habitus were taken by a Canon EOS 6D with Canon EF 100mm f/2.8 Macro lens and optimised by Helicon Remote software. Stacking was performed under Helicon Focus 6. Drawings were made using a drawing tube, and figures were improved with Photoshop and Illustrator CC/PC (Adobe Inc.).

Abbreviations

Ant.	antennal segment	mic	microchaeta(e)
Abd.	abdominal segment	psp	pseudopore
AIIO	apical organ of Ant. III	tric	trichobothria
Th.	thoracic segment	ms	S-microchaeta(e)
Tita	tibiotarsus	s or sens	S-chaeta(e)
mac	macrochaetae	VT	ventral tube
mes	mesochaeta(e)		

NHM-PSU Princess Maha Chakri Sirindhorn Natural History Museum, Prince of Songkla University, Songkhla, Thailand

MNHN Muséum national d'Histoire naturelle, Paris, France.

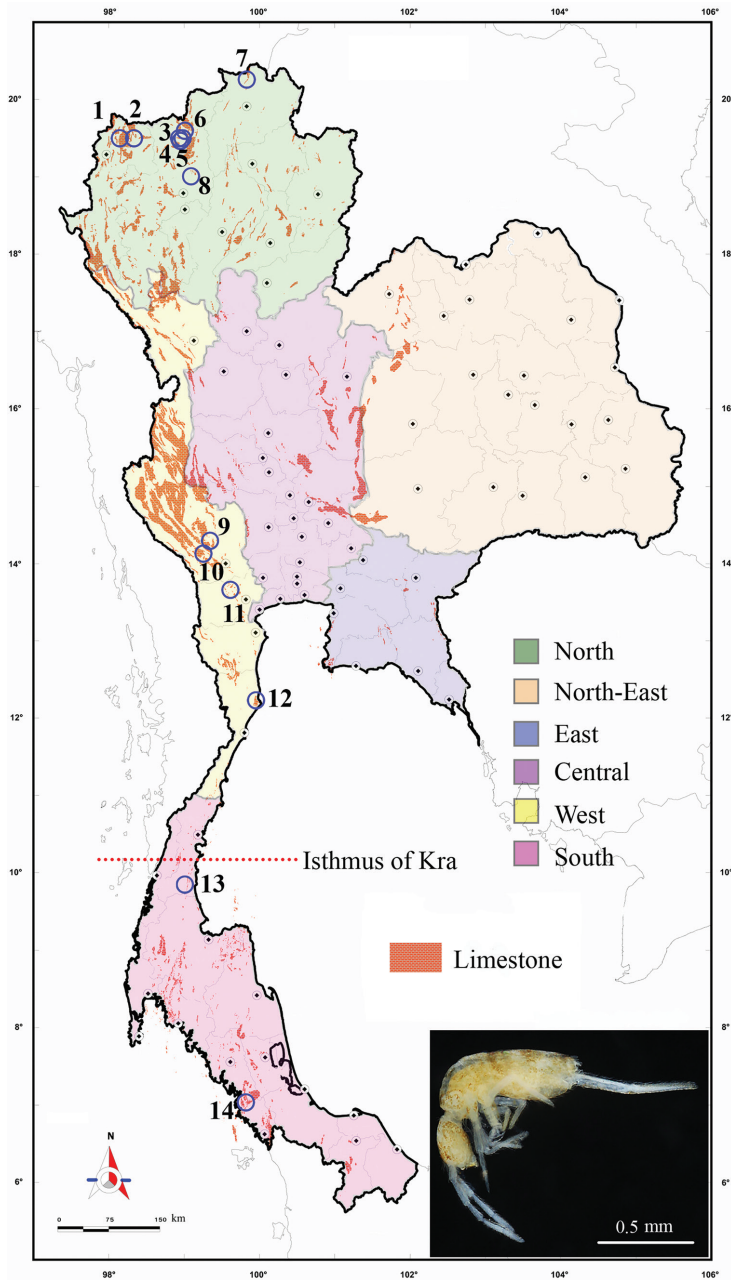


Figure 1. Distribution of *Troglopedetes* in Thailand (empty blue circles) with distributed limestone (orange colour) of the country **1** *T. maffrei* Deharveng & Gers, 1993 **2** *T. longicornis* Deharveng & Gers, 1993 **3** *T. centralis* Deharveng & Gers, 1993 **4** *T. fredstonei* Deharveng, 1988 **5** *T. leclerci* Deharveng, 1990 **6** *T. microps* Deharveng & Gers, 1993 **7** *T. multispinosus* Deharveng & Gers, 1993 **8** *T. maunonensis* Deharveng & Gers, 1993 **9** *T. calvus* Deharveng & Gers, 1993 **10** *T. dispersus* Deharveng & Gers, 1993 **11** *T. convergens* Deharveng & Gers, 1993 **12** *T. paucisetosus* Deharveng & Gers, 1993 **13** *T. meridionalis* sp. nov. **14** *T. kae* sp. nov. and its habitus (small colour picture). Small dark dots indicate province capitals; scale 1:250,000.

Conventions for describing chaetotaxic and pseudopore patterns

Pseudopore arrangement follows Deharveng et al. (2018). The formula of tergite pseudopores is given by half-tergite from Th. II to Abd. IV (Jantarit et al. 2013). The formula for labium basis chaetae follows the system of Gisin (1967) with the upper-case letter used for ciliated and lower-case letter for smooth chaetae. Labial chaetotaxy follows Fjellberg (1999). Dorsal chaetotaxy and chaetal areas of head follow Deharveng and Gers (1993), Jordana and Baquero (2005), and Mitra (1993). Dorsal macrochaetotaxy description combines notation of individual chaetae derived from Szeptycki (1979) with chaetal group notation (rationale explained below). Formula for dorsal macrochaetae and trichobothria are given by half-tergite from head to Abd. IV; for S-chaetae by half-tergite from head to Abd. V. Homologising ordinary chaetae between different taxa is not an easy task within Entomobryoidea where chaetotaxy has been strongly modified compared to the simple chaetotaxy of Poduromorpha, due to oligochaetosis, polychaetosis, variability, and usually unequally sized tergites (Yoshii 1989, Soto-Adames et al. 2014) as well as the important shift and secondary grouping of chaetae. It has been stressed for many years that homologies should be rooted in the analysis of first instars (Deharveng 1979; Szeptycki 1979; Zhang et al. 2011; Soto-Adames and Bellini 2015), but this has been done for a very few species only. Mitra (1973) recorded the development of tergite chaetae in the different stages of a species of *Callyntrura*; for Troglopedetinae, the only information we have in this respect is the description of the first instar of *Campylothorax sabanus* (Wray) by Soto-Adames (2016). For *Troglopedetes*, which is clearly oligochaetotic with several displaced mac, we opted for a cautious approach, using homologies by chaetal groups, less precise but more robust than chaeta-to-chaeta homologies, in cases of uncertainty. S-chaetae terminology of tergites follows Zhang and Deharveng (2014). The S-microchaeta (ms) of Th. II corresponds to S-chaetae type 1 of Jantarit et al. (2013) and microsensillum of Soto-Adames et al. (2014). The S-chaeta “sens” corresponds to S-chaetae type 2 of Jantarit et al. (2013) and to lateral sensillum of Soto-Adames et al. (2014).

Taxonomy

Family Paronellidae

Subfamily Troglopedetinae

In the concept of Soto-Adames et al. (2014), the tribe Troglopedetini is considered a synonym of Paronellini. This is plausible, but not supported by the last detailed redescription of *Paronella fusca* Schött, 1893, type species of the genus *Paronella*, by Mitra (1992), who gives 2+2 trichobothria on Abd. IV (vs. 3+3 in Troglopedetini), the main character separating the two tribes. Re-examination of the type material of the species is needed before accepting such a taxonomic decision.

Genus *Troglopedetes* Joseph, 1872

Type species. *Troglopedetes albus* Joseph, 1872

Medium sized Paronellidae. Body colour white, sometimes with light orange to red pigment dots. Eyes per side 0–3. Scales present on antenna, head, body and ventral side of furca, absent on ventral tube and legs. Pseudopores on tergites arranged as 1, 1/1, 1, 1, 1 by half tergite from Th. II to Abd. IV, with a row of 4+4 pseudopores behind the posterior row of chaetae of Abd. IV. Labial basis chaetotaxy as M1M2R(r)E(e)L1(11)L2(12). Presence of one or two sublobal hairs on maxillary outer lobe. Antennae of various length, composed of four segments, with Ant. IV always divided into two equal or subequal sub-segments and devoid of apical bulb. Suture zone of head when visible follows divergent lines. Trichobothrial pattern 0, 0/0, 2, 3, 3. Dorsal macrochaetotaxy oligochaetotic, polychaetotic on the collar. Macrochaetae on head present as 0–7+0–7 in area dorsalis (central mac). Th. II with a compact group of 6+6 mac accompanied by 0–4+0–4 mac anteriorly. Th. III with a group of 3+3 mac accompanied by 0–1+0–1 mac anterior-externally. Claw with 0–2 inner teeth, a pair of lateral ones and a dorsal tooth. Dens elongated with one or two rows of spines, those on external row larger, more serrated than those on internal row. Mucro of various length, 2–16 × shorter than dens, with 3–5(6) main teeth, proximal tooth sometimes with 1–5 basal toothlets.

Remarks. The number and arrangement of trichobothria on Abd. IV allows clear separation of Troglopedetinae (3+3 trichobothria) from other Paronellidae (2+2 trichobothria). Many characters are unknown for several species of *Troglopedetes*, including its type species. Two characters complementary to those listed by Soto-Adames et al. (2014) are discussed below. A new set of characters present in *Troglopedetes* are presented below as a result of this work.

Pseudopores. Pseudopores are arranged on tergites as in other Entomobryoidea: 1, 1/1, 1, 1, 1 from Th. II to Abd. IV. Additionally, a row of 4+4 pseudopores is constant behind the posterior row of chaetae of Abd. IV (Deharveng, 1988a). These pseudopores are present in *Cyphoderopsis* (Jantarit et al. 2013) and were reported in various number (4–10+4–10) under the name “lenticular organs” sensu Christiansen and Bellinger (1996) in *Trogolaphysa* (Soto-Adames and Taylor 2013) and in *Troglobius* (Cipola et al. 2016). They have also been detected in Cyphoderidae (Jantarit et al. 2014), but not in other families of Entomobryoidea, pointing to relatedness between the cited genera and Cyphoderidae, which have led some Collembologists to consider Cyphoderidae as a subfamily of Paronellidae.

Macrochaetotaxy. Dorsal clothing of macrochaetae is clearly oligochaetotic in the *Troglopedetes* species where it has been described. Pattern on Th. II includes a compact group of six chaetae (P3 complex of Soto-Adames et al. 2014) which is very obvious and constant. The same group, including 3–6 mac, is present in *Trogolaphysa* (Soto-Adames 2015, Soto-Adames and Taylor 2013), and a group of three or four mac in a line is found in *Cyphoderopsis* (Jantarit et al. 2013). The pattern on Th. III exhibits a group of three mac in *Troglopedetes* whereas *Trogolaphysa* shows 0–3 mac and *Cyphoderopsis* has none.

Dental spines. Dens of *Troglopedetes* is elongated with either one or two rows of spines, those of the external row larger and more serrated than those of the internal one that are rather short and smooth. Soto-Adames et al. (2014) mistakenly stated that *Troglopedetes* has a single row of dental spines. In fact, species of the Mediterranean region, Africa, south-west and central Asia known so far have only one row of 8–45 dental spines, but all Thai species have two rows of dental spines (internal row with 9–45 spines, external one with fewer spines).

***Troglopedetes kae* sp. nov.**

<http://zoobank.org/99807B93-C5B7-4F80-8499-3FF951526C20>

Figures 2–10

Type material. Holotype male and seven paratypes on slides (one male, four females and two subadults). Thailand: Satun Province: La-Ngu district, Tham Kae, 6°53'41"N, 99°46'44"E, 24 m a.s.l., 25 Jul 2017, S. Jantarit, A. Nilsai and K. Surakhambhaeng leg., dark zone of cave, by aspirator (sample # THA_SJ_STN04). Holotype and five paratypes deposited in NHM-PSU, two paratypes deposited in MNHN. Measurements of holotype in Table 1.

Description. Habitus. Slightly troglomorphic, slender, with elongate legs, furca and antennae. Body length 1.3–1.6 mm. Fourth abdominal segment $3.5\text{--}6 \times$ ($n = 9$, all adults) as long as the third one along dorsal axis. Furca well developed, ca. $1.6\text{--}2.2$ ($n = 8$) \times shorter than body length. Body colour white with spots of orange pigment. Eyes absent, no ocular patch.

Chaetal types. Four types of chaetae on somites, appendages (except antennae) and mouthparts: scales, present on antennae I and II, head, body and furca, absent on legs and ventral tube; ordinary chaetae on all body parts; S-chaetae and trichobothria on tergites; hairs devoid of sockets on outer maxillary lobe and labial papilla. Chaetal types on antennae are much more diverse and described further separately.

Pseudopores (Figs 2A, 3B–D, 4B, 8A–D, 10B, 10D, E). Pseudopores present as round flat disks larger than mac sockets, on antennae, head and tergites. Dorsal pseudopore formula: 1–(2)/1, 1/1, 1, 1, 1+4 (Fig. 8A–D). On antenna, two psp detected ventro-distally on Ant. I, one ventro-distally on Ant. II and one ventro-distally on Ant. III (Figs 3B, D, 4B). On head, 1–(2) psp close to antennal basis (Fig. 2A). On legs, psp present externally on coxae (two for legs I and II and 2–(3) for leg III). On manubrium, two psp on the dorso-distal plaque (Fig. 10B, D, E), on dens (new location for *Troglopedetes*) two psp dorso-basally near the internal spine on each side (Fig. 10D, E).

Mouthparts. Labral formula 4/5,5,4 (Fig. 2G); prelabral chaetae short, bent and ciliated, labral chaetae thinner, longer, smooth and acuminate, those of the distal row slightly shorter than those of the median row. Ventro-distal complex of labrum well differentiated, asymmetrical, with 2 distal combs (a larger one with 6–8 teeth on the left side, a smaller one with more than ten minute teeth on the right side) and an axial pair of sinuous tubules as in *Cyphoderopsis* (Jantarit et al. 2013) (Fig. 2F). Distal part of

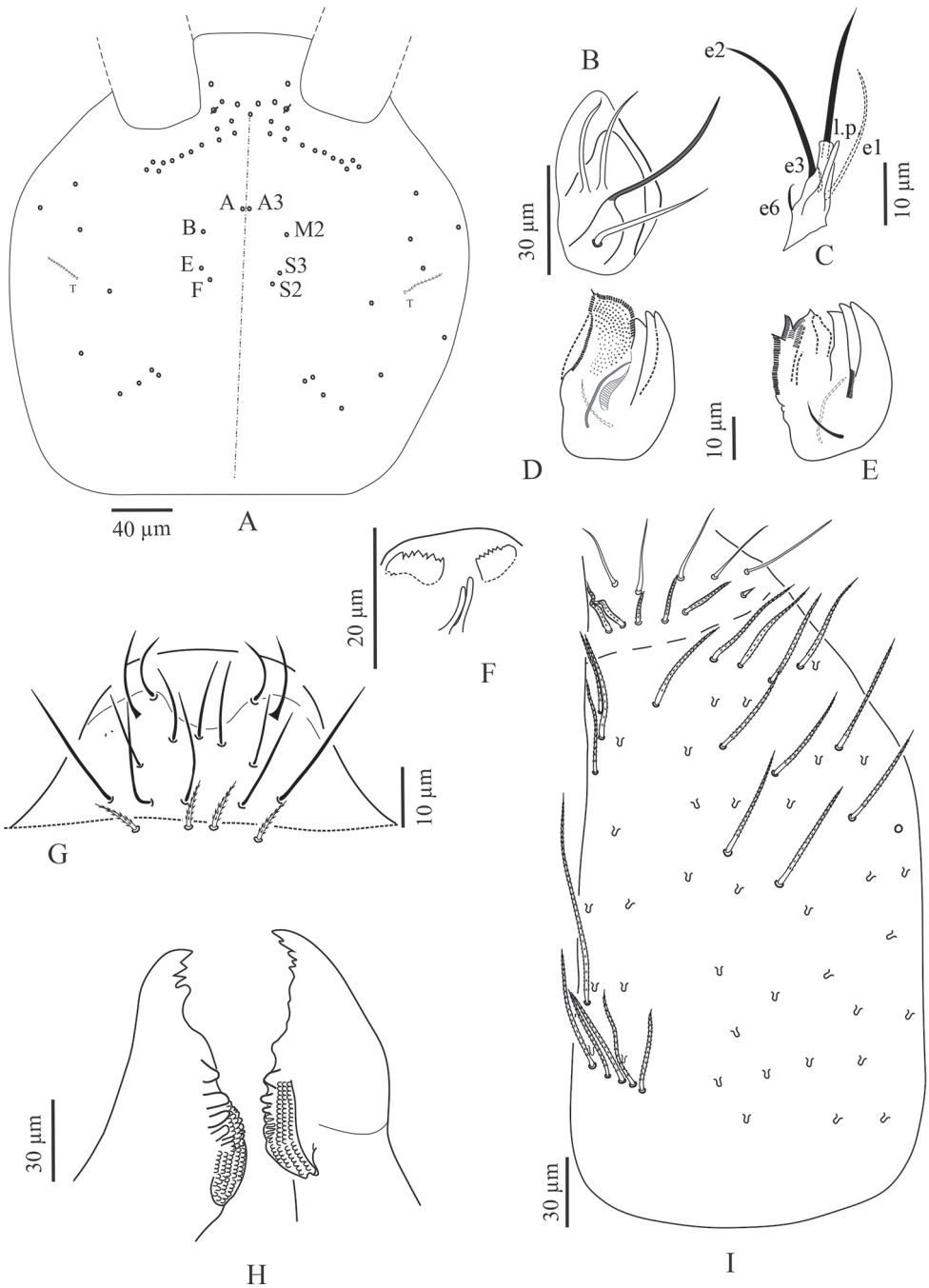


Figure 2. *Troglopedetes kae* sp. nov. **A** head chaetotaxy (left = **A** to **G** mac nomenclature; right = AMS nomenclature) **B** outer maxillary lobe **C** labial palp of papillae **D** maxillary head of ventral sides **E** maxillary head of dorsal sides **F** ventro-distal complex of labrum **G** labrum **H** mandible **I** labial basis and ventral chaetotaxy of head, right side.

labrum not adorned with spines dorso-distally. Labial palp similar to that described by Fjellberg (1999) for *Troglopedetes* sp., with strong papillate chaetae. Indicative number of guards for each major papillate chaetae: A (0), B (5), C (0), D (4) and E (4); lateral process subcylindrical, reaching slightly above the apex of papilla E (Fig. 2C); five smooth proximal chaetae. Chaetae of labial basis as M1M2REL1l2, with M1, M2, E and L1 subequal and ciliated, R shorter than others and ciliated, l2 short, smooth and acuminate (Fig. 2I). Outer maxillary lobe with one papillate chaeta, one basal chaeta and two sublobal hairs, shorter than others (Fig. 2B). Maxillary head with a 3-toothed claw, several stout shortly ciliated lamellae not observed in detail and three thin elongate structures (two dorsally and one ventrally) (Fig. 2D, E). Mandible head strong, asymmetrical (left side with four teeth, right side with five teeth); molar plate with three strong pointed basal teeth, and other two or three inner distal teeth, identical in both mandibles (Fig. 2H).

Ventral chaetotaxy of head (Fig. 2I). Head densely covered with oval scales (40–50 μm), postlabial chaetae along the linea ventralis as three mes anteriorly, one mac and an oblique line of five mes posteriorly on each side.

Antennae (Figs 3–7). Antennae shorter than body, $2.2 \times$ ($n = 6$) as long as cephalic diagonal. Ant. IV subdivided into two subequal segments, without apical bulb (Fig. 5). Lengths of antennal segments I–IV (IVa+IVb) as 1:1.9:1.3:2.5 (average, $n = 6$). Two other specimens with Ant. II and III fused (Figs 6, 7). Antennal chaetae (scales, five types of ordinary chaetae, 14 types of S-chaetae and subapical organite) described separately. Antennal scales oval, present dorsally only on Ant. I and II and ventrally on Ant. II, absent ventrally on Ant. I, and absent on Ant. III and IV (Figs 3A, C, D, 6B–D).

Body dorsal chaetotaxy (Figs 2A, 8A–D). Dorsal macrochaetae formula: 4,4/8,4/0,2,4,3 (Figs 2A, 8A). Trichobothrial pattern: 1/0, 0/0, 2, 3, 3 (Figs 2A, 8A). Trichobothrial complexes well developed with modified mes of various sizes (Fig. 8A–D) described below for each segment. The figured mes pattern is not complete.

Head with 12–13 peri-antennal mac in line on each side, with 4+4 central mac (chaetae A, B, E, F of Deharveng and Gers (1993), absence of the chaetae C, D and G, cephalic mes short, feebly serrated, equal, symmetrically arranged (not analysed). One lateral cephalic trichobothrium much shorter than closest mac on each side; su-

Table 1. *Troglopedetes kae* sp. nov., measurements in μm (from holotype).

	Head		Body		Appendages
Ant. I	90	Th. II	137	Man	305
Ant. II	215	Th. III	133	Dens	283
Ant. III	148	Abd. I	101	Mucro	30
Ant. IVa	136	Abd. II	130	Furca	618
Ant. IVb	138	Abd. III	144	Claw I	37
Ant.	727	Abd. IV	515	Claw II	35
Head	286	Abd. V	75	Claw III	36
		Abd. VI	71		
		Body	1,592		

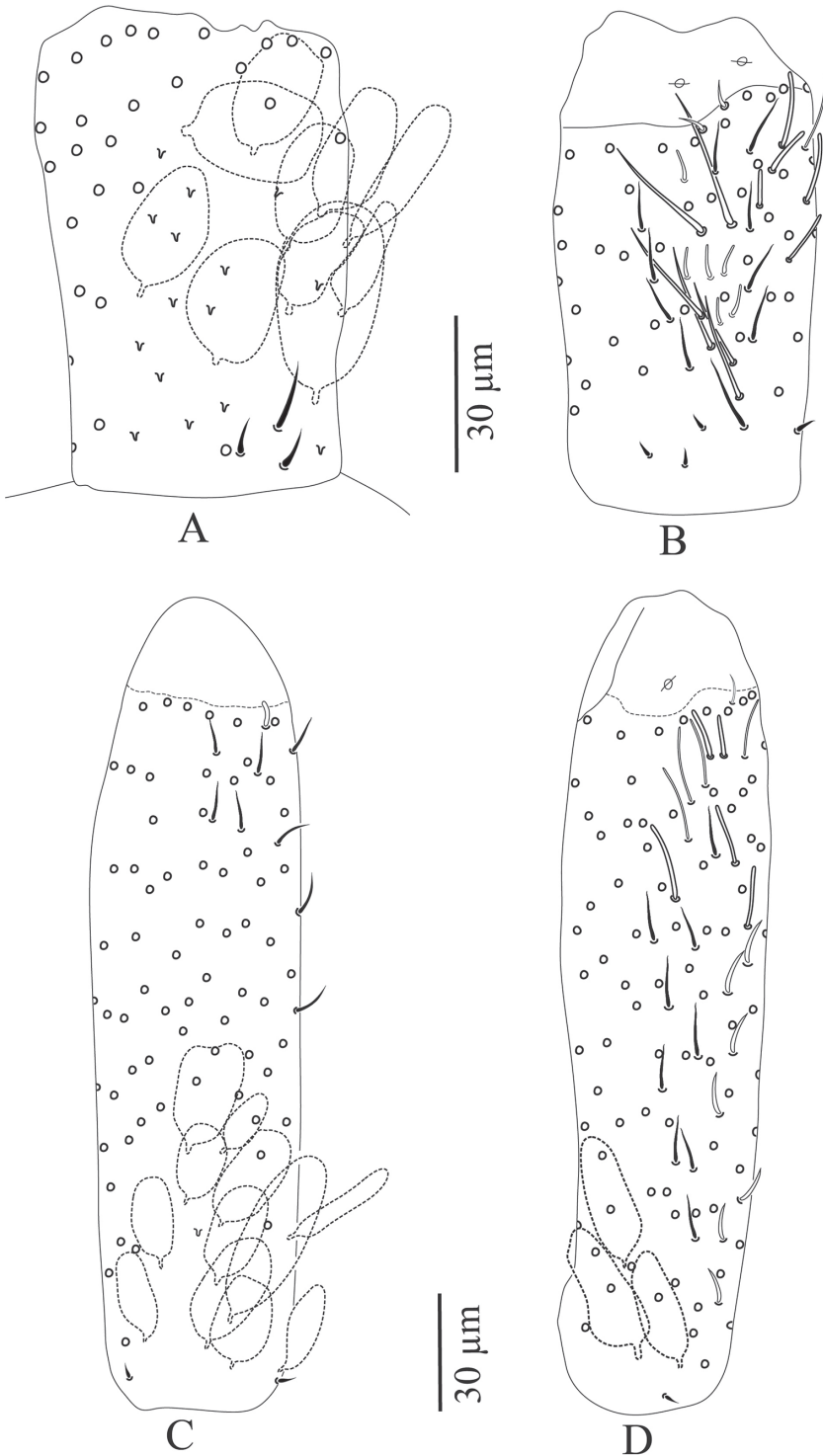


Figure 3. *Troglopedetes kae* sp. nov. continued **A** dorsal side of Ant. I, right side **B** ventral side of Ant. I, right side **C** dorsal side of Ant. II, right side **D** ventral side of Ant. II, right side.

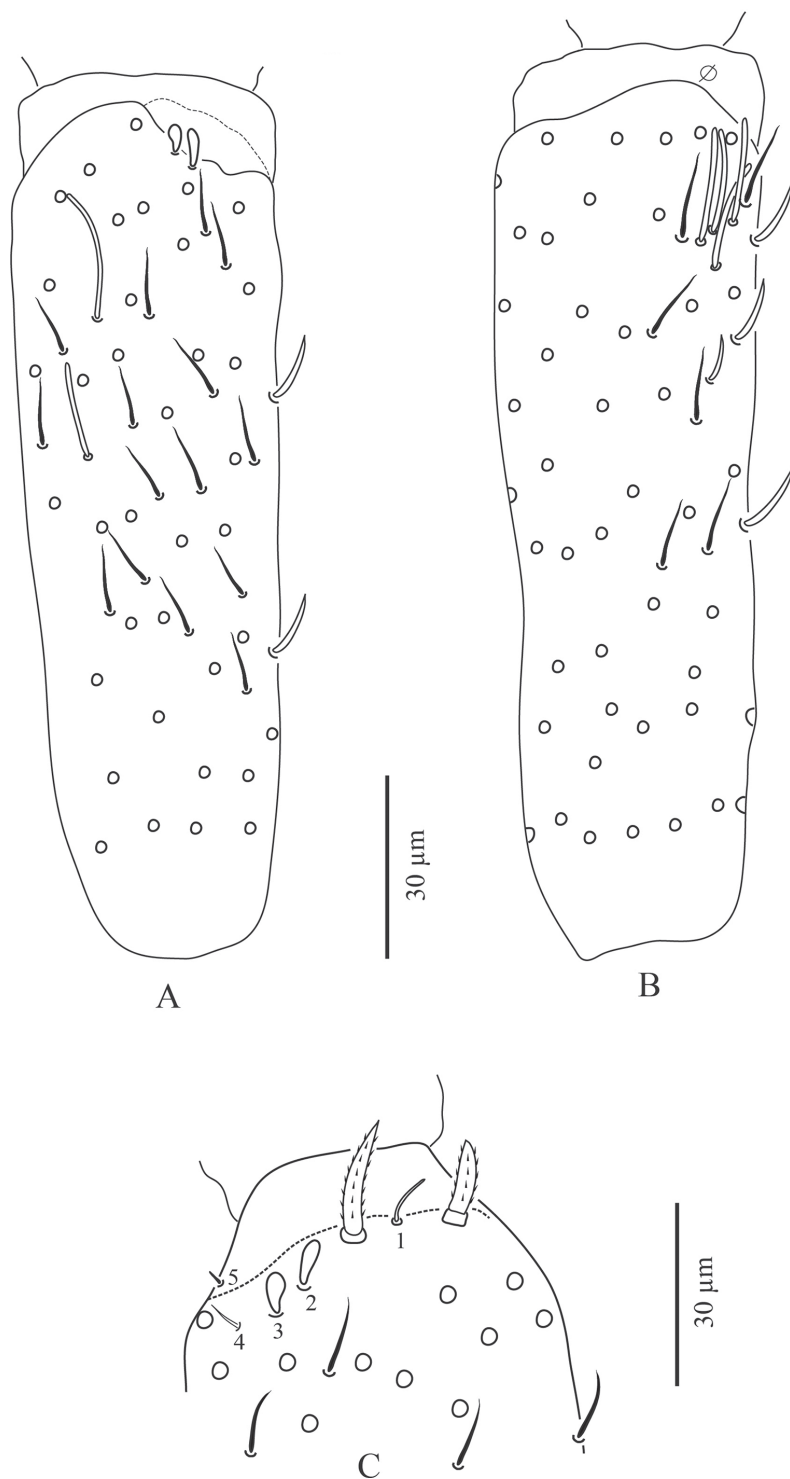


Figure 4. *Troglopedetes kae* sp. nov. continued **A** dorsal side of Ant. III, right side **B** ventral side of Ant. III, right side **C** distal organ of Ant. III, left side.

ture zone not visible (Fig. 2A). Head dorsally densely covered with round to oval scales (20–35 μm). Body densely covered with oval scales (15–50 μm).

Th. II with a collar consisting of a few rows of mac along its anterior and antero-lateral margins, a compact group of six central mac on each side (“P3 complex” of Soto-Adames et al. (2014) and two antero-lateral mac; one antero-lateral ms; one antero-lateral sens; two or three short mic laterally, and a few others not counted centrally (Fig. 8A).

Th. III with four mac by side (a group of three central and one anterior to them), one sens at antero-lateral margins, and ca. eight or nine mac or long mes at lateral margins (Fig. 8A).

Abd. I without central mac, with one ms laterally on each side, and three mes laterally, mic not counted (Fig. 8A).

Abd. II with two tric on each side and six or seven modified mes around them (three or four around the internal tric and three near external tric), two mac (one near internal tric and one near external tric), one sens near internal tric (Fig. 8A, B), three mic (one close to internal tric and two close to external tric), others mes sockets internally visible, not counted.

Abd. III with three tric on each side (one internal, two external) and eight or nine modified mes around tric (two near internal tric, six or seven near the two external tric); four mac (one near internal tric and three near external tric); one sens anterior to internal tric and one ms posterior to the two external tric; several mes at lateral margins, not counted (Fig. 8A, C).

Abd. IV with three tric on each side (two antero-lateral, one postero-lateral) and ca. 7–9 modified mes around the two antero-lateral tric; postero-lateral tric without modified mes. Mac distributed as three central on each side (one antero-external to pseudopore, two anterior to posterior tergite margin), one near postero-lateral tric, and at least four external, mixed with many mes or smaller mac on lateral to posterior margins (not counted); probably three sens anteriorly; at least six S-like chaetae *sensu* Lukić et al. (2015) anteriorly, and several mes or S-like chaetae uniformly distributed (not counted); six serrated mes in line in the posterior row, four near axis and two along pseudopore line, from medium to short size (Fig. 8A, D).

Abd. V with only one sens detected on each side, and several ordinary chaetae from mes to mac, not counted (Fig. 8A). Abd. VI chaetotaxy not analysed.

Legs (Fig. 9A–C). Legs long. Tita III as long as head diagonal, slightly longer than Tita I and II. Legs devoid of scales, mostly covered with ordinary ciliated chaetae of various length, from mes to mac. Trochanteral organ of leg III with eight smooth, straight, unequal, spiny chaetae ($n = 1$) (Fig. 9C). Tibiotarsus chaetotaxy mostly composed of strong ciliated-serrated mes, the basal ones longer and thicker (50–60 μm), slightly shorter distally (up to 15–20 μm). Distal row with 8–10 subequal ciliated mes and a dorso-apical tenent hair thin, smooth and acuminate on all tita; a ventro-distal strong smooth erected chaeta present on Tita III (Fig. 9A). Praetarsal mic minute (2.5–3 μm) (Fig. 9A). Unguis slender and relatively short (25–30 μm long, 6–7 μm wide at basis), 8–9 \times shorter than tita, with one rather strong tooth at 30% of inner edge and a pair of inner basal teeth of unequal size;

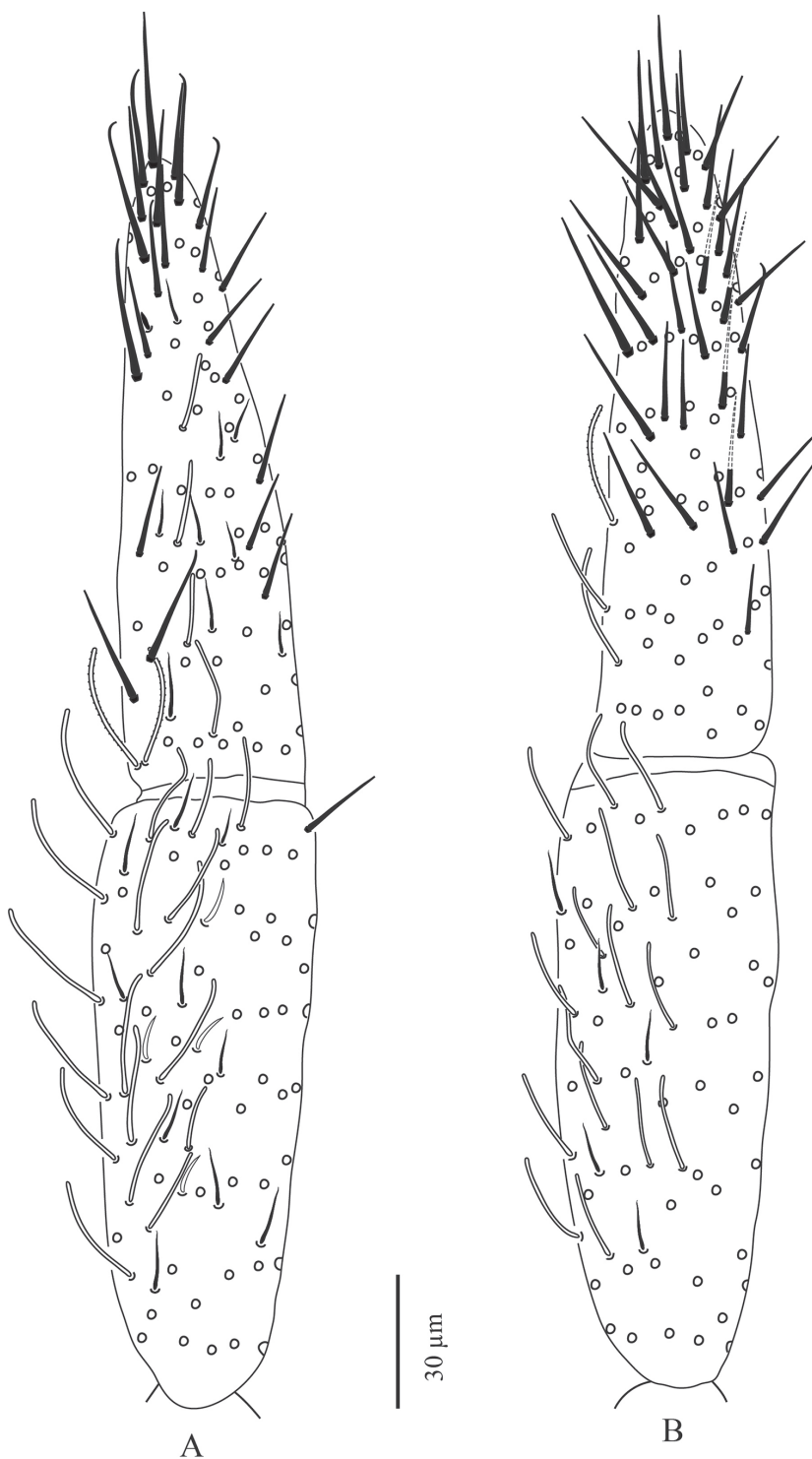


Figure 5. *Troglopedetes kae* sp. nov. continued **A** dorsal side of Ant. IV, right side **B** ventral side of Ant. IV, right side.

unguiculus pointed, narrow, lanceolate and elongate, ca. $0.6 \times$ as long as claw, its external edge smooth (Fig. 9A).

Ventral tube (Fig. 9D–F). Ventral tube ca. $4 \times$ longer than wide, with 3+3 long serrated mac anteriorly (Fig. 9D) and six mes (two ciliated and four smooth) on each lateral flap (Fig. 9E); posteriorly with at least 31 long ciliated mes and two distal smooth mes (Fig. 9F).

Furcal complex (Fig. 10A–E). Tenaculum with four teeth on each ramus, of decreasing size from the basal to the distal one, on a prominent, irregular body, with a postero-basal strong, densely serrated, distally bent chaeta (Fig. 10A). Manubrium ca. $0.82 \times$ ($n = 8$) shorter than mucrodens (mucro+dens). Manubrium dorsally with subequal ciliated mes (none smooth), irregularly arranged in three or four rows in two longitudinal stripes separated by a glabrous axial stripe, external row of chaetae distally with at least 7–11 long ciliated mes, dorso-distal plaque with 4+4 mes and 2+2 pseudopores (Fig. 10B). Ventrally, dense cover of round to oval ($22\text{--}38 \mu\text{m}$) and thin elongated scales ($20\text{--}25 \mu\text{m}$). Dens straight, elongate, hairy, slightly and progressively tapering, dorsally with two rows of spines, mixed with ciliated mes of various length, thickness and shape. Dorso-external row with 15–22 spines, dorso-internal row with 26–40 spines (asymmetries between dentes); external spines larger and less sclerotised than internal ones. Some short ciliated mes interspersed with spines in the external row; dorsally between the two rows of spines a mix of short and long ciliated mes, irregularly arranged in one row distally turning to three or four rows proximally; laterally, many short ciliated mes; dorso-distally, 3–(4) stronger ciliated mes; 2+2 psp on dorso-basally between the two rows of spine, sometimes inconspicuous (Fig 10C, D). Dens ventrally entirely and densely scaled, the scales elongate ($20\text{--}38 \mu\text{m}$) (oval shape distally), arranged in short lines from 3–5 (distally) to 6–8 scales (proximally) (Fig. 10D). Mucro rather stout, short, 9.3–13.7 (average 12, $n = 8$) \times shorter than dens (Fig. 10D, E), with five main teeth, the apical one blunt and strong, the subapical one acute and strong, a latero-distal one small and acute, and two dorso-basal, one minute and acute and one strong, acute and longer without toothlets basally (Fig. 10E).

Genital plate (Fig. 10F, G). Male genital plate of the circinate type, with six genital mic and 16 circumgenital short, thin, smooth mes (Fig. 10F); female genital plate with 2+2 mic (Fig. 10G).

Ecology. *Troglopedetes kae* sp. nov. is only known from a small chamber in the dark zone of a cave, accessible by a very low and narrow passage. Specimens were found as small populations in an oligotrophic habitat, i.e., on wall and ground with very humid and wet environment, without any trace of organic matter.

Etymology. The species name is taken from the type locality (Tham Kae).

Remarks. *Troglopedetes kae* sp. nov. has four medial head macrochaetae, three medial Abd. IV macrochaetae, one inner teeth of claw and mucro with five teeth. It is near *T. centralis* Deharveng & Gers, 1993 from a cave in Doi Chiang Dao, Chiang Mai province in the absence of eyes, chaetotaxy of labial basis and of outer maxillary lobe, dorsal macrochaetotaxy from head to Abd. IV, chaetotaxy of anterior side of ventral tube and claw morphology. However, *T. kae* sp. nov. differs from *T. centralis* by its smaller size

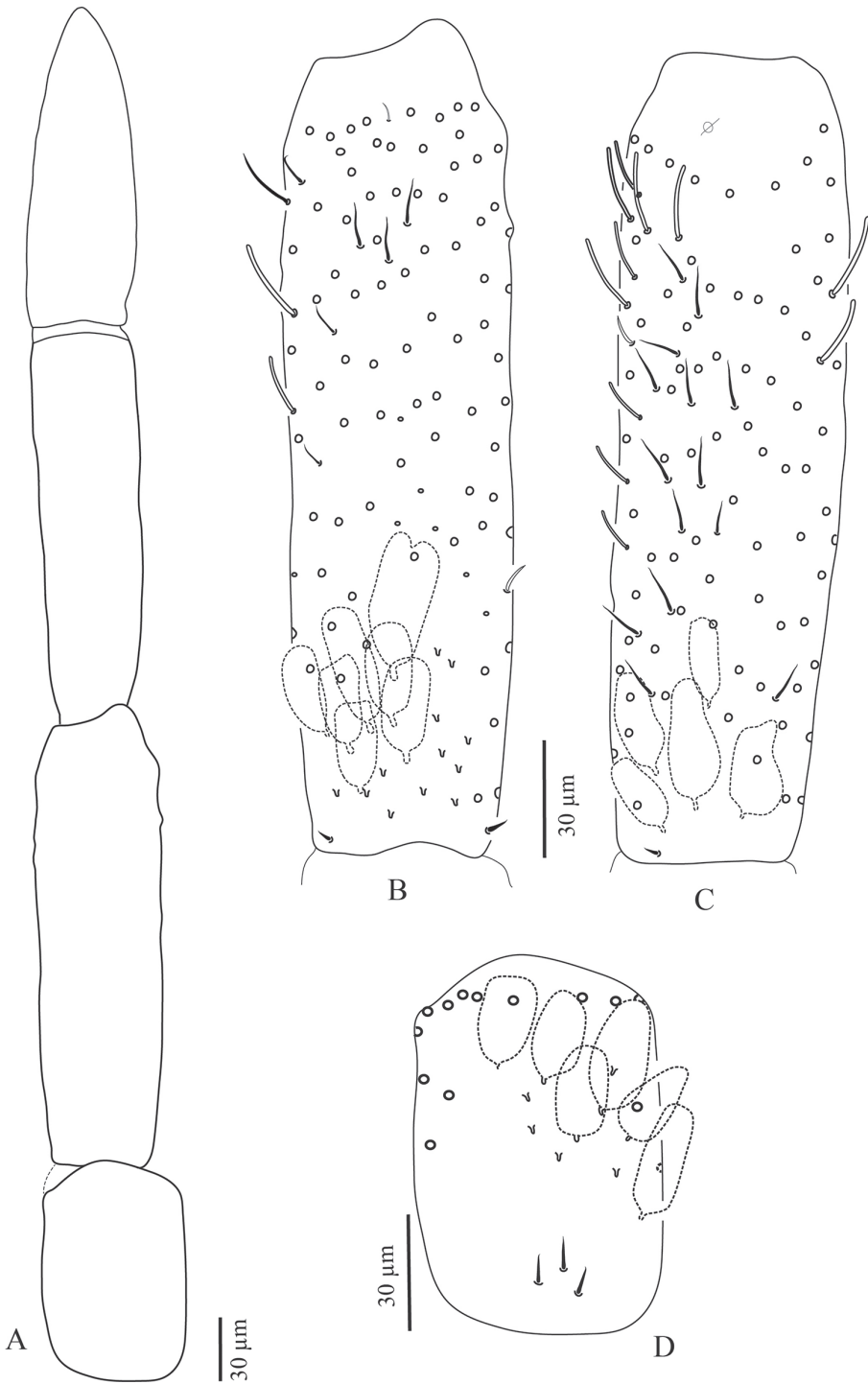


Figure 6. *Troglopedetes kae* sp. nov. continued **A** abnormal antenna with fusion of Ant. II and III, left side **B** dorsal side of fused Ant. II and III, left side **C** ventral side of fused Ant. II and III, left side **D** dorsal side of Ant. I, right side.

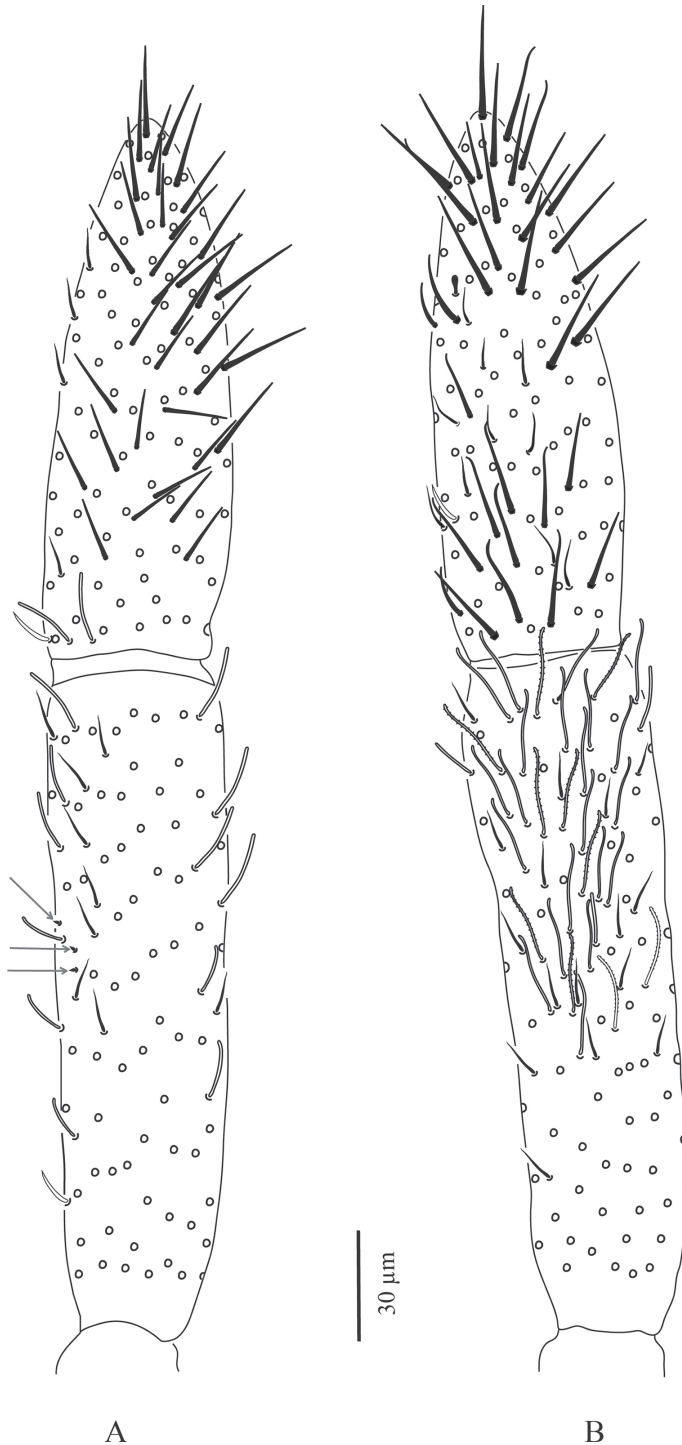


Figure 7. *Troglopedetes kae* sp. nov. continued **A** dorsal side of Ant. IV of a specimen with fused Ant. II and III, left side, arrows indicate new type of S-chaetae type 13 **B** ventral side of Ant. IV of a specimen with fused Ant. II and III, left side.

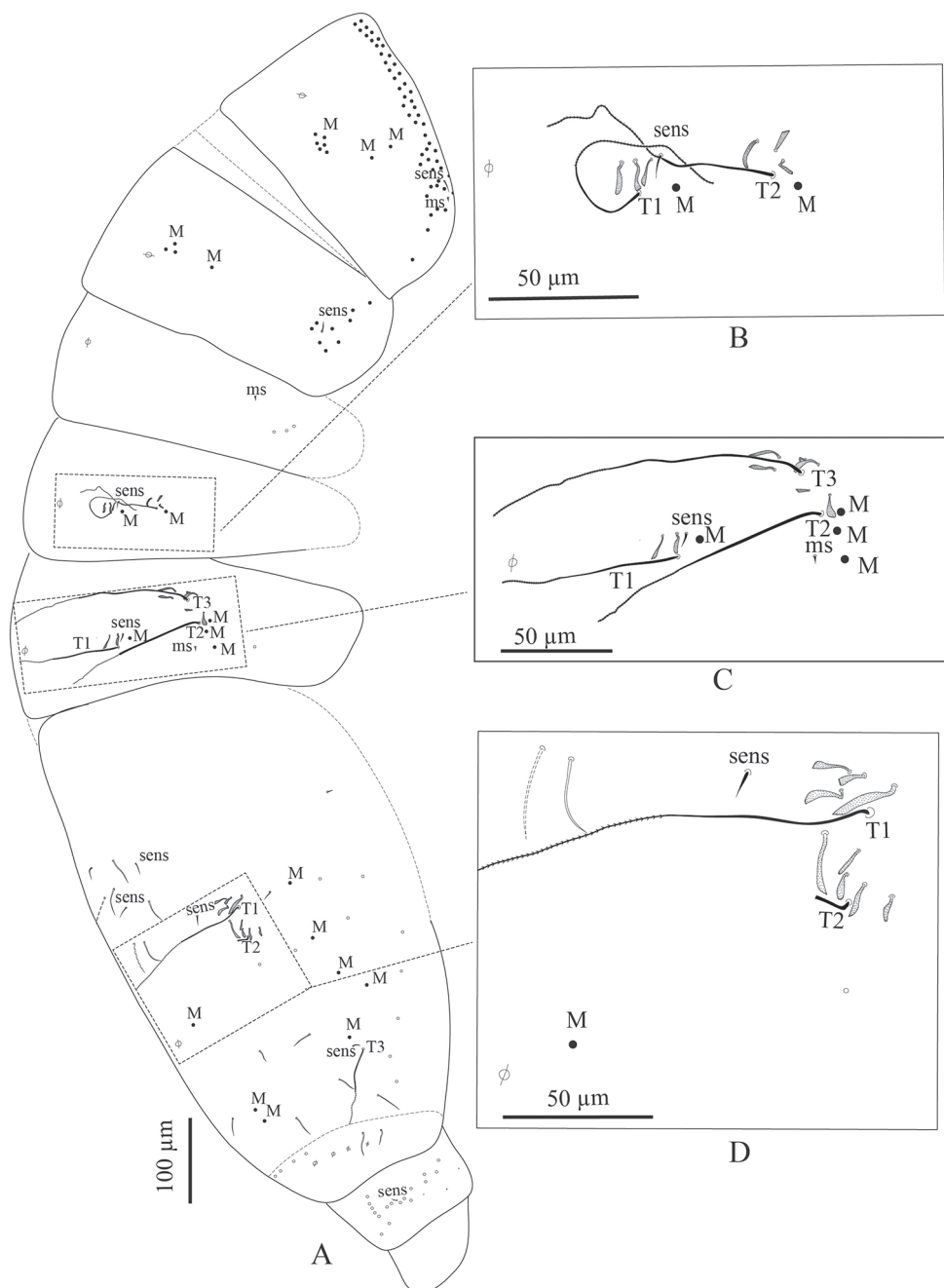


Figure 8. *Troglopedetes kae* sp. nov. continued **A** chaetotaxy of tergites **B** trichobothrial complexes of Abd. II **C** trichobothrial complexes of Abd. III **D** trichobothrial complex of Abd. IV.

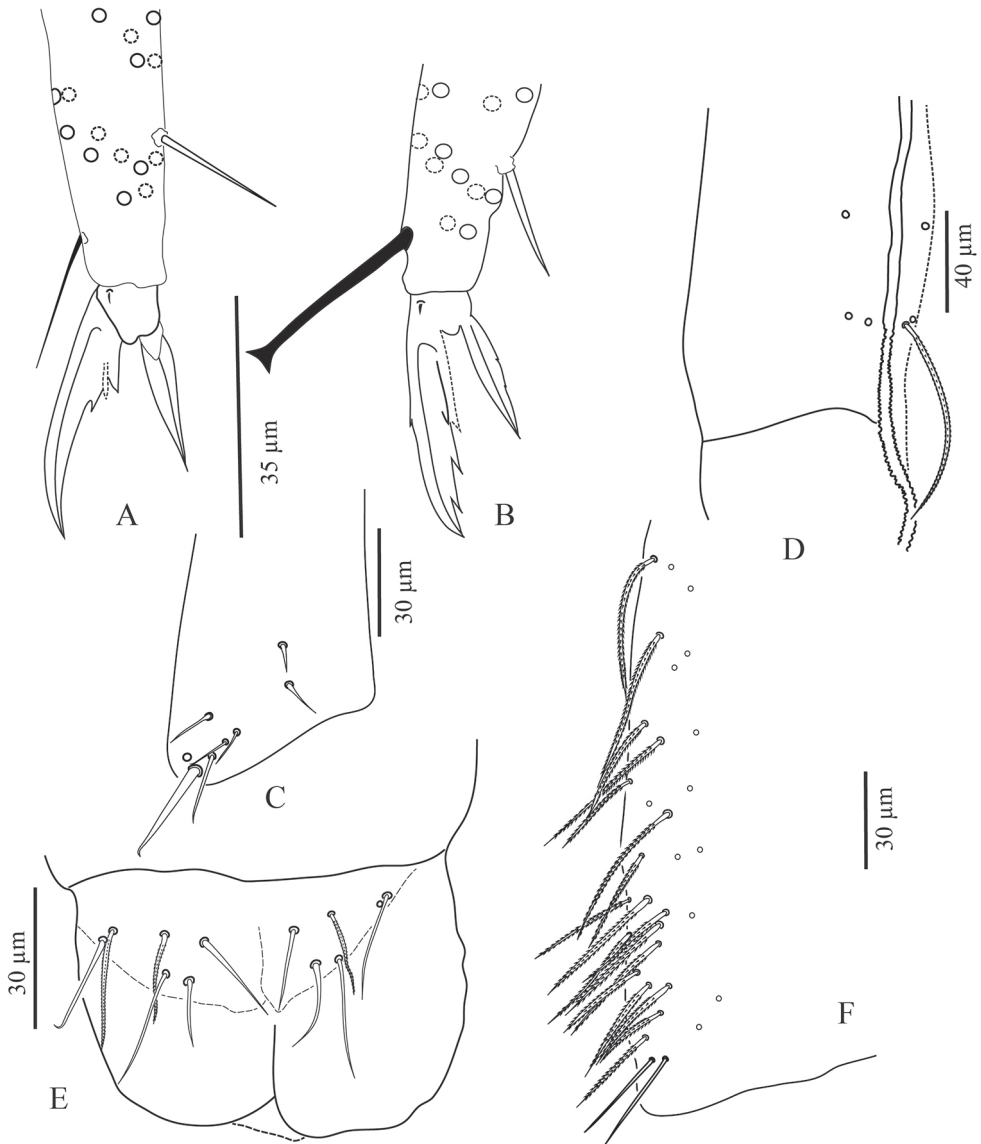
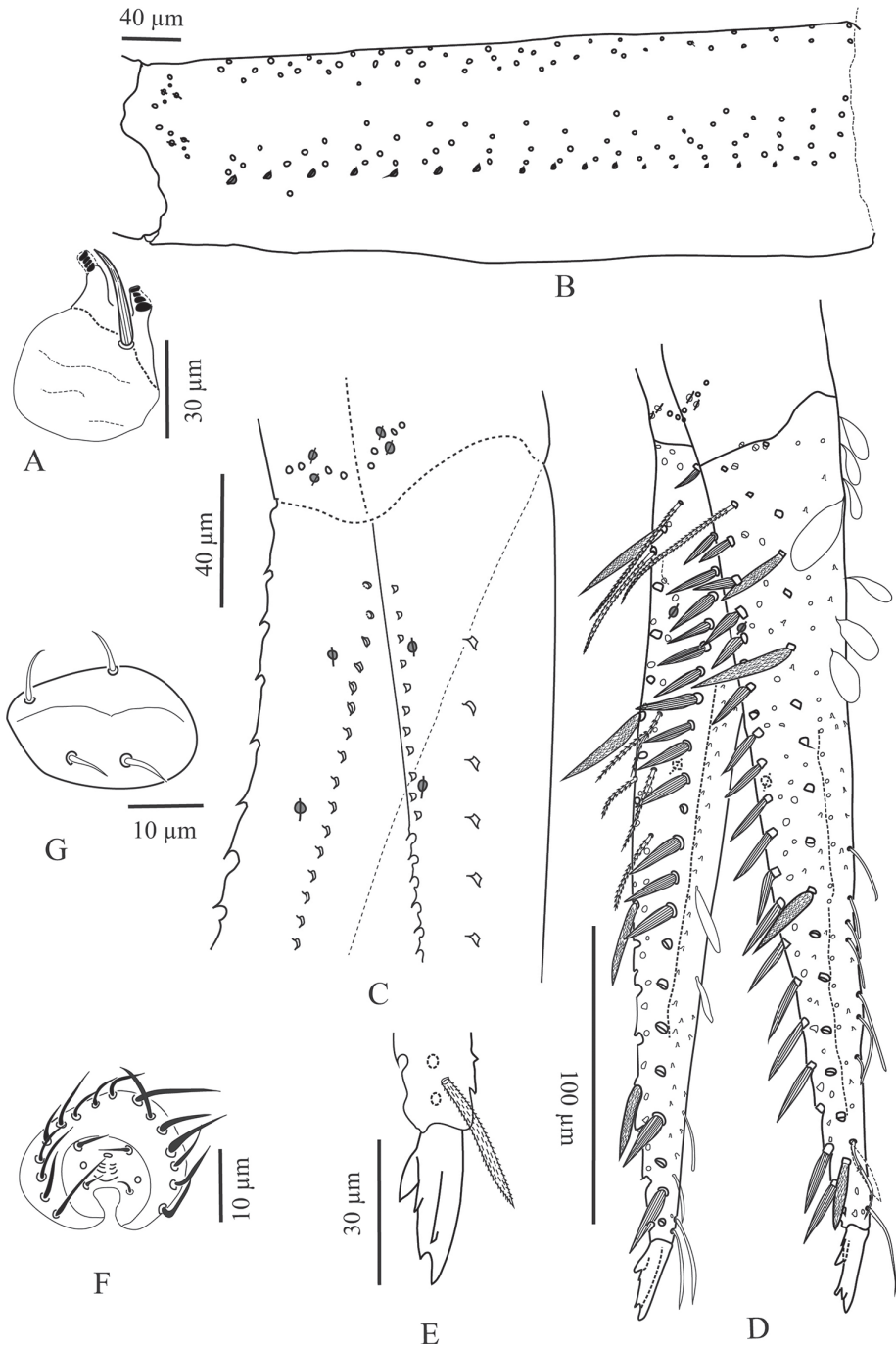


Figure 9. *Troglopedetes kae* sp. nov. continued **A** distal part of tibia-tarsus III and claw complex with pointed tenent hair **B** distal part of tibia-tarsus III and claw complex with clavate tenent hair **C** trochanteral organ **D** anterior side of ventral tube **E** lateral flap of ventral tube **F** posterior side of ventral tube.

(1.3–1.6 vs. 1.7–2.1 mm), body colour with spots of orange pigment (vs. white), longer antennae ($0.5\text{--}0.6 \times$ as long as body vs. 0.4), thinner claw with an internal tooth at 30 vs. 50–65% from the basis, chaetae on lateral flap of the ventral tube (6+6 vs. 7+7), higher ratio dens:mucro (9.3–13.7 vs. 8.8), and mucro with five teeth (vs. four).

In the same cave and same habitat, we found another morphotype with very different claw complex; thick and clavate tenent hair, two strong inner teeth on claw at



Symbols: ● Mac; ○ mac to mes; ○ mes; ● psp; ∪ scales; ∪∪ spine sockets

Figure 10. *Troglopedetes kae* sp. nov. continued **A** tenaculum **B** manubrium dorsal side **C** distal part of Manubrium and basal part of dens indicate the location of pseudopore **D** distal part of Manubrium and Microdens **E** micro **F** male genital plate **G** female genital plate.

74% and 91% of inner edge, and external edge of unguiculus with two or three minute outer basal teeth, sometimes inconspicuous (Fig. 9B). However, material was not enough to describe it in detail.

The locality where *T. kae* sp. nov. was collected is located 400 km south of the Isthmus of Kra, i.e., more south than other described *Troglopedetes* from Thailand. The Isthmus of Kra is well-known to be a biogeographical transition zone between Indo-chinese and Sundaic fauna (Fig. 1). It was previously considered to be the southern distribution limit for the genus *Troglopedetes*, and the northern limit for the closely related genus *Cyphoderopsis* in Thailand (Deharveng and Gers 1993, Jantarit et al. 2013). This discovery provides evidence that the two genera may actually overlap in southern Thailand, and questions the role of the Isthmus of Kra as biogeographical barrier for cave fauna.

***Troglopedetes meridionalis* sp. nov.**

<http://zoobank.org/9FA46FCC-4ED7-4DE0-9362-EC8425E63AAD>

Figures 11–16

Type material. Holotype male and four paratypes (one female, three subadults) on slides. Thailand: Chumphon Province: Lang Suan district, Tham Don Non (Tapan), 9°54'14"N, 99°02'41"E, ca 60 m a.s.l., 25 Jul. 2015, S. Jantarit leg., dark zone of cave, by aspirator (sample # THA_SJ_CPN01). Holotype and two paratypes deposited in NHM-PSU. Two paratypes deposited in MNHN. Measurements of holotype in Table 2.

Description. Habitus. Slightly troglomorphic, slender, with elongate legs, furca and antennae (Figs 1, 11A). Body length 1.3–1.5 mm. Fourth abdominal segment 3 × as long as the third one along dorsal axis. Furca well developed, ca. 2 × shorter than body length. Body colour white with spots of orange pigment. Eyes absent, no ocular patch.

Chaetal types. Four types of chaetae on somites, appendages (except antennae) and mouthparts: scales, present on antennae I and II, head, body and furca, absent on legs and ventral tube; ordinary chaetae on all body parts; S-chaetae and trichobothria on tergites; hairs devoid of sockets on outer maxillary lobe. Chaetal types on antennae are much more diverse and described separately further.

Table 2. *Troglopedetes meridionalis* sp. nov., measurements in µm (from holotype).

Head		Body		Appendages	
Ant. I	78	Th. II	137	Man	345
Ant. II	150	Th. III	114	Dens	340
Ant. III	125	Abd. I	62	Mucro	30
Ant. IVa	125	Abd. II	76	Furca	715
Ant. IVb	125	Abd. III	110	Claw I	27
Ant.	603	Abd. IV	400	Claw II	27
Head	300	Abd. V	62	Claw III	27
		Abd. VI	40		
		Body	1,301		

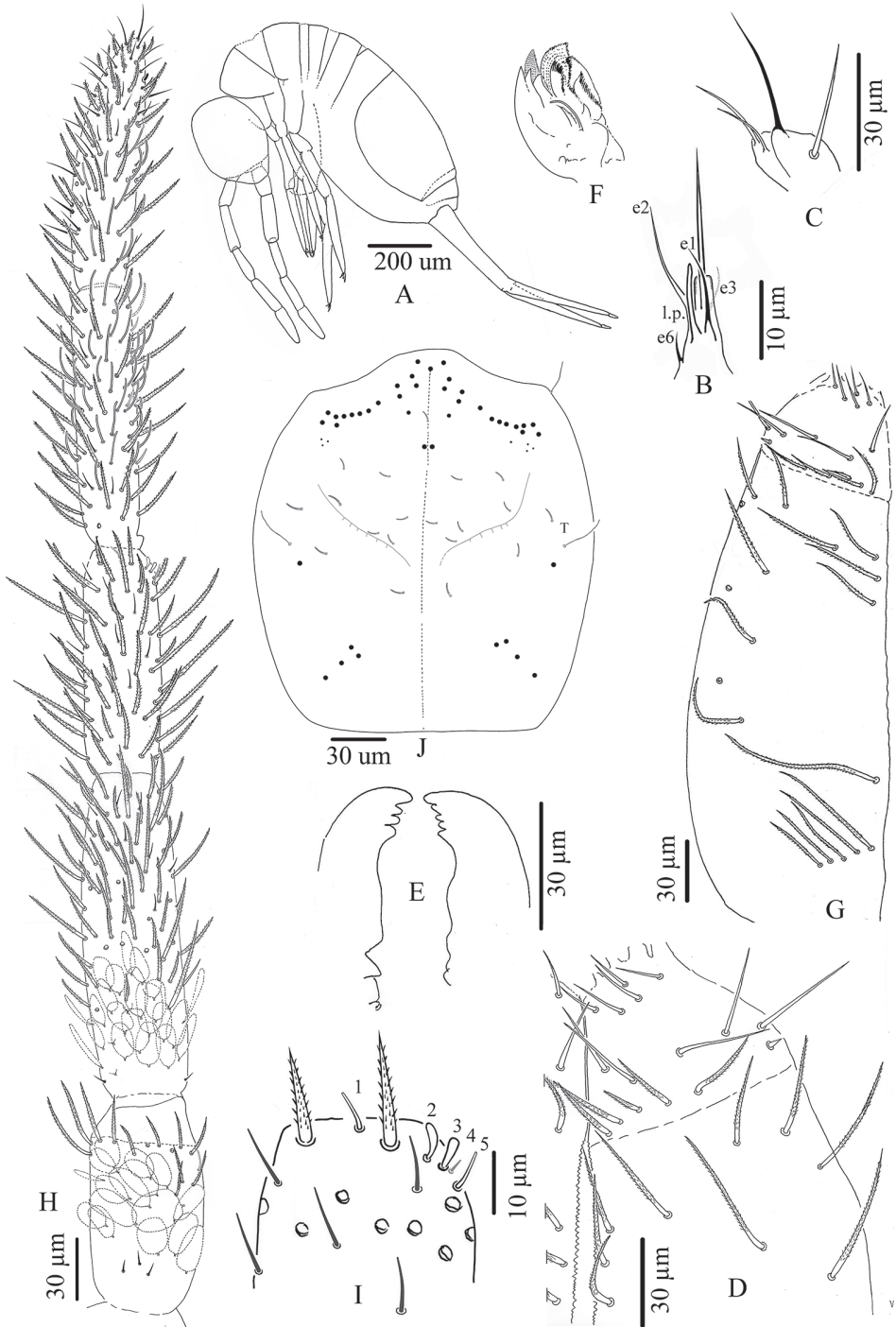


Figure 11. *Troglopedetes meridionalis* sp. nov. **A** habitus **B** labial palp of papillae **E C** outer maxillary lobe, right side **D** chaetotaxy of basal area of labium, right side **E** mandible **F** maxilla **G** ventral chaetotaxy of head, left side **H** antenna, right side **I** distal organ of Ant. III, right side **J** dorsal chaetotaxy of head.

Pseudopores (Figs 12C, 13D, 15A, B, D). Pseudopores present as round flat disks larger than mac sockets, on antennae, head and tergites. Dorsal pseudopore formula: 1–(2)/1, 1/1, 1, 1, 1+4 (Figs 11J, 15A). On antenna, 1–(2) psp detected ventro-distally on Ant. I., one ventro-distally on Ant. II and one ventro-distally on Ant. III, sometimes not clearly seen (Figs 12C, 13D). On head, 1–(2) psp close to antennal basis. On legs, psp present externally on coxae (two for legs I and II and 2–(3) for leg III). On manubrium, two psp on each dorso-distal plaque, on dens (new location for *Troglope-detes*) two psp dorso-basally near the internal spine on each side (Fig. 16E).

Mouthparts. Labral formula 4/5,5,4; prelabral chaetae short, bent and ciliated, labral chaetae thinner, smooth and acuminate, those of the distal row slightly shorter than those of the median row. Ventro-distal complex of labrum well differentiated, asymmetrical, with two distal combs (a larger one with 6–8 teeth on the left side, a smaller one with more than ten minute teeth on the right side) and an axial pair of sinuous tubules. Distal part of labrum not adorned with spines dorso-distally. Labial palp similar to that of *T. kae* sp. nov. (Fig. 11B). Chaetae of labial basis as M1M2REL112. Chaetae M1, M2, E and L1 subequal and ciliated, R shorter than others and ciliated, l2 short, smooth and acuminate (Fig. 11D, G). Outer maxillary lobe with one papillate chaeta, one basal chaeta and two sublobal hairs, shorter than others (Fig. 11C). Maxillary head with a 3-toothed claw, several stout shortly ciliated lamellae not detailed here; special structures present on the maxilla head, i.e., a thin elongate structure, arising from the basis of the maxilla head and reaching claw basis; close to it a spiny structure and a thin structure in an opposite side (Fig. 11F). Mandible heads strong, asymmetrical (left side with four teeth, right side with five teeth); molar plate with three strong pointed basal teeth, and other two or three inner distal teeth, identical in both mandibles (Fig. 11E).

Ventral chaetotaxy of head (Fig. 11D, G). Head densely covered with oval scales (40–50 µm), postlabial chaetae along the linea ventralis as three mes anteriorly, one mac and one oblique line of four or five mes posteriorly on each side.

Antennae (Figs 11H–I, 12A–D, 13A–F, 14A–C). Antennae shorter than body, ca. $2 \times (n = 3)$ as long as cephalic diagonal. Ant. IV subdivided into two subequal segments, without apical bulb. Lengths of antennal segments I to (IVa+IVb) as 1:1.8:1.5:2.9 (average, $n = 3$). Antennal chaetae (scales, five types of ordinary chaetae, 13 types of S-chaetae and subapical organite) described separately. Antennal scales oval, present dorsally only on Ant. I and II and ventrally on Ant. II, absent ventrally on Ant. I, and absent on Ant. III and IV (Figs 11H, 12A–D, 13D–F).

Dorsal chaetotaxy (Figs 11J, 15A, B, D). Dorsal macrochaetae formula: 1,4/8,4/0,2,4,3 (Figs 11J, 15A). Trichobothrial pattern: 1/0, 0/0, 2, 3, 3 (Figs 11J, 15A, B, D). Trichobothrial complexes well developed with modified mes of various sizes (Fig. 15A–D) as described below for each segment. The mes pattern is not complete. Head with 12 or 13 peri-antennal mac in line on each side; with 1+1 central mac (chaetae A of Deharveng and Gers 1993), chaetae B–F absent, at least 9+9 cephalic mes short, feebly serrated, equal in size, symmetrically arranged (Fig. 11J). One lateral cephalic trichobothria much shorter than closest mac on each side; suture zone visible,

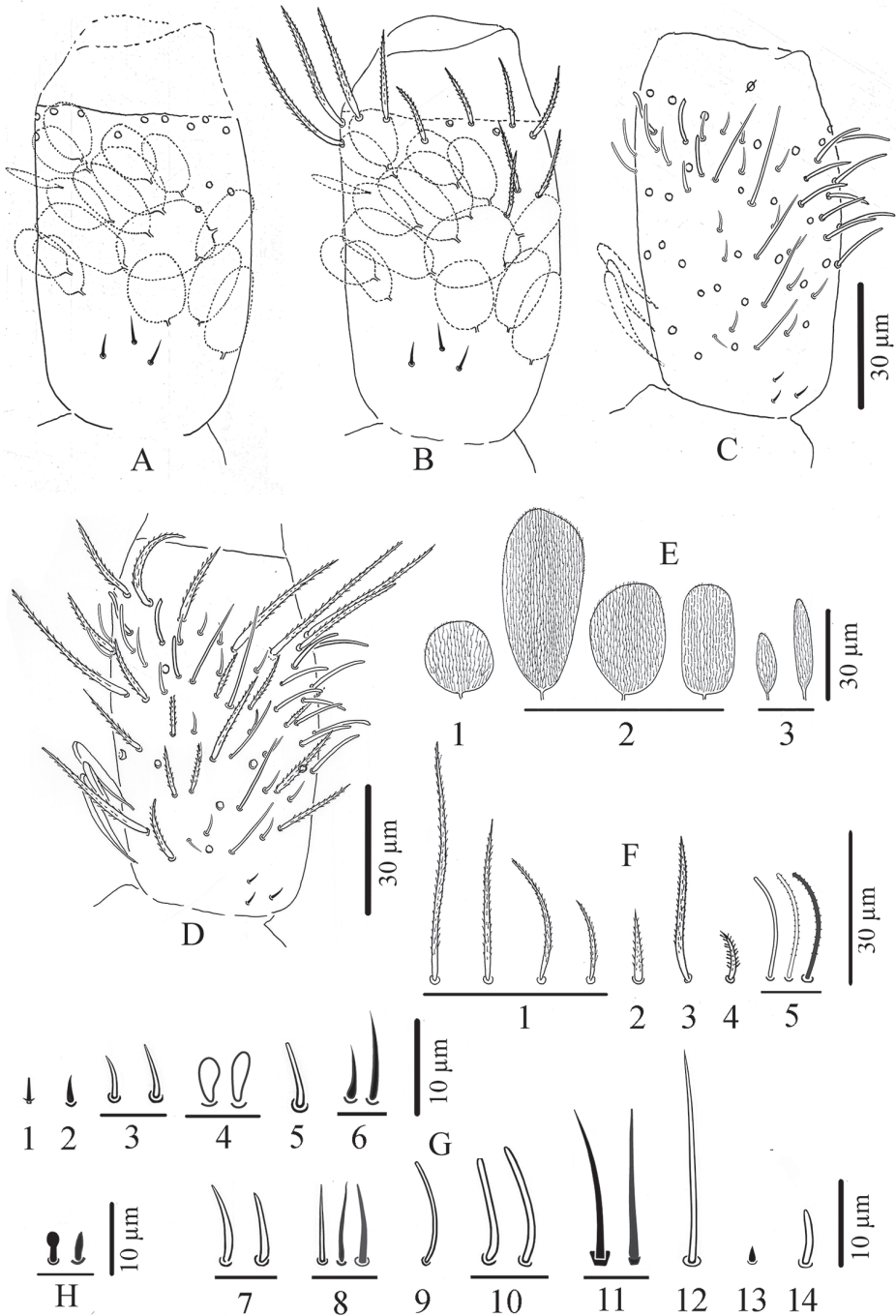


Figure 12. *Troglopedetes meridionalis* sp. nov. continued **A** dorsal side of Ant. I with scale and S-chaetae, right side **B** dorsal side of Ant. I with all chaetal types, right side **C** ventral side of Ant. I with scale and S-chaetae, right side **D** ventral side of Ant. I with all chaetal types, right side **E** type of scale **F** type of antennal ordinary chaetae **G** type of antennal S-chaetae **H** subapical organite of Ant. IV.

without associated mac (Fig. 11J). Head dorsally densely covered with round to oval scales (20–35 μm). Body densely covered with oval scales (15–50 μm).

Th. II collar consisting of a few rows of mac along its anterior and antero-lateral margins, a compact group of six central mac on each side (“P3 complex”) and two antero-lateral mac; one antero-lateral ms; one antero-lateral sens; two or three short mic laterally, and a few others not counted centrally (Fig. 15A).

Th. III with four mac on each side (a group of three central and one anterior to them); one sens at antero-lateral margins; one mic laterally; and ca. 11+11 mac or long mes at lateral margins (Fig. 15A).

Abd. I without central mac, with one ms laterally on each side; two or three mic arranged in line externally to pseudopore and two larger lateral mic; three mes laterally (Fig. 15A).

Abd. II with two tric on each side and six or seven modified mes around them (two around the internal tric and four or five near external tric), two mac (one near internal tric and one near external tric), one sens near internal tric; three mic (one close to internal tric and two close to external tric), others mes sockets internally visible, not counted (Fig. 15A, B).

Abd. III with three tric on each side (one internal, two external) and nine or ten modified mes around tric (two near internal tric and seven or eight near the two external tric); four mac (one near internal tric and three near external tric); one sens anterior to internal tric and one ms posterior to the two external tric; two mic/mes external to the external mac; several mes at lateral margins, not counted (Fig. 15A, C).

Abd. IV with three tric on each side (two antero-lateral, one postero-lateral); and ca. 6–9 modified mes around the two antero-lateral tric; postero-lateral tric without modified mes. Mac distributed as three central on each side (one antero-external to pseudopore, two anterior to posterior tergite margin), one near postero-lateral tric, and four or five external, mixed with many mes or smaller mac on lateral to posterior margins (not counted); probably three sens anteriorly; at least seven S-like chaetae *sensu* Lukić et al. (2015), and several mes or S-like chaetae uniformly distributed (not counted); six serrated mes in line in the posterior row (one near axis and five along pseudopore line, from medium to short) (Fig. 15A, D).

Abd. V with only two sens detected on each side, and several ordinary chaetae from mes to mac in size (Fig. 15A). Abd. VI chaetotaxy not analysed.

Legs (Fig 16A, B). Legs long; Tita III as long as head diagonal, slightly longer than Tita I and II. Legs devoid of scales, mostly covered with ordinary ciliated chaetae of various length, from mes to mac. Trochanteral organ of leg III with 11–13 smooth, straight, unequal spiny chaetae (Fig. 16B). Tibiotarsus chaetotaxy mostly composed of strong ciliated-serrated mes, basal ones longer and thicker (60 μm), the distal ones slightly shorter (up to 15–20 μm). Distal row with ten subequal ciliated mes and a dorso-apical tenent hair thin, smooth and acuminate on all tita; a ventro-distal strong smooth erected chaeta present on Tita III (Fig. 16A). Praetarsal mic minute (2.5–3 μm , Fig. 16A). Unguis slender and relatively short (27–30 μm long, 6–7 μm wide at basis), 8–9 \times shorter than tita; with one rather strong tooth at 50–55% of inner edge and a pair of inner basal teeth of unequal size (Fig. 16A). Unguiculus acuminate, 0.6

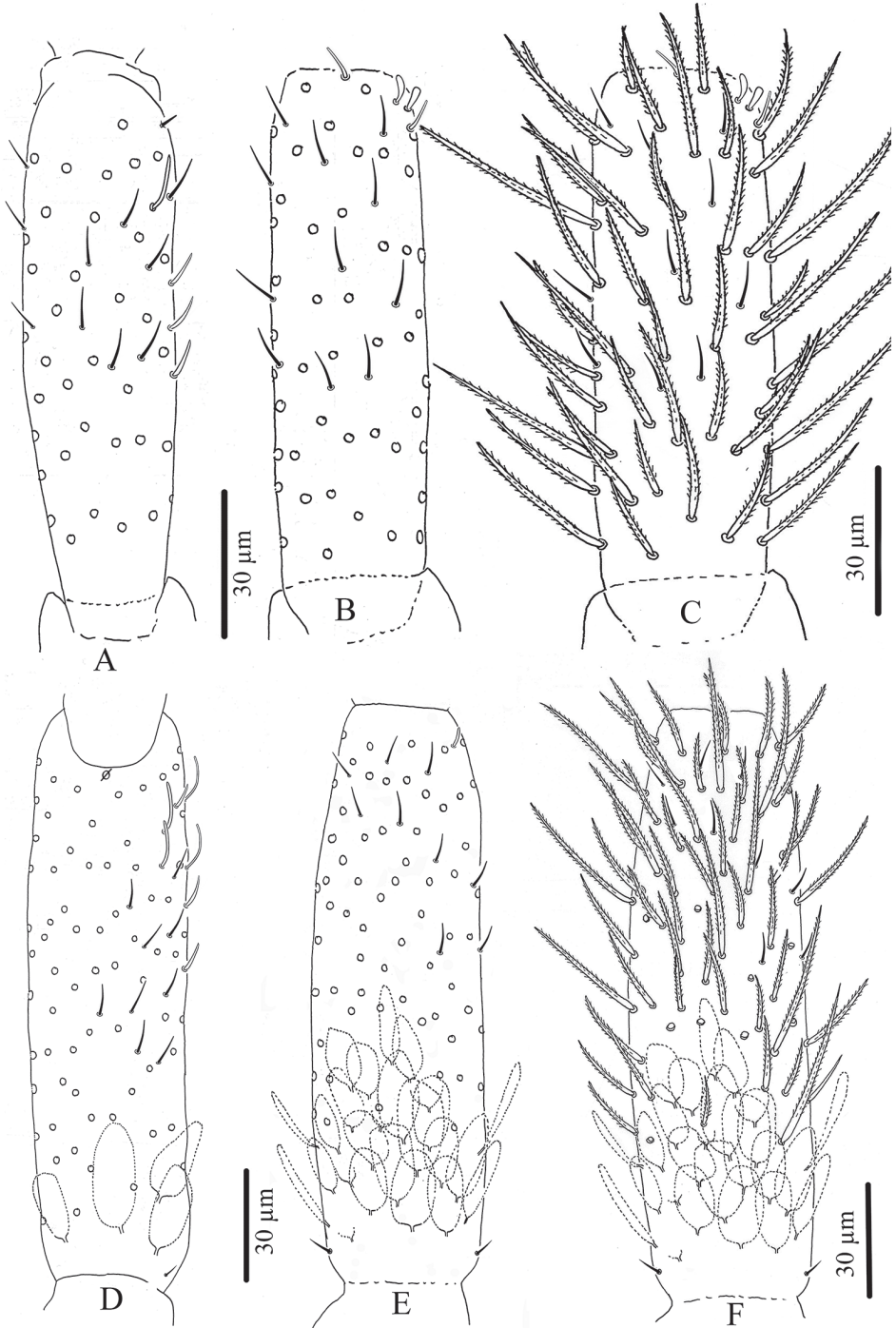


Figure 13. *Troglopedetes meridionalis* sp. nov. continued **A** ventral side of Ant. III with S-chaetae, right side **B** dorsal side of Ant. III with S-chaetae, right side **C** dorsal side of Ant. III with all chaetal types, right side **D** ventral side of Ant. II with scale and S-chaetae, right side **E** dorsal side of Ant. II with scale and S-chaetae, right side **F** dorsal side of Ant. II with all chaetal types, right side.

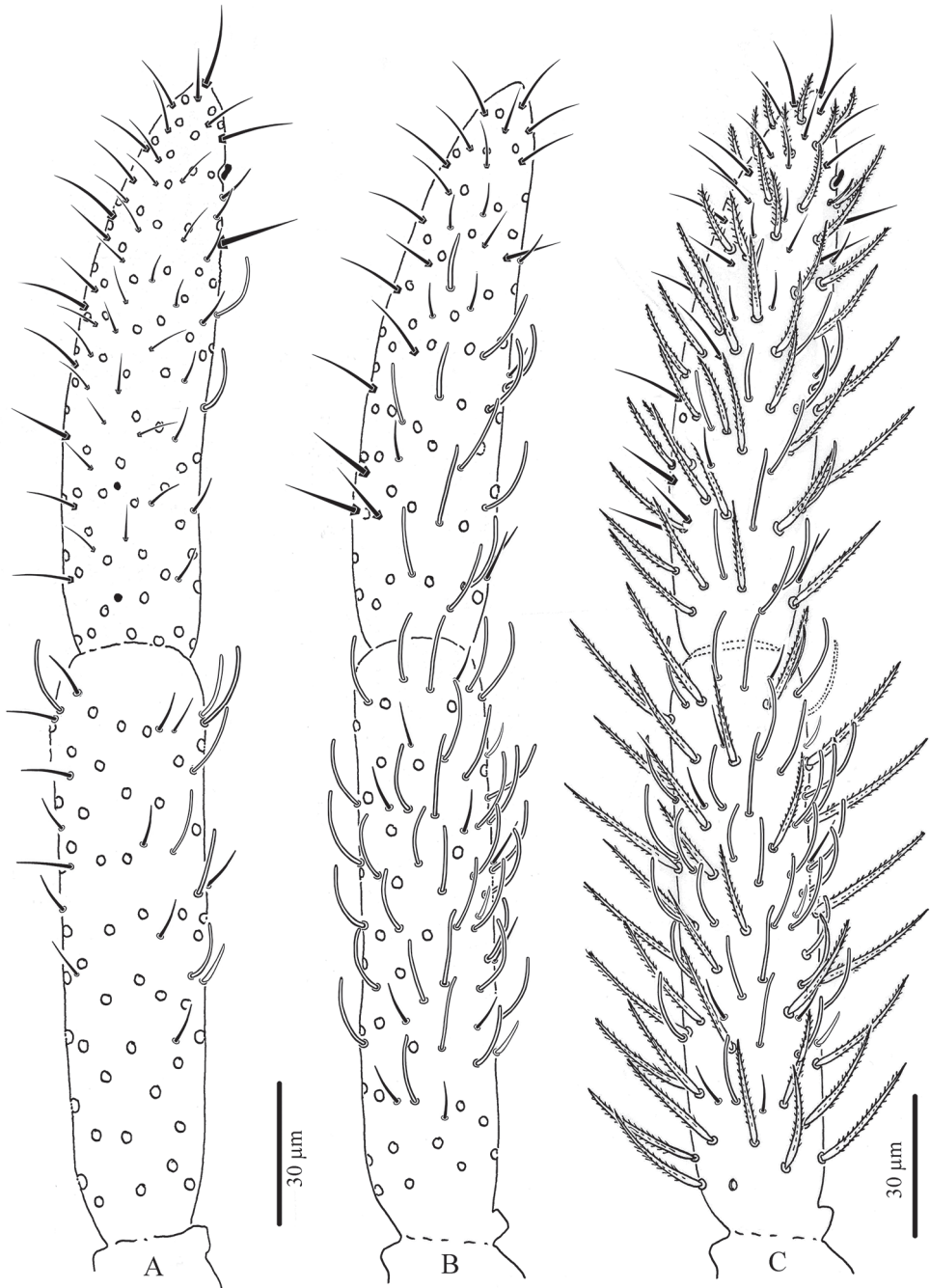


Figure 14. *Troglopedetes meridionalis* sp. nov. continued **A** ventral side of Ant. IV with S-chaetae, right side **B** dorsal side of Ant. IV with S-chaetae, right side **C** dorsal side of Ant. IV with all chaetal types, right side.

× as long as claw, its external edge with a minute outer basal tooth, sometimes inconspicuous (Fig. 16A).

Ventral tube (Fig. 16C). Ventral tube 4 × longer than wide; with 3+3 long serrated mac anteriorly and six mes (two ciliated and four smooth) on each lateral flap (Fig. 16C); posteriorly with many long ciliated mes, not suitable for observation in available specimens.

Furcal complex (Fig. 16D–F). Tenaculum with four large teeth on each ramus, of decreasing size from the basal to the distal one, on a prominent, irregular body, with a postero-basal strong, densely serrated, distally bent chaeta (Fig. 16D). Manubrium slightly shorter than mucrodens (ca. 0.95 ×). Manubrium dorsally with subequal ciliated mes (none smooth) irregularly arranged in 3–4 rows in two longitudinal stripes separated by a glabrous axial stripe, external row of chaetae distally with at least 5–7 long ciliated mes, dorso-distal plaque with 4+4 mes and 2+2 pseudopores. Ventrally, dense cover of round to oval (20–38 μm) and thin elongated scales (20–25 μm).

Dens straight, elongate, hairy, slightly and progressively tapering, dorsally with two rows of spines, mixed with ciliated mes of various length, thickness and shape. Dorso-external row with 17–20 subequal spines, dorso-internal row with 30–37 subequal spines (asymmetries between dentes); external spines larger and less sclerotised than internal ones. Short ciliated mes interspersed with spines in the external row; dorsally between the two rows of spines a mix of short and long ciliated mes, irregularly arranged in one row distally turning to 3–4 rows proximally; laterally, many short ciliated mes; dorso-distally, 3–(4) stronger ciliated mes; 2+2 psp on dorso-basally between the two rows of spine, sometimes inconspicuous. Dens ventrally entirely and densely scaled, scales elongate (20–38 μm), arranged in short lines from 3–5 (distally) to 6–8 scales (proximally) (Fig. 16E).

Mucro rather stout, short, 12–15 × shorter than dens (Fig. 16E, F), with four main teeth, the apical one blunt and strong, the two subapical ones smaller, the dorso-basal one slightly longer with one or two toothlets basally (Fig. 16F).

Genital plate. Genital plate not seen.

Ecology. *Troglopedetes meridionalis* sp. nov. was found in small populations in the dark zone of a cave, foraging on a small patch of old and humid bat guano.

Etymology. The name of the species, *meridionalis*, means southern in Latin, referring to the location of the species in the southern part of peninsular Thailand.

Remarks. *Troglopedetes meridionalis* sp. nov. is the only species of the genus with one medial head macrochaeta. It is similar to *T. convergens* Deharveng & Gers, 1993 from a cave of Ratchaburi province in the absence of eyes, two rows of dental spines, labial basis chaetotaxy, similar dorsal chaetotaxy from head to Abd. IV, anterior ventral tube chaetotaxy, and claw morphology. It can be distinguished by the combination of characters listed in Tables 3A and 3B, in particular the absence of the chaetae “E” on head, larger size (1.3–1.5 vs. 0.95–1.3 mm), antennae relatively shorter (0.35–0.4

Table 3A. Summary of main general and head characters of Thai *Troglopedetes* (N = northern Thailand, W = western Thailand, S = southern Thailand).

Species/ Characters	Length (mm)	Eyes	Colour	Ant.: Body	Labial basis	Sublobal hairs	Central mac on head	Mac on head	Locality (province)
<i>T. calvus</i>	0.90–1.37	0	white	0.6	M1M2REL112	2	0	–	Kanchanaburi (W)
<i>T. centralis</i>	1.7–2.1	0	white	0.4	M1M2REL112	2	4+4	A, B, E, F	Chiang Mai (N)
<i>T. convergens</i>	0.95–1.3	0	white	0.45–0.5	M1M2REL112	2	2+2	A, E	Ratchaburi (W)
<i>T. dispersus</i>	1.3–1.4	0	white with red pigment	0.6	M1M2Re(E) L112	2	3+3	A, C, E	Kanchanaburi (W)
<i>T. fredstonei</i>	1.4–2.1	0	white with red pigment	0.5	M1M2REL112	2	5+5	A, B, C, E, F	Chiang Mai (N)
<i>T. kae</i> sp. nov.	1.3–1.6	0	white with orange pigment	0.46	M1M2REL112	2	4+4	A, B, E, F	Satun (S)
<i>T. leclerci</i>	0.7–1.0	3+3	white	0.44	M1M2REL112	2	7+7	A, B, C, D, E, F, G	Chiang Mai (N)
<i>T. longicornis</i>	1.8–2.2	0	white	0.8	M1M2ReL112	2	5–6+5–6	A, B, C, D, E, (F)	Mae Hong Son (N)
<i>T. maffrei</i>	1.3–1.75	0	white	0.4	M1M2ReL112	1	7+7	A, B, C, D, E, F, G	Mae Hong Son (N)
<i>T. maungonensis</i>	1.1–1.2	0	white	0.5	M1M2REL112	1	7+7	A, B, C, D, E, F, G	Chiang Mai (N)
<i>T. meridionalis</i> sp. nov.	1.3–1.5	0	white with orange pigment	0.46	M1M2REL112	2	1+1	A	Chumphon (S)
<i>T. microps</i>	1.5–2.0	1–2+1–2	white	0.6	M1M2REL112	1	4–5+4–5	A, B, C, E, (F)	Chiang Mai (N)
<i>T. multispinosus</i>	1.8–2.2	0	white, red eye patch	0.9	M1M2ReL112	2	3+3	A, B, E	Chiang Rai (N)
<i>T. paucisetosus</i>	0.85–1.06	0	white with some red pigment	0.6	M1M2REL112	2	1–2+1–2	A, (E)	Prachuap Khiri Khan (W)

Table 3B. Summary of main characters of body and appendages of Thai *Troglopedetes* (N = northern Thailand, W = western Thailand, S = southern Thailand, ? = no information).

Species/ Characters	Central Mac on Th. II	Central Mac on Abd. IV	Claw (inner teeth)	Position of inner teeth	Tenent hair	Lateral flaps of VT	Internal row of spine	Dens: micro	Locality (province)
<i>T. calvus</i>	8+8	3+3	2	65%, 85%	capitate	7+7	14–32	8.5	Kanchanaburi (W)
<i>T. centralis</i>	8+8	3+3	1	50–65%	pointed	7+7	37–42	8.8	Chiang Mai (N)
<i>T. convergens</i>	8+8	3+3	1	55%	capitate	7+7	19–23	9	Ratchaburi (W)
<i>T. dispersus</i>	8+8	3+3	1(2)	50%–(80%)	pointed or capitate	7+7	25–29	8.5	Kanchanaburi (W)
<i>T. fredstonei</i>	8+8	3+3	1	58–60%	pointed or capitate	7+7	?	15	Chiang Mai (N)
<i>T. kae</i> sp. nov.	8+8	3+3	1	30–35%	pointed	6+6	26–33	9.3–13.7	Satun (S)
<i>T. leclerci</i>	8+8	2+2	1	50%	pointed or feebly capitate	6+6	18	5–6	Chiang Mai (N)
<i>T. longicornis</i>	8+8	3+3	1	30–45%	pointed	7+7	29–36	13.1	Mae Hong Son (N)
<i>T. maffrei</i>	9+9	3+3	2	65, 75–85%	pointed or capitate	6+6	21–28	9.4	Mae Hong Son (N)
<i>T. maungonensis</i>	9+9	3+3	2	65, 85%	capitate	?	27–30	9.7	Chiang Mai (N)
<i>T. meridionalis</i> sp. nov.	8+8	3+3	1	50–55%	pointed	6+6	30–37	12–15	Chumphon (S)
<i>T. microps</i>	8+8	3+3	1	65%	capitate	7+7	36–42	13.6	Chiang Mai (N)
<i>T. multispinosus</i>	8+8	3+3	1	35%	pointed	7+7	34–41	12.7	Chiang Rai (N)
<i>T. paucisetosus</i>	8+8	2+2	2	65, 80%	capitate	7+7	18–24	9.6	Prachuap Khiri Khan (W)

vs. 0.45–0.5 × as long as body), tenent hair acuminate vs. usually clavate, each lateral flap of ventral tube with six chaetae (vs. seven), dental spines of the internal row more numerous (30–37 vs. 19–23) and higher ratio of dens: micro (12–15 vs. 9).

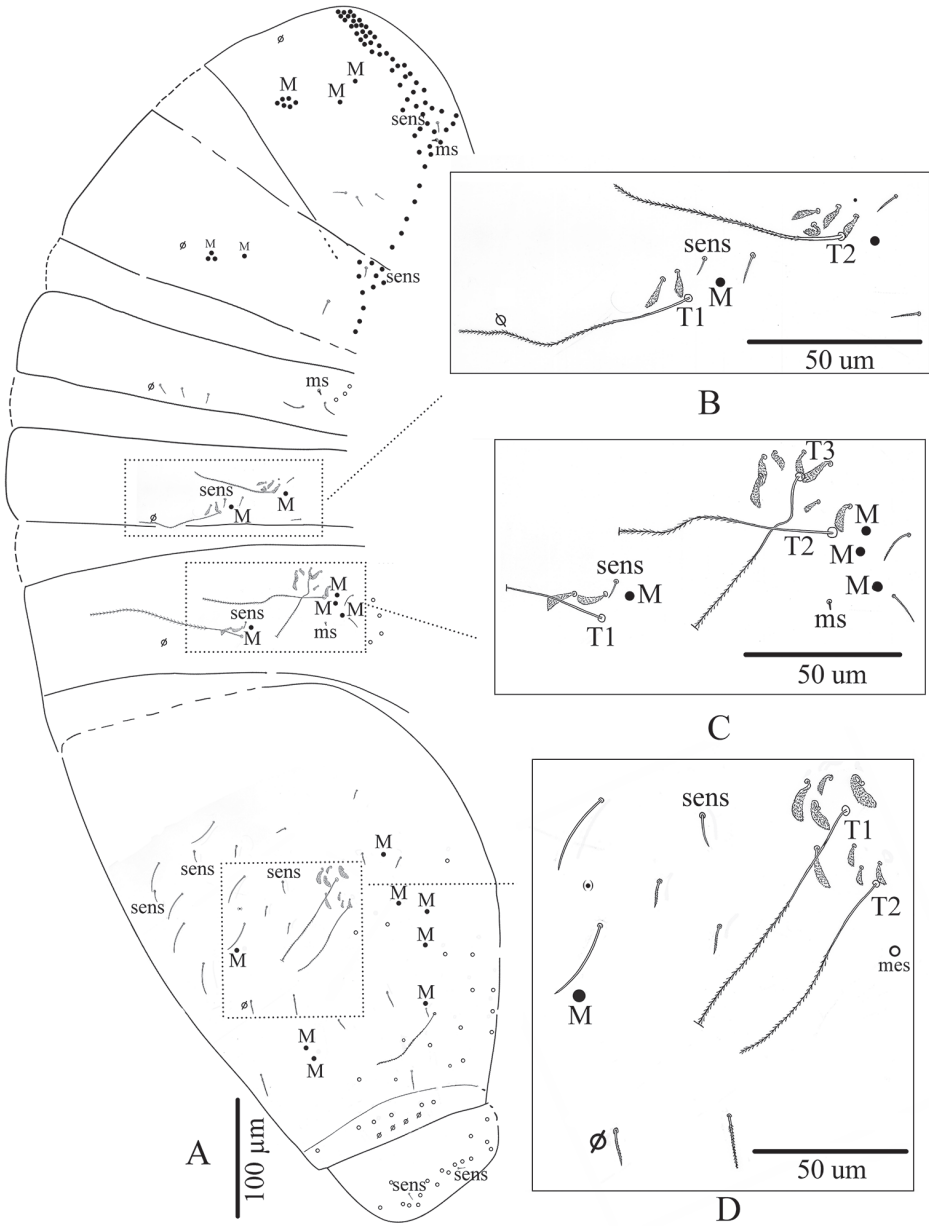


Figure 15. *Troglopedetes meridionalis* sp. nov. continued **A** chaetotaxy of tergites **B** trichobothrial complexes of Abd. II **C** trichobothrial complexes of Abd. III **D** trichobothrial complex of Abd. IV.

The pair of mac immediately ahead A and that ahead the uneven anterior mac on head are not figured in Deharveng and Gers (1993), as they were not considered as mac, but long mes. Their sockets in the new species are smaller than those of mac, but clearly marked.

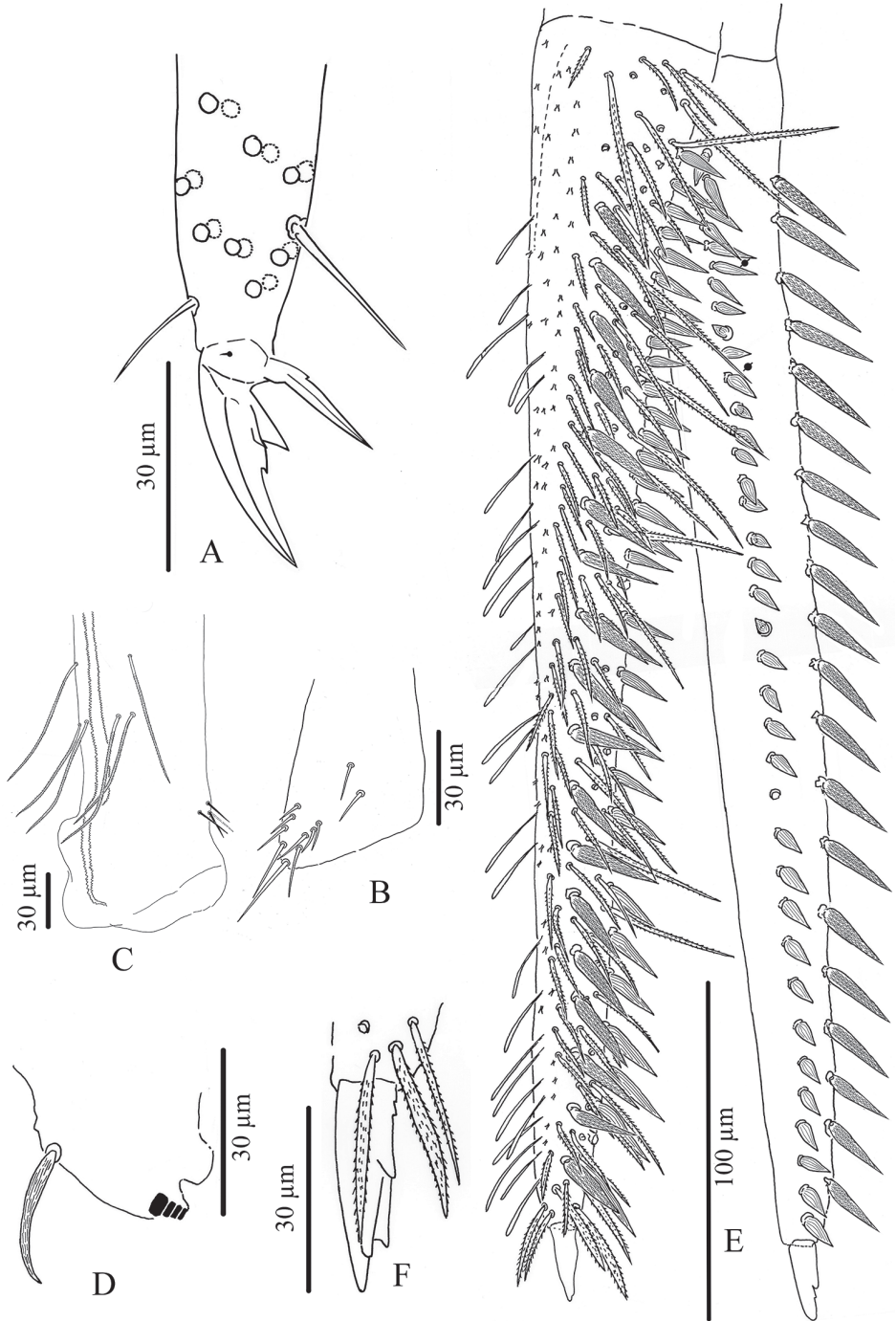


Figure 16. *Troglopedetes meridionalis* sp. nov. continued **A** distal part of tibiotarsus III and claw complex with pointed tenent hair **B** trochanteral organ **C** anterior side of ventral tube **D** tenaculum **E** microdens **F** enlargement of mucro and chaetae on tip of dens.

Diversity of antennal chaetae in *T. kae* sp. nov. and *T. meridionalis* sp. nov.

The work presented below is an attempt to build a comprehensive list of phanere types found on the antennae of an Entomobryoidea, to describe them morphologically, and to explore their distribution on antennal surface. Antennae bears many useful taxonomic and phylogenetic characters in Poduromorpha and has been the object of many studies (Deharveng 1981). In Entomobryoidea, antennal chaetotaxy is much more complex and variable, and has never been thoroughly explored for this reason. Only a few characters easy to observe are routinely used in taxonomy. Three recent papers, however (Lukić et al. 2015, 2018; Jantarit and Sangsiri 2020) provide detailed information on the chaetal investiture of *Verhoeffiella* and *Alloscopus* species (family Entomobryidae). Here, we carried out a detailed analysis of antennal chaetae of the adult of the two new *Troglopedetes* species described above, one female (normal antennae, Figs 3–5) and one female (fused antennae, Figs 6, 7) for *T. kae* sp. nov. and a male of *T. meridionalis* sp. nov. (Figs 11H, 12A–D, 13A–F, 14A–C).

Types of phaneres

There are five main types of phaneres (*sensu* Deharveng 1983) in *Troglopedetes*, like in all scaled Entomobryoidea: scales, ordinary chaetae (including spines), trichobothria, S-chaetae and subapical organite of Ant. IV. All, except trichobothria, are present on the antennae. We list phanere types that we recognise within each of these broad categories, mentioning putative homologies from the literature, and we summarise their arrangement pattern on each antennal segment.

Scales

Three types of scales were recognised in Thai *Troglopedetes*, but only one type was found on antennae of *T. kae* sp. nov. All scales are roundish, oval, variable in size on different organs, devoid of ridges but adorned by a dense and homogeneous cover of minute spicules (Fig. 12E).

Type 1 – round shape (20–30 μm long) on body and furca (Fig. 12E1).

Type 2 – oval shape (15–50 μm \times 7–30 μm) on antennae, body and furca (Fig. 12E2).

Type 3 – thin, elongated (20–40 μm \times 5–8 μm) on ventral side of dens (Fig. 12E3).

Antennal scales are of type 2 (25–35 μm long), oval, present dorsally only on Ant. I and II and ventrally on Ant. II, absent ventrally on Ant. I, and absent on Ant. III and IV (Figs 3A, C, D, 6B–D, 11H, 12A–D, 13D–F).

Ordinary chaetae

Ordinary chaetae are the most numerous chaetae on the body and appendages of *Troglopedetes*. They are well-diversified on antennae (Fig. 12F), where five types have

been recognised. In *Verboeffiella* and *Alloscopus*, Lukić et al. (2015) and Jantarit and Sangsiri (2020) recognised three types of ordinary chaetae on the antennae.

- Normal mes: serrated or ciliated (10–70 μm), of various thickness, shape and size, present on all antennal segments (Fig. 12F1).
- Short tapering mes: thicker than normal mes, straight or weakly bent, ciliated (15–18 μm), present dorso-distally on Ant. III (Figs 4C, 11I, 12F2).
- Long thick mes: thicker than normal mes, long and rather broadly ciliated (30–35 μm), present dorso-proximally on Ant. I (Figs 11H, 12B, 12F3).
- Short thick mes: thicker than normal mes, not clearly tapering, bent, ciliated ($\approx 10 \mu\text{m}$), limited to the tip of Ant. IV (Figs 11H, 14C, 12F4).
- Long, subcylindrical, hyaline, weakly bent and finely serrated mes ($> 15 \mu\text{m}$) (sometimes looking dark) mostly present on both dorsal and ventral sides of Ant. IV (Figs 5A, B, 7A, B, 12F5, 14A–C), that may appear smooth and qualified of S-chaetae under light microscope.

S-chaetae

S-chaetae (*sensu* Deharveng 1983) are present on all antennal segments, with a variety of thicknesses, shapes, and sizes (from mic to mes, 2–30 μm). The antennae of our species were carefully examined under light microscope. As a result, 14 types of S-chaetae were recognised in *T. kae* sp. nov. and 13 types in *T. meridionalis* sp. nov. based on morphology: thickness, length, bending (straight vs. bent), orientation (erected vs. oblique to the integument), shape (cylindrical vs. tapering vs. foliaceous), tip morphology (pointed vs. blunt), and opacity (hyaline vs. dark) (Fig. 12G). When possible, they were homologised with those of *Verboeffiella* (Lukić et al. 2015) and *Alloscopus* (Jantarit & Sangsiri, 2020) as described below.

Type 1—minute mic, thin, pointed and dark (3–4 μm) (Fig. 12G1); corresponding to antennal S-chaetae type j *sensu* Lukić et al. (2015) and Jantarit and Sangsiri (2020).

Type 2—short mic, thin, usually bent and dark mic (5–6 μm) (Fig. 12G2).

Type 3—short mic, thin, rather curved apically and hyaline (5–6 μm) (Fig. 12G3).

Type 4—short, hyaline and swollen mic (foliaceous sens) (5–6 μm) (Fig. 12G4); corresponding to antennal S-chaetae type h *sensu* Lukić et al. (2015) and Jantarit and Sangsiri (2020).

Type 5—short, thin, bent, hyaline mic (sometimes looks dark) (7–8 μm) (Fig. 12G5); corresponding to antennal S-chaetae type k *sensu* Lukić et al. (2015) and Jantarit and Sangsiri (2020).

Type 6—short, thin, erected and dark mic (6–12 μm) (Fig. 12G6); corresponding to antennal S-chaetae type g *sensu* Lukić et al. (2015) and Jantarit and Sangsiri (2020).

Type 7—rather long, bent, hyaline mic, thinner distally and broad basally (7–12 μm) (Fig. 12G7).

Type 8—rather long, thin, erected and hyaline mic (sometimes looking dark) (10–15 μm) (Fig. 12G8).

Type 9—long, subcylindrical, bent, hyaline mic (12–14 μm) (similar to type 10 but smaller and thinner) (Fig. 12G9).

Type 10—long, subcylindrical, bent, hyaline and rather broad mic (10–15 μm) (Fig. 12G10); corresponding to antennal S-chaetae type l *sensu* Lukić et al. (2015) and Jantarit and Sangsiri (2020).

Type 11—long, thin, erected and dark mic (10–20 μm) (Fig. 12G11); corresponding to antennal S-chaetae type f *sensu* Lukić et al. (2015) and Jantarit and Sangsiri (2020).

Type 12—long, thin and hyaline mic (24–30 μm) (Fig. 12G12); possibly corresponding to antennal S-chaetae type e *sensu* Lukić et al. (2015) and Jantarit and Sangsiri (2020).

Type 13—minute, pointed and dark mic (2 μm) (Fig. 7A (arrow), 12G13). This chaetal type was only found on the Ant. IV of two specimens of *T. kae* sp. nov. in which Ant. II and III are fused.

Type 14—rather short, subcylindrical, bent, hyaline (6–8 μm) (Fig. 12G14).

Subapical organite of Ant. IV

Short, thick, dark, swollen at tip (4 μm) phanere with protecting chaeta, inserted dorso-internally ca. 20–50 μm from the apex (Fig. 12H). This organite is present in all Entomobryoidea and most Collembola, with limited changes in morphology, size and position.

Distribution patterns of antennal phaneres

In this study, ordinary chaetae on a single antenna numbered 483 for *T. meridionalis* sp. nov. and 518 for *T. kae* sp. nov. and were assigned to the 5 categories described above; 208 S-chaetae were numbered for *T. meridionalis* sp. nov. and 207 for *T. kae* sp. nov. and were assigned to the 14 morphological categories described above. (Tables 4, 5). The ventral side of antenna is richer in both S-chaetae and ordinary chaetae than the dorsal side (ordinary chaetae = 278 vs. 240 in *T. kae* sp. nov., and 251 vs. 232 in *T. meridionalis* sp. nov.; S-chaetae = 115 vs. 92 in *T. kae* sp. nov., and 134 vs. 76 in *T. meridionalis* sp. nov.) (Tables 4, 5). The distribution of the different types of S-chaetae along the antennal segments is arranged in more or less clearly defined patterns which are described in the following paragraphs, summarised in Tables 4 and 5, and illustrated in Figures 3–7, 11H–I, 12A–D, 13, 14.

First antennal segment: eight types of S-chaetae are recognised (Figs 3A, B, 11H, 12A–D): type 2, type 3, type 5, type 6, type 8, type 9, type 10, and type 12. Only one type is present on the dorsal side (type 6), the others are located on the ventral side.

Second antennal segment: seven types of S-chaetae are recognised (Figs 3C, D, 11H, 13D–F): type 2, type 3, type 7, type 8, type 9, type 10, and type 14. Three types are present on the dorsal side (type 2, type 8 and type 14) and five on the ventral side (type 3, type 7, type 8, type 9, and type 10).

Third antennal segment: six types of S-chaetae are recognised (Figs 4A–C, 11H, I, 13A–C): type 1, type 4, type 5, type 7, type 8, and type 10. All are present on the dorsal side and three types are present on the ventral side (type 7, type 8, and type 10).

Table 4. Detailed distribution of antennal chaetae. Presence in *Verboeffiella* and *Alloscopus* by comparison with chaetal morphologies described by Lukic et al. (2015, 2018) and Jantarit and Sangsiri (2020) respectively, ? = no information.

Type of chaetae	Distribution on antenna	Location	Position on antennal segment	Number of chaetae		Presence in <i>Verboeffiella</i>	Presence in <i>Alloscopus</i>
				<i>T. meridionalis</i> sp. nov.	<i>T. kae</i> sp. nov.		
Type 1	Ant. III	dorsal	latero-proximal	1	1	x	x
Type 2	Ant. I	ventral	basal	4	4	–	–
	Ant. II	dorsal	basal	2	2	–	–
Type 3	Ant. I	ventral	proximal	2	2	–	–
	Ant. II	ventral	proximal	1	1	–	–
Type 4	Ant. III	dorsal	AIII	2	2	x	x
Type 5	Ant. I	ventral	all segment	7	6	x	x
	Ant. III	dorsal	AIII	2	2	–	–
Type 6	Ant. I	dorsal	basal	3	3	x	x
Type 7	Ant. II	ventral	all segment	3	7	–	–
	Ant. III	dorsal	lateral	0	2	–	–
	Ant. III	ventral	middle to proximal	3	4	–	–
	Ant. IVa	dorsal	middle to proximal	4	4	–	–
Type 8	Ant. I	ventral	all segment	6	10	–	–
	Ant. II	dorsal	middle to proximal	9	8	–	–
	Ant. II	ventral	all segment	9	9	–	–
	Ant. III	dorsal	all segment	10	15	–	–
	Ant. III	ventral	middle to proximal	11	6	–	–
	Ant. IVa	dorsal	all segment	9	10	–	–
	Ant. IVa	ventral	all segment	13	5	–	–
	Ant. IVb	dorsal	all segment	9	9	–	–
Type 9	Ant. IVb	ventral	all segment	11	0	–	–
	Ant. I	ventral	latero-proximal	2	1	–	–
Type 10	Ant. II	ventral	proximal	2	4	–	–
	Ant. I	ventral	latero-proximal	14	5	x	x
Type 11	Ant. II	ventral	proximal	2	5	–	x
	Ant. III	dorsal	upper middle	0	1	–	x
	Ant. III	ventral	proximal	1	4	–	x
	Ant. IVa	dorsal	middle to proximal	1	3	–	x
	Ant. IVb	dorsal	middle	2	3	–	x
	Ant. IVa	dorsal	latero-proximal	0	1	x	x
	Ant. IVb	dorsal	all segment	19	22	x	x
Ant. IVb	ventral	all segment	35	36	x	x	
Type 12	Ant. I	ventral	all segment	8	6	x	x
Type 13	Ant. IVa	dorsal	middle of Ant. IVa	0	3	–	–
Type 14	Ant. II	dorsal	proximal	1	1	–	–
Subapical organite	Ant. IVb	dorsal	proximal near the tip	1	1	x	x
Ordinary chaetae	Ant. I	dorsal	all segment	13	28	x	x
	Ant. I	ventral	all segment	27	38	x	x
	Ant. II	dorsal	all segment	63	67	x	x
	Ant. II	ventral	all segment	68	77	x	x
	Ant. III	dorsal	all segment	45	38	x	x
	Ant. III	ventral	all segment	36	45	x	x
	Ant. IVa	dorsal	all segment	62	59	x	x
	Ant. IVa	ventral	all segment	53	60	x	x
	Ant. IVb	dorsal	all segment	49	48	x	x
	Ant. IVb	ventral	all segment	67	58	x	x
Overall				692	726	?	945

Table 5. Number of chaetae of each type along antennal segments.

Type of S-chaetae/ antennal segment	<i>Troglopedetes meridionalis</i> sp. nov.					<i>Troglopedetes kae</i> sp. nov.						
	Ant. I	Ant. II	Ant. III	Ant. IV		Total	Ant. I	Ant. II	Ant. III	Ant. IV		Total
				Ant. IVa	Ant. IVb					Ant. IVa	Ant. IVb	
Type 1	–	–	1	–	–	1	–	–	1	–	–	1
Type 2	4	2	–	–	–	6	4	2	–	–	–	6
Type 3	2	1	–	–	–	3	2	1	–	–	–	3
Type 4	–	–	2	–	–	2	–	–	2	–	–	2
Type 5	7	–	2	–	–	9	6	–	2	–	–	8
Type 6	3	–	–	–	–	3	3	–	–	–	–	3
Type 7	–	3	3	4	–	10	–	7	6	4	–	17
Type 8	6	18	21	22	20	87	10	17	21	15	9	72
Type 9	2	2	–	–	–	4	1	4	–	–	–	5
Type 10	14	2	1	1	2	20	5	5	5	3	3	21
Type 11	–	–	–	–	54	54	–	–	–	1	58	59
Type 12	8	–	–	–	–	8	6	–	–	–	–	6
Type 13	–	–	–	–	–	0	–	–	–	3	–	3
Type 14	–	1	–	–	–	1	–	1	–	–	–	1
Overall S-chaetae	46	29	30	27	76	208	37	37	37	26	70	207
Subapical organite	–	–	–	–	1	1	–	–	–	–	1	1
Overall ordinary chaetae	40	131	81	115	116	483	66	144	83	119	106	518
Total	86	160	111	142	193	692	103	181	119	145	177	726

Fourth antennal segment: five types of S-chaetae are recognised (Figs 5A, B, 7A, B, 11H, 14A–C): type 7, type 8, type 10, type 11, and type 13. All are present on the dorsal side, but only two types are present on the ventral side (type 8 and type 11). They are distributed as follows on each subsegment.

Fourth antennal segment I (a): five types of S-chaetae are recognised: type 7, type 8, type 10, type 11 and type 13 (*T. meridionalis* sp. nov. has only three types while *T. kae* sp. nov. has all types), all present on the dorsal side.

Fourth antennal segment II (b): three types of S-chaetae are recognised: type 8, type 10, and type 11, all present on the dorsal side. Two types are present on the ventral side (type 8 and type 11).

The most frequent S-chaetae are type 8 and type 10 that are present all along antennal segments, followed by type 7 that was found on three antennal segments (Ant. II, III, IVa), but not on Ant. I. Type 2, type 3, and type 9 were found on only two segments (Ant. I and Ant. II). Type 5 was found on only two segments (Ant. I and Ant. III). Other types are all limited to a single antennal segment: Ant. I (type 6 and type 12), Ant. II (type 14), Ant. III (type 1, type 4) or Ant. IV (type 11, and type 13 in *T. kae* sp. nov.) (see Tables 4, 5 for details).

With regard to the abundance of S-chaetae along antennal segments, type 8 is the most common followed by type 11 (Tables 4, 5). Ant. IV has the highest number of S-chaetae in both species followed by Ant. I, III, and II respectively in *T. meridionalis* sp. nov. and Ant. III, I and II respectively in *T. kae* sp. nov. (Table 5), while ordinary chaetae abundance ranks as Ant. IV, II, III and I (Table 5). The distal subsegment of antenna IV (Ant. IVb) is richer in S-chaetae than the proximal subsegment Ant. IVa, but their respective number of ordinary chaetae is rather similar (Table 5).

Discussion

The diversity of chaetal types was very similar in the two studied species, and between-species differences in the relative numbers of each chaetal type were limited, probably only reflecting individual variability. Similarities with *Verhoeffiella* and *Alloscopus* have been noted, but there was also many differences regarding the types of chaetae. It is not clear whether chaetal morphologies which seem special to one of the three genera are really taxon-specific receptors, or the result of undetected homologies due to different morphological evolution of some chaetae in the two genera. The only way to test these hypotheses will be to investigate thoroughly Entomobryoidea of other lineages.

The antennal phaneres of *T. meridionalis* sp. nov. and *T. kae* sp. nov. are arranged in a complex pattern. On the 20 morphological types of chaetae that we recognised (five types for ordinary chaetae, 14 types for S-chaetae and subapical organite of Ant. IV), 12 types were located at a fixed position on antennal segments (four types of ordinary mes; S-chaetae type 1, type 4, type 6, type 11, type 12, type 13, and type 14; subapical organite of Ant. IV) (Tables 4, 5). It would be expected that the number of chaetae should directly vary with the length of antennal segments, ranked as Ant. IV > II > III > I. This applies only to the overall result and to ordinary chaetae (Table 5) but not or only partly to S-chaetae. In particular, Ant. IV (a and b) is longer than other segments, but less rich in types of S-chaetae (Tables 4 and 5). Interestingly, however, the distal subsegment of antenna IV (Ant. IVb) possesses more kinds and a higher density of S- and ordinary chaetae than the proximal one (Ant. IVa), with a complex arrangement of type 11 S-chaetae (Figs 5A, B, 7A–B, 11H, 14A–C). Ant. II, though longer than Ant. I or Ant. III, has a similar or lower number of S-chaetae than Ant. I and III, but it bears more ordinary chaetae than the others (Tables 4, 5). Ant. I, the shortest segment, is proportionally the richest in diversity and number of S-chaetae (eight different types, Tables 4, 5), highlighting the importance of this segment for sensory reception. Ant. III, as common in Collembola, bears a complex sensorial structure (AIIIO) with typically five S-chaetae, conserved across most species of Collembola and widely used in taxonomy (Figs 4A–C, 11I). Antennae appears therefore as a mosaic of sensorial areas, with probably different sensorial functions which remain undocumented in Entomobryoidea.

It is rather common that Ant. II and III fuse together (Fig. 6A–C). It can be found asymmetrically in a single antenna or in both antennae, making the antenna(e) a little shorter (Deharveng and Gers 1993; Lukić et al. 2018), with a chaetotaxic pattern strongly modified. For example, in *T. kae* sp. nov., S-chaetae type 13 is found only in the specimens with fused Ant. II and III. Such fusing may be due to regeneration after the loss of antennal segments following predator attack as observed by Ernsting and Fokkema (1983) in *Orchesella*.

S-chaetae on antennal segments vary in number and probably type diversity, depending on size, age, and sex of Collembola, but this remains to be documented. They are also related to species ecology. Cave adapted species in particular are said to have more developed sensory structures than surface species (Deharveng 1988b; Thibaud and

Deharveng 1994; Lukić 2019). A group of subcylindrical S-chaetae (type 10) on antennal segments II and III is for instance present in three Mediterranean cave species of the genus (*T. ruffoi* in Delamare-Deboutteville 1951 and Fanciulli et al. 2003, and *T. absoloni* and *T. ildumensis* in Soto-Adames et al. 2014). This character, however, is unknown in other Mediterranean species. It is absent in the described Thai species, all of which are so far cave-restricted, where chaetae of type 10 never clusters, and are in significantly lower number (Figs 3C, D, 4A, B, 13A–F). The multiplication of type 10 S-chaetae cannot be therefore considered a troglomorphic character at the moment. This character has evolved in caves for Mediterranean lineages cannot be ruled out, but this could only be confirmed by examination of antennal morphology of surface species in the region, which has not been done so far. Nevertheless, antennal elongation observed in most cave *Troglopedetes* is associated to an increase of the number of antennal receptors.

Antennal chaetotaxic characters are widely used for the supraspecific taxonomy of Poduromorpha (Deharveng 1981), but much less in Entomobryoidea (Chen and Christiansen 1993; Deharveng and Bedos 1996; Lukić et al. 2015, 2018), due to their complexity. The diversity and pattern of antennal chaetae described in this work are intended serve as reference for further comparisons in this respect. The recognised chaetal types need to be homologised in morphology and distribution across more genera of Entomobryoidea, and limited data available in the literature or from personal observation already indicate that this is possible in many cases. Knowledge of antennal S-chaetae in Entomobryoidea may prove to be as taxonomically significant as it has been in Poduromorpha.

In a broader context, the complexity of chaetal types and distribution patterns described illustrate the functional complexity of arthropod antennae. Though information is lacking, chaetal pattern of distribution on antennae is probably mostly related to their function and the abiotic environment (light, soil, water, food) and interaction within communities. Antennal sensilla ultrastructure and functions in Collembola were studied by Altner's team in several papers (e.g., Altner and Kuhn 1989), but very few taxa and antennal sensilla have been examined, e.g., Waldorf (1976), Verhoef et al. (1977), Altner and Thies (1978), Slifer and Sekhon (1978). In a further step, the chaetal types we recognised here, useful for taxonomical purpose, will have to be assigned as far as possible to the categories used by morphologists (Zacharuk 1985), in order to gain insight into their functional organisation on the antenna.

Acknowledgements

We would like to thank Anne Bedos and two anonymous reviewers for many useful suggestions. We also thank Rueangrit Promdam, Areeruk Nilsai, and Kanchana Jantapaso for offering help in the field. This work is supported by Division of Biological Science, Faculty of Science, Prince of Songkla University, the National Science and Technology Development Agency (FDA-CO-2563-11031-TH), and the Thailand Research Fund (RSA6280063).

References

- Absolon K (1907) Zwei neue Collembolen-Gattungen. *Weiner Entomologischen Zeitung* 26: 335–343.
- Altner H, Kuhn KH (1989) The terminal antennal sensory complex of Collembola. In: Dallai R (Ed.) *Third International Seminar on Apterygota*, University of Siena, Italy, 199–206.
- Altner H, Thies G (1978) The multifunctional sensory complex in the antennae of *Allacma fusca* (Insecta). *Zoomorphologie* 91(2): 119–131. <https://doi.org/10.1007/BF00993856>
- Bellinger PE, Christiansen KA, Janssens F (1996–2020) Checklist of the Collembola of the world. <http://www.collembola.org> [6 October 2020]
- Chen JX, Christiansen KA (1993) The Genus *Sinella* with Special Reference to *Sinella* s.s. (Collembola: Entomobryidae) of China. *Oriental Insects* 27: 1–54. <https://doi.org/10.1080/0305316.1993.10432236>
- Christiansen K, Bellinger P (1996) Cave *Pseudosinella* and *Oncopodura* new to Science. *Journal of Caves and Karst Studies* 58: 38–53.
- Cipola NG, de Morais JW, Bellini BC (2016) A new epigeous species of *Troglobius* (Collembola: Paronellidae: Cyphoderinae) from Brazil and notes on the chaetotaxy of the genus. *Florida Entomologist* 99(4): 658–666. <https://doi.org/10.1653/024.099.0412>
- Deharveng L (1979) Chétotaxie sensillaire et phylogénèse chez les Collemboles Arthropleona. *Travaux du Laboratoire d'Ecobiologie des Arthropodes Edaphiques*. Toulouse 1(3): 1–15.
- Deharveng L (1981) La chétotaxie dorsale de l'antenne et son intérêt phylogénétique chez les Collemboles Neanuridae. *Nouvelle Revue d'Entomologie* 11(1): 3–13.
- Deharveng L (1983) Morphologie évolutive des Collemboles Neanurinae en particulier de la lignée Neanurienne. *Travaux du Laboratoire d'Ecobiologie des Arthropodes Edaphiques*, Toulouse 4: 1–63.
- Deharveng L (1987) Cave Collembola of South-East Asia. *The Korean Journal of Systematic Zoology* 3: 165–174.
- Deharveng L (1988a) A new troglomorphic Collembola from Thailand: *Troglopedetes fredstonei*, new species (Collembola: Paronellidae). *Bishop Museum occasional papers* 30: 279–287.
- Deharveng L (1988b) Collemboles cavernicoles VII- *Pseudosinella bessoni* n. sp. et note sur l'évolution morphologique de la griffe chez les *Pseudosinella*. *Revue Suisse de Zoologie* 95(1): 203–208. <https://doi.org/10.5962/bhl.part.79648>
- Deharveng L (1990) Fauna of Thai caves II. New Entomobryoidea Collembola from Chiang Dao cave, Thailand. *Bishop Museum occasional papers* 28: 95–98.
- Deharveng L, Bedos A (1996) *Rambutsinella*, a new genus of Entomobryidae (Insecta: Collembola) from Southeast Asia. *The Raffles Bulletin of Zoology* 44(1): 279–285.
- Deharveng L, Gers C (1993) Ten new species of *Troglopedetes* Absolon, 1907 from caves of Thailand (Collembola, Paronellidae). *Bijdragen tot de Dierkunde* 63: 103–113. <https://doi.org/10.1163/26660644-06302002>
- Deharveng L, Jantarit S, Bedos A (2018) Revisiting *Lepidonella* Yosii (Collembola: Paronellidae): character overview, checklist of world species and reassessment of *Pseudoparonella doveri* Carpenter. *Annales de la Société entomologique de France (N.S.)*, 54(5): 381–400. <https://doi.org/10.1080/00379271.2018.1507687>

- Delamare-Deboutteville C (1951) Collemboles cavernicole des Pouilles avec la description d'une espèce italienne du genre *Troglopedetes* Absolon. *Memorie di Biogeografia Adriatica* 2: 43–47.
- Ellis WN, Bellinger PF (1973) An annotated list of the generic names of Collembola (Insecta) and their type species. *Monografieën van de Nederlandse Entomologische Vereniging* 7: 1–74.
- Ernsting G, Fokkema DS (1983) Antennal damage and regeneration in springtails (Collembola) in relation to predation. *Netherlands Journal of Zoology* 33(4): 476–484. <https://doi.org/10.1163/002829683X00200>
- Fanciulli PP, Inguscio S, Rossi E, Dallai R (2003) Nuovi ritrovamenti di *Troglopedetes ruffoi* Delamare Deboutteville (Collembola, Paronellidae). *Thalassia Salentina* 26: 201–206.
- Fjellberg A (1999) The labial palp in Collembola. *Zoologischer Anzeiger* 237: 309–330.
- Gisin H (1967) Espèces nouvelles et lignées évolutives de *Pseudosinella* endogées (Collembola). *Memorias e Estudos do Museu Zoológico da Universidade de Coimbra* 30: 1–21.
- Jantarit S, Bedos A, Deharveng L (2016) An annotated checklist of the collembolan fauna of Thailand. *Zootaxa* 4169(2): 301–360. <https://doi.org/10.11646/zootaxa.4169.2.4>
- Jantarit S, Sangsiri T (2020) Two new species of *Alloscopus* from caves in Thailand, with a key to world species of the genus (Hexapoda: Collembola). *Raffles Bulletin of Zoology (Suppl.)* 35: 48–60.
- Jantarit S, Satasook C, Deharveng L (2013) The genus *Cyphoderopsis* (Collembola: Paronellidae) in Thailand and a faunal transition at the Isthmus of Kra in Troglopedetinae. *Zootaxa* 3721(1): 49–70. <https://doi.org/10.11646/zootaxa.3721.1.2>
- Jantarit S, Satasook C, Deharveng L (2014) *Cyphoderus* (Cyphoderidae) as a major component of collembolan cave fauna in Thailand, with description of two new species. *Zookeys* 368: 1–21. <https://doi.org/10.3897/zookeys.368.6393>
- Jordana R, Baquero E (2005) A proposal of characters for taxonomic identification of *Entomobrya* species (Collembola, Entomobryomorpha) with description of a new species. *Abhandlungen und Berichte Naturkundemuseums Goerlitz* 76: 117–134.
- Joseph G (1872) Beobachtungen über die Lebensweise und Vorkommen den in den Krainer Gebirgsgrotten einheimischen Arten der blinden Gattungen *Machaerites*, *Leptodirus*, *Oryotus* und *Troglorrhynchus*. *Jahres-Bericht der Schlesischen Gesellschaft für Vaterländische Cultur* 49: 171–182.
- Lukić M (2019) Collembola. In: White WB, Culver DC, Pipan T (Eds) *Encyclopedia of Caves*, (3rd edn.). Academic Press, Elsevier, 308–318. <https://doi.org/10.1016/B978-0-12-814124-3.00034-0>
- Lukić M, Porco D, Bedos A, Deharveng L (2015) The puzzling distribution of *Heteromurus (Verhoeffiella) absoloni* Kseneman, 1938 (Collembola: Entomobryidae: Heteromurinae) resolved: detailed redescription of the nominal species and description of a new species from Catalonia (Spain). *Zootaxa* 4039(2): 249–275. <https://doi.org/10.11646/zootaxa.4039.2.3>
- Lukić M, Delić T, Zagmajster M, Deharveng L (2018) Setting a morphological framework for the genus *Verhoeffiella* (Collembola, Entomobryidae) for describing new troglomorphic species from the Dinaric karst (Western Balkans). *Invertebrate Systematics* 32: 1118–1170. <https://doi.org/10.1071/IS17088>
- Mitra SK (1973) Observations on the postembryonic morphological differentiations including chaetotaxy in *Callyntura (Handschinphysa) lineata* (Parona 1892) (Collembola: Entomobryidae: Paronellinae). *Zoologischer Anzeiger* 191(3/4): 209–218.

- Mitra SK (1992) Fixation of the concept of *Paronella* Schött, 1893 (Collembola; Entomobryidae). Records of the Zoological Survey of India 92(1–4): 211–224.
- Mitra SK (1993) Chaetotaxy, phylogeny and biogeography of Paronellinae (Collembola: Entomobryidae). Records of the Zoological survey of India, Occasional paper 154: 1–100.
- Schött H (1893) Beiträge zur Kenntniss der Insektenfauna von Kamerun. I. Collembola. Bi-hang till Kongliga Svenska Vetenskaps-akademiens Handlingar 19(2): 1–28.
- Slifer EH, Sekhon SS (1978) Sense organs on the antennae of two species of Collembola (Insecta). Journal of Morphology 157(1): 1–19. <https://doi.org/10.1002/jmor.1051570102>
- Soto-Adames FN (2015) The dorsal chaetotaxy of first instar *Trogolaphysa jataca*, with description of twelve new species of Neotropical *Trogolaphysa* (Hexapoda: Collembola: Paronellidae). Zootaxa 4032(1): 1–41. <https://doi.org/10.11646/zootaxa.4032.1.1>
- Soto-Adames FN (2016) Chaetotaxy of first-instar *Campylothorax sabanus* (Wray), and description of three new *Campylothorax* species from Hispaniola (Collembola, Paronellidae). Journal of Natural History 50: 1583–1612. <https://doi.org/10.1080/00222933.2016.1145272>
- Soto-Adames FN, Bellini BC (2015) Dorsal chaetotaxy of neotropical species supports a basal position for the genus *Lepidonella* among scaled Paronellidae (Collembola, Entomobryoidea). Florida Entomologist 98(1): 330–341. <https://doi.org/10.1653/024.098.0152>
- Soto-Adames FN, Taylor SJ (2013) The dorsal chaetotaxy of *Trogolaphysa* (Collembola, Paronellidae), with descriptions of two new species from caves in Belize. Zookeys 13(323): 35–74. <https://doi.org/10.3897/zookeys.323.4950>
- Soto-Adames FN, Barra J-A, Christiansen K, Jordana R (2008) Suprageneric classification of Collembola Entomobryomorpha. Annals of the Entomological Society of America 101(3): 501–513. [https://doi.org/10.1603/0013-8746\(2008\)101\[501:SCOCE\]2.0.CO;2](https://doi.org/10.1603/0013-8746(2008)101[501:SCOCE]2.0.CO;2)
- Szeptycki A (1979) Chaetotaxy of the Entomobryidae and its phylogenetical significance. Morpho-systematic studies on Collembola. IV. Polska Akademia Nauk, Zakład Zoologii Systematycznej i Doświadczalnej, Państwowe Wydawnictwo Naukowe, Warszawa-Kraków, 219 pp.
- Thibaud JM, Deharveng L (1994) Collembola. In: Juberthie C, Decu V (Eds) Encyclopaedia Biospeologica (Vol. 1). Société de Biospéologie, Moulis, Bucarest, 267–276.
- Verhoef HA, Nagelkerke CJ, Joosse ENG (1977) Aggregation pheromones in Collembola. Journal of Insect Physiology 23(8): 1009–1013. [https://doi.org/10.1016/0022-1910\(77\)90128-7](https://doi.org/10.1016/0022-1910(77)90128-7)
- Waldorf ES (1976) Antennal Amputations in *Sinella curviseta* (Collembola: Entomobryidae). Annals of the Entomological Society of America 69(5): 841–842. <https://doi.org/10.1093/aesa/69.5.841>
- Yoshii R (1989) On some Collembola of New Caledonia, with notes on the “colour pattern species”. Contributions of the Biological Laboratory of Kyoto University 27(3): 233–259.
- Zacharuk RY (1985) Antennae and sensilla. In: Kerkut GA, Gilbert LY (Eds) Comprehensive insect physiology, biochemistry and pharmacology. Oxford, Pergamon Press, 69 pp.
- Zhang F, Deharveng L (2014) Systematic revision of Entomobryidae (Collembola) by integrating molecular and new morphological evidence. Zoologica Scripta 44(3): 298–311. <https://doi.org/10.1111/zsc.12100>
- Zhang F, Yu D, Guoliang X (2011) Transformational homology of the tergal setae during postembryonic development in the *Sinella-Coecobrya* group (Collembola: Entomobryidae). Contributions to Zoology 80(4): 213–230. <https://doi.org/10.1163/18759866-08004001>

On some new species of Stenheiliinae Brady, 1880 (Copepoda, Harpacticoida, Miraciidae) from north-western Mexico, with the proposal of *Lonchoeidenstenhelia* gen. nov.

Samuel Gómez^{1,2}

¹ Instituto de Ciencias del Mar y Limnología, Unidad Académica Mazatlán, Universidad Nacional Autónoma de México, Joel Montes Camarena s/n, Fracc. Playa Sur, Mazatlán, 82040, Sinaloa, Mexico

Corresponding author: Samuel Gómez (samuelgomez@ola.icmyl.unam.mx)

Academic editor: Kai H. George | Received 5 April 2020 | Accepted 8 September 2020 | Published 6 November 2020

<http://zoobank.org/D8C4A3A6-6A30-43E4-BF02-B74E7A670C96>

Citation: Gómez S (2020) On some new species of Stenheiliinae Brady, 1880 (Copepoda, Harpacticoida, Miraciidae) from north-western Mexico, with the proposal of *Lonchoeidenstenhelia* gen. nov.. ZooKeys 987: 41–79. <https://doi.org/10.3897/zookeys.987.52906>

Abstract

Quarterly sampling campaigns during 2019 to study the diversity of meiofauna in a polluted estuary in northwestern Mexico revealed the subfamily Stenheiliinae Brady, 1880 as one of the most important contributors to the diversity of benthic harpacticoids. Two new stenheiliin species are described here. One of them was assigned to the, so far, monotypic genus *Lonchoeidenstenhelia* **gen. nov.** defined by the autapomorphic modified proximal outer spinules on the sigmoid process of the male P2 ENP2. The other species was assigned to *Willenstenhelia* Karanovic and Kim, 2014. *Lonchoeidenstenhelia* **gen. nov.** shares the armature formula of the P1 EXP2 with *Stenhelia*, *Anisostenhelia*, and *Beatricella*, but seems to bear a sister-group relationship with the former two genera by the loss of one inner seta on the P2–P3 EXP3, the presence of two outer spine-like elements on the male P5 EXP, and the displacement of the outer spine and medial and inner distal setae of P2 ENP3, to an apical and subapical inner position, respectively, but is more closely related to *Anisostenhelia* by the overall shape of the male P2 ENP2. *Willenstenhelia reducta* **sp. nov.** is attributed to a group of species composed of *Wi. minuta*, *Wi. urania*, and *Wi. terpsichore* characterized by the strongly reduced inner seta of the female P5 baseopod, but differs in the discrete female P5 baseopods and in the presence of one outer seta only on that segment. *Willenstenhelia reducta* **sp. nov.** is defined here by the autapomorphic loss of the outermost seta of the female P5 baseopod.

Keywords

Diversity, new genus, new species, pollution, taxonomy, *Willenstenhelia*

Introduction

A series of quarterly sampling campaigns were carried out during 2019 in the frame of a short-term project financed by the Universidad Nacional Autónoma de México, aiming at assessing the present effects of organic pollution on the distribution and diversity of meiofauna in an estuary in northwestern Mexico. Preliminary analyses revealed the sub-family Stenheliinae Brady, 1880 (Miraciidae Dana, 1846) to be one of the most important contributors to the overall diversity and density of benthic harpacticoids. In addition to the new species presented here, *Pseudostenhelia wellsii* Coull and Fleeger, 1977 was also found, although its overall contribution to the diversity and density of harpacticoid copepods in the study area was far less important. Here I present the description of two new stenheliin species. One of them was assigned to a new genus, *Lonchoeidestenhelia* gen. nov. as *L. prote* sp. nov., defined here by the autapomorphic modified proximal outer spinules on the sigmoid process of the male P2 ENP2. Some comments on the relationships amongst *Stenhelia* Boeck, 1865, *Anisostenhelia* Mu and Huys, 2002, *Beatricella* Scott, 1905, and *Lonchoeidestenhelia* gen. nov. are given. The other species was assigned to *Willenstenhelia* Karanovic and Kim, 2014 as *Wi. reducta* sp. nov. Some comments on the relationships amongst the species of *Willenstenhelia* are given.

Materials and methods

Sediment samples were taken from a series of sampling stations along Urías system (Fig. 1), a polluted estuary in southern Sinaloa State (north-western Mexico), using an Eckman grab of 25×25 cm (sampling surface, 625 cm²). Triplicate sediment cores were taken at each station using acrylic corers of 5.6 cm ID (24.6 cm²) and 20 cm in length, from which the upper 3 cm layer was retrieved. Each sample was fixed in pure ethanol and sieved through 500 µm and 38 µm sieves to separate macro- and meiofauna. Meiofauna was extracted through centrifugation with Ludox® HS-40 following Burgess (2001) and Rohal et al. (2016) and preserved in pure ethanol. Meiofauna was sorted at a magnification of 40× using an Olympus SZX12 stereomicroscope equipped with DF PLAPO 1× objective and WHS10× eyepieces, and harpacticoid copepods were stored separately in 1-ml vials containing pure ethanol.

Illustrations and figures were made from whole individuals and their dissected parts using a Leica DMLB microscope equipped with L PLAN 10× eyepieces, N PLAN 100× oil immersion objective, and drawing tube. The dissected parts were mounted on separate slides using lactophenol as mounting medium.

Huys and Boxshall (1991) was followed for general terminology. Abbreviations used in the text:

acro	acrothek;	EXP	exopod;
ae	aesthetasc;	EXP/ENP1(2,3)	exopodal/endopodal
BENP	baseoendopod;		1 st (2 nd , 3 rd) segment;
ENP	endopod;	P1–P6	first to sixth legs.



Figure 1. Sampling locations in Urías estuary, Mazatlán, Sinaloa State, Mexico. Coordinates as follows: stn 1 (23.15194°N, 106.3128°W); stn 2 (23.1587°N, 106.3326°W); stn 3 (23.1735°N, 106.3504°W); stn 4 (23.1840°N, 106.3579°W); stn 5 (23.2056°N, 106.3715°W); stn 6 (23.2123°N, 106.3780°W); stn 7 (23.2174°N, 106.3917°W); stn 8 (23.2128°N, 106.4047°W); stn 9 (23.1904°N, 106.4121°W); stn 10 (23.1815°N, 106.4214°W). Map data 2020 Google.

Repositories

The type material was deposited in the Copepoda collection of the Instituto de Ciencias del Mar y Limnología, Unidad Académica Mazatlán (ICML–EMUCOP).

Taxonomy

Order Harpacticoida Sars, 1903

Family Miraciidae Dana, 1846

Subfamily Stenheliinae Brady, 1880

Genus *Lonchoeidenstehelia* gen. nov.

<http://zoobank.org/67AB6B9E-4DDA-45FB-A9E8-D68A716B750F>

Type and only species. *Lonchoeidenstehelia prote* sp. nov., by monotypy.

Diagnosis (based on its only species, *L. prote* sp. nov.). Stenheliinae. **Female:** Anal somite twice as long as broad; anal operculum rounded, with minute spinules along its posterior margin, with one sensillum on each side. Caudal rami cylindrical, twice as long as broad, and slightly longer than anal somite; with seven setae, of which seta I spine-like, setae IV and V with fracture plane, rat-tail-like. Rostrum trapezoidal, not fused to cephalothorax, bifid, with medial pore and two subdistal sensilla. Antennule

seven-segmented; all setae smooth except for one and two pinnate setae on first and second segments; second and third segments each with one seta with fracture plane; sixth and seventh segments each with two articulated setae; aesthetasc on segments 4 and 7. Antenna with allobasis; exopod three-segmented, armature formula 1,1,[1 lateral + 3 apical, two of which fused basally]. Mandible with elongate basis tapering distally; exopod arising from short pedestal, one-segmented, ca. 4× as long as wide, tapering distally, with three lateral and three apical slender setae; endopod recurved, twisted over exopod, with three lateral setae, and five distal elements (one short seta and long pinnate element fused basally and to endopod, one slender pinnate and one strong bare element, and one long element fused to endopod and with hyaline flange in middle part). Maxillule without modified elements on arthrite; basis with two endites, proximal endite with four, distal endite with three slender setae; exopod and endopod fused basally, separated from basis, one-segmented, endopod with four setae, exopod with two setae. Maxilliped subchelate; syncoxa with one bare and two spinulose strong elements; basis with two slender distal setae unequal in length; endopod one-segmented, slender, with one claw and one accompanying seta. Armature seta of P1–P4 as follows:

	P1	P2	P3	P4
EXP	0,0,022	1,1,123	1,1,223	1,1,323
ENP	1,1,111	1,2,121	1,1,221	1,1,221

P5 baseoendopod transversely elongate, with five setae, all setae normal; exopod with six setae. **Male:** Habitus, anal somite, and caudal rami as in female. Sexual dimorphism expressed in A1, P2 ENP, P5, and P6. Antennule 10-segmented, haplocer; all segments smooth except for first and seventh segment with spinules; all setae smooth except for one and two pinnate setae on first and second segments, and one and two modified spine-like elements on seventh and eighth segments; aesthetasc on third, fifth, and tenth segments. P2 ENP2 transformed, proximal half globular, distal half triangular, without hyaline flange, with two inner (one proximal and one medial) small setae, one inner subdistal strong pinnate element, and one apical sigmoid pinnate process with proximal row of modified (lanceolate) outer spinules. Baseoendopods of both P5 fused medially, each endopodal lobe with two setae, of which the inner well-developed, the outer small; exopod small, discrete, with four elements, of which two outermost spine-like. P6 asymmetrical, only one leg functional, each leg with three normal setae.

Etymology. The genus name from the Greek *λονχοειδής*, *lonchoeidēs*, lanceolate, makes reference to the shape of the proximal spinules on the distal outer process of the male P2 ENP2. Gender feminine.

***Lonchoeidenbelia prote* sp. nov.**

<http://zoobank.org/D1A4C714-C914-40D5-B141-4CA9828E2BEE>

Figs 2–11

Specimens examined. One female holotype (ICML–EMUCOP-180119-01), one male allotype (ICML–EMUCOP-180119-02), and 14 paratypes (10 females and four

males) (ICML–EMUCOP-180119-03) preserved in alcohol, and two female (ICML–EMUCOP-180119-05, ICML–EMUCOP-180119-06) and one male (ICML–EMUCOP-180119-07) paratypes dissected and mounted onto 11, six and seven slides, respectively, all from the type locality; six paratypes (two females and four males) (ICML–EMUCOP-180119-04) from stn 1, preserved in alcohol; one female paratype partially dissected (ICML–EMUCOP-180119-08) (P1–P4 dissected and mounted onto one slide, the rest left intact and preserved in alcohol), and nine paratypes (eight females and one male) (ICML–EMUCOP-180119-09) from stn 10, preserved in alcohol; 18 Jan. 2019. S. Gómez leg.

Additional material examined. One intersexual individual partially dissected (ICML–EMUCOP-180119-10) (P1–P4 dissected and mounted onto one slide, the rest left intact and preserved in alcohol) from stn 4; 18 Jan. 2019. S. Gómez leg.

Differential diagnosis. Stenheliinae. Anal operculum present, with minute spinules along posterior margin. P1 EXP2 without inner armature. P2–P4 EXP1 with inner seta. Armature formula of P2 EXP3 and P3 EXP3, 123 and 223, respectively. Female P2 ENP3 with outer apical spinous process, with displacement of medial and inner apical setae to subapical inner margin, the latter setae normal, not swollen basally. Female P5 baseoendopod without modified setae. Male P2 ENP2 without hyaline flange; outer apical sigmoid, bipinnate, flagellate process with incomplete suture indicating original articulation with the supporting segment, with longitudinal row of modified lanceolate spinules proximally. Outer spine of the male P4 ENP3 normal, not sexually dimorphic. Male P5 EXP and baseoendopod not fused; exopod with two outermost elements modified into spines. Innermost seta of the male P6 normal.

Description. Female. Total body length measured from tip of rostrum to posterior margin of caudal rami ranging from 415 μm to 563 μm (mean, 491 μm ; n, 12; total body length of holotype, 563 μm); habitus pyriform, widest at posterior end of cephalothorax in dorsal view, tapering posteriad (Fig. 2A).

Prosome (Fig. 2A, B): Consisting of cephalothorax with fused first pedigerous somite, and second to fourth free pedigerous somites, the latter without expansions nor spinular ornamentation; posterior hyaline frill of cephalothorax and pedigerous somites plain, of fourth pedigerous somite visibly narrower; integument smooth, weakly sclerotized.

Urosome (Figs 2A, B, 3A–C): Consisting of fifth pedigerous somite (first urosomite), genital double-somite (genital (second urosomite) and third urosomites fused), two free urosomites, and anal somite; urosomites without expansions laterally nor dorsally; integument weakly sclerotized.

First urosomite (fifth pedigerous somite): Visibly narrower than preceding somites in dorsal view (Fig. 2A), without spinular ornamentation, with dorsolateral sensilla as shown (Fig. 2A, C).

Genital double-somite: Slightly wider than long, widest at proximal half; with dorsolateral internal rib marking original division between second (genital) and third urosomite (Figs 2A, C, 3A, B), completely fused dorsally (Figs 2A, 3A) and ventrally (Fig. 3C); proximal half (genital somite) without spinular ornamentation, with poste-

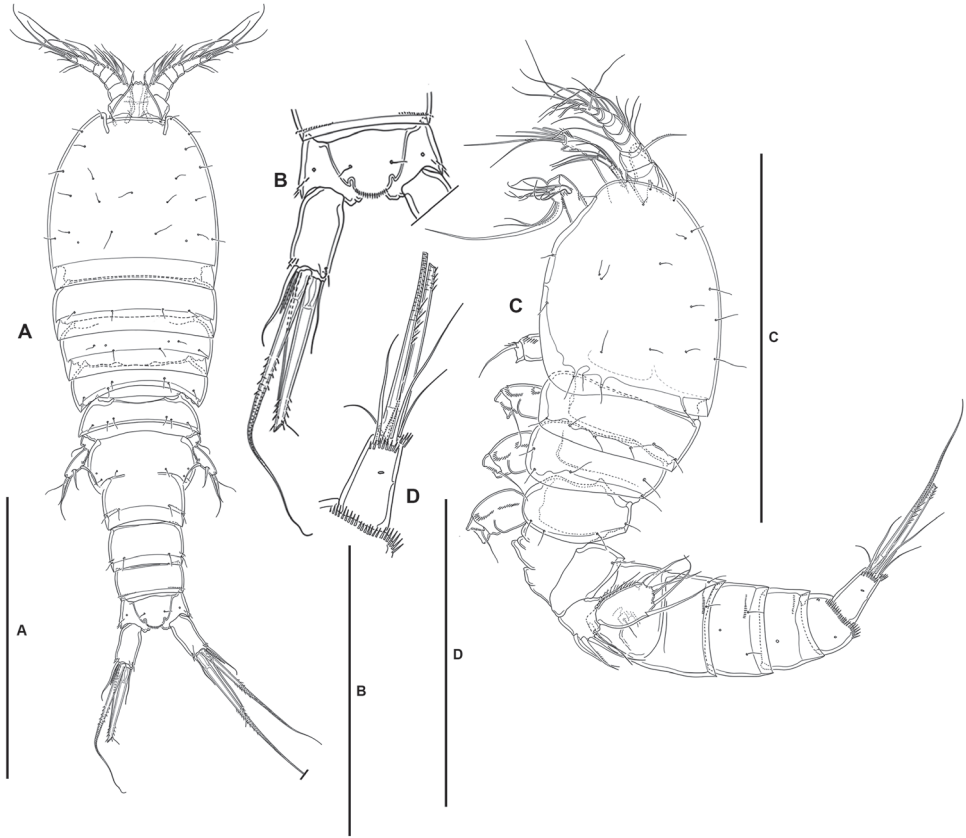


Figure 2. *Lonchoidestenhelia prote* gen. et sp. nov., female **A** habitus, dorsal **B** anal somite and left caudal ramus, dorsal **C** habitus, lateral **D** left caudal ramus, lateral. Scale bars: 200 μ m (**A, C**); 100 μ m (**B, D**).

rior sensilla as depicted; distal half (third urosomite) with short transverse row of small dorsolateral spinules (Figs 2A, 3A), with sensilla as shown.

Fourth urosomite: With spinular ornamentation (Fig. 3A–C) as in distal half of genital double-somite, with sensilla as shown.

Fifth urosomite: With spinular ornamentation (Fig. 3A–C) as in distal half of genital double-somite, without sensilla.

Anal somite (Figs 2A–C, 3A–C): Twice as long as broad, maximum breadth measured proximally; maximum length measured at the middle from anterior margin of somite to distal margin of anal operculum, with row of dorsolateral spinules close to joint with caudal rami, with one lateral pore on each side (Figs 2C, 3A, B); anal operculum rounded, with minute spinules along its posterior margin, with one sensillum on each side; ventrally cleft medially, with one pore on each side, with spinular row close to joint with caudal rami (Fig. 3C).

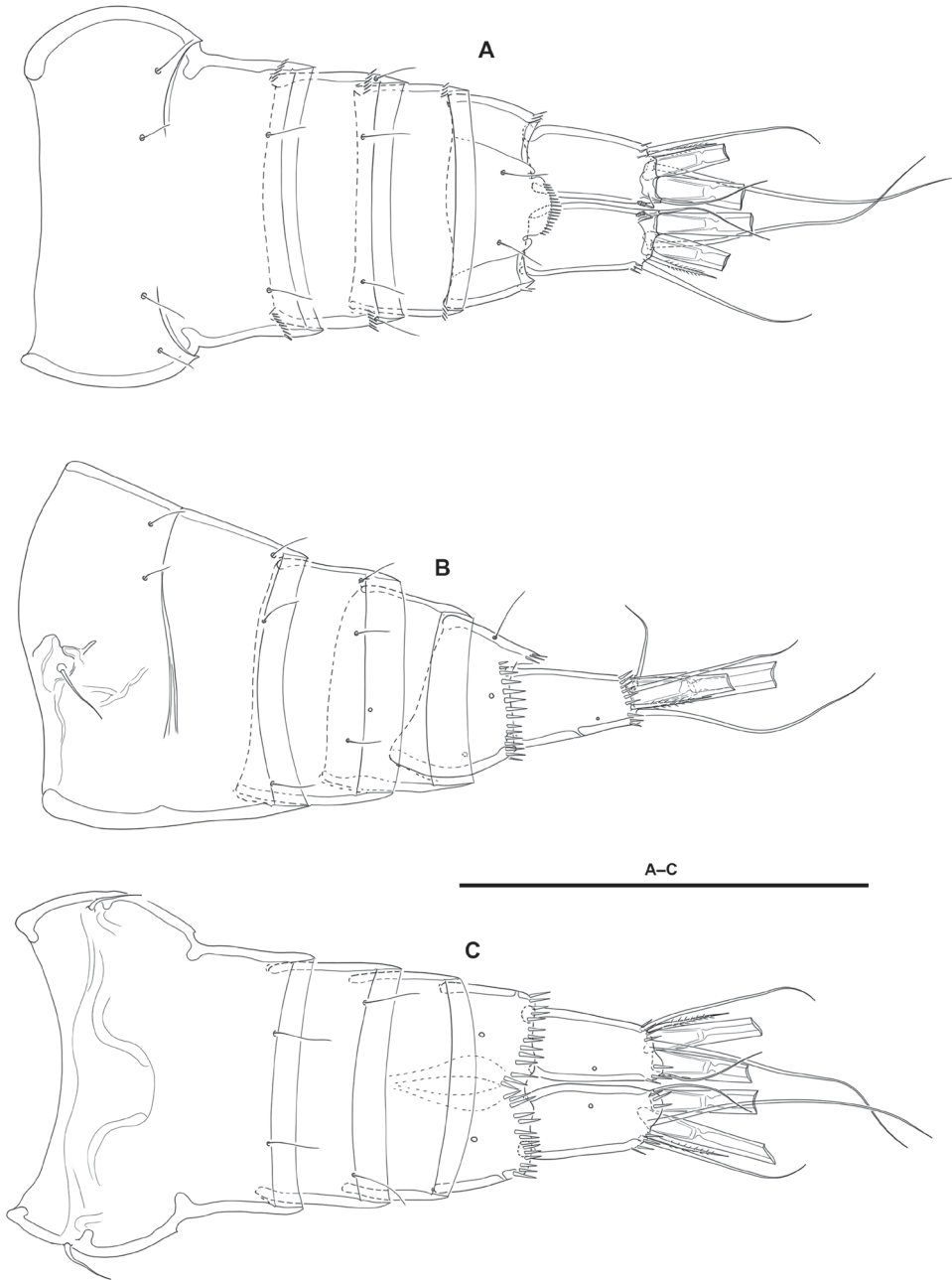


Figure 3. *Lonchoidestenhelia prote* gen. et sp. nov., female **A** urosome, dorsal (P5-bearing somite omitted) **B** urosome, lateral (P5-bearing somite omitted) **C** urosome, ventral (P5-bearing somite omitted). Scale bars: 100 μ m (**A-C**).

Caudal rami (Figs 2A–D, 3A–C): Typically divergent (Fig. 2A, B), but sometimes parallel (Fig. 3A, C), cylindrical, twice as long as broad, and slightly longer than anal somite; each ramus with one lateral (Fig. 2C, D) and one ventral pore (Fig. 3B, C); with spinules at base of setae I and II (Figs 2C, D, 3B), and ventrally close to insertion site of seta III (Fig. 3C); with seven elements as follows: seta I spine-like, ventral to seta II, the former visibly shorter, both arising subdistally on lateral margin; seta III ventral, subdistal, slightly longer than seta II; seta IV and V situated distally, with fracture plane, rat-tail-like; seta VI issuing at inner distal corner; dorsal seta VII triarticulate at base, situated subdistally close to inner margin.

Rostrum (Figs 2A, 4A): Trapezoidal, not fused to cephalothorax, reaching middle of second antennular segment, bifid, with medial pore and two subdistal sensilla.

Antennule (Fig. 4A): Seven-segmented; all segments smooth, except for first segment with spinular row. All setae smooth except for one and two pinnate setae on first and second segments, respectively; second and third segments each with one seta with fracture plane; sixth and seventh segments each with two articulated setae. Armature formula: 1(1); 2(11); 3(8); 4(5+(1+ae)), 5(3); 6(8); 7(4+acro). Acrothek consisting of two setae and one slender aesthetasc fused at their bases.

Antenna (Fig. 4B): Allobasis as long as free endopodal segment, inner margin with long spinules on proximal third, with one abexopodal seta arising midway inner margin. Exopod three-segmented, issuing proximally; first and third segments longest, each 3× as long as wide, second segment shortest, ca. 1.5× as long as broad; first and second segments with one subdistal pinnate seta each, first segment with spinular row as shown, second segment unornamented; third segment with one lateral proximal pinnate element, and three distal setae, of which two fused basally, with spinular row as depicted. Free endopodal segment elongate, inner margin with spinular row proximally, subdistally with curved row of strong spinules, with medial and subdistal outer fringes; armature consisting of two lateral spines and two accompanying setae, one non-geniculate inner distal element, three distal geniculate spines (of which innermost shortest) and one slender seta, and one outer distal geniculate seta fused basally to slender element.

Mandible (Fig. 5A): With relatively short coxa. Gnathobasis wide; with two strong bicuspidate teeth, several smaller bicuspidate teeth, some spinules, and one lanceolate element accompanied by seta. Basis elongate, tapering distally; with transverse spinular rows as shown; with three subdistal setae. Exopod arising from short pedestal, one-segmented, elongate, ca. 4× as long as wide, tapering distally; with three lateral and three apical slender setae, none of which fused basally. Endopod recurved, twisted over exopod; with three lateral setae, and five distal elements (one short seta and long pinnate element fused basally and to endopod, indicated with an asterisk in Fig. 5A, one slender pinnate and one strong bare element, and one long element fused to endopod and with hyaline flange in middle part, indicated with an asterisk in Fig. 5A).

Maxillule (Fig. 5B): Arthrite of praecoxa with two surface setae and seven bare distal elements (one of which a slender seta arising next to ventralmost spine), one spinulose dorsal spine, and one lateral spinulose recurved seta. Coxal endite with three setae. Basis with two endites; proximal endite with four, distal endite with three slender

setae. Exopod and endopod fused basally, separated from basis, one-segmented; endopod larger than exopod, with four setae; exopod small, with two setae.

Maxilla (Fig. 6A): With large syncoxa with outer spinules as shown; with three endites; proximal endite smallest, with one proximal and two distal setae; middle and distal endites elongate, the latter slightly longer, with three elements each as figured. Basis drawn out into strong claw, additionally with strong spine and two slender setae, one of which arising from elongate setophore. Endopod one-segmented, $2\times$ as long as wide, with six slender setae.

Maxilliped (Fig. 6B): Subchelate. Syncoxa rectangular, ca. $1.5\times$ as long as wide, outer margin irregular and with medial protrusion; with spinules as shown; with one bare and two spinulose strong elements, of which the bare seta and one spinulose element subdistal and both at the same level, the other arising distally from long pedestal. Basis shorter than syncoxa, oval; with inner and outer spinules as depicted, and two slender distal setae, one of which visibly shorter. Endopod one-segmented, slender, with one claw-like element and one seta.

P1 (Fig. 7A): Intercoxal sclerite narrow and elongate, without surface ornamentation. Praecoxa large, triangular, unornamented. Coxa quadrate, with spinular rows as shown. Basis with inner robust and strongly spinulose spine, and outer slender pinnate element; with strong spinules at the bases of inner and outer elements and between rami, and with long slender inner spinules. Exopod three-segmented, reaching tip of first endopodal segment, situated at a lower level than ENP; first segment longest, third segment shortest; all segments without outer nor inner distal processes; with spinular ornamentation as shown; first and second segments without inner seta, third segment with four elements. Endopod three-segmented, situated distally on medial circular outgrowth of basis and at a higher level than EXP; ENP1:EXP length ratio 0.9, ENP1 ca. $1.4\times$ as long as ENP2 and ENP3 combined; ENP1 and ENP3 without, ENP2 with outer acute distal process; segments with spinular ornamentation as figured; ENP1 with pinnate inner seta arising subdistally; ENP2 with one slender inner seta; ENP3 with three elements (one slender inner seta, one apical pinnate element, and one apical outer spine).

P2 (Fig. 7B): Intercoxal sclerite not transversely elongate, trapezoidal, with strong pointed process on distal outer corners, without surface ornamentation. Praecoxa small, triangular, unornamented. Coxa massive, quadrate, with outer spinules proximally and subdistally, with subdistal spinules and one pore close to inner margin. Basis with outer setiform element and strong acute process between rami and on inner distal corner, the latter with slender spinules proximally. Exopod three-segmented, reaching slightly beyond ENP3; EXP1 and EXP2 with inner distal frill, with outer acute distal process, with spinular ornamentation as shown, and with one inner seta; EXP3 with processes as shown, with small outer spinules at base of proximal outer spine, with subdistal pore, with one inner and two apical setae, and three outer spines. Endopod three-segmented; segments with spinules as shown; ENP1 shortest, with subdistal inner pore, with inner and outer acute processes, the former slightly larger, with one slender short inner seta; ENP2 and ENP3 subequal in length, the former with outer

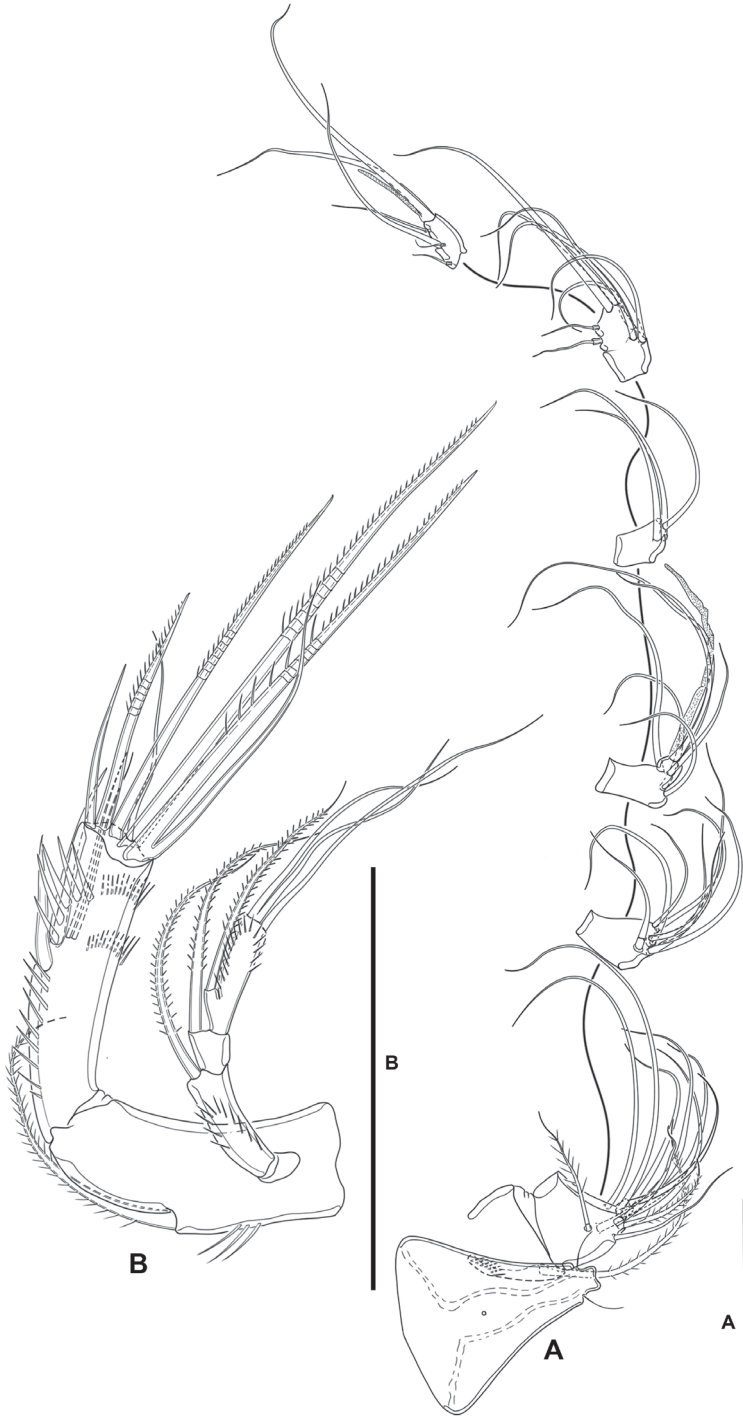


Figure 4. *Lonchoidestenhelia prote* gen. et sp. nov., female **A** rostrum and antennule **B** antenna. Scale bars: 50 μ m (**A**, **B**).

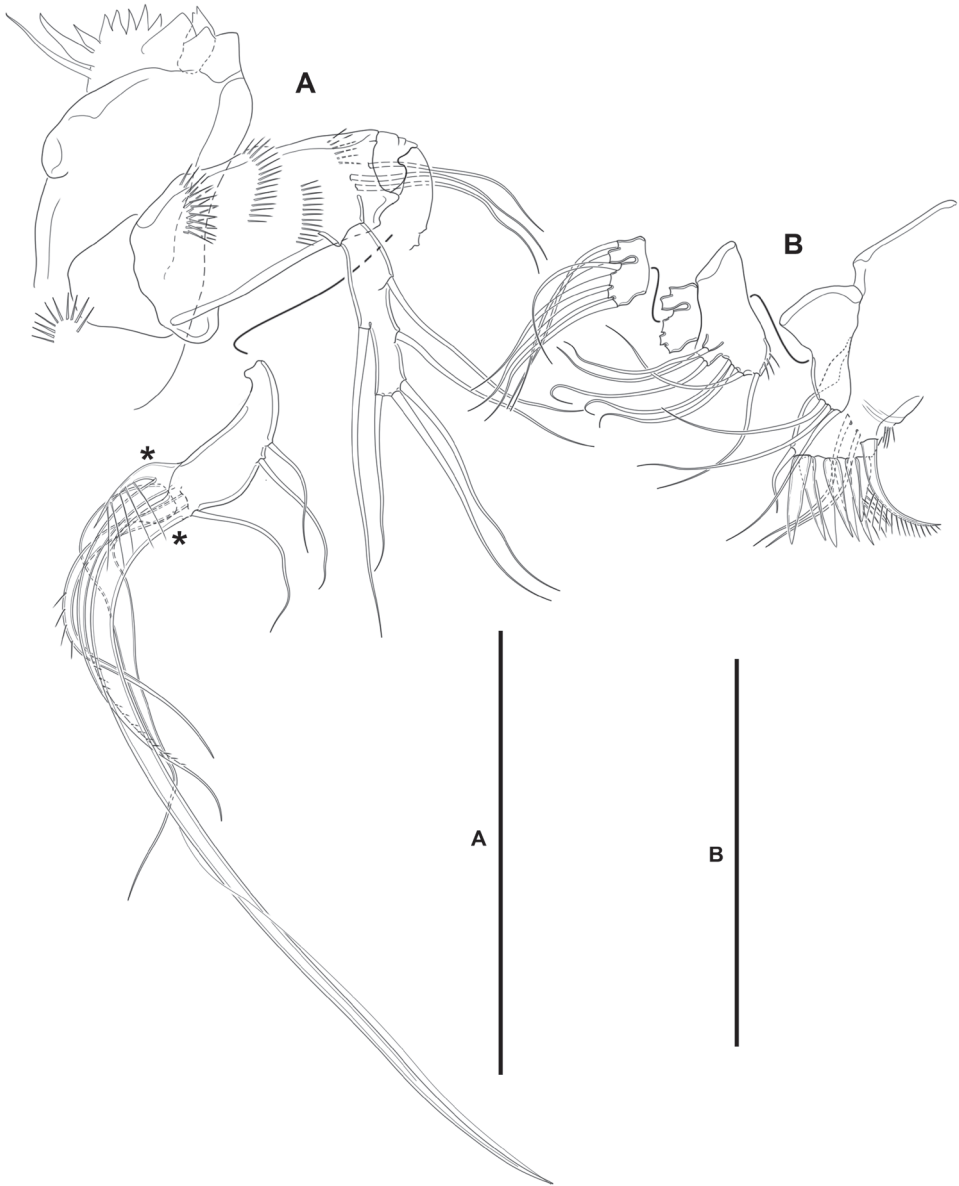


Figure 5. *Lonchoidestenhelia prote* gen. et sp. nov., female **A** mandible (asterisks indicate two elements fused basally and to ramus, and single element fused to ramus) **B** maxillule. Scale bars: 50 μm (**A**, **B**).

acute and small inner process, with two inner setae subequal in length; ENP3 with distal processes as shown, with subdistal inner pore, with one inner seta, two inner apical elements, and one outer distal spine.

P3 (Fig. 8A): Intercoxal sclerite not transversely elongate; trapezoidal; wider than in P2; with strong pointed process on distal outer corners; without surface ornamentation.

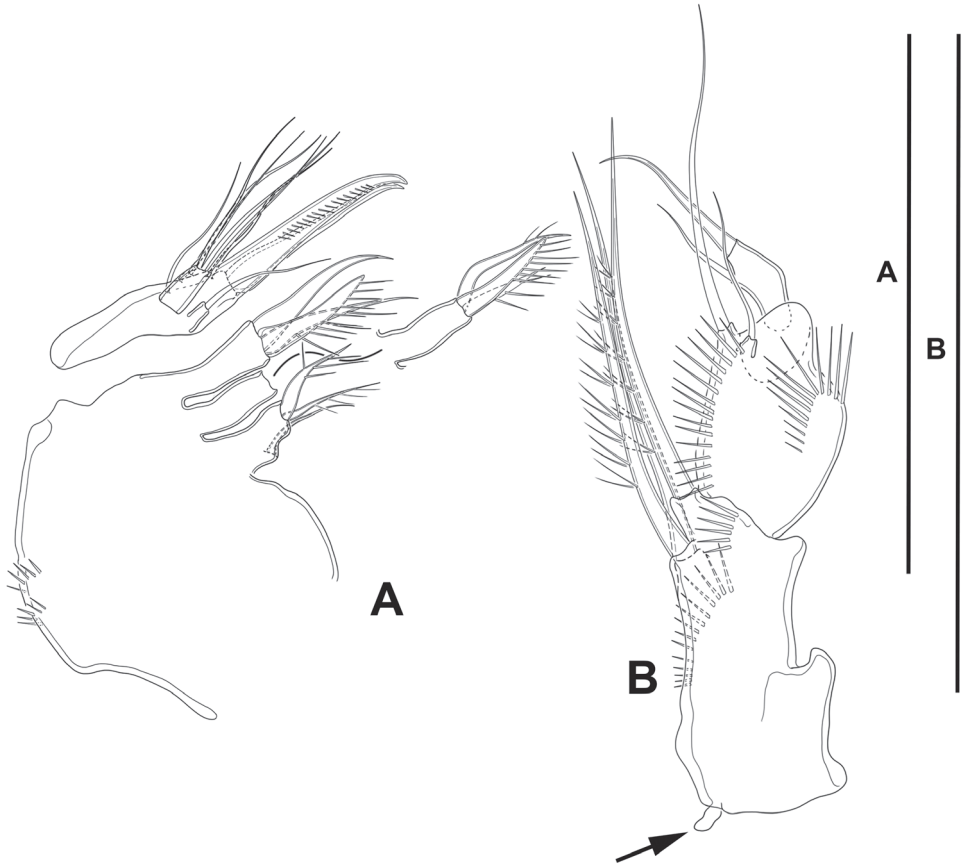


Figure 6. *Lonchoeidenstenhelia prote* gen. et sp. nov., female **A** maxilla **B** maxilliped (arrow indicates minute intercoxal sclerite). Scale bars: 50 μ m (**A**, **B**).

tation. Praecoxa triangular, small. Coxa as in P2 but without inner spinules. Basis as in P2, but with somewhat more slender outer seta. Exopod three-segmented, slightly longer than ENP; segments with spinules as shown; EXP1 and EXP2 with outer acute distal process, without pores, with inner distal frill, and with one inner seta each; EXP3 with outer subdistal pore, with two inner setae, two apical elements, and three outer spines. Endopod three-segmented; spinular ornamentation of segments as depicted; ENP1 shortest, ENP3 longest; ENP1 with small outer and inner distal processes, with inner seta; ENP2 with well-developed outer and small inner distal process, with inner pinnate seta; ENP3 with distal processes as shown, with subdistal outer pore, with two inner and two apical setae, and one outer apical spine.

P4 (Fig. 8B): Intercoxal sclerite not transversely elongate; trapezoidal; smaller than in P3; with strong pointed process on distal outer corners; without surface ornamentation. Praecoxa, coxa and basis as in P3 except for comparatively smaller inner distal process of basis. Exopod three-segmented, longer than ENP; spinular ornamentation

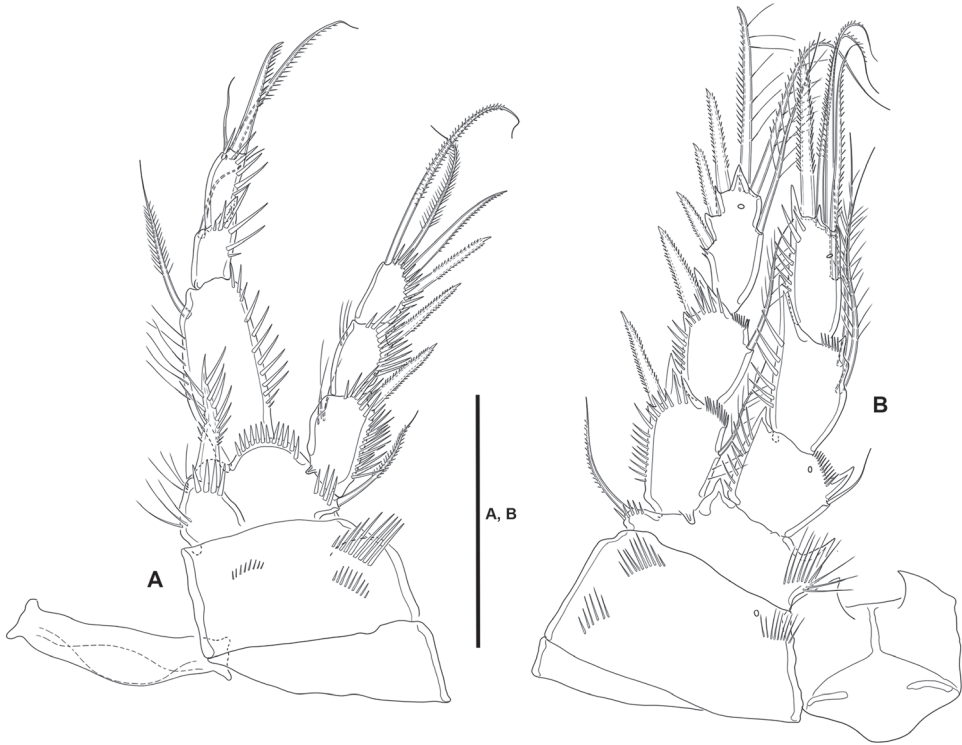


Figure 7. *Lonchoidstenbelia prote* gen. et sp. nov., female **A** P1, anterior **B** P2, anterior. Scale bars: 50 μ m (**A, B**).

of segments as shown; EXP1 and EXP2 with outer distal process less developed than in P3, without pores, with inner distal frill, and with inner seta; EXP3 with subdistal outer pore, with three inner setae of which medial visibly stronger, two apical elements, and three outer spines. Endopod three-segmented, reaching tip of EXP2; spinular ornamentation of segments as shown; ENP1 shortest, ENP3 longest; ENP1 with small outer distal process, without pore, with inner pinnate seta; ENP2 with well-developed outer distal process, armature as in previous segment; ENP3 with distal processes as shown, with subdistal inner pore, with two inner setae, two apical elements, and one outer apical spine.

Setal formula of swimming legs as follows:

	P1	P2	P3	P4
EXP	0,0,022	1,1,123	1,1,223	1,1,323
ENP	1,1,111	1,2,121	1,1,221	1,1,221

P5 (Fig. 8C): Baseopod transversely elongate; with five setae, of which outermost shortest and set close to adjoining element, all setae whip-like without any transformation. Exopod oval, with some outer proximal spinules, with six setae, of which fourth from outer to inner margin shortest.

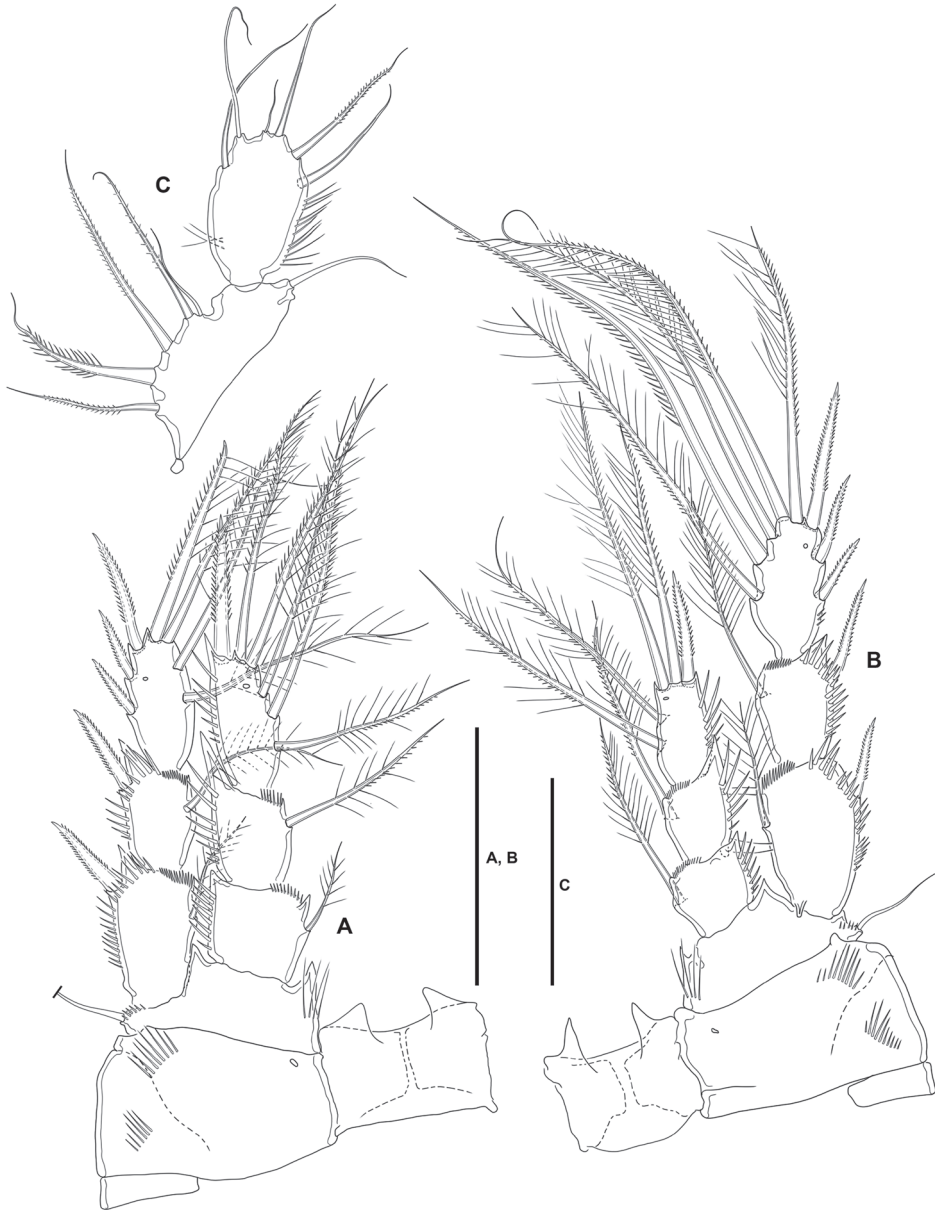


Figure 8. *Lonchoeidenstenhelia prote* gen. et sp. nov., female **A** P3, anterior **B** P4, anterior **C** P5, anterior. Scale bars: 50 μm (**A–C**).

P6 (Fig. 3B, C): Represented by a minute flap covering ventrolateral genital aperture, fused to somite, without surface ornamentation, with one slender seta.

Male. Total body length measured from tip of rostrum to posterior margin of caudal rami ranging from 289 μm to 460 μm (mean, 377 μm ; n, 7; total body length of allotype, 415 μm).

Prosome: As in female.

Urosome (Fig. 9A–C): Largely as in female except for genital somite and third urosomite separated, and for lateral and ventral spinular ornamentation.

Caudal rami (Fig. 9A–C): As in female.

Sexual dimorphism: Expressed in A1, P2 ENP, P5, and P6.

Antennule (Fig. 10A, B): 10-segmented, haplocer. All segments smooth except for first and seventh segment with spinules as shown. All setae smooth except for one and two pinnate setae on first and second segments, respectively, and one and two modified spine-like elements on seventh and eighth segments. Armature formula: 1(1); 2(11); 3(7+ae); 4(2), 5(5+(1+ae)); 6(1); 7(3); 8(3); 9(4); 10(4+acro). Acrothek consisting of two setae and one minute aesthetasc fused at their bases.

Antenna, mandible, maxillule, maxilla, and maxilliped: As in female.

P1: As in female.

P2: EXP (not shown) as in female. ENP (Fig. 10C) sexually dimorphic; basis, coxa and ENP1 largely as in female; ENP2 transformed, proximal half globular, distal half triangular, with inner notch indicating former division between ENP2 and ENP3, proximal half with inner long setules, distal half with subdistal pore, proximal half with two inner (one proximal and one medial) small setae, distal half with one inner subdistal strong pinnate element, and one apical sigmoid pinnate process with proximal row of outer spinules modified into lanceolate ornaments.

P3 and P4: As in female.

P5 (Figs 9B, C, 10D): Baseoendopods of both legs fused medially forming a continuous plate; each endopodal lobe with two setae, of which inner well-developed, outer small. Exopod small, discrete; with four elements, of which two outermost spine-like, third element from outer to inner margin shortest, innermost seta longest.

P6 (Fig. 9B, C, 10E): Asymmetrical, only one leg functional; each leg with three setae, of which medial longest, inner and outer elements subequal in length.

Variability. One intersexual specimen (ICML–EMUCOP–180119–10) possesses female antennules, displays genital double-somite (Fig. 11B), and lacks dimorphism in swimming legs, but the P5 (Fig. 11A, B) seems more of the male type with exopod bearing four elements (but two outer elements long and seta-like), and both baseoendopods fused medially and with two setae (outer small, inner long and pinnate), and the P6 possesses two setae.

Etymology. The specific epithet from the Greek *πρώτη*, *prôtē*, first, makes reference to the first species of *Lonchoidestenhelia* gen. nov. described so far. Gender feminine.

Type locality. Mexico, Sinaloa State: Urías estuary, stn 2, 23.1587°N, 106.3326°W, depth 1.8 m, organic carbon content 3.99%, organic matter content 6.86%, sand 80.42%, clay 8.29%, silt 11.28%.

Other localities. Mexico, Sinaloa State: Urías estuary, stn 1: 23.15194°N, 106.3128°W, depth 1.5 m, organic carbon content 3.74%, organic matter content 6.43%, sand 25.31%, clay 35.75%, silt 38.94%, stn 4: 23.1840°N, 106.3579°W, depth 0.7 m, organic carbon content 1.13%, organic matter content 1.94%, sand 82.44%, clay 8.27%, silt 9.29%, stn 7: 23.2174°N, 106.3917°W, depth 3.7 m, organ-

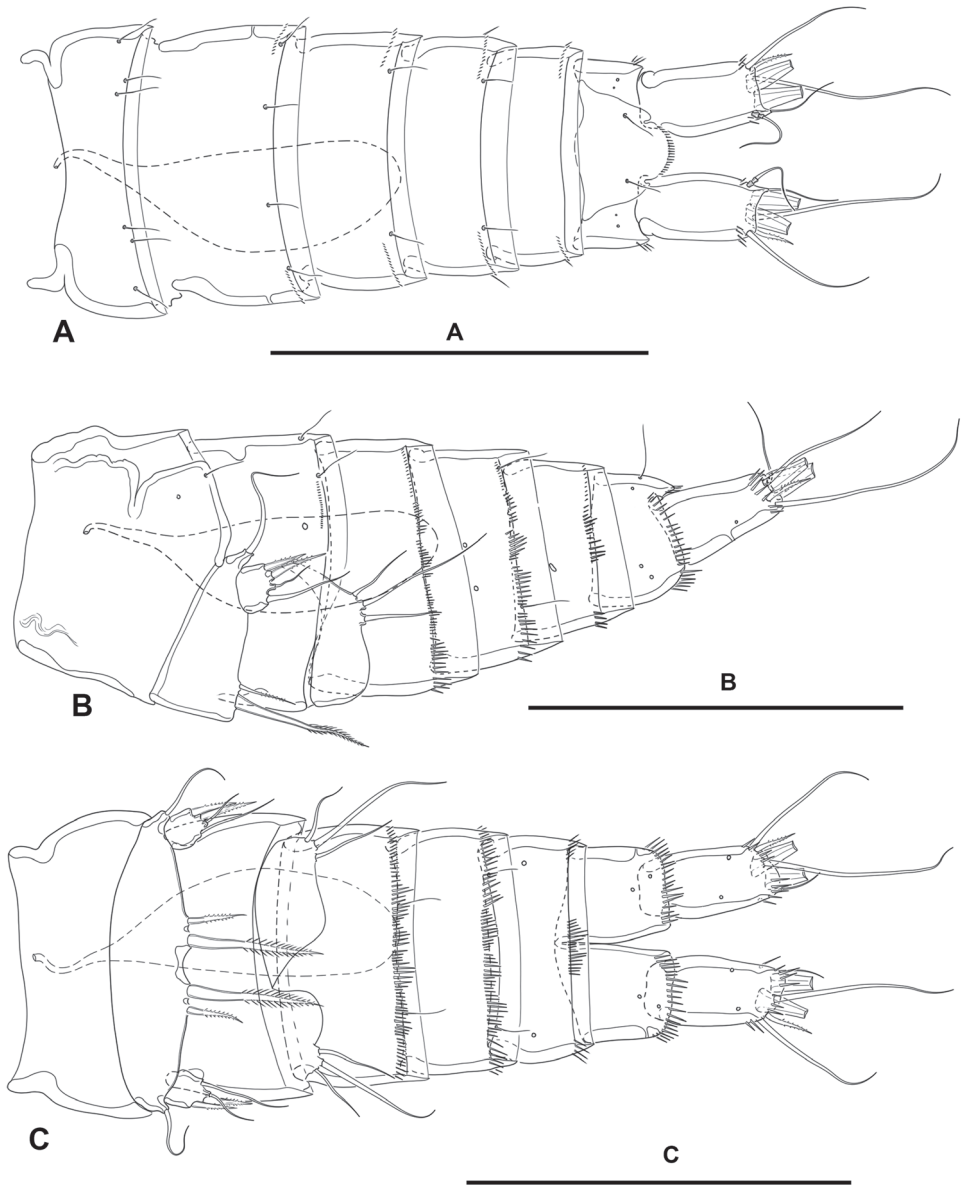


Figure 9. *Lonchoidestenbelia prote* gen. et sp. nov., male **A** urosome, dorsal **B** urosome, lateral **C** urosome, ventral. Scale bars: 100 μm (**A–C**).

ic carbon content 5.59%, organic matter content 9.62%, sand 10.78%, clay 37.54%, silt 51.68%, stn 9: 23.1904°N, 106.4121°W, depth 5.4 m, organic carbon content 1.41%, organic matter content 2.43%, sand 64.81%, clay 8.09%, silt 27.11%, and stn 10: 23.1815°N, 106.4214°W, depth 6.0 m, organic carbon content 1.2%, organic matter content 2.07%, sand 69.12%, clay 7.91%, silt 22.97%.

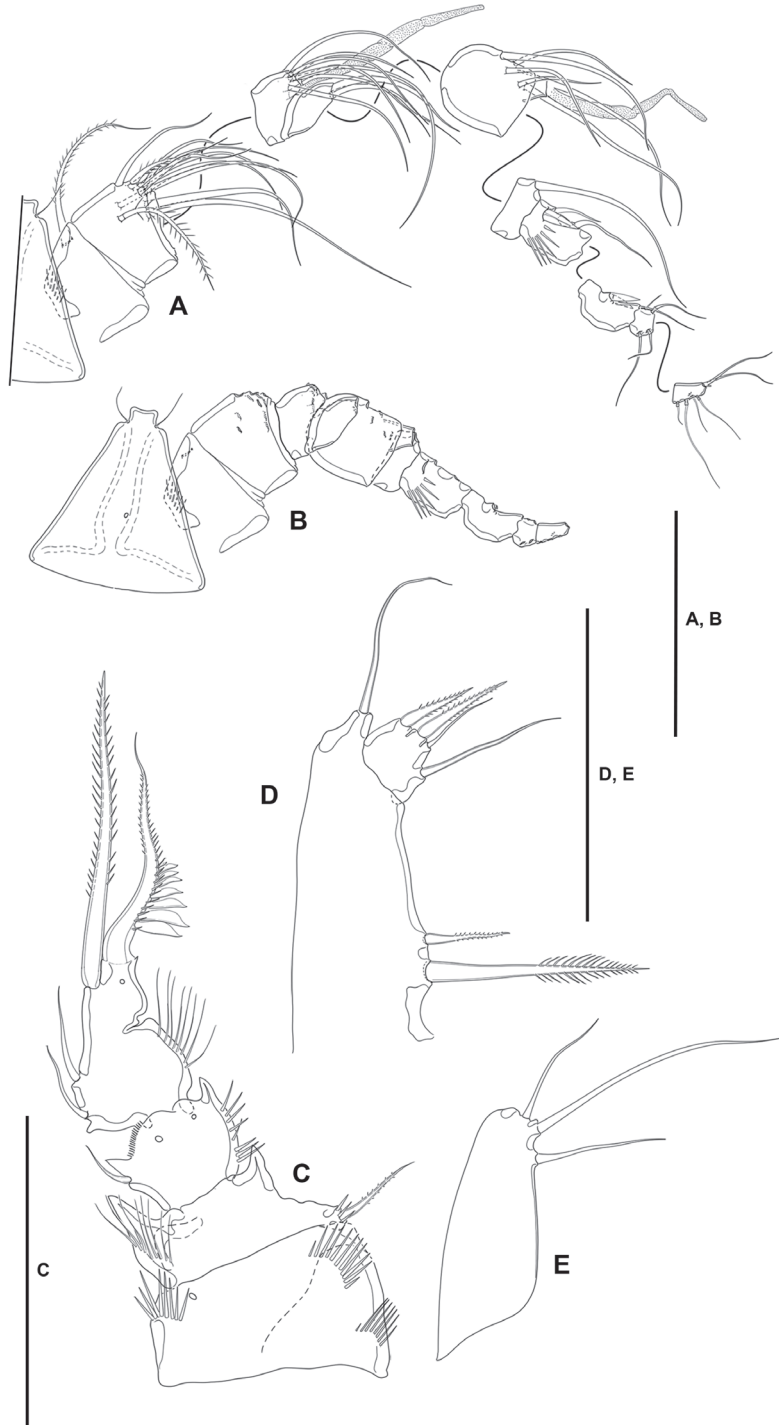


Figure 10. *Lonchoeidenstenhelia prote* gen. et sp. nov., male **A** rostrum antennule with armature **B** rostrum and antennule without armature **C** P2 ENP, anterior **D** P5, anterior **E** P6, anterior. Scale bars: 50 μ m (**A-E**).

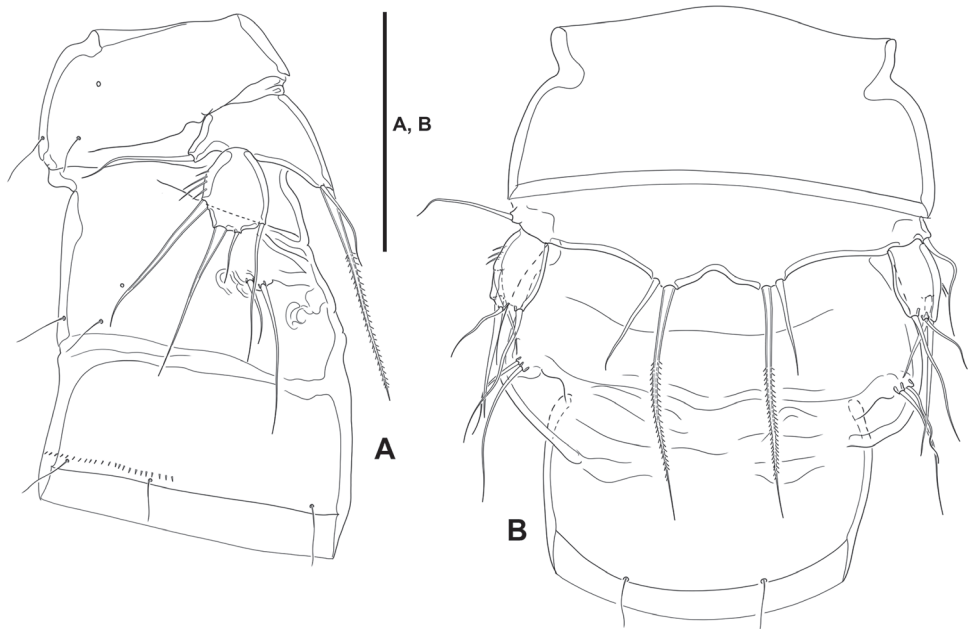


Figure 11. *Lonchoeidstenhelia prote* gen. et sp. nov., intersex individual **A** P5-bearing somite and double genital-somite, lateral **B** P5-bearing somite and double genital-somite, ventral. Scale bar: 50 μ m (**A**, **B**).

Genus *Willenstenhelia* Karanovic and Kim, 2014

Type species. *Willenstenhelia thalia* Karanovic and Kim, 2014, by original designation.

Other species. *Wi. minuta* (A. Scott, 1902) (= *D. minuta* A. Scott, 1902), *Wi. unisetosa* (Wells, 1967) (= *Stenhelia (Delavalia) unisetosa* Wells, 1967), *Wi. reducta* sp. nov., *Wi. urania* Karanovic and Kim, 2014, and *Wi. terpsichore* Karanovic and Kim, 2014.

Willenstenhelia reducta sp. nov.

<http://zoobank.org/F5070C00-3D05-4EE1-9E9B-310C1E6335E8>

Figs 12–21

Specimens examined. One female holotype (ICML–EMUCOP-180119-25) from the type locality and one male allotype (ICML–EMUCOP-180119-26) from stn 4; four (ICML–EMUCOP-180119-31) and one (ICML–EMUCOP-180119-32) female paratypes from the type locality; one female and one male paratype (ICML–EMUCOP-180119-33), one female paratype (ICML–EMUCOP-180119-34), and two female paratypes (ICML–EMUCOP-180119-35) from stn 4; one female and one male paratype (ICML–EMUCOP-180119-36), one female paratype (ICML–EMU-

COP-180119-37), and one CIV, one CV, one female and two male paratypes (ICML–EMUCOP-180119-38) from stn 9; one CIII, one CIV, and two female paratypes (ICML–EMUCOP-180119-39) from stn 10; all preserved in alcohol. Two dissected female paratypes (ICML–EMUCOP-180119-27, ICML–EMUCOP-180119-28) mounted onto eight and six slides, respectively, and one dissected male paratype (ICML–EMUCOP-180119-29) mounted onto three slides, all from stn 2; one dissected male paratype (ICML–EMUCOP-180119-30) from stn 4 mounted onto eight slides. 18 Jan. 2019. S. Gómez leg.

Differential diagnosis. Stenheliinae: *Willenstenhelia*. Female antennule eight-segmented. Armature formula of P4 EXP, 0,1,122. Female P5 baseoendopods not fused medially; endopodal lobe with two setae separated by wide gap, outer seta well-developed, inner seta minute; exopod with five setae, of which innermost as long as two outermost setae, middle seta smallest, inner neighboring seta longest. Male antennule ten-segmented. Male P5 EXP discrete, with four elements, of which apical a strong spine, two medial ones small and subequal in length, innermost smallest arising midway inner margin; baseoendopods fused medially forming a continuous plate, each endopodal lobe with one strong spine-like element fused to endopod, both elements set close to each other.

Description. Female. Total body length measured from tip of rostrum to posterior margin of caudal rami ranging from 445 μm to 510 μm (mean, 477 μm ; n, 3; total body length of holotype, 510 μm); habitus (Fig. 12A) pyriform, widest at posterior end of cephalothorax in dorsal view, tapering posteriad.

Prosome (Fig. 12A): Consisting of cephalothorax with fused first pedigerous somite, and second to fourth free pedigerous somites, the latter without expansions nor spinular ornamentation; posterior hyaline frill of cephalothorax and pedigerous somites plain, of fourth pedigerous somite visibly narrower; integument smooth, weakly sclerotized.

Urosome (Figs 12A, B, 13A, B): Consisting of fifth pedigerous somite (first urosomite), genital double-somite (genital second urosomite and third urosomite fused), two free urosomites, and anal somite; urosomites without expansions laterally nor dorsally; integument weakly sclerotized.

First urosomite (fifth pedigerous somite): Visibly narrower than preceding somites in dorsal view (Fig. 12A, B), without spinular ornamentation (Figs 12A, B, 13A, B).

Genital double-somite: Ca. 1.5 \times as wide as long, widest part at proximal half (Fig. 12A, B); separated dorsolaterally (Figs 12A, B, 13A), completely fused ventrally (Fig 13B); without spinular ornamentation, with posterior sensilla as depicted.

Fourth urosomite: With short spinular row and pore laterally on each side (Fig. 13A) and with sensilla as shown.

Fifth urosomite (Fig. 13A): Without sensilla; spinular ornamentation and pores as in previous somite.

Anal somite (Figs 12A, B, 13A, B): Twice as long as broad, maximum breadth measured at proximal margin; maximum length measured at the middle from anterior margin of somite to distal margin of anal operculum, with row of dorsolateral spinules

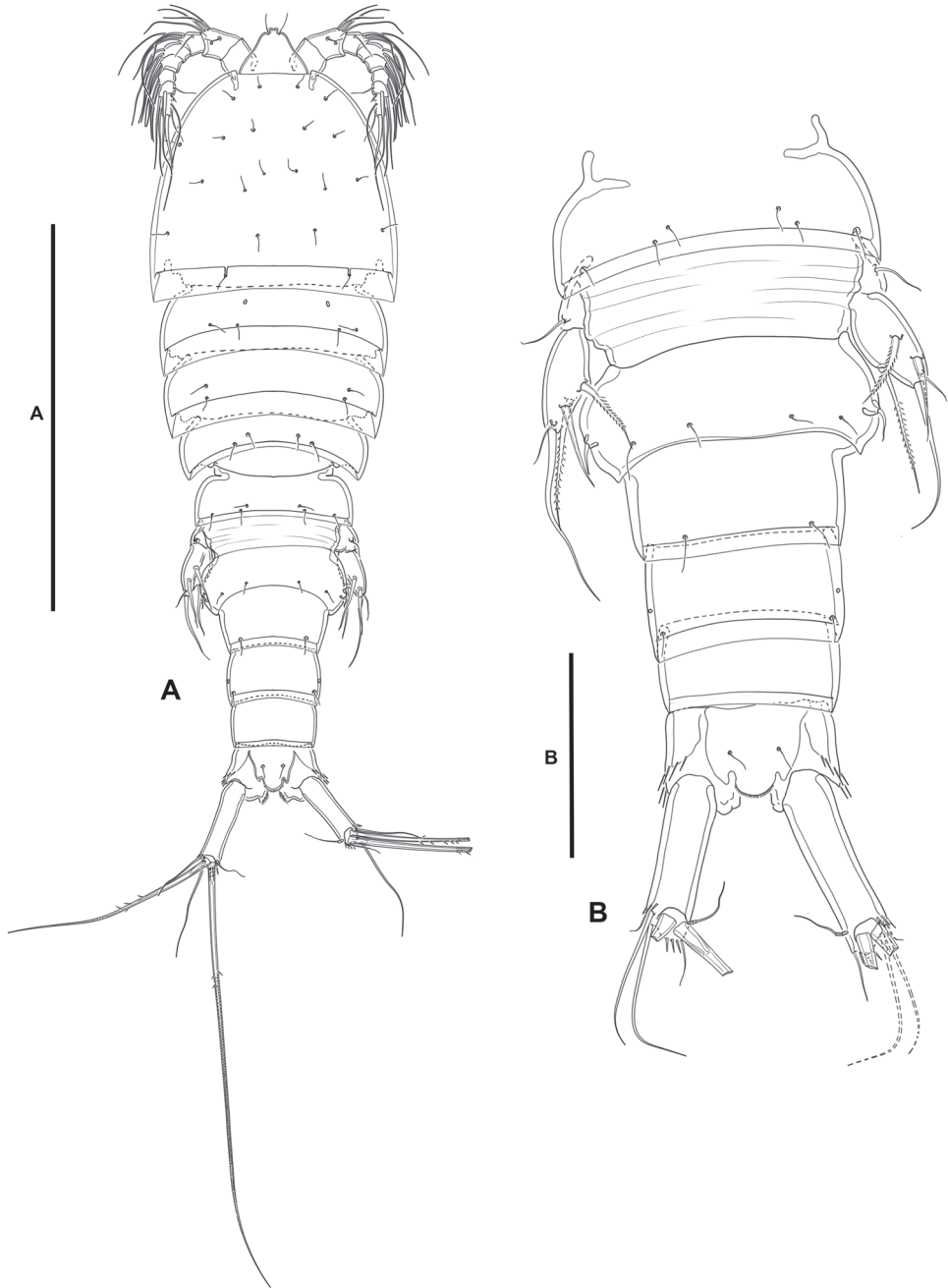


Figure 12. *Willenstenbelia reducta* sp. nov., female **A** habitus, dorsal **B** urosome, dorsal. Scale bars: 200 µm (**A**); 50 µm (**B**).

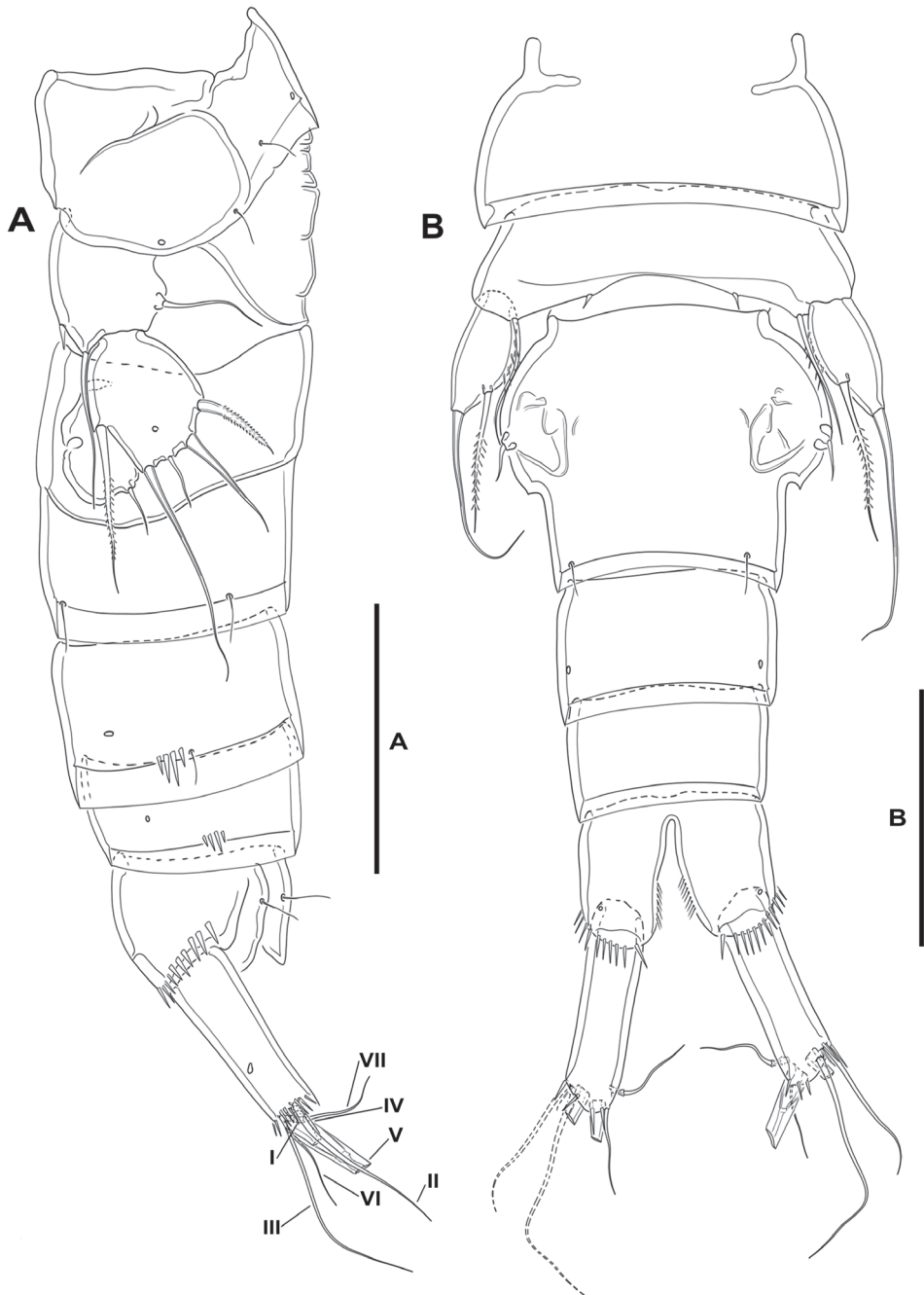


Figure 13. *Willenstenhelia reducta* sp. nov., female **A** urosome, lateral **B** urosome, ventral. Scale bars: 50 μ m (**A**, **B**).

close to joint with caudal rami (Figs 12A, B, 13A), ventrally cleft medially (Fig. 13B), with one subdistal pore on each side, with spinular row close to joint with caudal rami; anal operculum (Fig. 12A, B) rounded, with minute spinules along its posterior margin, with one sensilla on each side.

Caudal rami (Figs 12A, B, 13B): Typically divergent, cylindrical, ca. 2.7× as long as broad, and 1.4× as long as anal somite in dorsal view; each ramus with one subdistal lateral pore (Fig. 13A); with spinules at base of setae I and II (Figs 12B, 13A), and ventrally (Fig. 13B); with seven elements; seta I very small, often masked behind spinules, ventral to seta II, the latter long, both arising subdistally on lateral margin; seta III ventral, subdistal, longer than seta II; seta IV and V situated distally, with fracture plane; seta VI issuing at inner distal corner; dorsal seta VII tri-articulate at base, situated subdistally close to inner margin.

Rostrum (Fig. 12A): Trapezoidal, not fused to cephalothorax, reaching tip of first antennular segment, bifid at tip, without pore, with two subdistal sensilla.

Antennule (Fig. 14A, B): Eight-segmented; all segments smooth, except for first segment with spinular row. All setae seemingly smooth; second and third segments each with one seta with fracture plane; seventh and eighth segments with two articulated setae each. Armature formula: 1(1); 2(11); 3(8); 4(5+(1+ae)), 5(3); 6(4); 7(4); 8(3+(2 setae fused basally)). Eighth segment seemingly without aesthetasc.

Antenna (Fig. 14C): Coxa small, with some outer spinules. Allobasis as long as free endopodal segment, inner margin with some proximal spinules, with one (pinnate?) abexopodal seta arising midway on inner margin. Exopod three-segmented, issuing proximally; first and third segments longest, each 3× as long as wide, second segment shortest and ca. 1.5× as long as broad; first and second segments with one pinnate seta each, spinular ornamentation of first segment a single spinule, second segment unornamented; third segment with small spinules as shown, with one lateral pinnate element proximally, and three distal setae, of which two fused basally. Free endopodal segment elongate, inner margin with proximal row of small spinules, with medial and subdistal inner fringe; armature consisting of two lateral spines and two accompanying setae, one geniculate inner distal element, three geniculate distal spines (of which innermost shortest) and one slender seta, and one outer distal geniculate seta fused basally to pinnate element.

Mandible (Fig. 15A, B): With relatively short coxa. Gnathobasis wide; with two strong bicuspidate teeth, several smaller bicuspidate teeth, some spinules, and one strong lanceolate element accompanied by slender seta. Basis elongate, tapering distally, with transverse spinular rows as shown, with three subdistal setae. Exopod arising from short pedestal, one-segmented, elongate, ca. 3.5× as long as wide, tapering distally; with three lateral and three apical slender setae, none of which fused basally. Endopod recurved, twisted over exopod; with three lateral setae, and five distal elements (one smooth and one long pinnate element, two long setae fused basally and fused to endopod, and one long element fused to endopod and with hyaline flange in middle part).

Maxillule (Fig. 15C): Arthrite of praecoxa with two surface setae and seven bare distal elements (one of which a slender seta arising next to ventralmost spine), one

spinulose dorsal spine, and one lateral spinulose recurved seta. Coxal endite with three setae. Basis with two endites; proximal endite with four, distal endite with three slender setae. Exopod and endopod fused basally, and fused also to basis, each ramus one-segmented; endopod larger than exopod, with four setae; exopod small, with two setae.

Maxilla (Fig. 15D): Large syncoxa with outer spinules as shown; with three endites; proximal endite smallest, with one slender proximal and two strong distal setae; middle and distal endites elongate, the latter slightly longer, with three elements each as figured. Basis drawn out into strong claw, additionally with strong spine and two slender setae, one of which arising from elongate setophore. Endopod one-segmented, 2× as long as wide, with six slender setae.

Maxilliped (Fig. 15E): Non-prehensile. Syncoxa rectangular, ca. 2× as long as wide; with anterior and posterior spinules as shown; with two proximal elements arising from short pedestals, and one apical element arising from long pedestal. Basis shorter than syncoxa, oval; with inner and outer spinules as depicted, and two slender distal setae subequal in length. Endopod absorbed into basis, with two slender setae.

P1 (Fig. 16A): Intercoxal sclerite narrow and elongate, without surface ornamentation. Praecoxa triangular, unornamented. Coxa quadrate, with spinular rows as shown. Basis with inner robust and pinnate spine, and outer smaller pinnate spine, with strong spinules at the base of inner spine and between rami. Exopod three-segmented, as long as endopod; first and third segments longest, second segment shortest; all segments without outer nor inner acute distal processes; with spinular ornamentation as shown; first segment without, second segment with inner seta, third segment with four elements. Endopod two-segmented; ENP1 reaching slightly beyond EXP1, ca. 1.5× as long as wide, and 0.7× as long as ENP2, with outer and distal spinules as depicted; with one inner long seta; ENP2 longer than ENP1, with outer and distal spinules as shown, with one inner proximal, one inner subdistal, and two apical elements of which outermost a spine.

P2 (Fig. 16B): Intercoxal sclerite not transversely elongate, trapezoidal, with strong pointed process on distal outer corners, without surface ornamentation. Praecoxa triangular, unornamented. Coxa massive, quadrate, with outer spinules proximally and subdistally, with one pore close to inner distal margin. Basis with outer setiform element with small spinules at its base, and strong acute process between rami and on inner distal corner, the latter with slender spinules proximally. Exopod three-segmented, shorter than endopod, reaching middle of ENP3; spinular ornamentation of segments as shown; EXP1 and EXP2 with inner distal frill, with outer acute distal process, EXP1 without, EXP2 with medial pore and inner seta; EXP3 with processes as shown, with subdistal pore, with one inner and two apical setae, and three outer spines. Endopod three-segmented; ENP1 shortest, ENP2 and ENP3 subequal in length; spinular ornamentation of segments as shown; ENP1 and ENP2 with inner and outer acute processes, ENP1 with one, ENP2 with two inner seta; ENP3 with distal processes as shown, with medial pore, with one inner seta, two apical elements, and one outer distal spine.

P3 (Fig. 17A): Intercoxal sclerite not transversely elongate, trapezoidal, with strong pointed process on distal outer corners, without surface ornamentation. Coxa as in P2.

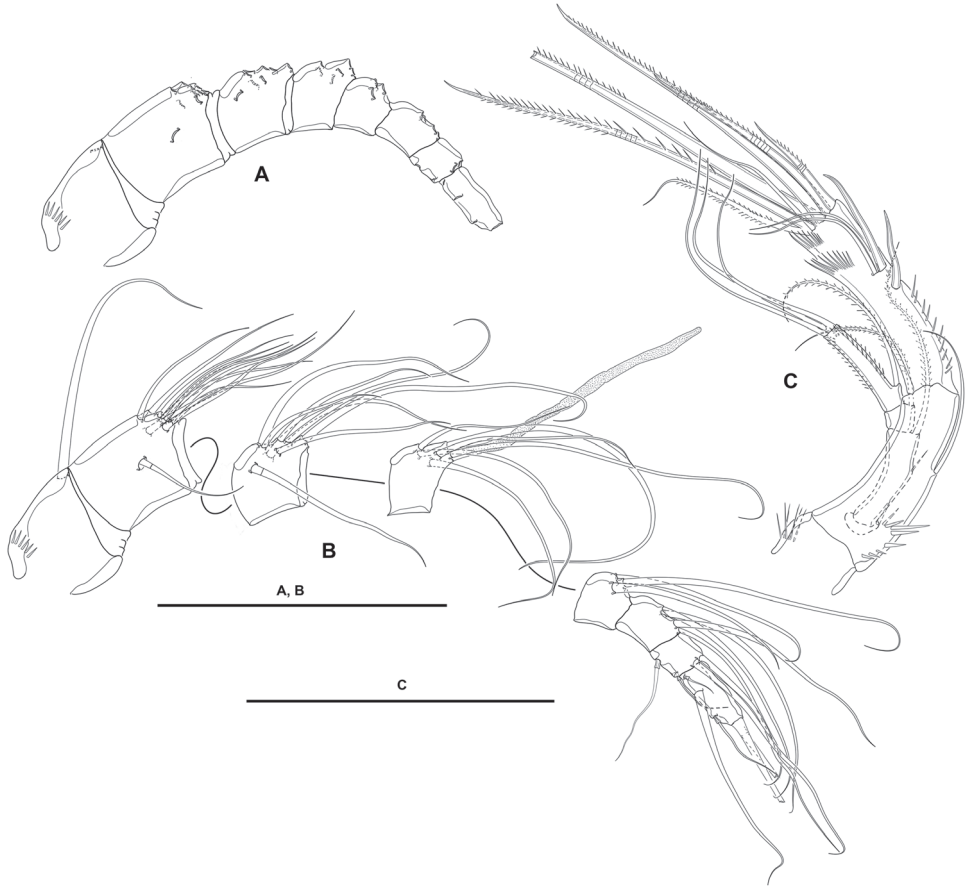


Figure 14. *Willenstenhelia reducta* sp. nov., female **A** antennule without armature **B** antennule with armature **C** antenna. Scale bars: 50 μ m (**A–C**).

Basis as in P2, but with somewhat more slender outer seta. Exopod three-segmented, as long as ENP; spinular ornamentation of segments as shown; EXP1 and EXP2 with outer acute distal process, without pores, with inner distal frill, EXP1 without, EXP2 with inner seta; EXP3 with subdistal pore, with two inner setae of which the distal is visibly stronger, two apical elements, and three outer spines. Endopod three-segmented; ENP1 shortest, ENP3 longest; spinular ornamentation of segments as shown; ENP1 with small outer and inner distal processes, with inner seta; ENP2 with well-developed outer and small inner distal process, with inner seta; ENP3 with distal processes as shown, with subdistal pore, with one inner and two apical setae, and one outer apical spine.

P4 (Fig. 17B): Intercoxal sclerite not transversely elongate, trapezoidal, with strong pointed process on distal outer corners; without surface ornamentation. Praecoxa triangular, unornamented; coxa and basis as in P3 except for comparatively smaller inner distal process of basis. Exopod three-segmented, longer than ENP; spinular ornamentation

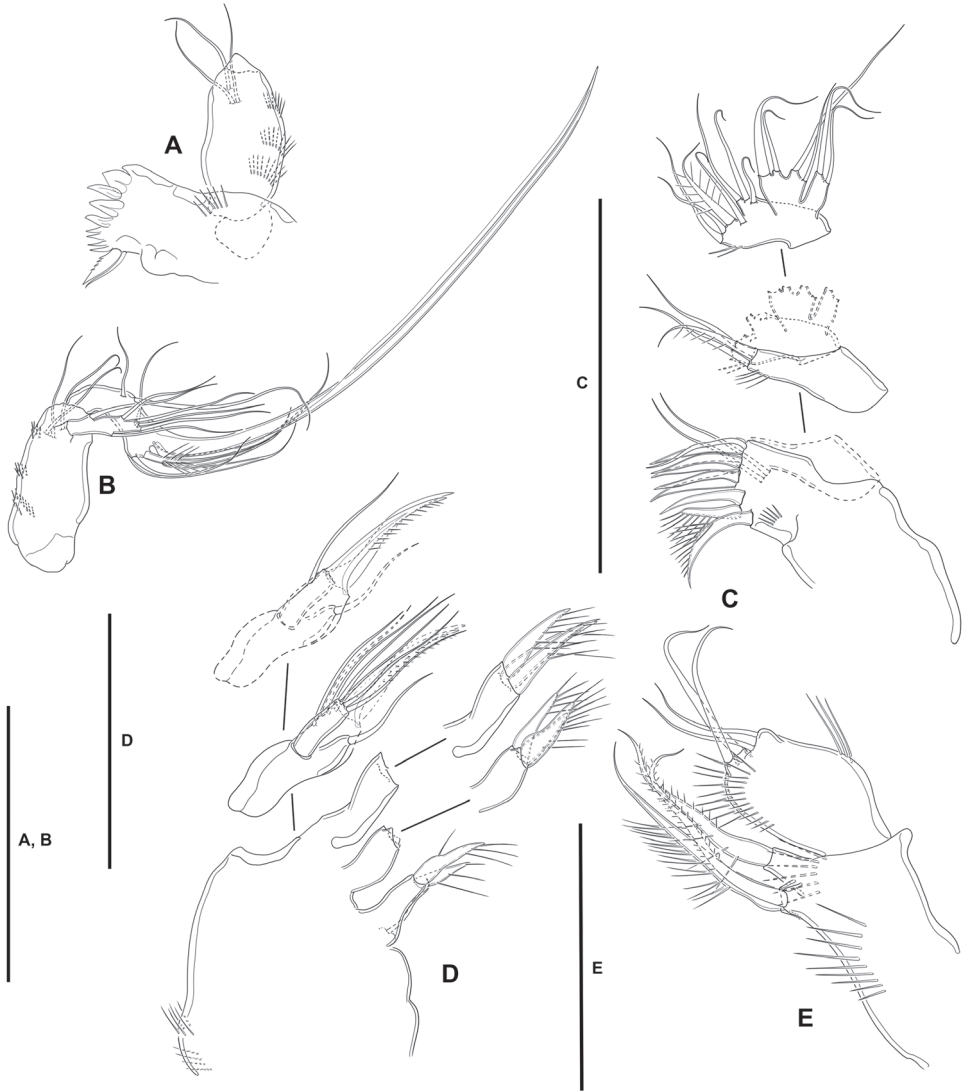


Figure 15. *Willenstenbelia reducta* sp. nov., female **A** mandibular coxa and basis **B** another mandibular basis, exopod and endopod **C** maxillule **D** maxilla **E** maxilliped. Scale bars: 50 μ m (**A–C**); 25 μ m (**D, E**).

tation of segments as shown; EXP1 and EXP2 with outer distal process less developed than in P3, with inner distal frill, EXP1 without, EXP2 with subdistal pore and inner seta; EXP3 with subdistal pore, with one inner seta, two apical elements, and two outer spines. Endopod three-segmented, reaching proximal third of EXP3; ENP1 shortest, ENP3 longest; spinular ornamentation of segments as depicted; ENP1 with small outer distal process, with inner long stiff pinnate element; ENP2 with well-developed outer distal process, without inner armature; ENP3 with distal processes as shown, with subdistal pore, with one inner seta, two apical elements, and one outer apical spine.

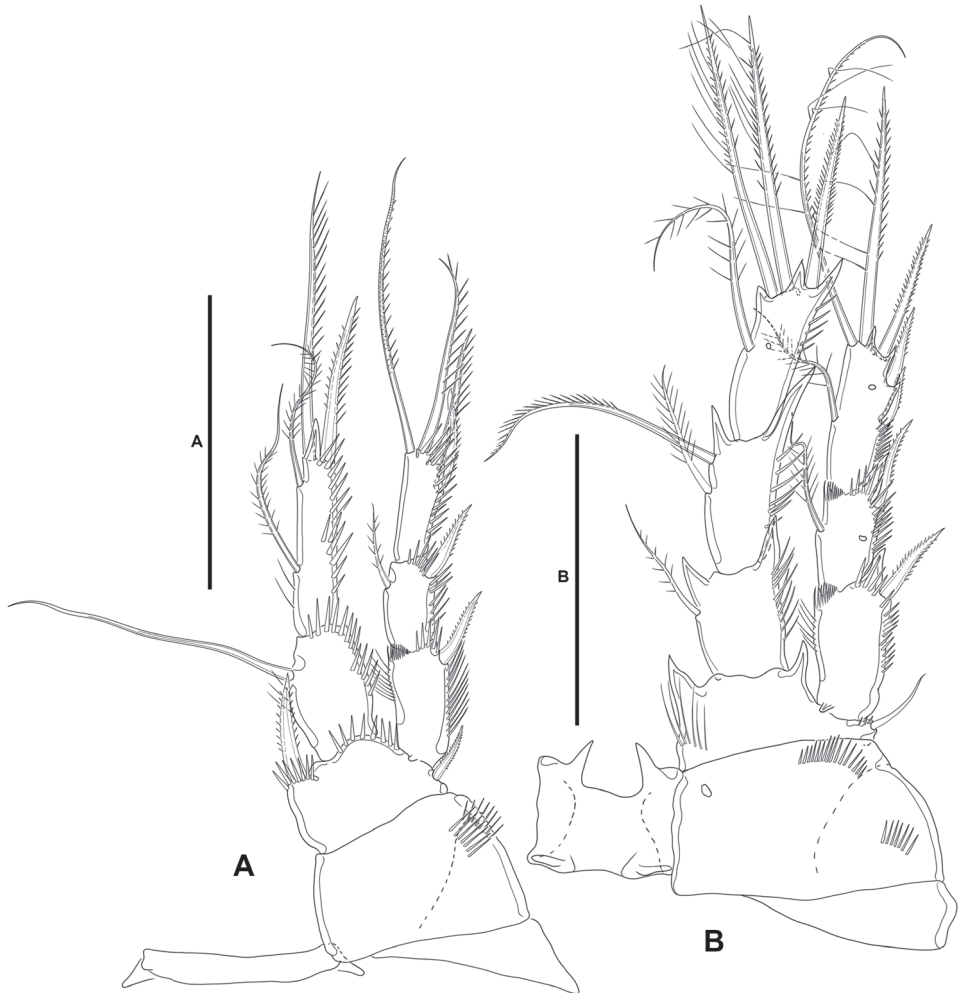


Figure 16. *Willenstenhelia reducta* sp. nov., female **A** P1, anterior **B** P2, anterior. Scale bars: 50 μ m (**A**, **B**).

Setal formula of swimming legs as follows:

	P1	P2	P3	P4
EXP	0,1,022	0,1,123	0,1,223	0,1,122
ENP	1,211	1,2,121	1,1,121	1,0,121

P5 (Fig. 17C): Baseoendopod transversely elongate; endopodal lobe with two setae, of which outer well-developed, inner minute, both separated by wide gap. Exopod trapezoidal, with some inner proximal spinules; with five setae, of which outermost, medial outer, and innermost setae pinnate and subequal in length, middle seta shortest and slender, medial inner seta bare and longest.

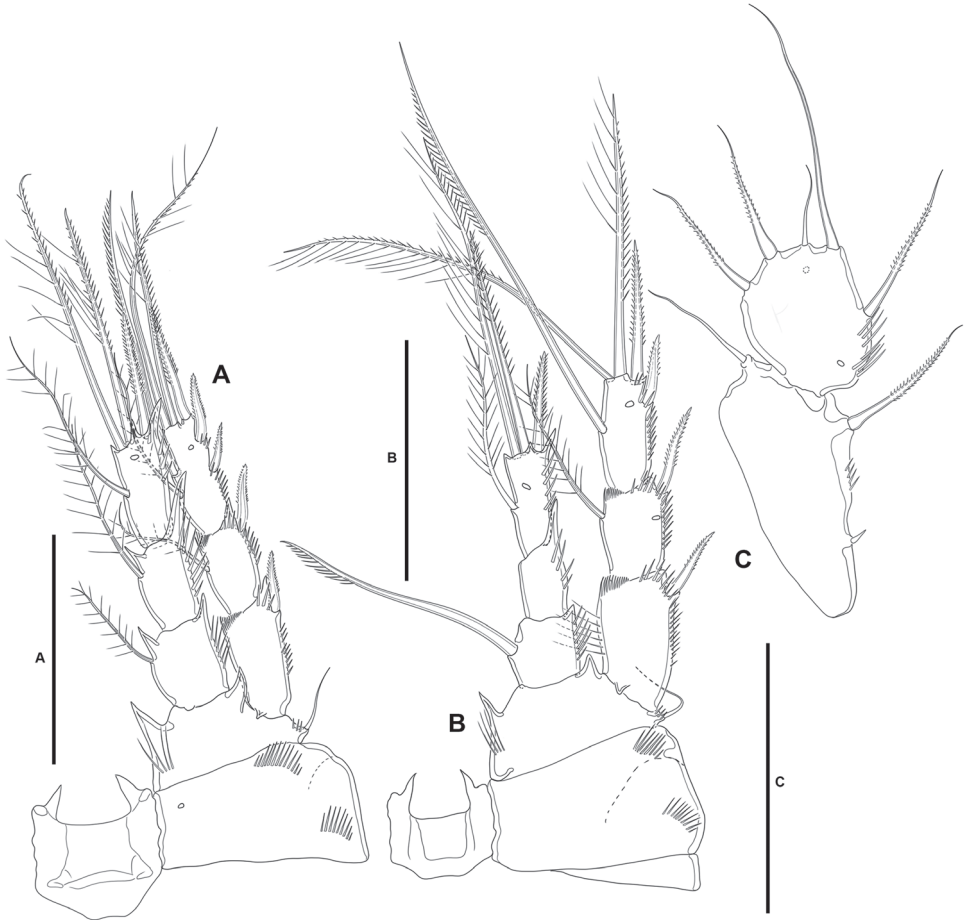


Figure 17. *Willenstenhelia reducta* sp. nov., female **A** P3, anterior **B** P4, anterior **C** P5, anterior. Scale bars: 50 μ m (**A–C**).

P6 (Figs 12B, 13A, B): Represented by a minute flap covering ventrolateral genital aperture, fused to somite, without surface ornamentation, with one small seta.

Male. Total body length measured from tip of rostrum to posterior margin of caudal rami ranging from 251 μ m to 363 μ m (mean, 309 μ m; n, 5; total body length of allotype, 363 μ m).

Prosome: As in female.

Urosome: Largely as in female except for genital and third urosomites separated, and spinular ornamentation of fourth and fifth urosomites (Figs 18C, 19A, B).

Caudal rami (Figs 18C, 19A, B): As in female.

Sexual dimorphism: Expressed in A1, P2 ENP, P3, P4, P5, and P6.

Antennule (Fig. 18A, B): 10-segmented, haplocer. All segments smooth except for first and seventh segment with spinules as shown. All setae seemingly smooth; with

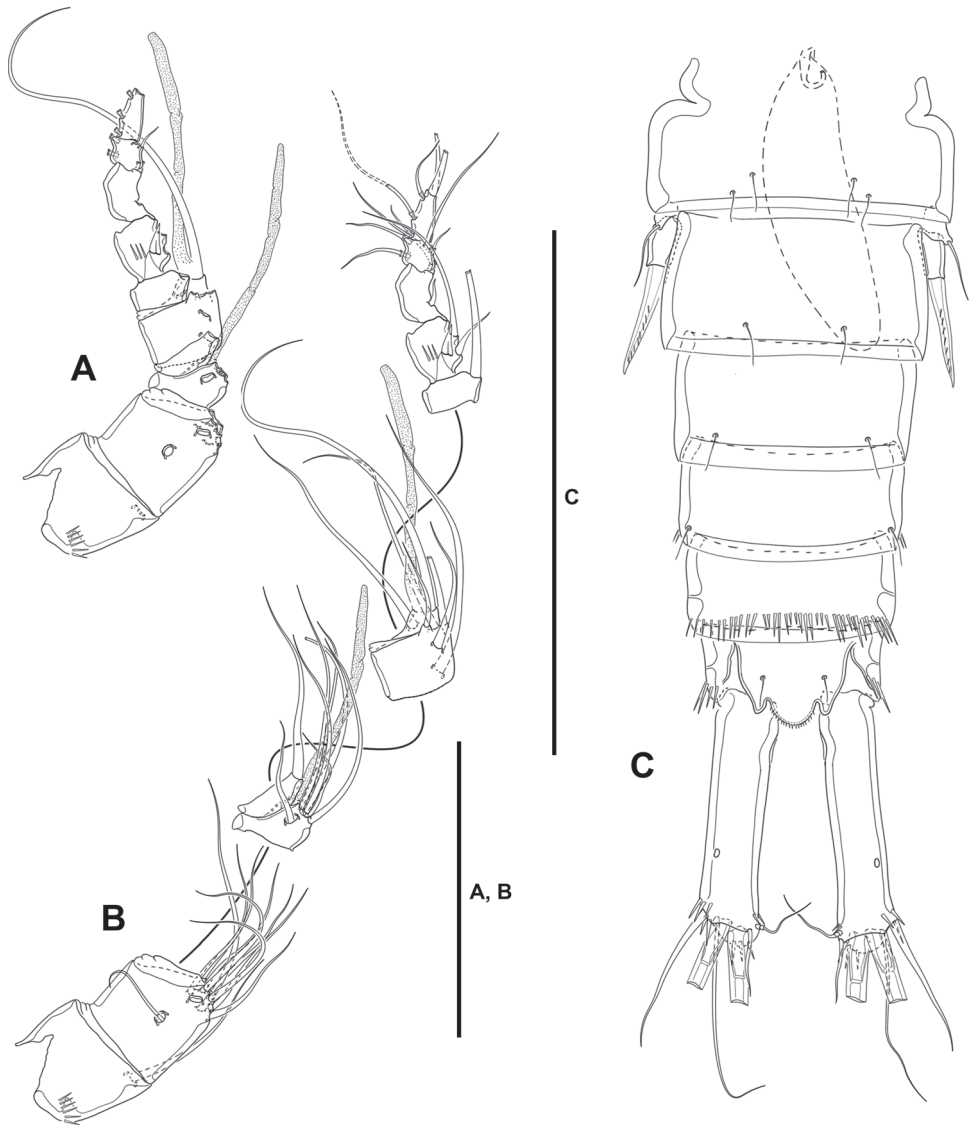


Figure 18. *Willenstenbelia reducta* sp. nov., male **A** antennule without armature **B** antennule with armature **C** urosome, dorsal. Scale bars: 50 μm (**A, B**); 100 μm (**C**).

one modified spine-like element on seventh segment. Armature formula: 1(1); 2(11); 3(7+ae); 4(1), 5(6+(1+ae)); 6(1); 7(3); 8(2); 9(4); 10(3+2 setae fused basally).

Antenna, mandible, maxillule, maxilla, and maxilliped: As in female.

P1: As in female.

P2 (Fig. 20A): Praecoxa, coxa, basis, and exopod as in female. Endopod sexually dimorphic, two segmented; first segment as in female; second segment with one proxi-

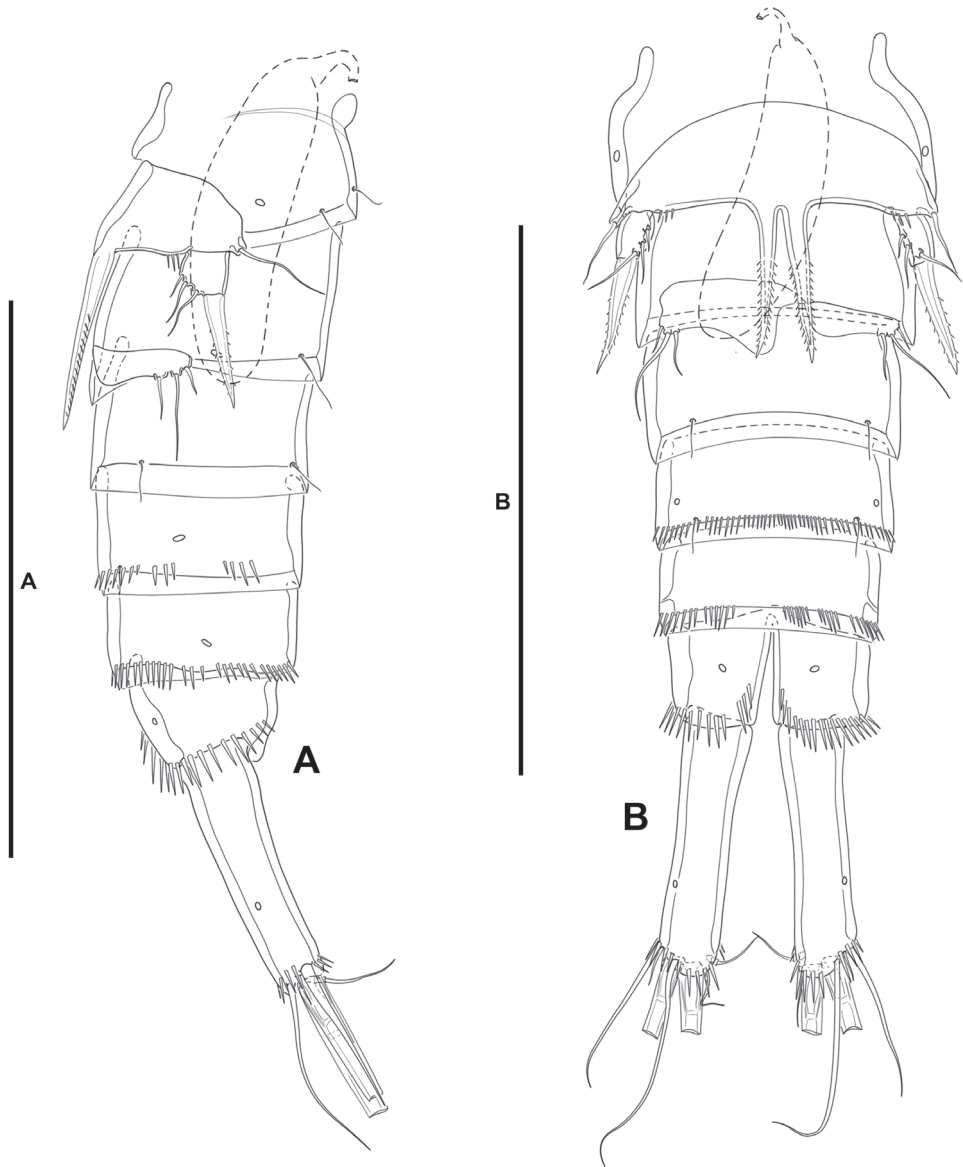


Figure 19. *Willenstenbelia reducta* sp. nov., male **A** urosome, lateral **B** urosome, ventral. Scale bars: 100 μm (**A**, **B**).

mal and one subdistal longitudinal row of spinules separated by medial process indicating division between ENP2 and ENP3 of the female ENP, with two inner elements homologues to the inner elements of the female ENP2, with subdistal pore, with one inner subdistal strong outer element, and one inner apical slender seta, and one apical outer spine-like element.

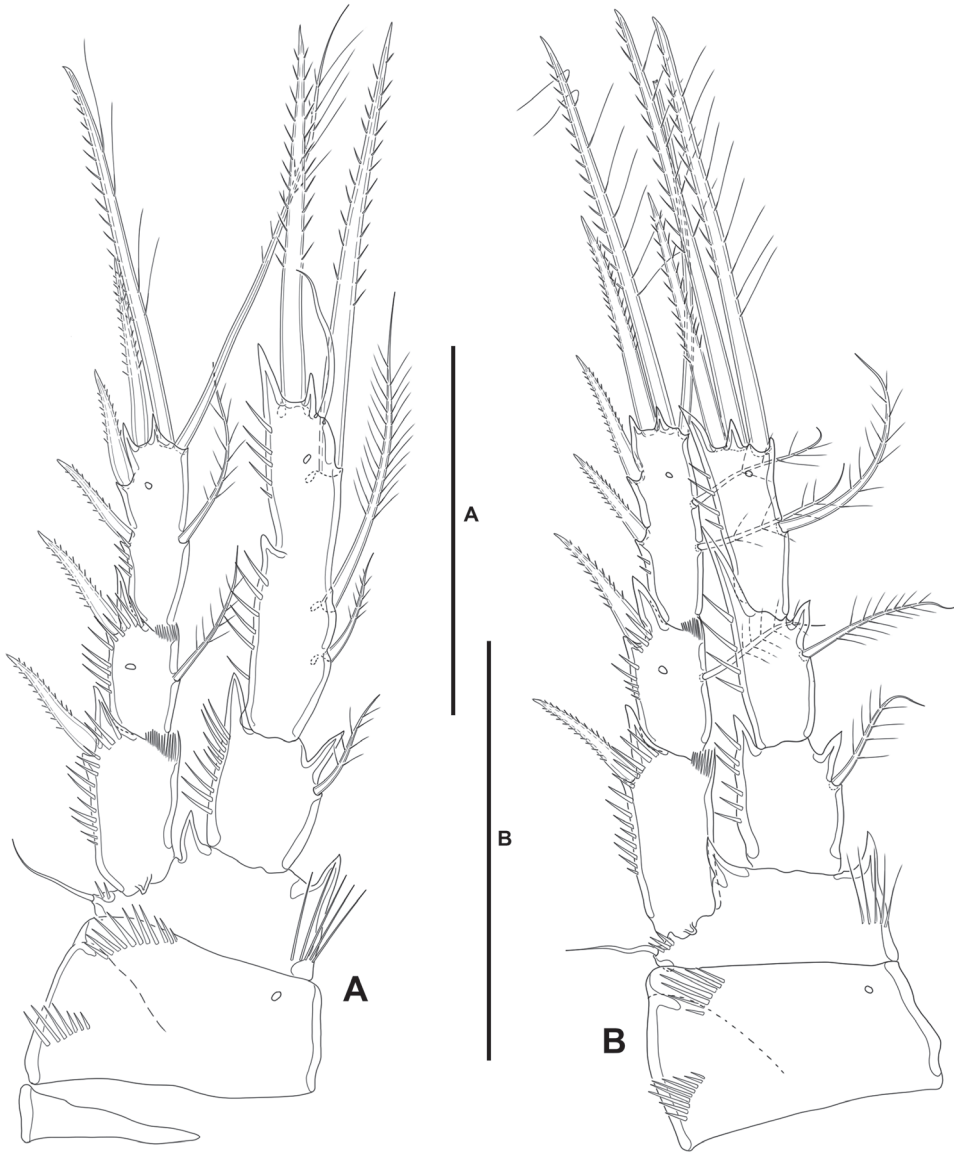


Figure 20. *Willenstenhelia reducta* sp. nov., male **A** P2, anterior **B** P3, anterior. Scale bars: 50 μ m (**A**, **B**).

P3 (Fig. 20B): Largely as in female, the general shape of the distalmost inner seta of EXP3 the only difference detected: very long, and pinnate element as in the female, but a visibly shorter and plumose seta in the male.

P4 (Fig. 21A): Largely as in female, the relative length and shape of the inner seta on ENP1, inner seta of EXP2, and outer spine of EXP2 the only differences detected:

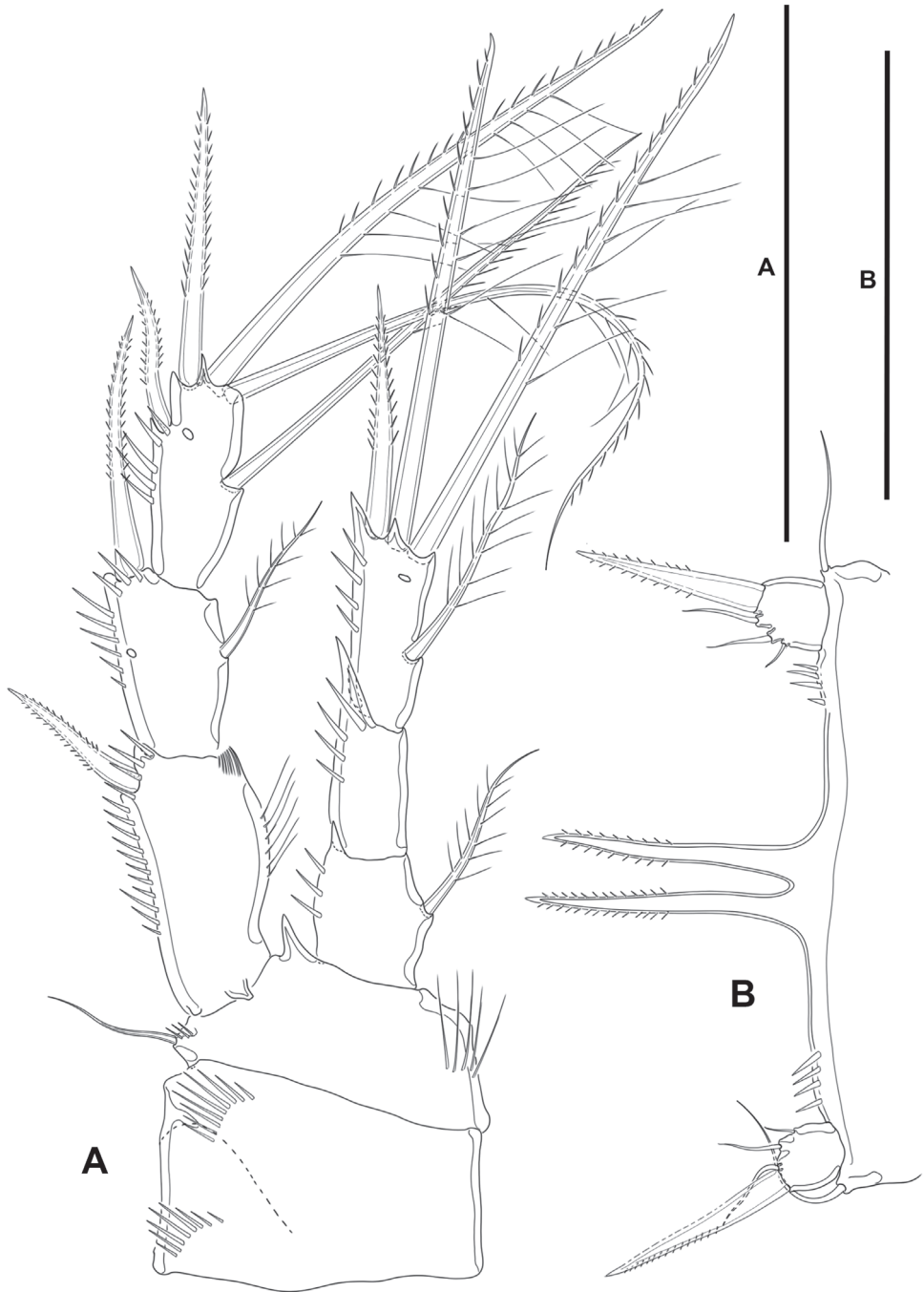


Figure 21. *Willenstenhelia reducta* sp. nov., male **A** P4, anterior **B** P5, anterior. Scale bars: 50 μ m (**A**, **B**).

inner seta of ENP1 very long and stiff in the female, but comparatively shorter, slender and plumose in the male; inner seta on the female EXP2 reaching beyond tip of EXP3 in the female, but visibly shorter in the male; outer spine of EXP2 of normal length not reaching tip of EXP3 in the female, but comparatively longer and reaching beyond tip of EXP3 in the male.

P5 (Figs 19A, B, 21B): Baseoendopods of both P5 fused forming a continuous plate; each endopodal lobe with short row of spinules close to insertion of exopod, and with one element (the two elements are set very close together) fused to endopodal lobe. Exopod small, discrete; with four elements, of which apical a strong spine, two medial ones small and subequal in length, innermost smallest arising midway inner margin.

P6 (Fig. 19A, B): Asymmetrical; each leg with three setae, of which medial longest, outer shortest.

Variability. No variability was observed in the inspected material.

Etymology. The specific epithet from the Latin *reducta*, reduced, in reference to the reduced inner seta on the female P5 baseoendopod, and to the reduced armature complement on the female and male P5 BENP. It is an adjective in the nominative singular; gender feminine.

Type locality. Mexico, Sinaloa State: Urías estuary, stn 2: 23.1587°N, 106.3326°W, depth 1.8 m, organic carbon content 3.99%, organic matter content 6.86%, sand 80.42%, clay 8.29%, silt 11.28%.

Other localities. Mexico, Sinaloa State: Urías estuary, stn 4: 23.1840°N, 106.3579°W, depth 0.7 m, organic carbon content 1.13%, organic matter content 1.94%, sand 82.44%, clay 8.27%, silt 9.29%, stn 9: 23.1904°N, 106.4121°W, depth 5.4 m, organic carbon content 1.41%, organic matter content 2.43%, sand 64.81%, clay 8.09%, silt 27.11%, stn 10: 23.1815°N, 106.4214°W, depth 6.0 m, organic carbon content 1.20%, organic matter content 2.07%, sand 69.12%, clay 7.91%, silt 22.97%.

Discussion

Affinities of *Lonchoidestenhelia prote* sp. nov.

In their paper, Mu and Huys (2002) proposed the abandonment of the traditional subgeneric division of the genus *Stenhelia* and restricted the genus to a core of species of the former subgenus *Stenhelia* (*Stenhelia*) Boeck, 1865, the type species *S. gibba* Boeck, 1865, and *S. proxima* Sars, 1906, *S. curviseta* Lang, 1936, *S. divergens* Nicholls, 1940, *S. peniculata* Lang, 1965, *S. pubescens* Chislenko, 1978, *S. sheni* Mu and Huys, 2002, and *S. taiiae* Mu and Huys, 2002 (Mu and Huys 2002, Karanovic et al. 2014). Additionally, Mu and Huys (2002) reinstated the genus *Beatricella* for *S. (S.) aemula* T. Scott, 1893, created the genus *Anisostenhelia* for *S. asetosa* Thistle and Coull, 1979, and reassigned *S. diegensis* Thistle and Coull, 1979 *Delavalia* Brady, 1868. In their paper, Mu and Huys (2002) proposed the monophyly of *Stenhelia* based on the presence of a modified seta on the P5 baseoendopodal lobe (second innermost seta in the female;

innermost element in the male) and on the probable presence of a hyaline flange on the P2 ENP2 in the male of all its species. Their view was later corroborated by Karanovic et al. (2014). Additionally, Mu and Huys (2002) suggested a sister-group relationship with *Anisostenhelia* by the synapomorphic (i) loss of one inner seta on the P2 EXP3, resulting in the armature formula 123, (ii) loss of one inner seta on P3 EXP3, resulting in the armature formula 223, (iii) P2–P3 ENP3 produced into an apical spinous process, resulting in the displacement of the outer spine to an apical situation, and both apical setae to the inner (subapical) margin, (iv) male P5 EXP with two outermost elements modified into spines, (v) innermost element of male P6 modified into an outwardly recurved spine, and (vi) anal operculum absent. Also, Mu and Huys (2002) detected a potential synapomorphy for *Stenhelia*, *Anisostenhelia*, and *Beatricella*, the loss of the inner seta on the P1 EXP2. The genus *Anisostenhelia* was defined by Mu and Huys (2002) by the apomorphic (i) loss of the inner seta on P2–P4 EXP1, (ii) basal part of both apical setae on the female P2 ENP3 typically swollen, (iii) male sexual dimorphism expressed in the modification of the outer spine of the P4 ENP into a strongly recurved spine, and (iv) male P5 with exopod and baseoendopod fused. Finally, Mu and Huys (2002) defined the genus *Beatricella* by the apomorphic (i) male P2 ENP drawn out into sigmoid finely pinnate process with long outer spinules, (ii) P4 ENP1 with very long stout seta, and (iii) male P5 EXP and baseoendopod fused and outermost exopodal element modified into strong spine.

Lonchoeidestenhelia gen. nov. shares the potentially synapomorphic loss of the inner seta on the P1 EXP2 (Mu and Huys 2002) with *Stenhelia*, *Anisostenhelia*, and *Beatricella*. *Lonchoeidestenhelia* gen. nov. seems to be more closely allied to *Stenhelia*–*Anisostenhelia* than to *Beatricella*. *Stenhelia*, *Anisostenhelia*, and *Lonchoeidestenhelia* gen. nov. share (i) the apomorphic loss of one inner seta on the P2 EXP3 (formula 123) and P3 EXP3 (formula 223), *Beatricella* displays a more primitive condition, with armature complement of 223 and 323 on the P2 EXP3 and P3 EXP3, respectively, (ii) P2 ENP3 with apical outer spinous process with subsequent displacement of the outer spine to an apical situation, and medial and inner distal setae to a subapical inner position, and (iii) male P5 EXP with two outermost elements modified into spines; only outermost element modified into a spine in the male P5 EXP of *Beatricella*. *Lonchoeidestenhelia* gen. nov. seems to be more closely related to *Anisostenhelia* than to *Stenhelia*, by the overall shape of the male P2 ENP2, with proximal half globular, distal half triangular in these two species, but proximal half visibly less globular and gradually tapering distally in *Stenhelia* and *Beatricella*. *Lonchoeidestenhelia* gen. nov. share the plesiomorphic non-modified setae of the female P5 baseoendopod and lack of hyaline flange on the male P2 ENP2 with *Anisostenhelia*, and *Beatricella*; the plesiomorphic presence of one inner seta on P2–P4 EXP1, the apical setae on the female P2 ENP3 not swollen basally, and the outer spine of the male P4 ENP3 not sexually dimorphic with *Stenhelia* and *Beatricella*; and the plesiomorphic normal (unmodified) setae of the male P6 with normal, and presence of anal operculum with *Beatricella*. Finally, *Lonchoeidestenhelia* gen. nov. is defined here by the autapomorphic modified (lanceolate) proximal spinules on the outer distal process of the male P2 ENP2.

Affinities of *Willenstenhelia reducta* sp. nov. The genus *Delavalia* is not only the most species-rich genus within the Stenheliinae, but also the most morphologically diverse. Although past decades have witnessed important advancements in the study of the genus, its monophyletic status is far from resolved (Mu and Huys 2002, Willen 2002, Karanovic et al. 2014). Probably, the most important contribution towards the monophyly of the genera *Stenhelia* Boeck and *Delavalia* was that of Mu and Huys (2002) who, amongst other things, challenged and abandoned the subgeneric classification of the genus *Stenhelia*, and consequently gave the subgenus *Stenhelia* (*Delavalia*) full generic rank. The genus *Delavalia* remained, nevertheless, polyphyletic (Mu and Huys 2002, Karanovic et al. 2014). Later, Willen (2003) proposed six groups/subgroups upon (i) the shape of the anal operculum, (ii) the combination of a specialized setation pattern on the female P5, (iii) presence/reduction/absence of the distal inner setae on P2–P4 EXP3, (iv) shape of the male and female P5, and (v) reduction of the setation of swimming legs; Dahms and Bresciani (1993) and Dahms et al. (2005) proposed some apomorphies for the genus based on naupliar morphology. Some years later, Huys and Mu (2008) discussed Willen (2003) and Dahms et al. (2005), and presented a subdivision of the genus *Delavalia* based on (i) the segmentation pattern of the antennary exopod, and (ii) number of outer spines on P2–P4 EXP3. More recently, Karanovic and Kim (2014) proved the polyphyly of the genus and proposed three genera with two-segmented P1 endopods, *Wellstenhelia* Karanovic and Kim, 2014 for its type species *We. calliope* Karanovic and Kim, 2014, and *We. clio* Karanovic and Kim, 2014, *We. erato* Karanovic and Kim, 2014, *We. euterpe* Karanovic and Kim, 2014, *We. melpomene* Karanovic and Kim, 2014, *We. qingdaoensis* (Ma and Li, 2011), *We. hanstroemi* (Lang, 1948), and *We. bocqueti* (Soyer, 1972), *Willenstenhelia* for its type species *Wi. thalia*, and *Wi. minuta*, *Wi. unisetosa*, *Wi. urania*, and *Wi. terpsichore*, and *Itostenhelia* Karanovic and Kim, 2014 for its type species *I. polyhymnia* Karanovic and Kim, 2014, and *I. golikovi* (Chislenko, 1978) (= *Stenhelia* (*Delavalia*) *golikovi* Chislenko, 1978).

Karanovic and Kim (2014) gave a list of autapomorphies for *Willenstenhelia*. These are:

- i. inner apical seta on the male P2 ENP2 shorter than outer spine,
- ii. outer spine on the male P4 EXP2 more sclerotized than other spines and strongly curved inwards,
- iii. female P5 BENP with three elements only, and with a large gap between the innermost one and the other two setae,
- iv. P4 ENP2 without inner armature, and
- v. female P5 EXP with five setae only, of which innermost element displaced to the inner margin.

Additionally, they (Karanovic and Kim 2014) suggested that *D. palustris palustris* Brady, 1868 known from salt marshes of Northumberland and Durham, the widely distributed *D. palustris bispinosa* (Bodin, 1970) which could be a separate species or a

species complex (Karanovic and Kim 2014), *D. clavus* (Wells and Rao, 1987), *D. paraclavus* (Wells and Rao, 1987), and *D. valens* (Wells and Rao, 1987) all known from Andaman and Nicobar Islands, might be distant relatives of *Willenstenhelia*. Interestingly, the above species, along with *D. schminkei* (Willen, 2002) and an unidentified species, “*St. spec. 5*”, both found in sediment samples from Papua New Guinea (Willen 2002, 2003), belong to Willen’s (2003) “*S. clavus* group”, which seems to be restricted the Indo-Pacific region (Willen 2002, 2003). The “*S. clavus* group” was defined by Willen (2002, 2003) upon:

- i. the lack of inner armature on P2–P4 EXP1,
- ii. presence of one inner seta at most on P2 EXP3,
- iii. presence of two inner setae at most on P3 EXP3,
- iv. P3 ENP3 with one inner seta at most,
- v. P4 EXP3 with two outer spines only,
- vi. loss of distalmost inner seta of P4 EXP3,
- vii. loss of inner armature of P4 ENP2,
- viii. presence of one inner seta at most on P4 ENP3,
- ix. baseoendopods of pair of female P5 fused medially,
- x. outermost element on the male P5 EXP modified into a strong spine fused to segment (the male of *D. valens* remains unknown though), and
- xi. the non-prehensile maxilliped with globular allobasis (endopod absorbed into basis) (Willen 2002, 2003).

Similarly, Huys and Mu (2008) attributed *D. palustris palustris*, *D. incerta* (Por, 1964) known from the Israeli coasts, and *D. schminkei*, *D. clavus*, *D. paraclavus*, *D. valens*, and *D. unisetosa* (Wells, 1967) from Inhaca Island to their group III of the genus *Delavalia*, defined by the presence of 3, 3, 2 outer spines on P2–P4 EXP3. Karanovic and Kim (2014) reallocated *D. unisetosa* into *Willenstenhelia*.

Karanovic and Kim (2014) noted, that the assumed autapomorphic characters (iv) P4 ENP2 without inner armature and (v) female P5 EXP with five setae only, of which the innermost element is displaced to the inner margin, for *Willenstenhelia* might have evolved convergently in some other stenheliins. As an example of this, they mentioned the lack of inner armature on the P4 ENP2 of *Muohuysia xylophila* (Hicks, 1988), a genus pertaining to a different lineage as evidenced by the three-segmented P1 endopods. The lack of inner armature on P4 ENP2 is present, however, in some other species somehow related to *Willenstenhelia*, e.g., *D. schminkei*, *D. valens*, *D. clavus*, and *D. paraclavus* (Karanovic and Kim 2014), rendering the autapomorphic status of this character, doubtful, but apomorphic for *Willenstenhelia* if convergence is assumed. Similarly, the autapomorphic status of the reduction of the inner apical seta on the male P2 ENP2, shorter than the apical outer spine, is questionable, since a similar condition is present in *D. oblonga* (Lang, 1965) (see Lang 1965: 248, fig. 137f), and is regarded here as apomorphic for *Willenstenhelia* if convergence is invoked.

To the best of my knowledge, the innermost seta of the pentasetose female P5 EXP displaced to the inner margin of the ramus is present only in *Willenstenhelia*, and its autapomorphic status for the genus is confirmed. Also, I could not find any other species, for which the male is known, with the outer spine of the male P4 EXP2 comparatively more sclerotized and longer than in the female, and curved inwards, and its autapomorphic status for *Willenstenhelia* is provisionally accepted. Some other species in other related genera, e.g., *Wellstenhelia euterpe*, display a reduced armature complement of the female P5 BENP from five to three setae, but *Willenstenhelia* is unique in the wide gap between the innermost element and its outer neighboring seta. This wide gap between the innermost element and its next outer neighboring seta is accepted here as autapomorphic for *Willenstenhelia*.

As with other stenheliins with a two-segmented P1 endopod, *Wi. reducta* sp. nov. was initially attributed to *Delavalia*. However, it was subsequently allocated into *Willenstenhelia* on account of (i) the pentasetose female P5 EXP in which the innermost seta is displaced to the inner margin, (ii) the reduced armature complement of the female P5 BENP, with two setae only, and with a wide gap between the innermost element and its outer neighboring seta, and (iii) presence of a sclerotized long and recurved outer spine on the male P4 EXP2.

The interspecific relationships amongst the species of *Willenstenhelia* are not clear. The Mexican *Wi. reducta* sp. nov. seems to belong to a core of species composed of *Wi. minuta*, *Wi. urania*, and *Wi. terpsichore* characterized by the strongly reduced inner seta of the female P5 baseoendopod. However, *Wi. reducta* sp. nov. is different from the other three species in the presence of one outer seta only on the discrete, not fused medially, baseoendopods of the female P5, i.e. *Wi. reducta* sp. nov. underwent loss of the outermost shorter seta of the female P5 baseoendopod which is still present in *Wi. minuta*, *Wi. urania*, and *Wi. terpsichore*, and unlike these three species, both baseoendopods of the female P5 of *Wi. reducta* sp. nov. are not fused medially. The loss of the outermost seta of the female P5 baseoendopod of *Wi. reducta* sp. nov. is regarded here as autapomorphic for the species. The innermost seta of the female P5 EXP and the outermost seta of the female P5 baseoendopod of *Willenstenhelia thalia* underwent reduction, but the innermost seta of the female P5 baseoendopod is visibly larger than in *Wi. minuta*, *Wi. urania*, and *Wi. terpsichore*. The reduction of the innermost seta of the female P5 EXP of *Wi. thalia* is considered here as autapomorphic for that species. *Willenstenhelia unisetosa* stands out for its three well-developed setae on the female P5 baseoendopod and for the discrete baseoendopods of the female P5 which are regarded here as the most plesiomorphic conditions. *Willenstenhelia unisetosa* and *Wi. reducta* sp. nov. share the discrete baseoendopods of the female P5. The male is known only for *Wi. thalia*, *Wi. terpsichore*, *Wi. unisetosa* and *Wi. reducta* sp. nov. *Willenstenhelia reducta* sp. nov. shares the male P5 EXP with three small inner setae and the discrete apical spine with *Wi. unisetosa*, but it also shares the endopodal spines fused to the baseoendopod with *Wi. terpsichore*. The most plesiomorphic condition seems to be that of *Wi. thalia* with two (or three?) inner setae on the male P5 baseoendopod, and the inner medial seta of the exopod well-developed.

Acknowledgements

I am deeply indebted to Abraham Guerrero Ruíz (Centro de Investigación en Alimentación y Desarrollo, Unidad Mazatlán) and to Sergio Rendón Rodríguez (Instituto de Ciencias del Mar y Limnología, Unidad Académica Mazatlán) for their help during the sampling campaigns. Thanks also goes to Nataly Ortíz Gálvez and Ángel A. Valenzuela Cruz for their help during the sampling campaigns and for processing the sediment samples. I wish to express my gratitude to Dr. Paulo H. Costa Corgosinho and to Dr. Kai Horst George for their comments to the first draft of the manuscript. This is a contribution to project IN202019 Biodiversidad de la meiofauna en un ecosistema costero contaminado del sur de Sinaloa: un enfoque integrativo de técnicas taxonómicas clásicas y moleculares financed by the Programa de Apoyo a Proyectos de Investigación e Innovación Tecnológica (DGAPA-PAPIIT) of the Universidad Nacional Autónoma de México.

References

- Bodin P (1970) Copépodes harpacticoides marins des environs de la Rochelle. 1. Espèces de la vase intertidale de Chatelaillon. *Téthys* 2: 385–436.
- Boeck A (1865) Oversigt over de ved Norges Kyster iagttagne Copepoder henhörende til Calanidernes, Cyclopidernes og Harpacticidernes Familier. *Forhandlinger i Videnskabselskabet i Kristiania* 1864: 226–282.
- Brady GS (1868) On the crustacean fauna of the salt-marshes of Northumberland and Durham. *Natural History Transactions of Northumberland and Durham* 3: 120–136. <https://www.biodiversitylibrary.org/page/34814697#page/11/mode/1up>
- Brady GS (1880) A monograph of the free and semi-parasitic Copepoda of the British Islands. Vol. II. The Ray Society, London, 182 pp. <https://www.biodiversitylibrary.org/item/67810#page/7/mode/1up>
- Burgess R (2001) An improved protocol for separating meiofauna from sediments using colloidal silica sols. *Marine Ecology Progress Series* 214: 161–165. <https://doi.org/10.3354/meps214161>
- Chislenko LL (1978) New species of harpacticoid copepods (Copepoda, Harpacticoida) from Poss'yet Bay, Sea of Japan. *Trudy Zoologicheskogo Instituta, Akademii Nauk SSSR, Leningrad* 61: 161–192.
- Coull BC, Fleeger JW (1977) A new species of *Pseudostenhelia*, and morphological variations in *Nannopus palustris* (Copepoda, Harpacticoida). *Transactions of the American Microscopical Society* 96: 332–340. <https://doi.org/10.2307/3225863>
- Dahms H-U, Bresciani J (1993) Naupliar development of *Stenhelia* (*D.*) *palustris* (Copepoda, Harpacticoida). *Ophelia* 37: 101–116. <https://doi.org/10.1080/00785326.1993.10429911>
- Dahms H-U, Schizas N V, Shirley TC (2005) Naupliar evolutionary novelties of *Stenhelia peniculata* (Copepoda, Harpacticoida) from Alaska affirming taxa belonging to different categorical rank. *Invertebrate Zoology* 2: 1–14. <https://doi.org/10.15298/invertzool.02.1.01>

- Dana JD (1846) Notice of some genera of Cyclopacea. The American Journal of Science and Arts 2: 225–229. <https://www.biodiversitylibrary.org/item/51994#page/255/mode/1up>
- Hicks GRF (1988) Harpacticoid copepods from biogenic substrata in offshore waters of New Zealand. 1: New species of *Paradactylopodia*, *Stenhelia* (St.) and *Laophonte*. Journal of the Royal Society of New Zealand 18: 437–452. <https://doi.org/10.1080/03036758.1988.10426467>
- Huys R, Boxshall GA (1991) Copepod evolution. The Ray Society, London, 468 pp. <https://doi.org/10.4319/lo.1993.38.2.0478>
- Huys R, Mu FH (2008) Description of a new species of *Onychostenhelia* Itô (Copepoda, Harpacticoida, Miraciidae) from the Bohai Sea, China. Zootaxa 1706: 51–68. <https://doi.org/10.11646/zootaxa.1706.1.2>
- Karanovic T, Kim K (2014) New insights into polyphyly of the harpacticoid genus *Delavalia* (Crustacea, Copepoda) through morphological and molecular study of an unprecedented diversity of sympatric species in a small South Korean bay. Zootaxa 3783: 1–96. <https://doi.org/10.11646/zootaxa.3783.1.1>
- Karanovic T, Kim K, Lee W (2014) Morphological and molecular affinities of two East Asian species of *Stenhelia* (Crustacea, Copepoda, Harpacticoida). ZooKeys 411: 105–143. <https://doi.org/10.3897/zookeys.411.7346>
- Lang K (1936) Die während der Schwedischen Expedition nach Spitzbergen 1898 und nach Grönland 1899 eingesammelten Harpacticiden. Kungliga Svenska Vetenskapsakademiens Handlingar 15: 1–55.
- Lang K (1948) Monographie der Harpacticiden Vols. I & II. Nordiska Bokhandeln, Stockholm, 1682 pp.
- Lang K (1965) Copepoda Harpacticoida from the Californian Pacific coast. Kungliga Svenska Vetenskapsakademiens Handlingar (4)10: 1–560. <http://www.vliz.be/imis/imis.php?refid=78667>
- Ma L, Li X (2011) *Delavalia qingdaoensis* sp. nov. (Harpacticoida, Miraciidae), a new copepod species from Jiaozhou Bay, Yellow Sea. Crustaceana 84: 1085–1097. <https://doi.org/10.1163/001121611X584334>
- Mu F, Huys R (2002) New species of *Stenhelia* (Copepoda, Harpacticoida, Diosaccidae) from the Bohai Sea (China) with notes on subgeneric division and phylogenetic relationships. Cahiers de Biologie Marine 43: 179–206. <https://doi.org/10.21411/CBM.A.C482EC6A>
- Nicholls AG (1940) Marine harpacticoids and cyclopoids from the shores of the St. Lawrence. Fauna et Flora Laurentianae 2: 240–316.
- Por FD (1964) A study of the Levantine and Pontic Harpacticoida (Crustacea, Copepoda). Zoologische Verhandelingen 64: 1–128. <https://www.repository.naturalis.nl/document/149025>
- Rohal M, Thistle D, Easton EE (2016) Extraction of metazoan meiofauna from muddy deep-sea samples: operator and taxon effects on efficiency. Journal of Experimental Marine Biology and Ecology. <https://doi.org/10.1016/j.jembe.2017.01.006>
- Sars GO (1903) Copepoda Harpacticoida. Parts I & II. Misophriidae, Longipediidae, Cerviniidae, Ectinosomidae. An account of the Crustacea of Norway, with short descriptions and figures of all the species. V: 1–28. <https://www.biodiversitylibrary.org/item/15960#page/36/mode/1up>
- Sars GO (1906) Copepoda Harpacticoida. Parts XI & XII. Thalestridae (concluded), Diosaccidae (part). An account of the Crustacea of Norway with short descriptions and figures

- of all the species V: 133–156. <https://www.biodiversitylibrary.org/item/15960#page/307/mode/1up>
- Scott A (1902) On some Red Sea and Indian Ocean Copepoda. Proceedings and Transactions of the Liverpool Biological Society 16: 397–428. <http://www.biodiversitylibrary.org/item/129204>
- Scott T (1893) Additions to the fauna of the Firth of Forth. Annual Report of the Fishery Board for Scotland 11: 197–219. <https://www.biodiversitylibrary.org/item/177823#page/226/mode/1up>
- Scott T (1905) Notes on British Copepoda: Change of names. Annals and Magazine of Natural History 16: 1–16. <https://doi.org/10.5962/bhl.title.38696>
- Soyer J (1971) Contribution à l'étude des copépodes harpacticoides de Méditerranée Occidentale. 5. *Stenbelia (Delavalia) coineauae* n. sp., *Stenbelia (D.) bocqueti* n. sp. et *Typhlamphiascus bouligandi* n. sp. (Diosaccidae, Sars). Vie et Milieu (A)22: 263–280. https://www.php.obs-banyuls.fr/Viemilieu/images/Archives_1950-2002/vie-et-milieu/VOLUME_1971_22_fasc2_A.pdf
- Thistle D, Coull BC (1979) A revised key to *Stenbelia (Stenbelia)* (Copepoda: Harpacticoida) including two new species from the Pacific. Zoological Journal of the Linnean Society 66: 63–72. <https://doi.org/10.1111/j.1096-3642.1979.tb01901.x>
- Wells JBJ (1967) The littoral Copepoda (Crustacea) of Inhaca, Island, Mozambique. Transactions of the Royal Society of Edinburgh 67: 189–358. <https://doi.org/10.1017/S0080456800024017>
- Wells JBJ, Rao GC (1987) Littoral Harpacticoida (Crustacea: Copepoda) from Andaman and Nicobar Islands. Memoirs of the Zoological Survey of India 16: 1–385.
- Willen E (2002) Notes on the systematic position of the Stenheleinae (Copepoda, Harpacticoida) within the Thalestridimorpha and description of two new species from Motupore Island, Papua New Guinea. Cahiers de Biologie Marine 43: 27–42. <https://doi.org/10.21411/CBM.A.FCF07EC3>
- Willen E (2003) A new species of *Stenbelia* (Copepoda, Harpacticoida) from a hydrothermal, active, submarine volcano in the New Ireland Fore-Arc system (Papua New Guinea) with notes on deep sea colonization within the Stenheleinae. Journal of Natural History 37: 1691–1711. <https://doi.org/10.1080/00222930110114437>

Description of three new species of oak gallwasps of the genus *Amphibolips* Reinhard from Mexico (Hymenoptera, Cynipidae)

Dohuglas Eliseo Castillejos-Lemus¹, Ken Oyama¹, José Luis Nieves-Aldrey²

¹ *Escuela Nacional de Estudios Superiores (ENES) Unidad Morelia, Universidad Nacional Autónoma de México (UNAM). Antigua Carretera a Pátzcuaro 8701, Ex-Hacienda de San José de la Huerta, 58190, Morelia, Michoacán, México* ² *Departamento de Biodiversidad y Biología Evolutiva, Museo Nacional de Ciencias Naturales (CSIC). José Gutiérrez Abascal 2, 28006 Madrid, Spain*

Corresponding author: Dohuglas Eliseo Castillejos-Lemus (castillejos.lemus@gmail.com)

Academic editor: A. Köhler | Received 25 February 2020 | Accepted 7 October 2020 | Published 6 November 2020

<http://zoobank.org/CFC20F09-580A-49BE-BE3D-DA64C11F12B0>

Citation: Castillejos-Lemus DE, Oyama K, Nieves-Aldrey JL (2020) Description of three new species of oak gallwasps of the genus *Amphibolips* Reinhard from Mexico (Hymenoptera, Cynipidae). ZooKeys 987: 81–114. <https://doi.org/10.3897/zookeys.987.51366>

Abstract

Three new species of oak gall wasps of the genus *Amphibolips* Reinhard, 1865 (Hymenoptera: Cynipidae: Cynipini) are described from Mexico: *Amphibolips magnigalla* Nieves-Aldrey & Castillejos-Lemus, *Amphibolips kinseyi* Nieves-Aldrey & Castillejos-Lemus and *Amphibolips nigrialatus* Nieves-Aldrey & Castillejos-Lemus. The specimens of the first two species were representative of sexual generations and come from the State of Oaxaca, while only a female, collected in the State of Veracruz, is described for *A. nigrialatus*. The new species induces galls on *Quercus zempoaltepecana* and *Q. sapotifolia* (Fagaceae, section *Lobatae*, red oaks). Descriptions of the diagnostic morphological characteristics of the three species and a key for their identification are provided. The taxonomic relationships of the new species with other species of *Amphibolips* are discussed; the three new species are closely allied amongst themselves and are related to *A. dampfi* Kinsey, 1937. With the three newly-described species, the number of *Amphibolips* in Mexico is increased to 23.

Keywords

Amphibolips, Cynipini, *Lobatae*, Mexico, oak apple gall, oak gallwasps, *Quercus*

Introduction

Oak gall wasps (Cynipidae: Cynipini) include approximately 41 genera with circa 1,000 species (Liljeblad et al. 2008, Péntzes et al. 2018) distributed mainly in the Holarctic, Neotropical and Oriental regions (Ronquist et al. 2015). They represent the largest tribe of Cynipidae and are a monophyletic group of wasps that induce relatively more structurally complex and diverse galls of the known gall types (Cornell 1983, Stone and Cook 1998, Nieves-Aldrey 2001, Csöka et al. 2005). Cynipini species are predominantly associated with host species of *Quercus* (Liljeblad et al. 2008), but some genera of Cynipini use other hosts within the Fagaceae, such as *Castanea*, *Castanopsis*, *Lithocarpus*, *Chrysolepis* and *Notholithocarpus* (Stone et al. 2002, Nicholls et al. 2018). A particularity of the Cynipini is that most species exhibit life histories with alternating generations (e.g. asexual and sexual) (Stone et al. 2002).

The Nearctic region, particularly Mexico, is one of the centres of diversity of the oak gall wasps, which have been estimated to include more than 700 species (Stone et al. 2002, Liu et al. 2007). This diversity is directly related to the diversity of *Quercus* species, with more than 90 species recorded from the United States and Canada and 161 from Mexico (Valencia 2004, Liu and Ronquist 2006). The most recent work on the number of Cynipidae species recorded from Mexico indicates the presence of 183 species in 16 genera (Pujade-Villar and Ferrer-Suay 2015) associated with approximately 35 *Quercus* species.

Amphibolips is exclusively associated with the *Lobatae* section of *Quercus* genus and is restricted to the American continent (Nieves-Aldrey et al. 2012). Fifty-three species of *Amphibolips* are recognised; the vast majority are found in the Nearctic region, three species are distributed in Panama, 19 species are endemic to Mexico and one is shared with the United States (Burks 1979, Melika and Abrahamson 2002, Medianero and Nieves-Aldrey 2010, Melika et al. 2011, Nieves-Aldrey et al. 2012, Pujade-Villar et al. 2018).

The morphological characteristics of adults and their galls are very uniform amongst the most well-known *Amphibolips* species. The galls induced by species of this genus develop mainly in buds, stems or leaves and are rarely found in acorns. They are usually globose or spindle-shaped and detachable, with a spongy parenchyma surrounding a central larval cell, sometimes supported by radiating filaments (Beutenmüller 1909, Kinsey 1937, Melika and Abrahamson 2002). The species of this genus can be easily recognised by the following diagnostic characteristics: antennae with 12 to 14 segments in females and 15 to 16 segments in males; body robust with strong coarse reticulate sculpture, notauli not well marked, mesoscutellum often emarginate posteriorly; metasomal tergites punctate posteriorly; metatarsal claws with a large secondary basal tooth; forewings usually more or less smoky and showing spots, bands or completely obscured; radial cell open; ventral spine of the hypopygium usually long and pointed apically, without setae forming an apical tuft (Melika and Abrahamson 2002, Medianero and Nieves-Aldrey 2010, Melika et al. 2011).

Before 1937, only two species had been described in Mexico (*A. palmeri* Bassett, 1890 and *A. nigra* Beutenmüller, 1911) (Bassett 1890; Beutenmüller 1911, 1917). In 1937, Kinsey described nine species, six of which he grouped in the “*niger*” complex;

the remaining three (*A. dampfi* Kinsey, 1937, *A. nassa* Kinsey, 1937 and *A. fusus* Kinsey, 1937) were not grouped. Melika et al. (2011) described two new species: *A. zacatecaensis* Melika & Pujade-Villar, 2011 and *A. hidalgoensis* Pujade-Villar & Melika, 2011. Parallel to the “*niger*” complex proposed by Kinsey (1937), a second group, the “*nassa*” species complex, was proposed and a species identification key was provided for *A. palmeri*, *A. dampfi*, *A. nassa*, *A. hidalgoensis*, *A. zacatecaensis* and *A. fusus*. Nieves-Aldrey et al. (2012) described seven new species outside of those in the “*niger*” group, raising the number of known species to 13. In the referenced paper, the “*nassa*” complex was criticised as useless, based on the assumption that it did not reflect the extant species diversity outside of the “*niger*” group, as the complex omitted the anterior wing colouration pattern, which was important for some of the species described by Kinsey, such as *A. dampfi*, *A. fusus* and *A. nassa* (Nieves-Aldrey et al. 2012). More recently, an additional species (*A. cibriani* Pujade-Villar, 2018) was described within the “*nassa*” group (Pujade-Villar et al. 2018), resulting in a total of 20 species of *Amphibolips* recorded from Mexico.

The objective of this study is to present a description of three new species of the *Amphibolips* genus in Mexico. One of these species represents the first record of *Amphibolips* for the State of Veracruz (*A. nigrialatus* Nieves-Aldrey & Castillejos-Lemus, new species) and the other two species were collected in the State of Oaxaca. One of the species from Oaxaca induces a strikingly-characteristic gall (*A. magnigalla* Nieves-Aldrey & Castillejos-Lemus, new species), while the other species from Oaxaca (*A. kinseyi* Nieves-Aldrey & Castillejos-Lemus, new species) shares characteristics with *A. magnigalla* and with another species previously described from Oaxaca (*A. dampfi* Kinsey, 1937). The species richness of this genus in Mexico is discussed, as well as the taxonomic problems existing within the group. An update to the identification key given in Nieves-Aldrey et al. (2012) is provided, including the new species described herein. This work is part of a larger study of the revision of the *Amphibolips* species of Mexico, which includes extensive sampling throughout most of Mexico. Rich materials of *Amphibolips* have been collected, including possible additional new species and are being studied with a phylogenetic approach, including genetic tools. The results will be published elsewhere.

Material and methods

Study material

Quercus species of the *Lobatae* section were sampled in Veracruz State in 2008 and in Oaxaca in 2018. The galls were collected directly from oak trees and stored in plastic containers with plastic or mesh lids until the emergence of the wasps. The emergence of the wasps occurred under laboratory conditions. The voucher specimens and their galls were deposited in the entomological collections of the Museo Nacional de Ciencias Naturales in Madrid, Spain and in the Colección Nacional de Insectos of the Instituto de Biología, Universidad Nacional Autónoma de México, Mexico City, Mexico. The *Quercus* species were identified by Dr Susana Valencia-Ávalos at the Facultad de

Ciencias of the Universidad Nacional Autónoma de México (UNAM). Voucher specimens were deposited in the Herbarium of the Facultad de Ciencias and in the Escuela Nacional de Estudios Superiores, Unidad Morelia (ENES-Morelia) of the UNAM. Observations on the habitats, distribution or affinities of the host *Quercus* species were mainly based on Valencia-Ávalos (2004), but other publications on *Quercus* species were also consulted.

Examination of types

The type specimen of *Amphibolips dampfi* Kinsey, 1937 was examined for comparison with the new species described. The male holotype of this species was borrowed from the American Museum of Natural History, New York (AMNH) (James Carpenter).

Specimen preparation

The images used for the morphological descriptions were taken with a FEI Quanta 200 (Oregon, EU) scanning electron microscope (SEM) in Madrid (Spain) and with a JEOL JSM-IT300 (Tokyo, Japan) SEM in Morelia (Mexico). For the SEM observations, two strategies were followed, depending on the number of individuals available for a given species. For the preservation of some unique specimens mounted in a conventional manner, a low vacuum technique was used without gold coating. When the number of specimens allowed it, some specimens were dissected in 99% alcohol and mounted in stubs to be coated with gold and observed with a high vacuum technique. The forewings were mounted on slides with euparal and examined with a Wild MZ8 and an Olympus SZX10 stereomicroscope. Images of the wings and adult habitus were acquired with a NIKON Coolpix 4500 digital camera attached to a Wild MZ8 light microscope, with the exception of some images taken with an Olympus SC100 camera with the help of CELLENS STANDARD software. Measurements were made with a micrometric eyepiece calibrated to a Wild M5A stereomicroscope. Photographs of galls in the field and of gall dissections were taken with a Nikon D5300 camera.

Morphological terms

The terminology of the morphological structures and abbreviations follow that of Ronquist and Nordlander (1989), Nieves-Aldrey (2001) and Liljeblad et al. (2008). For wing venation, we follow Ronquist and Nordlander (1989) and for the terminology of the forewing cells, we follow Richards and Davies (1977). For sculpture terminology, we follow Harris (1979). The measurements of the structures were made according to Nieves-Aldrey (2001). The abbreviations used include F1–F12 for the antennal flagellomeres, **POL** (post-ocellar distance) for the distance between the inner margins of the posterior ocelli, **OOL** (ocellar-ocular distance) for the distance from the outer margin of a posterior ocellus to the inner margin of a compound eye and **DOL** (diameter of a lateral ocellus).

Results

Amphibolips magnigalla Nieves-Aldrey & Castillejos-Lemus, sp. nov.

<http://zoobank.org/34858B85-8A3C-4675-9ADD-76BABA811ABA>

Figs 1–5

Type material. *Holotype*: 1♀ in the Museo Nacional de Ciencias Naturales, Madrid, Spain (MNCN), mounted (glued) on a card. Mexico, Oaxaca, Comaltepec, 17°33'50"N, 96°33'20"W, ca. 2330 m alt.; ex gall *Quercus zempoaltepecana* (*Quercus* sect. *Lobatae*), gall collected 21/04/2018, insect emerged 30/04/2018. D. Castillejos-Lemus leg. *Paratypes*: 5♂, same data as holotype but emerged 1-3/05/2018. Two paratype ♂ were dissected and mounted on a stub for SEM observation in the MNCN. Other materials: 4♂, same data as paratypes, preserved in ethanol (in MNCN and Castillejos-Lemus collection, Morelia, Mexico). Additional material: 3 galls, one dissected (in MNCN).

Etymology. Named after the strikingly-large size of the galls of this species.

Diagnosis and comments. This new species belongs to the group of *Amphibolips* species that have a forewing with a transversal clear band that is variable in size and extends towards medial and cubital veins to the ventral margin of the wing (Nieves-Aldrey et al. 2012). The aforementioned group comprises *Amphibolips castroviejo* from Panama, *Amphibolips trizonata* Ashmead, 1896 from Arizona (USA) and the Mexican *Amphibolips durangensis* Nieves-Aldrey & Maldonado, 2012, *A. dampfi* and the recently described *A. cibriani* Pujade-Villar, 2018 (Pujade-Villar et al. 2018). However, the forewing pattern of the new species is different from that of all the referenced species. The transversal clear band is larger and broader and extends to two-thirds of the radial cell in both sexes and the basal third of the wing is more heavily infuscate in the male (Fig. 4A, B).

Amphibolips magnigalla shares with *Amphibolips dampfi*, *A. castroviejo* and the other two new species described herein, a mesoscutellum emarginate posteriorly. However, the emargination is comparatively less deep in *A. magnigalla* (Figs 1C, 2C). Besides the main character of the forewing, the four species can be readily distinguished by the characters provided in the identification key in this paper.

Regarding the gall, the new species is easily distinguished by its large spindle-shaped gall (approximately 10 cm in length × 2.5 cm in diameter), which is at least 2× larger than any other spindle-shaped gall described from Mexico. *Amphibolips fusus* and *A. durangensis* induce galls morphologically similar to the gall of the new species. However, besides the differences in size, the inner structure of the gall induced by the referenced species is different, being filled with a dense soft tissue, while the inner structure of the gall induced by the new species is often almost empty, with visible radiating filaments from the central larval cell.

Description. Body length: 5.8 mm (n = 1) for females; 5.2 mm (n = 3) for males.

Female (Fig. 4C). Body almost entirely black; antennae, except two basal segments, mandibles, metasoma ventrally, hypopygium and parts of tibiae and tarsi, chestnut. Forewing predominantly black infuscate, except a wide clear transversal band that starts in the distal two thirds of radial cell and extends towards discoidal and

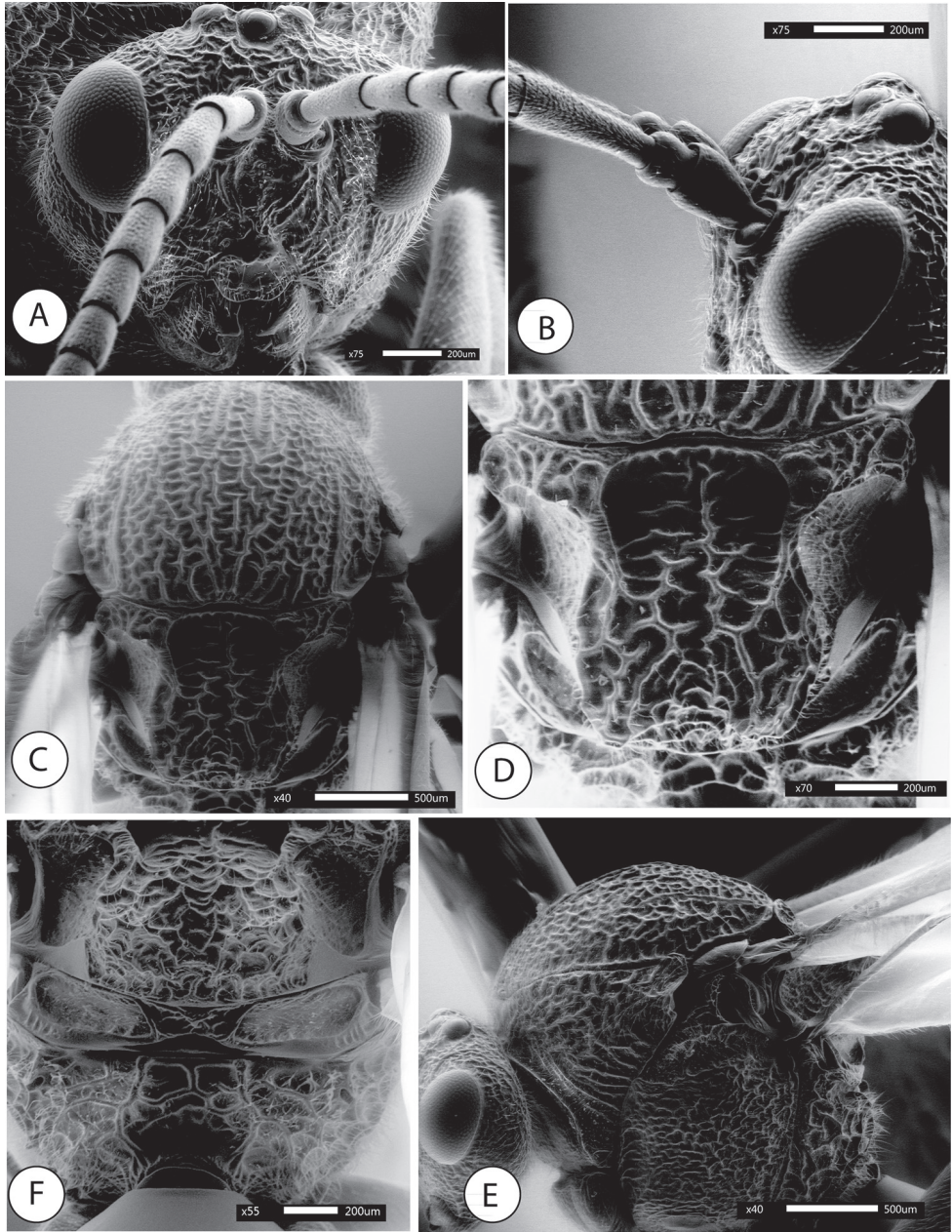


Figure 1. *Amphibolips magnigalla* sp. nov., female **A** head, anterior view **B** frons and vertex **C** mesosoma, dorsal view **D** scutellum, dorsal view **E** mesosoma, lateral view **F** propodeum.

cubital cell, almost reaching ventral margin of forewing. Another non-infusate band extended from the posterior part of the costal cell towards the Rs+M vein and reached the cubital vein (Fig. 4A).

Head, in dorsal view 2.3× wider than long. POL:OOL:DOL as 23:44:14. Head in anterior view (Fig. 1A) 1.2× wider than high, gena slightly broadened behind eye. Vertex, frons, lower face, gena and occiput with strong reticulate-rugose sculpture (Fig. 1B); two longitudinal carina present, extending from ventral margin of toruli to converge towards the anterior tentorial pits; irradiating carinae from clypeus absent; head moderately pubescent, except in vertex and frons. Clypeus more or less hexagonal, ventral margin strongly projecting over mandibles and slightly sinuate on anterior margin. Anterior tentorial pits well visible; epistomal sulcus and clypeo-pleurostomal lines slightly discernible. Malar space 0.7× height of compound eye. Toruli situated mid-height of compound eye; transfacial line 1.4× height of an eye; distance between antennal rim and compound eye slightly shorter than width of antennal socket including rim. Ocellar plate slightly raised.

Head posterior view (male) (Fig. 2B), heavily pubescent, with occiput coarsely rugose; dorsally the sculpture is transversely ribbed. Two carinae present, arising from dorsal part of the occipital foramen and ventrally continuing past posterior tentorial pits; posterior tentorial pits rounded; gular sulci united meeting at hypostoma. Posterodorsal margin of oral foramen not margined medially; hypostomal ridges well separated.

Mouthparts (male) (Fig. 2A), mandibles strong, exposed; with dense setae in base, right mandible with three teeth; left with two teeth. Cardo of maxilla not visible, maxillary stipes 4.1× as long as wide. Maxillary palp with five segments. Labial palp with three segments; apical peg of last labial and maxillary segments present.

Antenna (Fig. 3C), of moderate length, 0.5× as long as body length; with 13 antennomeres; flagellum not broadening towards apex; with relatively long, erect setae. Relative length/width of antennal segments as: 0.29(0.16):0.12(0.16):0.44(0.15):0.32(0.14):0.25(0.15):0.24(0.16):0.21(0.15):0.19(0.15):0.17(0.14):0.16(0.15):0.16(0.15):0.16(0.15):0.32(0.14). Pedicel (Fig. 3C) short, small, broader than long, 0.4× as long as scape; F1 1.4× as long as F2. F8-F10 as long as wide, F11 2.3× as long as wide, 2× as long as F10. Placodeal sensilla on F5-F11, disposed in dense rows of 6–8 sensilla, only in half dorsal area of each flagellomere.

Mesosoma in lateral view (Fig. 1E) 1.12× as long as high. Pronotum, moderately pubescent; lateral surface of pronotum with strong irregular reticulate rugose sculpture. Pronotum medially short; ratio of length of pronotum medially/laterally = 0.2. Pronotal plate indistinct dorsally.

Mesonotum. Mesoscutum (Fig. 1C) barely pubescent and with strong reticulate-rugose sculpture, the interspaces smooth and shining. Notauli somewhat obscured by the coarse sculpture, but visible; strongly convergent posteriorly; longitudinal median impression, not discernible. Anteroadmedian signa quite visible, extended back to near one half of mesoscutum; parapsidal signa distinct. Transscutal fissure narrow, sinuate. Mesoscutellum 1.2× as long as wide; about 0.7× as long as mesoscutum. Scutellar foveae (Fig. 1D) rounded, elongated posteriorly, about 0.5× as long as mesoscutellum, separated medially by a groove, the foveae are deep, mostly smooth anteriorly and crossed posteriorly by irregular transversal rugae, the intervals smooth, posterior margins indistinct. Mesoscutellum strongly coarsely rugose, with a deep and broad median

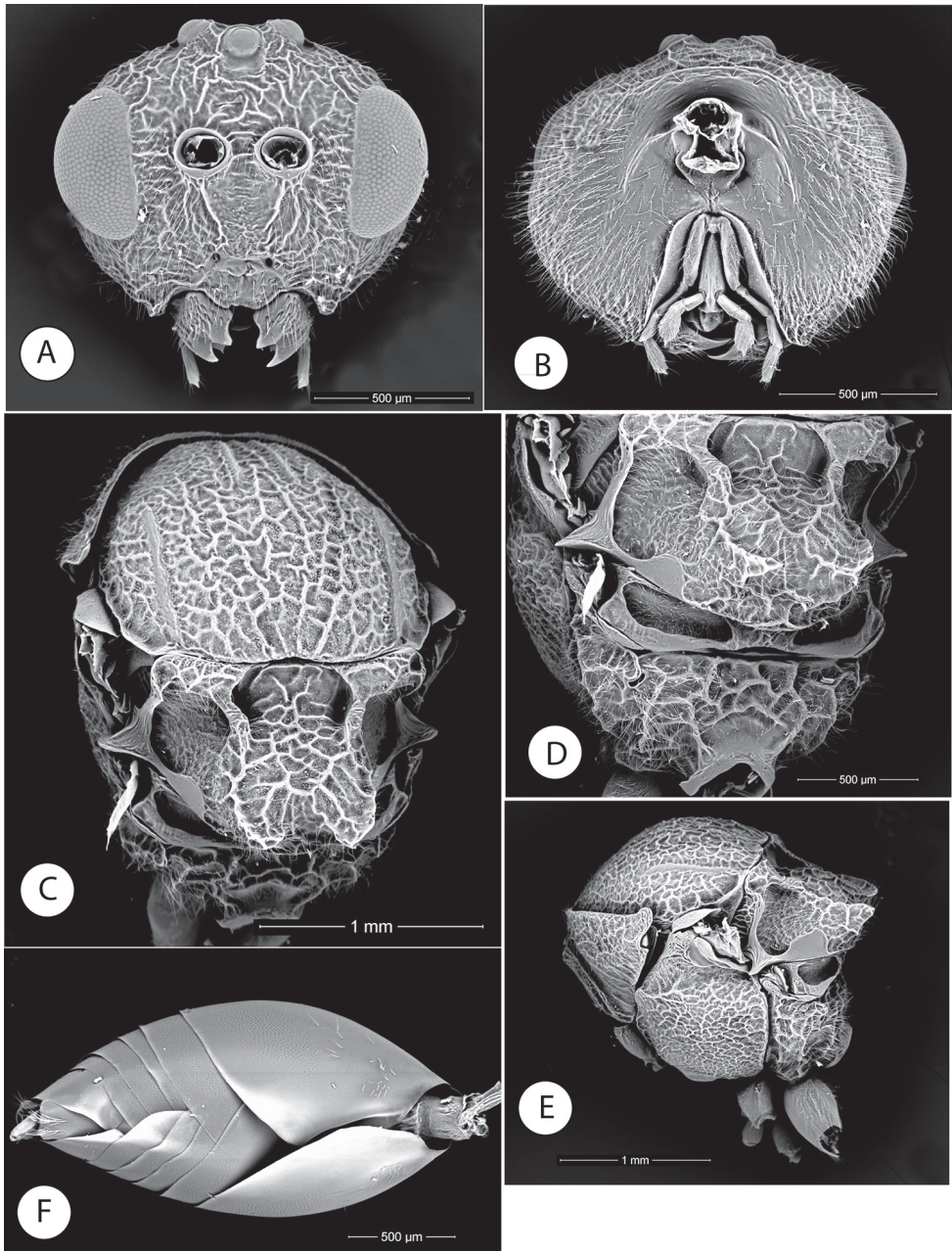


Figure 2. *Amphibolips magnigalla* sp. nov., male **A** head, anterior view **B** head, posterior view **C** mesosoma, dorsal view **D** scutellum and propodeum **E** mesosoma, lateral view **F** metasoma, ventral view.

longitudinal impression which makes the mesoscutellum strongly emarginate posteriorly (Fig. 1D); the emargination reaches anteriorly the scutellar foveae. In lateral view, the posterior emargination of mesoscutellum is seen as two, slightly curved upwards,

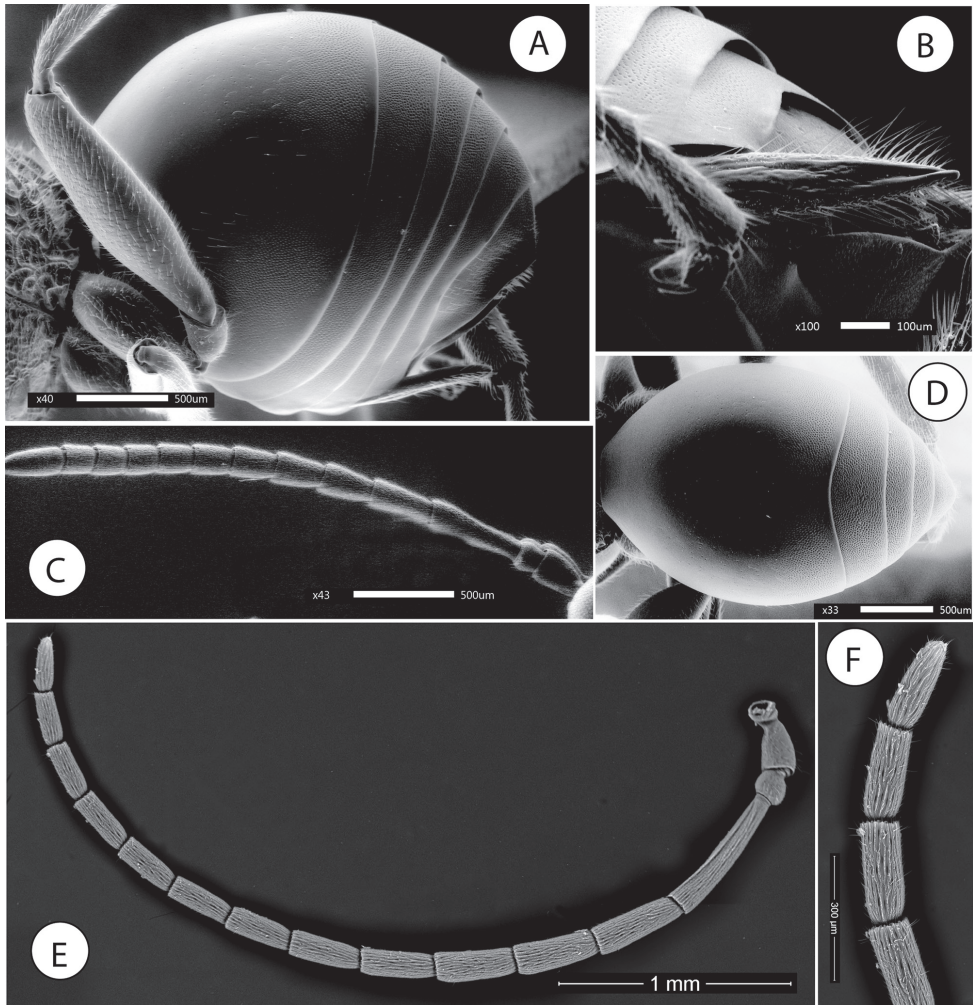


Figure 3. *Amphibolips magnigalla* sp. nov. **A** female metasoma, lateral view **B** female hypopygium, ventral view **C** female antenna **D** female metasoma, dorsal view **E** male antenna **F** detail of apical flagellomeres in male antenna.

horn-like projections. Mesoscutellum in lateral view with the posterodorsal extension of body of subaxillary strip short, not reaching one half of mesoscutellar height. Mesopleuron coarsely reticulate rugose, the rugae not as strong as in mesoscutum (Fig. 1E).

Metanotum. Metapectal-propodeal complex. Metapleural sulcus reaching posterior margin of mesopectus at about mid-height of metapectal-propodeal complex. Metascutellum rugose; metanotal trough smooth and pubescent. Median propodeal area (Fig. 1F) with some irregular strong longitudinal and transversal rugae; and densely pubescent; lateral propodeal carinae distinct, subparallel anteriorly and converging posteriorly.

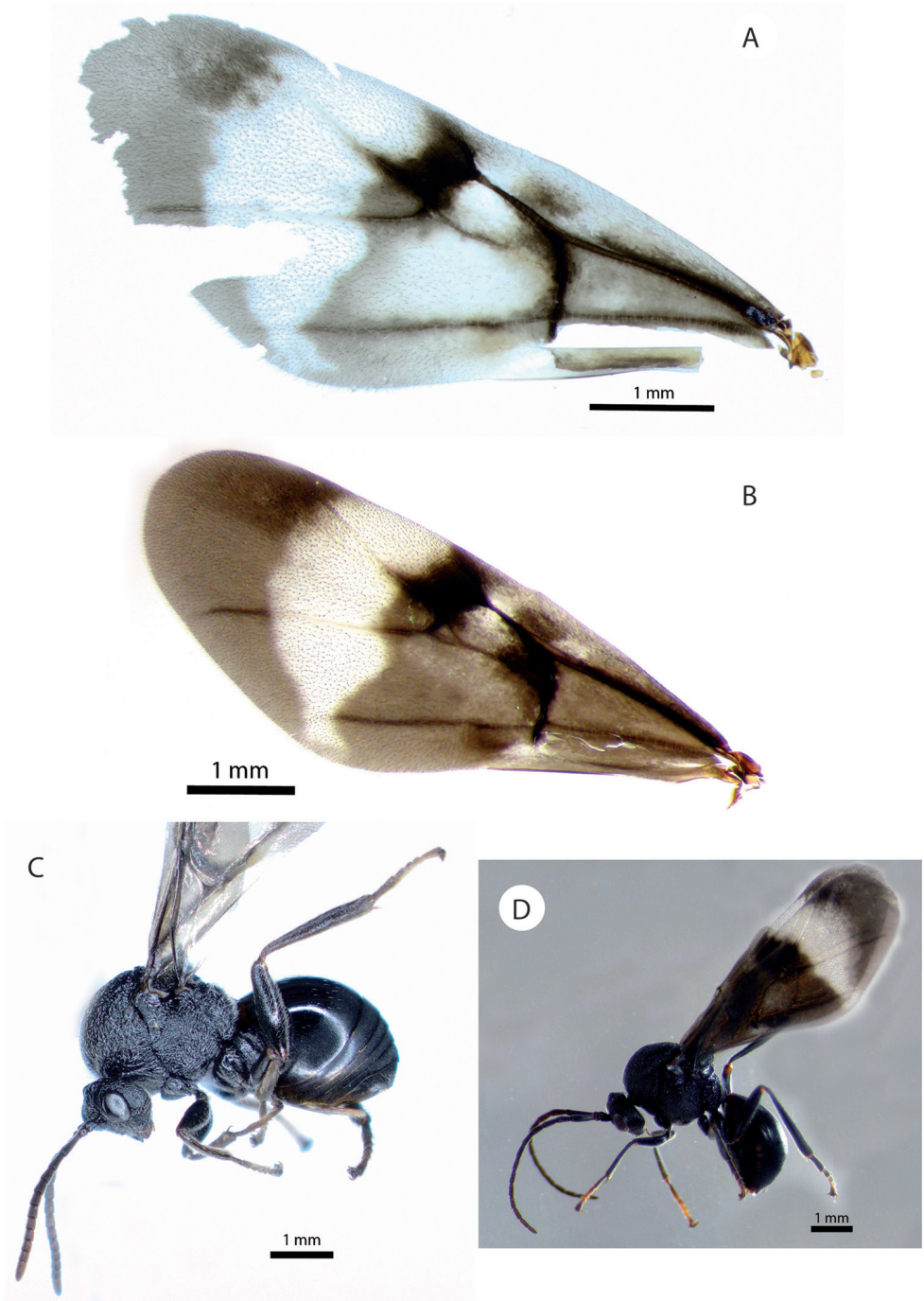


Figure 4. *Amphibolips magnigalla* sp. nov. **A** female forewing **B** male forewing **C** female habitus **D** male habitus.

Legs. Densely pubescent; femora and tibiae robust. Metatibia about as long as metatarsus; apical margin of metatarsomeres 1–4, with long strong erect setae. Metatarsal claws with strong triangular basal lobes or teeth.

Forewing (Fig. 4A), about as long as body, radial cell 3.2× longer than wide; open along anterior margin; areolet obsolete, obscured by infuscation. M and Cu1 veins nearly straight, not reaching wing margin. Rs+M not reaching basalis. First abscissa of radius (2r) slightly angled, not projected. Cu1 vein not branched in two veins. Apical margin with very short or obsolete hair fringe.

Metasoma (Fig. 3A, D), in dorsal view 1.6× as long as wide, in lateral view 1.2× as long as high. Second metasomal tergite covering about 0.7× length of metasoma. Anterior 2/3 smooth and shining; posterior one third with a band of micropunctures clearly visible; the punctate sculpture extended on subsequent tergites; ventral area of second metasomal tergite moderately pubescent. Projecting part of hypopygial spine moderately long (Fig. 3B); 4.6× as long as high in lateral view; laterally with long setae, longer than spine width, but not forming an apical patch.

Male (Figs 2A–F, 4B, D). Differs from the female as follows: smaller size, length 5.2 mm on average (n = 3). Body and wings almost completely black, except tarsomeres of anterior legs and apical segments of antennae. Antennae, legs and wings relatively longer. Antenna (Fig. 3E) with 14 segments. Antennal formula as: 0.24(0.15):0.13(0.15):0.6(0.11):0.39(0.13):0.35(0.14):0.35(0.14):0.32(0.12):0.31(0.11):0.28(0.11):0.27(0.1):0.27(0.1):0.27(0.1):0.26(0.1):0.24(0.1):0.23(0.08). F1 slightly curved and enlarged apically and flattened ventrally, 1.5× as long as F2; placodeal sensilla present in all the flagellomeres (Fig. 3F). Head 1.3× as wide as high; apical part of gena slightly expanded. Mesoscutellar impression not reaching the scutellar foveae (Fig. 2D). Scutellar foveae confluent, not separated by a sulcus. Forewing relatively longer 1.2× as long as body. Almost completely black, except the distal transversal clear band (Fig. 4B).

Gall (Fig. 5A–D). A large spindle-shaped gall with an elongated and narrow tip and base. The galls measure 100 × 25 mm on average. The surface of the gall is smooth, but some superficial longitudinal ridges are visible. The gall is monothalamic; the outer shell is thin, flexible and of fleshy consistency when it is fresh and becomes soft and light when it dries. They are light green without spots when they are fresh and light brown when they are dry. Internally (Fig. 5C), there is an oval larval cell in the centre of the gall (0.35 mm thick and 7 × 5 mm; n = 1). A spongy tissue occupies the entire space between the epidermis and the larval chamber, the outer shell is weakly attached to the internal spongy tissue when fresh and when the gall dries, the spongy tissue allows us to observe the radiant filaments, which extend from the larval chamber towards the internal walls of the galls (Fig. 5D). When it is dry, the gall is very fragile and can be easily crushed. At least half of the galls no longer showed spongy tissue when they were transferred to the laboratory. This caused the galls to collapse due to the fragility of the epidermis. Some of these collapsed galls presented internal modifications in the epidermis, probably caused by inquilines.

The galls develop on twigs of *Quercus zempoaltepecana* Trel. The gall closely resembles that of *Amphibolips durangensis* Nieves-Aldrey & Maldonado, 2012. However, the gall of *A. magnigalla* is distinguished by its larger size, which is at least 2× longer than that of *A. durangensis* and by its different internal structure, which is filled with less dense spongy tissue and radiant filaments (easily visible in the older galls).

Distribution. *A. magnigalla* was found only in one site: Comaltepec (Oaxaca State, Mexico). The galls were relatively abundant on a single isolated tree, while we did not find galls on the nearby trees.

Biology. Sexual generation. The galls were collected at the end of April and the insects emerged shortly thereafter, in early May. It seems that it is normal for many insects to feed on the tissue of this species. A detached gall was observed in a field, relatively far from the tree, probably carried by a bird.

***Amphibolips kinseyi* Nieves-Aldrey & Castillejos-Lemus, sp. nov.**

<http://zoobank.org/5542112A-D80F-4FF1-BB9F-623D326833BC>

Figs 6–8, 9B, D

Type material. *Holotype*: 1♀ in the Museo Nacional de Ciencias Naturales (MNCN), Madrid, Spain, mounted (glued) on a card. Mexico, Oaxaca, Pozuelos, Ixtlán, 17°22.52'N, 96°26.88'W, ca. 3040 m alt., ex gall *Quercus zempoaltepecana*. Collected 21/04/2018; emerged 04/05/2018. D. Castillejos-Lemus leg. *Paratypes*: 4♂ and 2♀, same data as that of holotype; 1♀ and 1♂ paratype dissected and mounted on a stub for SEM observation. Additional material in ethanol: 3♂ and 1♀ (in the collection of Castillejos-Lemus, Morelia, Mexico), 1♂ (in MNCN). Eighteen galls, one dissected (in the collection of Castillejos-Lemus and the Colección Nacional de Insectos-UNAM).

Etymology. Named after Dr Alfred Kinsey, one of the most prominent cynipidologists and the pioneer of the study of *Amphibolips* in Mexico.

Diagnosis and comments. *Amphibolips kinseyi* is very similar to *A. dampfi* Kinsey, 1937. We collected the new species in sites near where collections by A. Dampf were made (near Ixtlán, Oaxaca), the material of which was later described by Kinsey (Kinsey 1937). Both species share a strongly emarginate mesoscutellum and have a similar forewing colour pattern. However, after a close comparison with the male holotype, we found some diagnostic differences that allowed us to describe our specimens as different and new species. The forewings of the males of *A. dampfi* and *A. kinseyi* are similar, being predominantly black infuscate and have a reduced clear transversal band; however, in *A. dampfi*, the first radial abscissa (2r vein) is strongly angled and projected into the radial cell (Fig. 9C), while it is weakly angled and not projected in *A. kinseyi* (Fig. 9D). The postero-lateral projections of the mesoscutellum are more or less pointed or acute in the *A. dampfi* males (Fig. 9A), but are more rounded and flatter in the case of the new species (Fig. 9B). Additional distinguishing characters are given in the identification key provided herein. The female forewing of *A. dampfi* was not available for description, as it was apparently lost in the only female collected. However,

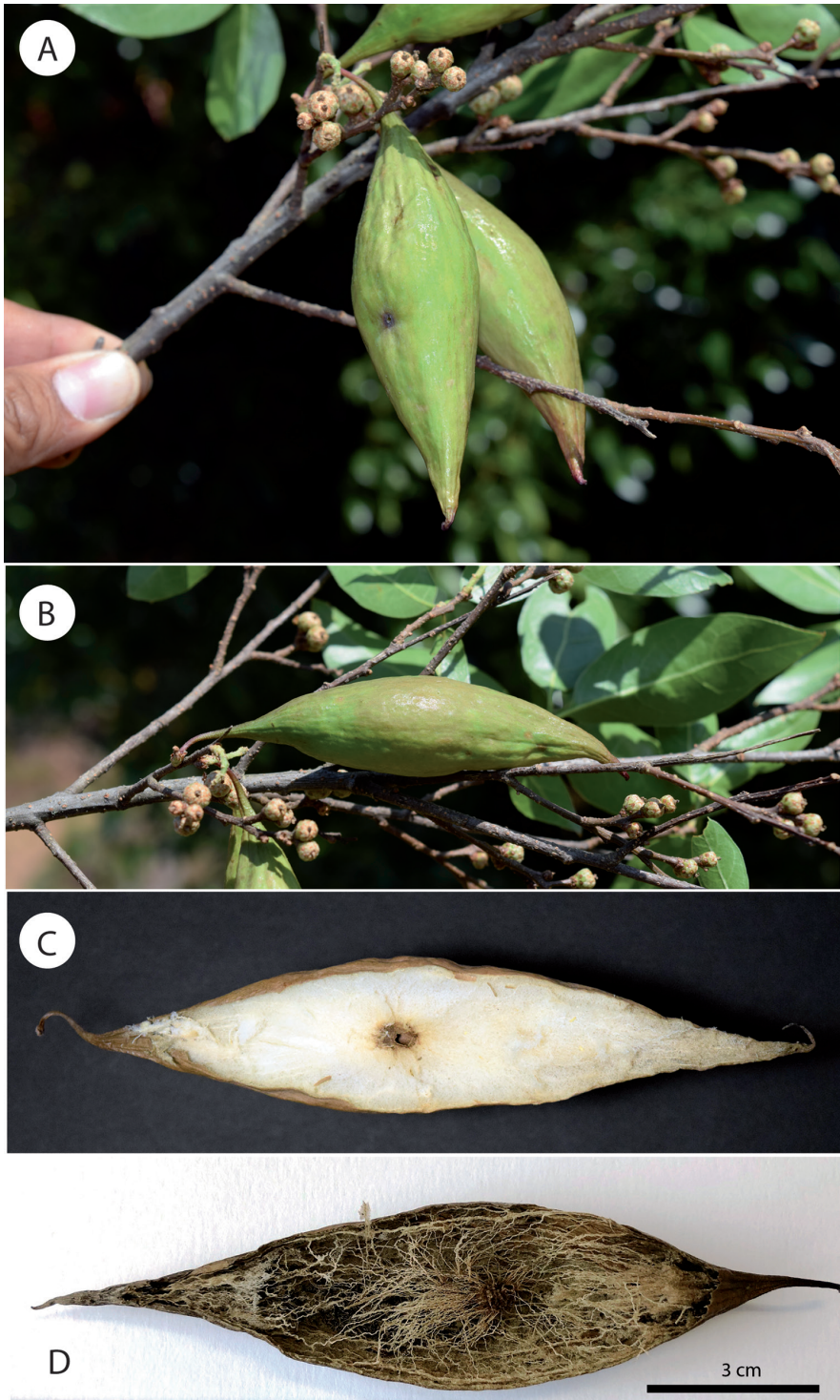


Figure 5. *Amphibolips magnigalla* sp. nov. **A–B** galls **C–D** sections of galls.

the female forewing of this closely-allied new species is described here. Consistent with other *Amphibolips* species from Mexico, the female forewing is different from the male forewing. In this case, the female forewing has a clear transversal band, which is larger and more extended than that of the male (Fig. 8C).

Description. Body length: 6.3 mm ($n = 1$) for females; 5.7 mm ($n = 3$) for males.

Female. Body predominantly black (Fig. 8A); head, except the red mandibles and the mesosoma, black; metasoma reddish postero-ventrally; antennal flagellum reddish in distal half; legs reddish except black basal part of coxae. Forewing (Fig. 8C) predominantly black infusate, but much less infusate above the cubital veins and below the M+Cu1 vein. There is a wide, clear, transversal band, which starts in the apex of the radial cell and extends towards the discoidal and cubital cells to the Cu1a vein but does not reach the latero-ventral margin of the forewing.

Head, in dorsal view $2.1\times$ as wide as long; $0.8\times$ as wide as mesosoma. POL $0.7\times$ the OOL; lateral ocelli separated from inner margin of an eye for a distance of $3\times$ the diameter of a lateral ocellus. Head in anterior view (Fig. 6A) $1.2\times$ wider than high, gena slightly broadened behind eye. Vertex, frons, lower face and gena, with strong coarsely-rugose sculpture. A medial frontal pit visible followed by a sulcus addressed to the median ocellus. Face with two longitudinal carinae visible, extending from ventral margin of toruli to converge towards the space between the anterior tentorial pits; irradiating carinae from clypeus virtually absent; head moderately pubescent, except in vertex and frons. Clypeus more or less hexagonal, ventral margin strongly projecting over mandibles and weakly sinuate on anterior margin. Anterior tentorial pits well visible; epistomal sulcus and clypeo-pleurostomal lines visible. Gena slightly depressed basally and projected over the mandibles. Malar space $0.7\times$ height of a compound eye. Toruli situated mid-height of compound eye; transfacial line $1.7\times$ height of an eye; distance between antennal rim and compound eye $0.8\times$ width of antennal socket including rim. Ocellar plate slightly raised.

Mouthparts (Fig. 6A), mandibles strong, exposed; with dense setae in base, right mandible with three teeth; left with two teeth.

Antenna (Fig. 6E), about one half as long as body length; with 13 antennomeres; 12 and 13 incompletely separated ventrally. Flagellum not broadening towards apex; with relatively long, erect setae. Relative length/width of antennal segments as: $0.28(0.16):0.16(0.16):0.52(0.16):0.38(0.16):0.3(0.17):0.24(0.16):0.24(0.17):0.2(0.17):0.2(0.17):0.2(0.16):0.18(0.16):0.16(0.15):0.3(0.14)$. Scape slightly longer than wide, flattened and smooth ventrally. Pedicel, short, small, as long as wide, $0.5\times$ as long as scape; F1 $1.3\times$ as long as F2, F11 2.3 times as long as wide, $2\times$ as long as F10. Placodeal sensilla present on flagellomeres F3-F11, disposed in dense rows of 6–8 sensilla, only in half dorsal area of each flagellomere. Coeloconic and trichoidea sensilla are also present and visible (Fig. 6F).

Mesosoma in lateral view $1.3\times$ as long as high. Pronotum, moderately pubescent; lateral surface of pronotum with strong irregular reticulate rugose sculpture (Fig. 6D). Pronotum medially short; ratio of length of pronotum medially/laterally = 0.2. Pronotal plate indistinct dorsally.

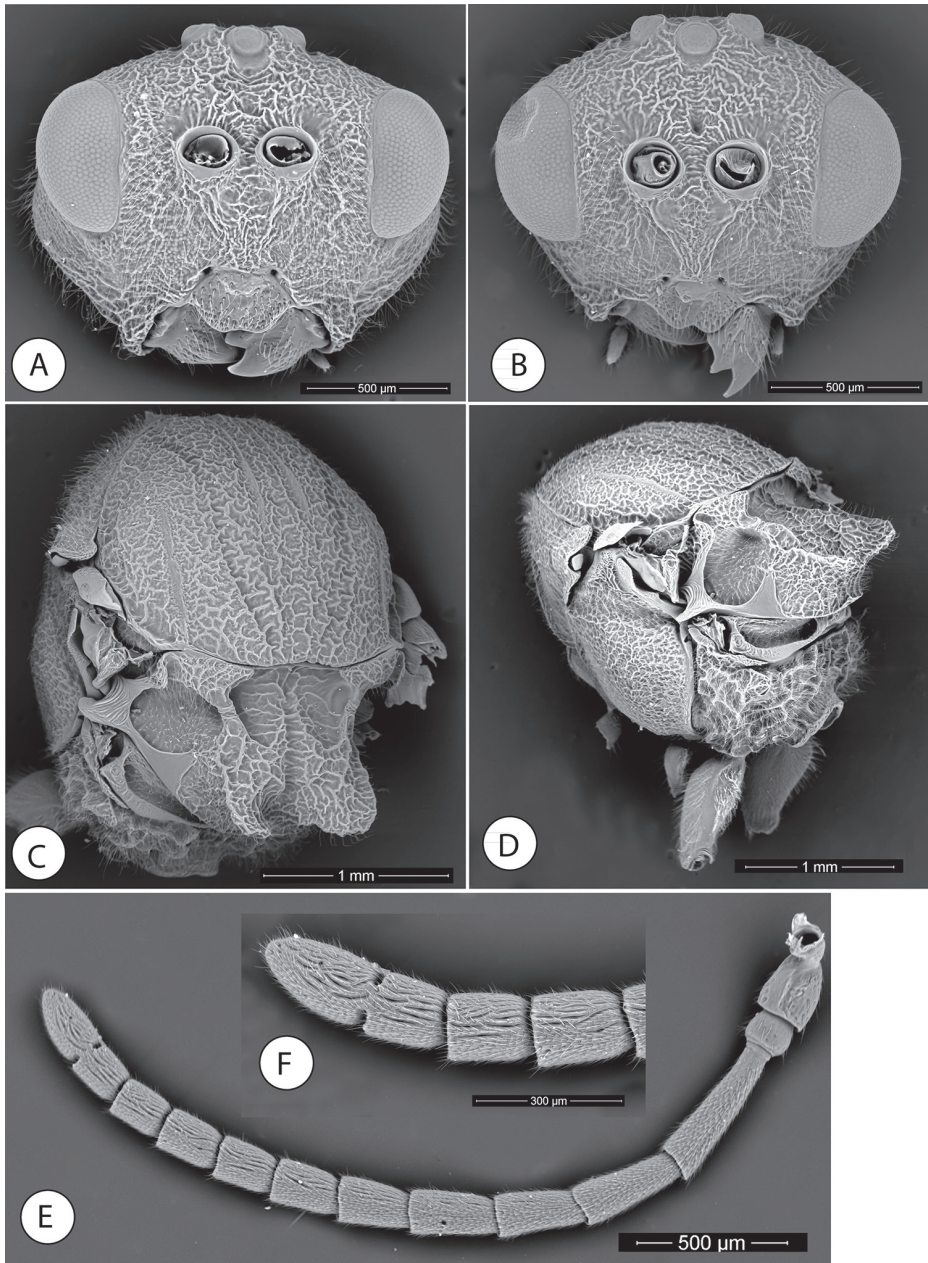


Figure 6. *Amphibolips kinseyi* sp. nov. **A** female head, anterior view **B** male head, anterior view **C–D** female mesosoma, dorsal and lateral view **E** female antenna **F** detail of last flagellomeres in female antenna.

Mesonotum. Mesoscutum (Fig. 6C) barely pubescent and with strong coarse reticulate sculpture, the interspaces smooth and shining. Notauli shallow and crossed by the general sculpture, but well visible and almost complete; longitudinal median

impression not visible. Anteromedian signa well marked, extended back to near one half of mesoscutum; parapsidal signa distinct. Transscutal fissure very narrow, sinuate. Mesoscutellum 1.3× as long as wide; about 0.5× as long as mesoscutum. Scutellar foveae ovoid elongated posteriorly, about 0.5× as long as mesoscutellum, separated medially by a deep groove, the foveae are deep, crossed by irregular transversal rugae, the intervals smooth, posterior margins shallowly indicated. Mesoscutellum strongly coarsely rugose, with a deep and broad median longitudinal impression which makes the mesoscutellum strongly emarginate posteriorly (Fig. 6C); the emargination reaches anteriorly the scutellar foveae. In lateral view, the posterior emargination of mesoscutellum appears as two rounded apically and slightly flat, curved upwards projections. In lateral view, the space between the mesoscutellar projections and the posterior limit of mesoscutellum is high. Axillula large, deep, heavily pubescent, with distinct margins. Mesoscutellum in lateral view with the posterodorsal extension of body of subaxillular strip long, nearly reaching upper margin of mesoscutellum. Mesopleuron coarsely reticulate rugose, the rugae not as strong as in mesoscutum.

Metanotum. Metapectal-propodeal complex. Metapleural sulcus obscured by the strong sculpture. Metascutellum weakly rugose; metanotal trough deep, smooth and pubescent. Median propodeal area with strong and coarse reticulate rugae; densely pubescent; lateral propodeal carinae distinct, subparallel anteriorly and converging posteriorly.

Legs. Densely pubescent; femora and tibiae robust. Femur 4× as long as wide; metatibia 1.6× as long as metatarsus; apical margin of metatarsomeres 1–4, with long strong erect setae. Metatarsal claws with strong triangular basal lobes or teeth.

Forewing (Fig. 8C), about 1.2× as long as body, radial cell 3.7× as long as wide; open along anterior margin; areolet very small, but visible. All veins heavily infuscate. M and Cu1 veins nearly straight, not reaching wing margin. Rs+M reaching basalis, well-marked. First abscissa of radius (2r) slightly angled, not projected. Cu1 vein not branched in two veins. Apical margin with very short or obsolete hair fringe.

Metasoma (Fig. 7D), in lateral view 1.3× as long as high. Second metasomal tergite covering about 0.6× length of metasoma. Anterior 2/3 smooth and shining; posterior one third with a band of micropunctures clearly visible; the punctate sculpture extended on subsequent tergites; ventral area of second metasomal tergite moderately pubescent, with a relatively dense patch of setae. Projecting part of hypopygial spine moderately long (Fig. 7D); about 5× as long as high in lateral view; laterally with long setae, longer than spine width, but not forming an apical tuft.

Male (Figs 6B, 7A, E, 8B, D). Differs from the female as follows: smaller size, length 5.7 mm on average ($n = 3$). Body and wings almost completely black, except the mandibles, metasoma ventrally, tarsomeres of legs and half of the apical flagellomeres of antennae which are more or less reddish (Fig. 8B). Antennae, legs and wings relatively longer. Antenna with 14 segments (Fig. 7A). Antennal formula (mean of four measured individuals) as: 0.29(0.18):0.15(0.16):0.69(0.16):0.46(0.15):0.40(0.15):0.41(0.15):0.38(0.14):0.36(0.14):0.34(0.14):0.34(0.14):0.31(0.14):0.32(0.13):0.29(0.12):0.25(0.11):0.23(0.11). F1 slightly curved, weakly enlarged apically and flattened ventrally, 1.5× as long as F2; placodeal sensilla present in all the flagellomeres. Head 1.3×

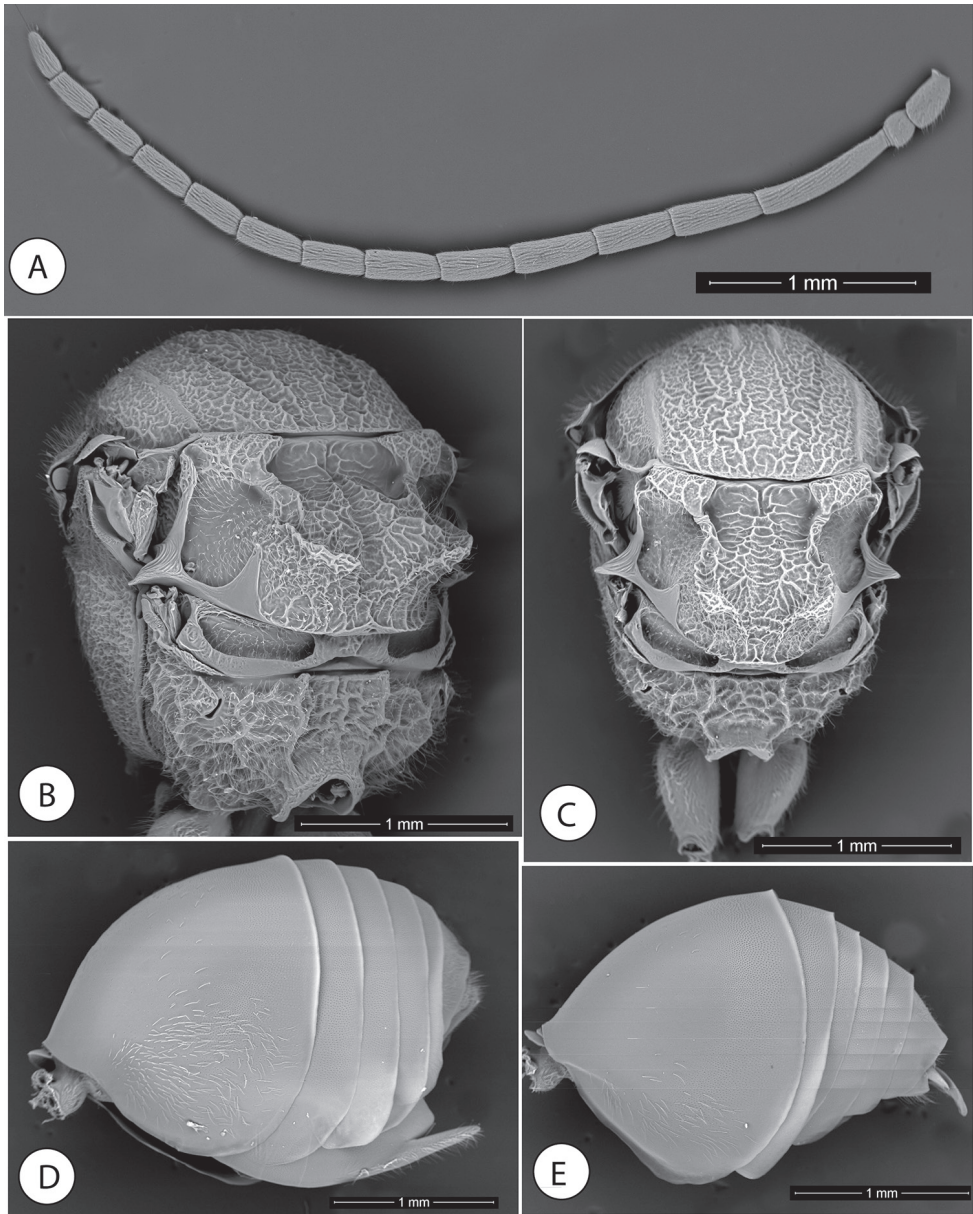


Figure 7. *Amphibolips kinseyi* sp. nov. **A** male antenna **B** female mesosoma, dorsolateral view **C** male mesosoma, dorsal view **D** female metasoma, lateral view **E** male metasoma, lateral view.

as wide as high; apical part of gena slightly expanded. Frontal pit distinct, prolonged by a groove towards median ocellus. Pair of frontal longitudinal carinae more convergent towards epistomal line (Fig. 6B). Projection of anterior margin of clypeus more incised. Forewing (Fig. 8D) relatively longer 1.3× as long as body. Almost completely black, except the distal transversal clear band that is much smaller and less extended.

Gall (Fig. 8E, F). The gall is similar to the gall of *Amphibolips dampfi* described by Kinsey (1937). A moderate to large “oak apple”, irregularly spherical gall with spongy inner consistency. Some are slightly elongated towards the apex. The surface is slightly rough when intact, but may have more pronounced irregularities, which cause deformations on the surface or in the general shape. Monothalamic. They are light green without spots when they are fresh and light brown when they are dry. The epidermis is thin, at 0.4 mm thick; firmly attached to the internal spongy tissue when fresh; firm and brittle when dry. The consistency is relatively hard and fleshy when green and brittle when dry. Internally, the spongy tissue occupies the entire space between the epidermis and the larval chamber (Fig. 8F). Diameter of 30 mm and height of 31 mm on average (diameter of 16 to 44 mm and height of 18 to 51 mm; $n = 18$). Rigid and oval larval cell, 0.4 mm thick and 6.5 mm long \times 5 mm in diameter on average ($n = 2$). Galls are formed on the twigs of *Quercus zempoaltepecana* Trel. Galls are relatively common in the study area.

Distribution. Known only from the type locality along the route from Ixtlán to Tepanzacoalcos (Oaxaca State, Mexico).

Biology. Sexual generation. The galls were collected in late April and the insects emerged shortly thereafter, in early May. It is normal to find galls deformed and/or attacked by inquilines and parasitoids; the deformed or attacked galls are usually relatively small.

***Amphibolips nigrialatus* Nieves-Aldrey & Castillejos-Lemus, sp. nov.**

<http://zoobank.org/679F3F98-B166-4677-832C-AF7C6E0DB97C>

Figs 10–13

Type material. Holotype: 1♀ in the Museo Nacional de Ciencias Naturales (MNCN), Madrid, Spain, mounted (glued) on a card. Mexico, Veracruz, Xico, in the Texolo waterfall, 19°24.11'N, 96°59.69'W, ca. 1170 m alt., ex gall *Quercus sapotifolia* Liebm. Collected 27/04/2008; emerged 04/2008. Nieves-Aldrey & Pascual leg.

Etymology. Named after the smoky black forewing.

Diagnosis and comments. *Amphibolips nigrialatus* is closely allied to *A. dampfi* Kinsey, 1937 and the new species *Amphibolips kinseyi*. Despite being based on a single female holotype, we found distinctive diagnostic characters that let us describe the specimen as belonging to a new species. The strongly-emarginate mesoscutellum relates the new species to *A. kinseyi* and *A. dampfi*, but in *A. nigrialatus*, the postero-lateral projections of the scutellum are pointed apically and curved upwards. Moreover, the scutellar foveae are very large in the new species, extending approximately one half of the length of the mesoscutellum, medially confluent and not separated by a carina or groove, while they are well separated by the mesoscutellar impression in the other two species. The forewing colour of *A. nigrialatus* is the darkest we have seen in females of *Amphibolips* species from Mexico and the black smoky colouration even extends to the costal and basal cells and below the cubital vein. In this last character,

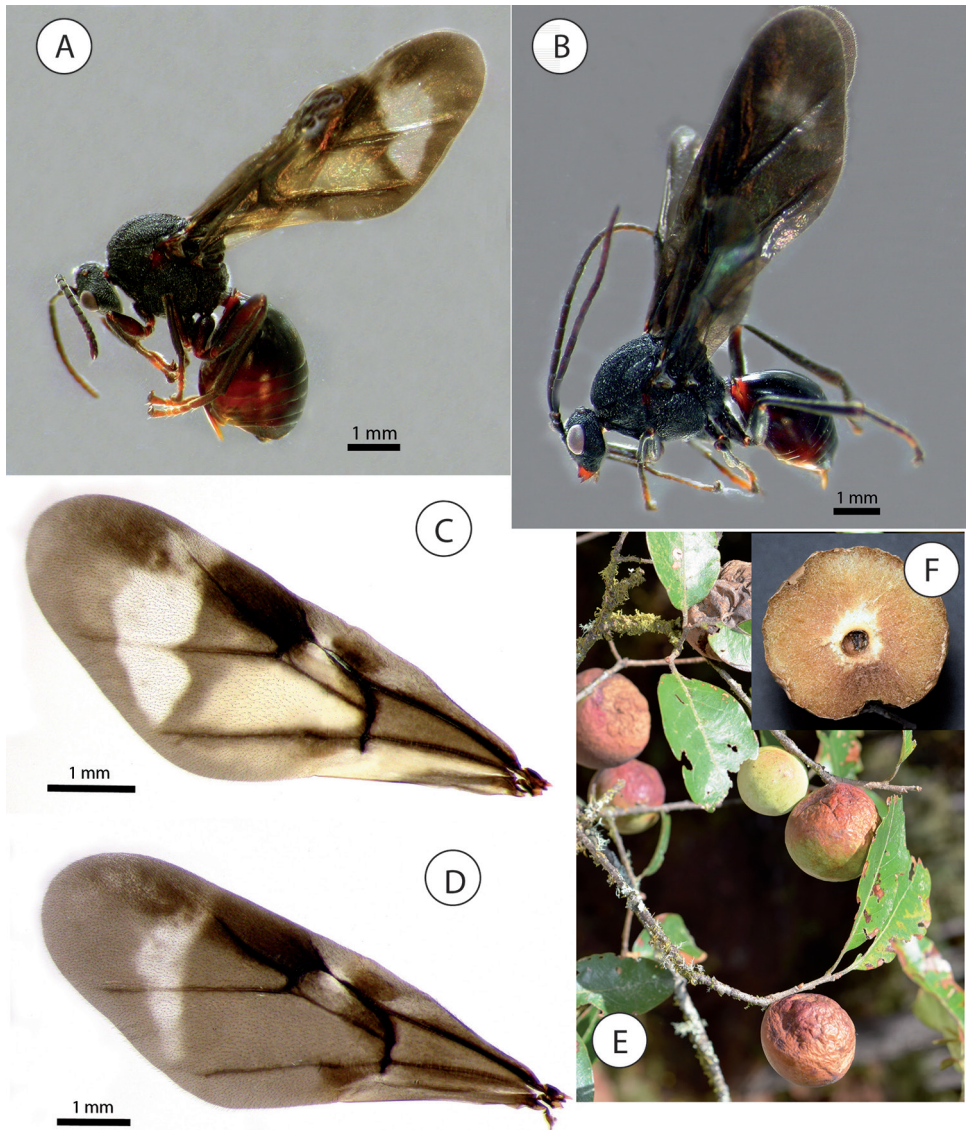


Figure 8. *Amphibolips kinseyi* sp. nov. **A** female habitus **B** male habitus **C** female forewing **D** male forewing **E** galls **F** section of a gall.

it resembles *A. castroviejoii* from Panama, but in this late species, the forewing area anterior to the transversal band is even darker (Fig. 15F), besides other distinguishing characters given in the identification key (transversal clear band larger, smooth scutellar foveae and visible notauli). The clear transversal band in the discoidal cell of forewing is very short and narrow in *A. nigrialatus*, measuring not more than one-fifth of the length of the radial cell (Fig. 13A), while in *A. kinseyi*, it is wider, measuring at least one-half the length of the radial cell (Fig. 8C). Additionally, the green spherical

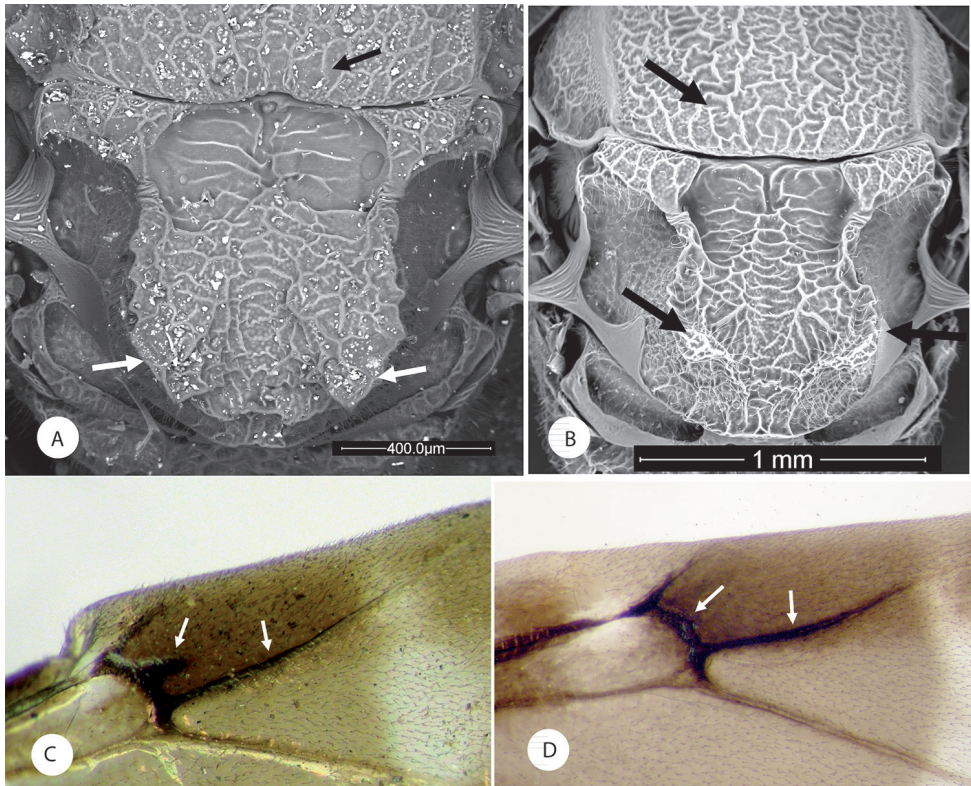


Figure 9. Comparison between *Amphibolips dampfi* and *A. kinseyi* sp. nov. **A** male mesoscutellum of *A. dampfi* **B** male mesoscutellum of *A. kinseyi* **C** radial cell of *A. dampfi* **D** radial cell of *A. kinseyi*.

gall of the new species (*A. nigrialatus*) on *Quercus sapotifolia* is distinguishable from the galls of *A. dampfi* and *A. kinseyi* on *Q. ocoteifolia* Liebm. and *Q. zempoaltepecana* Trel., respectively.

Description. Body length: 6.6 mm ($n = 1$) for the female.

Female. (Fig. 13B). Body almost completely black with the exception of the mandibles, the antennae apically, the metasoma ventrally, especially the hypopygium and parts of the legs, including the tarsi, which are reddish. Forewing predominantly black infusate, except a large basal area delimited by the medial and cubital veins and another smaller area above the medial vein. A small clear transversal band, that starts below the radial cell and extends towards the medial vein, but does not reach the cubital vein, is present (Fig. 13A).

Head, in dorsal view (Fig. 10A) $2.2\times$ as wide as long; narrower than mesosoma. OOL $1.4\times$ POL $0.7\times$ DOL; posterior ocelli separated from internal orbit of an eye by $2.2\times$ its diameter. Head in anterior view (Fig. 11A) $1.3\times$ as broad as high; gena slightly broadened behind eyes. Vertex, frons, lower face and gena, with coarse reticulate-rugose sculpture. Face with two longitudinal carinae, extending from ventral margin of toruli to converge towards the anterior tentorial pits; irradiating carinae from

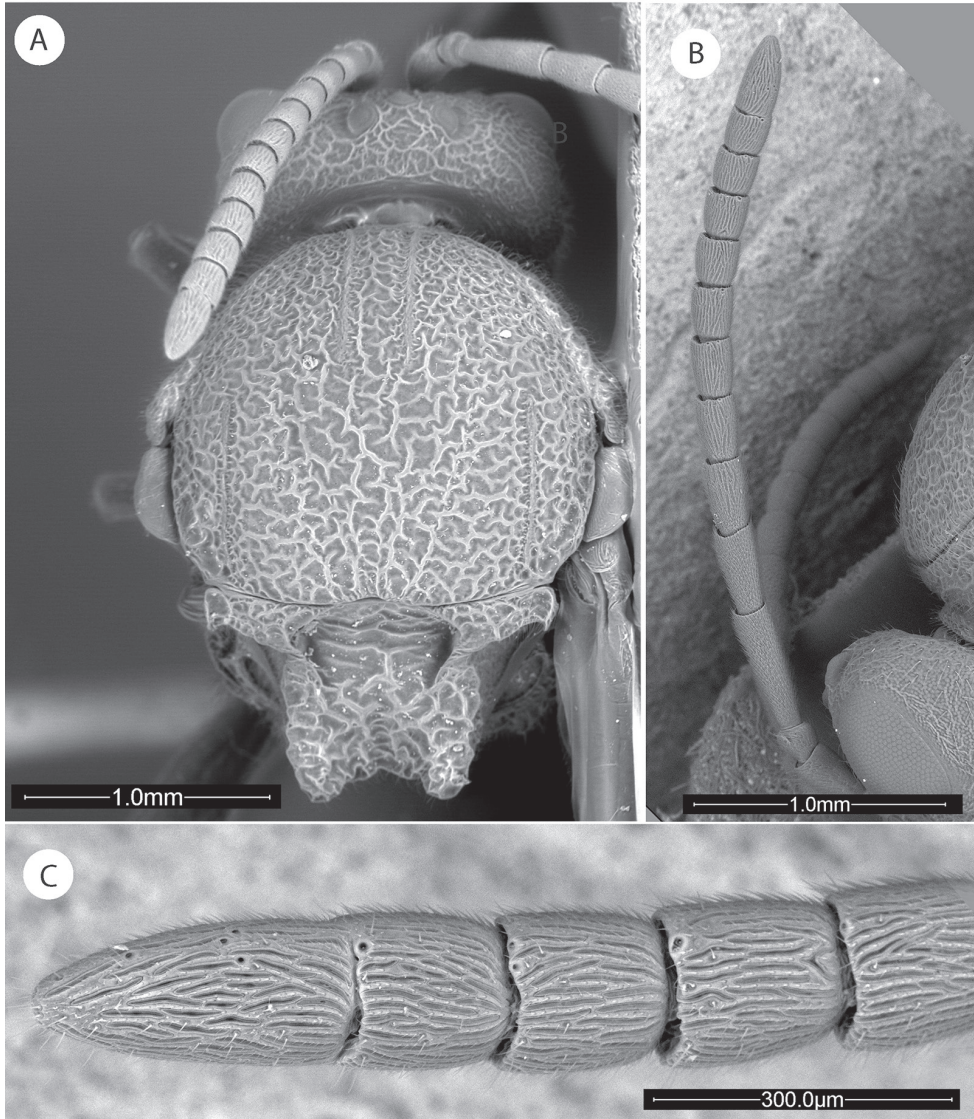


Figure 10. *Amphibolips nigrialatus* sp. nov., female. **A** head and mesosoma, dorsal view **B** antenna **C** detail of last flagellomeres.

clypeus indistinct or absent; head moderately pubescent, except in vertex and frons. Clypeus more or less hexagonal, ventral margin strongly projecting over mandibles and moderately incised or sinuate on anterior margin. Anterior tentorial pits well visible; epistomal sulcus and clypeo-pleurostomal lines also distinct. Malar space $0.8\times$ height of a compound eye. Toruli situated about mid-height of compound eye; transfacial line $1.7\times$ height of an eye; distance between antennal rim and compound eye almost equal to the width of antennal socket including rim. Ocellar plate slightly raised.

Mouthparts (Fig. 11A), mandibles strong, exposed, with dense setae in base, right mandible with three teeth, left with two teeth.

Antenna (Fig. 10B), 0.6× as long as body length; with 13 antennomeres; 12 and 13 incompletely separated (Fig. 10C). Flagellum not broadening towards apex; with relatively long, erect setae. Antennal formula : 0.4(0.22):0.16(0.18):0.58(0.18):0.36(0.18):0.32(0.18):0.28(0.18):0.26(0.18):0.24(0.18):0.23(0.18):0.2(0.18):0.2(0.18):0.18(0.18):0.34(0.16). Pedicel, short, 0.4× as long as scape and slightly broader than long. F1 1.6× as long as F2; F8–F10 as long as wide, F11 2.1× times as long as wide, 1.9× as long as F10. Placodeal sensilla present on flagellomeres F3–F11, disposed in dense rows of 8–10 sensilla, only in half dorsal area of each flagellomere.

Mesosoma in lateral view 1.1× as long as high. Pronotum, moderately pubescent; lateral surface of pronotum with strong irregular reticulate rugose sculpture (Fig. 11B). Pronotum medially short; ratio of length of pronotum medially/laterally = 0.23. Pronotal plate indistinct.

Mesonotum. Mesoscutum (Fig. 10A) barely pubescent and with strong coarse reticulate sculpture, the interspaces smooth and shining. Notauli indistinct, obscured by the coarse sculpture; more so in anterior one third of mesoscutum; longitudinal median impression indistinct. Anteroadmedian signa and parapsidal signa distinct. Transscutal fissure very narrow, sinuate. Mesoscutellum as long as wide; about 0.5× as long as mesoscutum. Scutellar foveae rounded transverse, about 0.5× as long as mesoscutellum, the scutellar foveae are confluent and not separated medially by a carina or groove; some transverse strong rugae visible with smooth and shining intervals. Mesoscutellum strongly coarsely rugose, with a deep and broad median longitudinal impression which makes the mesoscutellum strongly emarginate posteriorly (Fig. 10A); the emargination not reaching anteriorly the scutellar foveae. Postero-lateral projections of scutellum pointed apically and curved upwards (Fig. 11C, D). Mesopleuron coarsely reticulate rugose, the rugae not as strong as in mesoscutum (Fig. 11B). Mesoscutellum in lateral view with the posterodorsal extension of body of subaxillary strip short, not reaching one half of mesoscutellar upper margin.

Metanotum. Metapectal-propodeal complex. Metapleural sulcus distinct, reaching posterior margin of mesopectus at about mid-height of metapectal-propodeal complex. Metascutellum rugose; metanotal trough deep, smooth and pubescent. Median propodeal area with strong and coarse reticulate rugae; densely pubescent; lateral propodeal carinae distinct, subparallel anteriorly and converging posteriorly (Fig. 11E).

Legs. Densely pubescent; femora and tibiae robust. Metatibia about 1.7× as long as metatarsus. Metatarsal claws with strong triangular basal lobes or teeth (Fig. 12C).

Forewing (Fig. 13A), about 1.1× as long as body, radial cell 3.9× as long as wide; open along anterior margin; areolet absent. All veins heavily infuscate. M and Cu1 veins nearly straight, not reaching wing margin. Rs+M complete, reaching basalis. First abscissa of radius (2r) slightly angled, not projected into the radial cell. The two branches of the cubitalis vein are not interrupted by a gap. Apical margin with very short hair fringe.

Metasoma (Fig. 12A) in dorsal view 1.5× as long as wide; in lateral view 1.2× as long as high (Fig. 11F). Second metasomal tergite covering about 0.64× the length of metasoma. In dorsal view, anterior half of T2 smooth and somewhat shining, posterior half with two

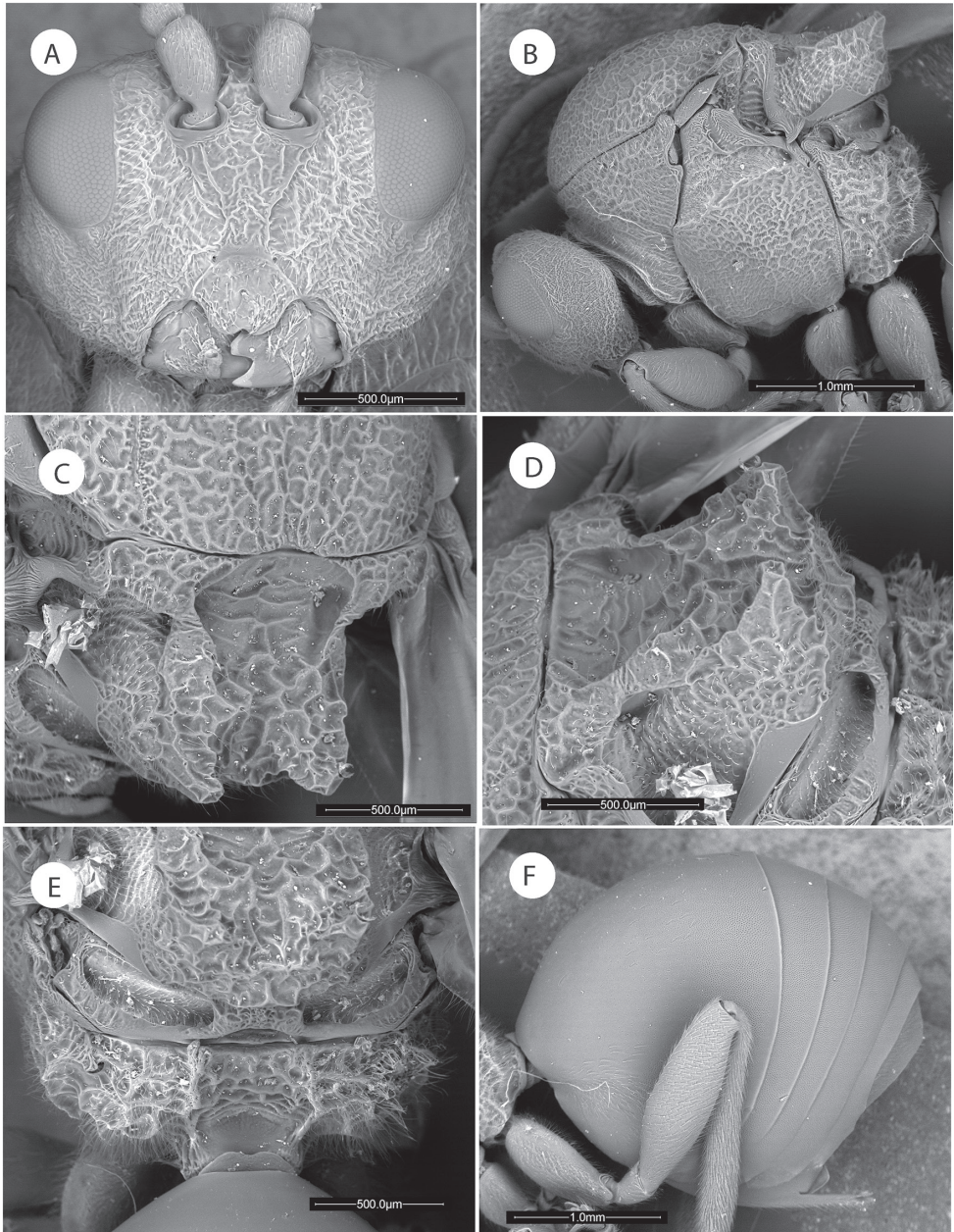


Figure 11. *Amphibolips nigrialatus* sp. nov., female. **A** head, anterior view **B** mesosoma, lateral view **C** mesoscutellum, dorsal view **D** mesoscutellum, lateral view **E** propodeum **F** metasoma, lateral view.

types of microsculpture clearly visible, first a series of slightly hexagonal cells and in the back micropunctures, both microstructures occupying the same proportion (Fig. 12B). In lateral view, anterior 2/3 smooth and somewhat shining; posterior one third with a band of micro-

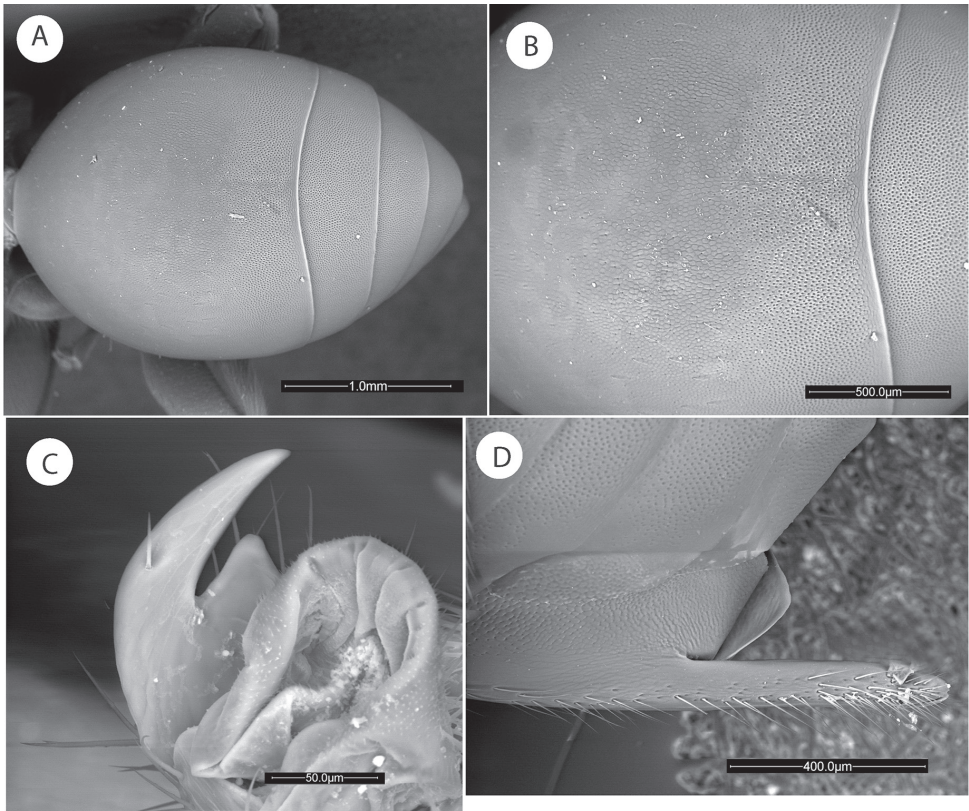


Figure 12. *Amphibolips nigrialatus* sp. nov., female. **A** metasoma, dorsal view **B** detail of sculpture **C** metatarsal claw **D** ventral spine of hypopygium, lateral view.

punctures clearly visible. The punctate sculpture extended on subsequent tergites. Ventral area of second metasomal tergite moderately pubescent, with a relatively dense patch of setae. Projecting part of hypopygial spine long (Fig. 12D); about 6.3× as long as high in lateral view; laterally with long setae, longer than spine width, but not forming an apical tuft.

Male. Unknown.

Gall (Fig. 13C). A regular, spherical, moderately-sized gall with a green colour when it is fresh. When dry, the gall acquires a rough and slightly elongated appearance and turns brown in colour. The galls measure on average 16.5 × 21.5 mm (diameter of 14 to 19 mm and length of 17 to 25 mm; n = 4). The gall is monothalamic. The outer shell is thin, flexible and of fleshy consistency when fresh and becomes rigid and hardly detachable from the parenchyma when dry. Internally, there is a spherical larval cell in the centre of the gall (5 × 5 mm; n = 1); a spongy tissue occupies the entire space between the epidermis and the larval chamber and is hardly separable from the larval chamber. When it is dry, the gall is moderately fragile.

On twigs of *Quercus sapotifolia* Liebm. Closely resembles that of *Amphibolips oaxaca* Nieves-Aldrey & Pascual, 2012, *A. michoacaensis* Nieves-Aldrey y Maldonado, 2012,

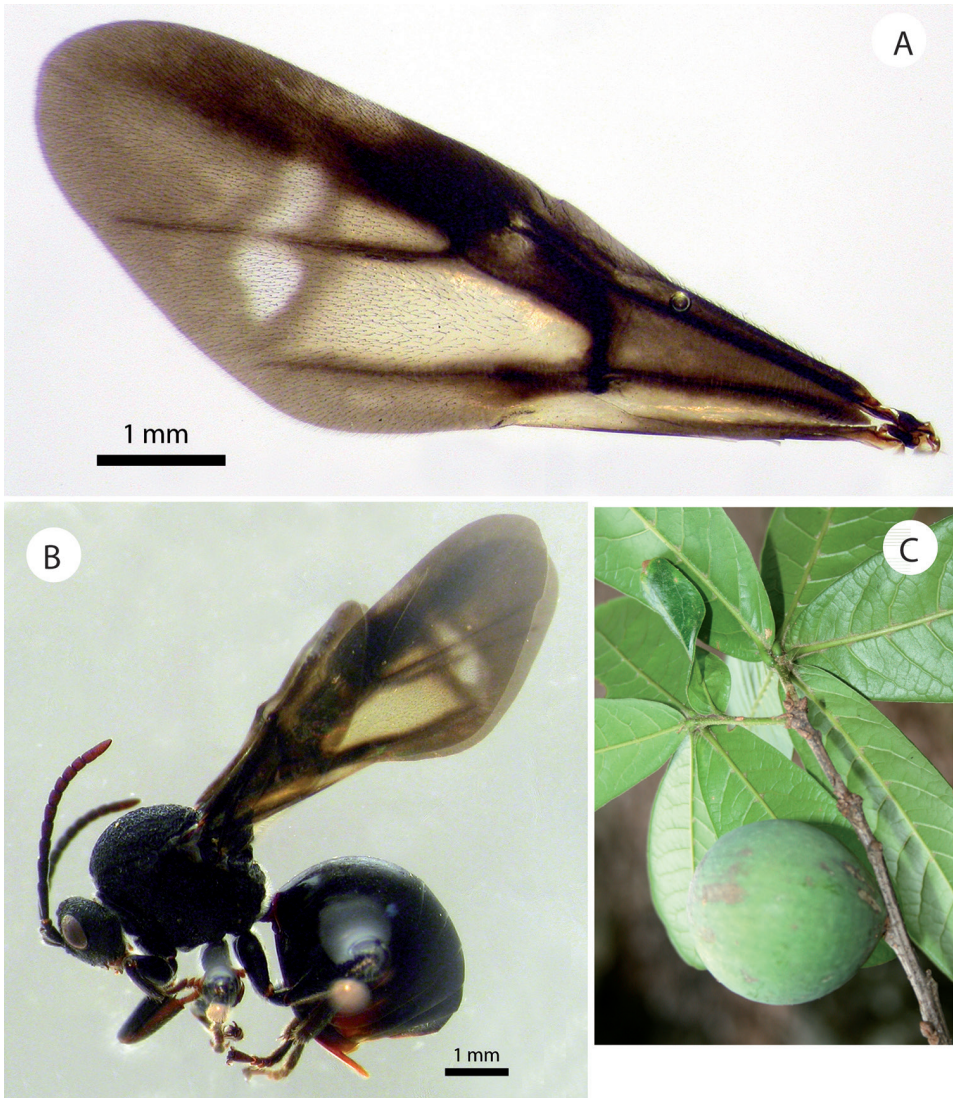


Figure 13. *Amphibolips nigrialatus* sp. nov., female. **A** forewing **B** habitus **C** gall on *Quercus sapotifolia* Liebm.

A. trizonata Ashmead, 1896 and *Amphibolips kinseyi* sp. nov. However, the gall of *A. nigrialatus* differs in its size, which is approximately half that of the other species. The gall is similar to that of *A. murata* Weld, 1957, but not as rough when dry and to that of *A. quercusfuliginosa* Ashmead, 1885, from which it is impossible to differentiate according to the original description of the gall. Nonetheless, the adults are completely different.

Distribution. Known only from the type locality in Veracruz State, Mexico.

Biology. Presumably, a sexual generation. The gall was collected in late April and the insect emerged shortly afterwards.

Key to adult *Amphibolips* species of Mexico and Panama (species of the “niger complex” excluded). Modified from Nieves-Aldrey et al. (2012) for including the new species described

- 1 Females. Antenna with 13–14 antennomeres; F1 not modified (Fig. 3C) ... **2**
 – Males. Antenna with 15 antennomeres; F1 modified, flattened ventrally (Fig. 3E) **9**
- 2 Forewing with a heavily-infusate spot on the basal area of radial cell; remainder of the forewing, hyaline to only slightly infusate (Fig. 15D)
 *aliciae* Medianero & Nieves-Aldrey
- Forewing entirely infusate, more heavily along a band on anterior margin of wing (Fig. 15G, H) **3**
- 3 More heavily infusate band along anterior margin of forewing with a clear transversal band on one-third apical part of radial cell which is more or less extended towards posterior margin of wing (Fig. 15F, G) **4**
- More heavily infusate band along the anterior margin of the forewing, without a clear transversal band on apical part of radial cell extended towards posterior margin of wing. If there is a clear colourless spot apically on the radial cell, it does not extend below the radial cell (Fig. 15H) *
- * To this couplet option run nine *Amphibolips* species from Mexico included in the above referred original key.
- 4 Basal and first cubital cells colourless or only weakly infusate prior to the heavily-infusate basal half of the radial cell (Fig. 15A, B). Mesoscutellum weakly emarginate posteriorly (Fig. 14C). F1 1.2× as long as F2 *fuscus* Kinsey*
 * To this couplet run also the recently described species *Amphibolips cibriani* Pujade-Villar. According the original description, we cannot find diagnostic morphological characters differentiating *A. cibriani* from *A. fuscus* Kinsey (Figs 14C, D). The authors comparing incorrectly the species only with *A. castroviejoii* Medianero & Nieves-Aldrey and *A. durangensis* Nieves-Aldrey & Pascual, which have a different forewing colour pattern and run to the alternative option in this couplet (compare Fig. 15B, C). However, the galls of the two species are quite different: spindle-shaped in *A. fuscus* while they are more or less spherical in *A. cibriani*.
- Basal and first cubital cells as heavily infusate as basal half of radial cell (Figs 4A, 15G). F1 1.4–1.5× as long as F2 **5**
- 5 Mesoscutellum slightly or moderately emarginate posteriorly (Fig. 14B). Forewing not as blackish infusate; the clear transversal band relatively large and broad and extended to ventral margin of forewing **6**
- Mesoscutellum strongly emarginate posteriorly (usually V-shaped in dorsal view) (Figs 6C, 7B, 10A). Forewing darker, heavily infusate and predominantly black; the clear transversal band usually smaller and not reaching ventral margin of forewing (Figs 8C, 13A); if reaching ventral margin (*A. castroviejoii*), then the scutellar foveae are smooth **7**

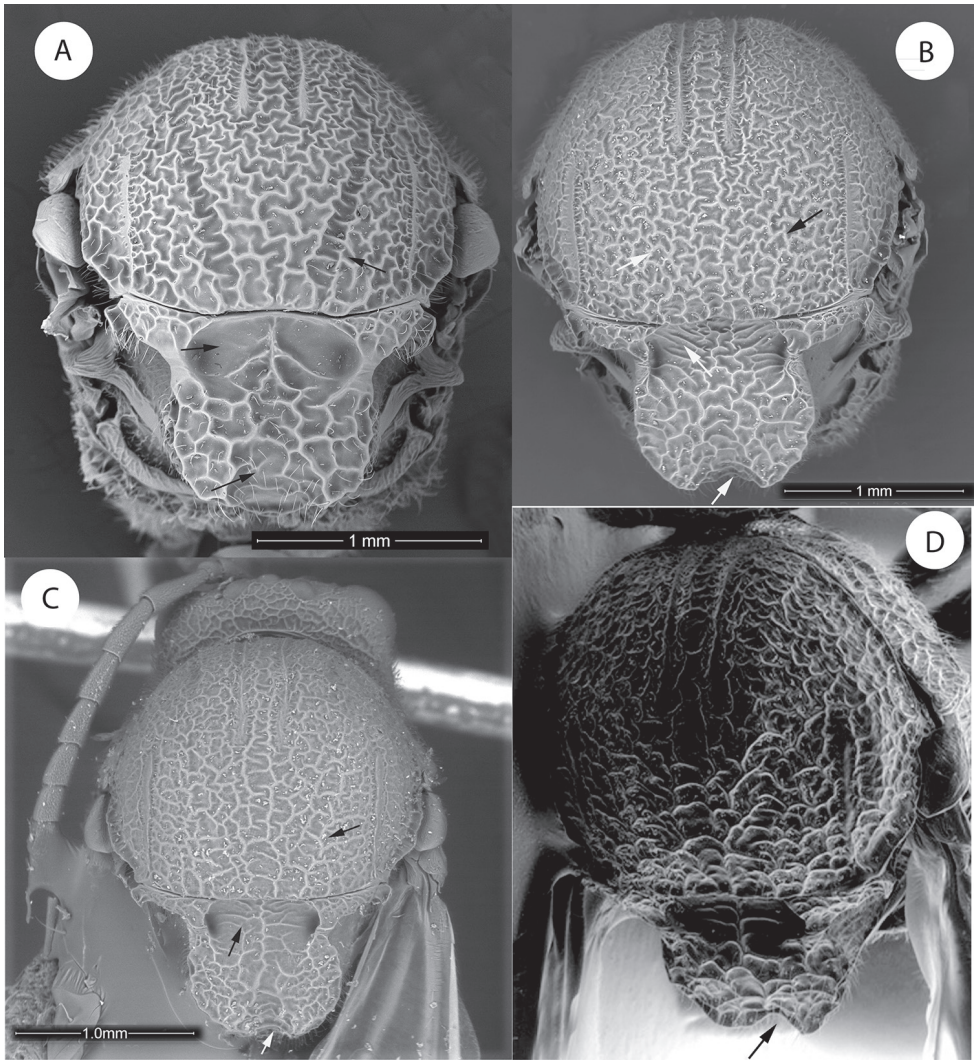


Figure 14. Details of mesoscutum and mesoscutellum (dorsal view) of *Amphibolips* species **A** *Amphibolips castroviejoi* Medianero & Nieves-Aldrey **B** *Amphibolips durangensis* Nieves-Aldrey & Maldonado **C** *Amphibolips fusus* Kinsey (type) **D** *Amphibolips cibriani* Pujade-Villar (last image taken from Pujade-Villar et al. 2018).

- 6 Mesoscutellum only slightly emarginate posteriorly (Fig. 14B). Clear transversal band relatively smaller and narrow (Fig. 15G) *durangensis* Nieves-Aldrey & Maldonado
- Mesoscutellum more deeply emarginate posteriorly; postero-lateral projections of mesoscutellum moderately expanded (Fig. 1D). Non-infusate clear forewing transversal band large and broad, almost reaching ventral margin of forewing; medially measuring approximately three-quarters of the length of the radial cell (Fig. 4A) *magnigalla* sp. nov.

- 7 Scutellar foveae smooth. Notauli visible (Fig. 14A). Basal area anteriorly the transversal clear band of forewing completely black; Costal cell infusate; without less infusate areas above the cubital veins and below the M+Cu1 vein (Fig. 15F). Transversal clear band relatively large, reaching ventrally the posterior margin of forewing (Fig. 15F) *castroviejo* Medianero & Nieves-Aldrey
- Scutellar foveae with carinate sculpture (Figs 2C, 10A). Notauli either visible (Fig. 6A) or almost invisible, hidden by sculpture on mesoscutum (Fig. 10A). Basal area anteriorly the transversal clear band of forewing with less infusate basal areas, above the cubital veins and below the M+Cu1 vein (Figs 8C, 13A). Transversal clear band small and not reaching ventral margin of forewing; occupying about one third or less of the radial cell (Figs 8C, 13A) **8**
- 8 Scutellar foveae large, extended approximately one-half of the length of mesoscutellum; medially confluent not separated by a carina or groove (Figs 11C, D). Posterolateral projections of scutellum pointed apically and curved upwards. Forewing strongly dark infusate, the clear transversal band of the forewing small, short and narrow; medially not more than one-fifth the length of the radial cell (Fig. 13A)..... *nigrialatus* sp. nov.
- Scutellar foveae not as large, extended approximately one-third of the length of the mesoscutellum and medially separated by the mesoscutellar impression (Figs 6C, D, 9A, B). Posterolateral projections of scutellum flat or less pointed apically, less upward curved. Clear forewing transversal band wider, medially about half of the radial cell *kinseyi* sp. nov.

Males

- 9 Forewing with a heavily infusate spot in the basal area of the radial cell; rest of the forewing only slightly infusate ... *aliciae* Medianero & Nieves-Aldrey
- Forewing entirely and heavily infusate, with a transversal clear band or with a more infusate longitudinal band on the anterior margin of the wing (Figs 4B, 8D, 15I) **10**
- 10 Forewing with a clear transversal band on one-third of the apical part of the radial cell, which is more or less extended towards the posterior margin of the wing (Figs 4B, 8D) **11**
- Forewing without a clear transversal band on one-third of the apical part of the radial cell; usually with a more infusate longitudinal band along dorsal margin of forewing; if there is a clear colourless spot apically on the radial cell, it does not extend below the radial cell (Fig. 15I) *
- * To this couplet option run other nine *Amphibolips* species from Mexico included in the above referred original key.
- 11 Transversal clear band large; dorsally extended on 2/3 of apical area of radial cell and extended posteriorly to reach margin of the wing (Fig. 4B) *magnigalla* sp. nov.

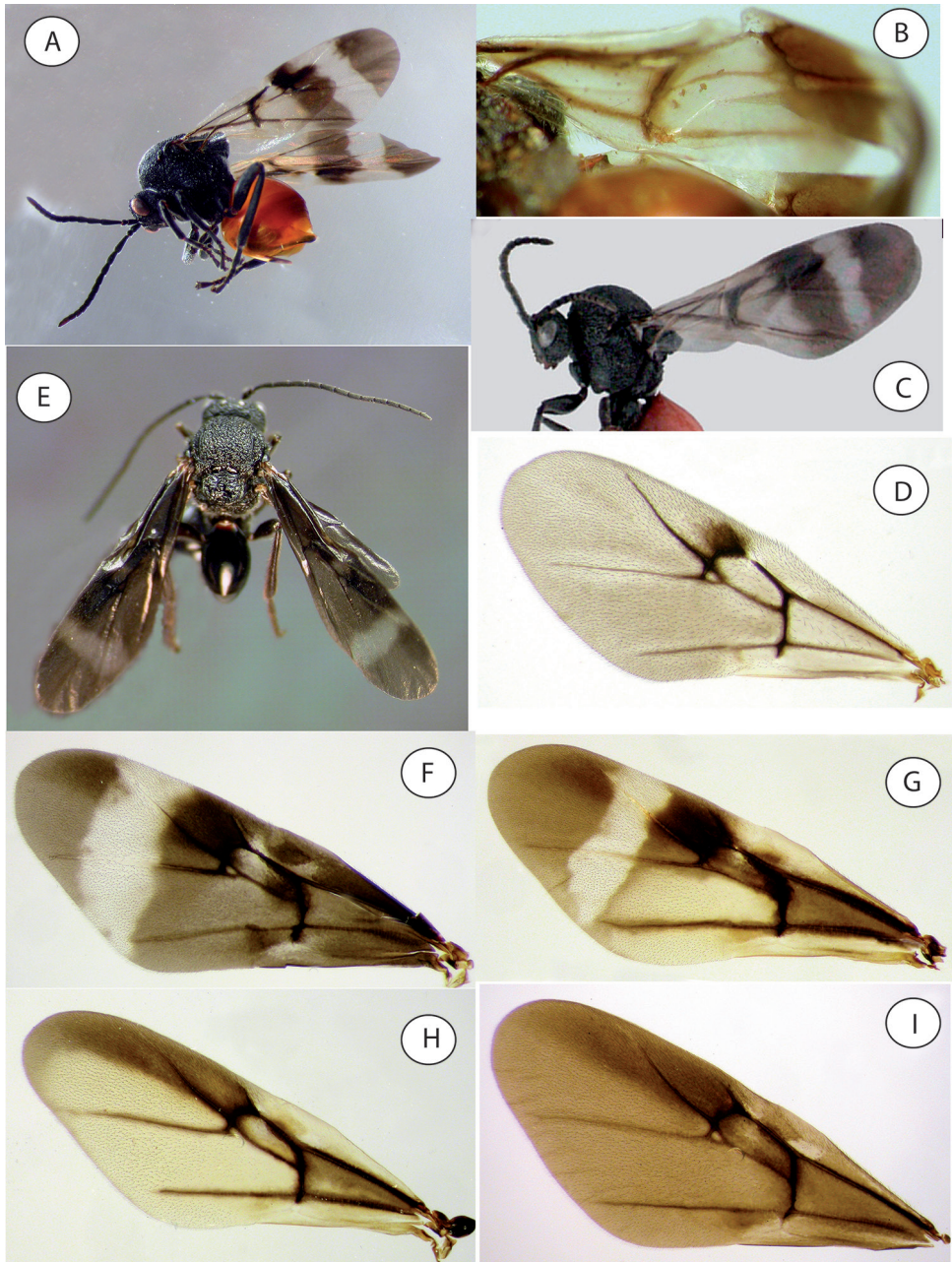


Figure 15. Details of wings and habitus of *Amphibolips* species **A** habitus of *Amphibolips* near *fuscus* from Zacatecas **B** detail of forewing of *Amphibolips fusus* Kinsey (type) **C** habitus of *Amphibolips cibriani* Pujade-Villar (image taken from Pujade-Villar et al. 2018) **D** forewing of female *Amphibolips aliciae* Medianero & Nieves-Aldrey **E** habitus of male *Amphibolips castroviejo* Medianero & Nieves-Aldrey **F** forewing of female *Amphibolips castroviejo* **G** forewing of female of *Amphibolips durangensis* Nieves-Aldrey & Maldonado **H** forewing female of *Amphibolips michoacaensis* Nieves-Aldrey & Pascual **I** forewing male of *Amphibolips michoacaensis*.

- Transversal clear band much more reduced in size; extended at most on one third of apical area of radial cell, and posteriorly not reaching the posterior margin of the wing (Figs 8D, 9C, 15E)..... **12**
- 12 Scutellar foveae smooth. Transversal clear band relatively larger and more extended (Fig. 15C). Mesoscutellum moderately emarginate posteriorly *castroviejo* **Medianero & Nieves-Aldrey**
- Scutellar foveae sculptured. Transversal clear band very reduced in size (Figs 8D, 9C). Mesoscutellum strongly emarginate posteriorly (Fig. 9A, B), with a sharp horn projection observed in lateral view. **13**
- 13 Posterolateral projections of the mesoscutellum acute pointed (Fig. 9A). Notauli hardly visible. Radial cell with first radial abscissa projected into the radial cell at tip of angle (Fig. 9C). F1 1.8× as long as F2 *dampfi* **Kinsey**
- Posterolateral projections of mesoscutellum flat and rounded apically (Fig. 9B). Notauli well indicated. Radial cell with first radial abscissa rounded or slightly angled, not projected into the radial cell at tip of angle (Fig. 9D). F1 1.6× as long as F2. *kinseyi* **sp. nov.**

Discussion

The current study increases the number of *Amphibolips* in Mexico from 20 to 23. However, this number may rapidly increase since fieldwork is revealing new species that are still being studied and will eventually be published elsewhere.

The three species described herein present the typical diagnostic features of the *Amphibolips* species out of the “*niger*” group (Kinsey 1937, Melika et al. 2011, Nieves-Aldrey et al. 2012). We observed one morphological character, which seems to be shared only by *Amphibolips* species, namely, the absence of a gap or space between the two branches of the cubital vein of the forewing. A second not previously noticed character, present in the species from Mexico, is a pair of longitudinal carinae running from the ventral margin of the toruli to the anterior tentorial pits or the epistomal sulcus. However, this feature needs to be checked in all the *Amphibolips* species.

Considering that the complete life cycle of most species is unknown, it is difficult to propose a pattern of morphologies or phenologies for these species. In some cases, mistakes could be made, for example, some descriptions may pertain to different generations of currently-recognised species. Nieves-Aldrey et al. (2012) mentioned the difficulties in separating *Amphibolips* species (excluding those of the “*niger*” complex) based on external morphology of their galls, considering that some species are very similar (e.g. *A. nigrialatus* new species and *A. kinseyi* new species). In the same study, the question arises about the variability in a single *Amphibolips* species and the need to use new tools (specifically, molecular markers) that allow the clarification of the boundaries between species.

The new species described herein are very similar and share a set of similar morphological characteristics. The forewings are very dark and heavily black infuscate, but with a clear transversal band that is more or less extended in both sexes; the mesoscutellum is very deeply emarginate posteriorly, with the emargination reaching the scutellar foveae and almost dividing the mesoscutellum into two parts. Another shared feature of the three new species is that all are distributed in the States of Oaxaca and Veracruz in southern Mexico and none exceeds the Trans-Mexican volcanic belt. Their host oak species (*Quercus zempoaltepecana* and *Q. sapotifolia*) are similar in their affinity for slopes in humid climates near the Gulf of Mexico and their occurrence within tropical communities with many *Quercus* species. After studying large collections of *Amphibolips* collected across extensive areas of Mexico, we observed a distinct morphological pattern within the geographic distribution of the species, which is also confirmed in the species from the United States (unpublished observations). The more southern a species is distributed, the stronger and deeper its mesoscutellar emargination appears. These two patterns are consistent within a north-south distribution in Mexico.

The presence of four described species from the State of Oaxaca (*Amphibolips oaxacae* Nieves-Aldrey & Pascual, *A. dampfi* Kinsey, *A. magnigalla* sp. nov. and *A. kinseyi* sp. nov.) and three species from Panama (*A. castroviejo* Medianero & Nieves-Aldrey, *A. aliciae* Medianero & Nieves-Aldrey and *A. salicifoliae* Medianero & Nieves-Aldrey) allows us to propose that *Amphibolips* must be present throughout Central America. Although they have not been cited from Chiapas, Mexico to Costa Rica, its presence in those geographic areas is likely, given that most host *Quercus* species recorded from south of Mexico and Panama are also present in Mesoamerica (Burger 1977, Breedlove 2001, Valencia 2004). Currently, broader work is being carried out to understand the relationships between the Mexican and Panamanian species of *Amphibolips*.

Acknowledgements

We thank George Melika, Matt Buffington and Zhiwei Liu their useful comments that contributed to improve the manuscript. JLNA was supported by the research project MINECO/FEDER, UE, CGL2015-66571-P. JLNA is grateful to Enrique Medianero (Panama) and Enrique Pascual (Mexico) for their help with sampling in Veracruz and DECL thanks Javier Piña and Antonio López for their help in sampling in Oaxaca. Thanks to the authorities of the communities of the Sierra Juárez, Oaxaca, for allowing us to carry out this work. We also thank Laura Tormo (MNCN), Alberto Jorge (MNCN) and Orlando Hernández (Microscopy Laboratory, ENES Morelia, UNAM) for technical assistance in the acquisition of SEM micrographs. This project is a partial requirement for the doctoral studies of DECL in the Posgrado en Ciencias Biológicas at UNAM. DECL received funds through a scholarship (330529) from the Consejo Nacional de Ciencia y Tecnología (CONACYT).

References

- Ashmead WH (1885) On the cynipidous galls of Florida with descriptions of new species. Proceedings of the Entomological Section of the Academy of Natural Sciences 12: 5–9. <https://www.jstor.org/stable/25076461>
- Ashmead WH (1896) Descriptions of new cynipidous galls and gallwasps in the United States National Museum. Proceedings United States National Museum 19: 113–136. <https://doi.org/10.5479/si.00963801.19-1102.113>
- Bassett HF (1890) New species of North American Cynipidae. Transactions of the American Entomological Society 17(1): 59–92. <https://www.jstor.org/stable/25076539>
- Beutenmüller W (1909) The species of *Amphibolips* and their galls. Bulletin of American Museum of Natural History 26: 47–66. <http://hdl.handle.net/2246/656>
- Beutenmüller W (1911) Three new species of Cynipidae (Hym.). Entomological News 22: 197–198. <https://www.biodiversitylibrary.org/page/2604288>
- Beutenmüller W (1917) Descriptions of new Cynipidae. The Canadian Entomologist 49(10): 345–349. <https://doi.org/10.4039/Ent49345-10>
- Breedlove D (2001) Fagaceae. In: Stevens WD, Ulloa UC, Pool A, Montiel OM (Eds) Flora de Nicaragua. Monographs in Systematic Botany, Missouri Botanical Garden 85(2): 1076–1084.
- Burger W (1977) Fagaceae. In: Burger W (Ed) Flora Costaricensis. Fieldiana: Botany 40: 59–82.
- Burks BD (1979) Superfamily Cynipoidea. In: Krombein KV, Hurd PD, Jr, Smith DR, Burks BD (Eds) Catalog of Hymenoptera in America North of Mexico. Volume 1. Symphyta and Apocrita. Smithsonian Institution Press, Washington, DC, 1045–1107.
- Cornell HV (1983) The secondary chemistry and complex morphology of galls formed by the Cynipinae (Hymenoptera): why and how? American Midland Naturalist 110(2): 225–234. <https://doi.org/10.2307/2425263>
- Csőka G, Stone GN, Melika G (2005) Biology, Ecology, and Evolution of gall-inducing Cynipidae. In: Raman A, Schaefer CW, Withers TM (Eds) Biology, Ecology, and Evolution of gall-inducing arthropods. Volume 2. Science Publishers Inc. New Hampshire, 573–642.
- Harris R (1979) A glossary of surface sculpturing. State of California, Department of Food and Agriculture. Occasional Papers in Entomology 28: 1–31.
- Kinsey AC (1937) New Mexican gall wasps (Hymenoptera, Cynipidae). II. Revista de Entomologia 7(4): 428–471.
- Liljeblad J, Ronquist F, Nieves-Aldrey JL, Fontal-Cazalla FM, Ros-Farré P, Pujade-Villar J (2008) A fully web-illustrated morphological phylogenetic study of relationships among oak gall wasps and their closest relatives (Hymenoptera: Cynipidae). Zootaxa 1796: 1–73. <https://doi.org/10.11646/zootaxa.1796.1.1>
- Liu Z, Ronquist F (2006) Familia Cynipidae. In: Fernández F, Sharkey MJ (Eds) Introducción a los Hymenoptera de la región Neotropical. Sociedad Colombiana de Entomología y Universidad Nacional de Colombia. Bogotá, 839–849.
- Liu Z, Engel MS, Grimaldi DA (2007) Phylogeny and geological history of the cynipoid wasps (Hymenoptera: Cynipoidea). American Museum Novitates 3583: 1–48. [https://doi.org/10.1206/0003-0082\(2007\)3583\[1:PAGHOT\]2.0.CO;2](https://doi.org/10.1206/0003-0082(2007)3583[1:PAGHOT]2.0.CO;2)

- Medianero E, Nieves-Aldrey JL (2010) The genus *Amphibolips* Reinhard (Hymenoptera: Cynipidae: Cynipini) in the Neotropics, with description of three new species from Panama. *Zootaxa* 2360: 47–62. <https://doi.org/10.11646/zootaxa.2360.1.3>
- Melika G, Abrahamson WG (2002) Review of the world genera of oak cynipid wasps (Hymenoptera: Cynipidae: Cynipini). In: Melika G, Thuróczy C (Eds) Parasitic wasps: evolution, systematics, biodiversity and biological control. International Symposium: Parasitic Hymenoptera: taxonomy and biological control, Koszeg (Hungary), May 2001, Agroinform, 150–190.
- Melika G, Equihua-Martínez A, Estrada-Venegas EG, Cibrián-Tovar D, Cibrián-Llenderal VD, Pujade-Villar J (2011) New *Amphibolips* gallwasp species from Mexico (Hymenoptera: Cynipidae). *Zootaxa* 3105: 47–59. <https://doi.org/10.11646/zootaxa.3105.1.2>
- Nicholls JA, Melika G, Demartini JD, Stone GN (2018) A new species of *Andricus* Hartig gallwasps from California (Hymenoptera: Cynipidae: Cynipini) galling *Notholithocarpus* (Fagaceae). *Integrative Systematics* 1: 17–24. <https://doi.org/10.18476/insy.v01.a3>
- Nieves-Aldrey JL (2001) Hymenoptera, Cynipidae. In: Ramos MA, Alba-Tercedor J, Bellés i Ros X, Gosálbez i Noguera J, Guerra-Sierra A, Macpherson-Mayol E, Martín-Piera F, Serrano-Marino J, Templado-González J (Eds) Fauna Ibérica. Volumen 16. Museo Nacional de Ciencias Naturales, CSIC, Madrid, 636 pp.
- Nieves-Aldrey JL, Pascual E, Maldonado-López Y, Medianero E, Oyama K (2012) Revision of the *Amphibolips* species of Mexico excluding the “*niger* complex” Kinsey (Hymenoptera: Cynipidae), with description of seven new species. *Zootaxa* 3545: 1–40. <https://doi.org/10.11646/zootaxa.3545.1.1>
- Pénzes Z, Tang CT, Stone GN, Nicholls JA, Schwéger S, Bozsó M, Melika G (2018) Current status of the oak gallwasp (Hymenoptera: Cynipidae: Cynipini) fauna of the Eastern Palearctic and Oriental regions. *Zootaxa* 4433(2): 245–289. <https://doi.org/10.11646/zootaxa.4433.2.2>
- Pujade-Villar J, Ferrer-Suay M (2015) Adjudicació genèrica d'espècies mexicanes d'ubicació dubtosa descrites per Kinsey i comentaris sobre la fauna mexicana (Hymenoptera: Cynipidae: Cynipini). *Butlletí de la Institució Catalana d'Història Natural* 79: 7–14. <http://hdl.handle.net/2445/102507>
- Pujade-Villar J, Barrera-Ruiz UM, Cuesta-Porta V (2018) Descripción de *Amphibolips cibriani* Pujade-Villar n. sp. para México (Hymenoptera: Cynipidae: Cynipini). *Dugesiana* 25(2): 151–158.
- Richards OW, Davies RG (1977) Hymenoptera. In: Imms' General Textbook of Entomology. Springer, Dordrecht, 1175–1279. https://doi.org/10.1007/978-94-011-6516-7_30
- Ronquist F, Nordlander G (1989) Skeletal morphology of an archaic cynipoid, *Ibalia rufipes* (Hymenoptera: Ibalidae). *Entomologica Scandinavica Supplement* 33: 1–60.
- Ronquist F, Nieves-Aldrey JL, Buffington ML, Liu Z, Liljeblad J, Nylander JAA (2015) Phylogeny, evolution and classification of gall wasps: the plot thickens. *PLoS ONE* 10(5): 1–40. <https://doi.org/10.1371/journal.pone.0123301>
- Stone GN, Cook JM (1998) The structure of cynipid oak galls: patterns in the evolution of an extended phenotype. *Proceedings of the Royal Society of London, B* 265: 979–988. <https://doi.org/10.1098/rspb.1998.0387>

- Stone GN, Schönrogge K, Atkinson RJ, Bellido D, Pujade-Villar J (2002) The population biology of oak gall wasps (Hymenoptera: Cynipidae). *Annual Review of Entomology* 47: 633–668. <https://doi.org/10.1146/annurev.ento.47.091201.145247>
- Valencia-A S (2004) Diversidad del género *Quercus* (Fagaceae) en México. *Boletín de la Sociedad Botánica de México* 75: 33–53. <https://doi.org/10.17129/botsoci.1692>
- Weld LH (1957) New American cynipid wasps from oak galls. *Proceedings of the United States National Museum* 107: 107–122. <https://doi.org/10.5479/si.00963801.107-3384.107>

Chinese species of *Carinostigmus* Tsuneki (Hymenoptera, Crabronidae), including three new species and a new record to China

Nawaz Haider Bashir¹, Li Ma¹, Qiang Li¹

¹ Department of Entomology, College of Plant Protection, Yunnan Agricultural University, Kunming, Yunnan, 650201, China

Corresponding author: Li Ma (maliwasps@aliyun.com); Qiang Li (liqiangkm@126.com)

Academic editor: T. Dörfel | Received 10 June 2020 | Accepted 6 October 2020 | Published 6 November 2020

<http://zoobank.org/BF3D3038-2C5A-4EC4-BAB4-7700D0DFB374>

Citation: Bashir NH, Ma L, Li Q (2020) Chinese species of *Carinostigmus* Tsuneki (Hymenoptera, Crabronidae), including three new species and a new record to China. ZooKeys 987: 115–134. <https://doi.org/10.3897/zookeys.987.55317>

Abstract

Three new species of *Carinostigmus* Tsuneki from the Oriental Region of China are described: *Carinostigmus frontirugatus* Bashir & Ma, **sp. nov.**, *C. latidentatus* Bashir & Ma, **sp. nov.**, and *C. vesulcatus* Bashir & Ma, **sp. nov.** In addition, ten species are reported, of which *Carinostigmus palawanensis* (Tsuneki) is recorded in China for the first time. A key to known and new species of the genus *Carinostigmus* Tsuneki from China is provided.

Keywords

Apoid wasps, Pemphredoninae, Stigmina, taxonomy, Yunnan

Introduction

Carinostigmus, first proposed by Tsuneki (1954) as a subgenus, was raised to the genus level by Bohart and Menke (1976). The females of *Carinostigmus* prey on small insects (leaf hoppers and aphids), males feed on nectar (flowering plants), and the larvae on aphids provided by the adults. The nests are generally built inside a burrow made in wooden logs or dried twigs. The aphid hunting wasp genus *Carinostigmus* Tsuneki belongs to subfamily Pemphredoninae and contains 35 species and one subspecies. Most

of the species are distributed across the Oriental (18 species), Afrotropical (11 species and one subspecies) and Palearctic regions (two species), and four species are present in both the Palearctic and Oriental regions (Maidl 1925; Gussakovskij 1934; Tsuneki 1954, 1956, 1966, 1974, 1976, 1977; Bohart and Menke 1976; Krombein 1984; Pulawski 2020). Previously, nine species have been recorded in China (Fig. 1), among them six species in Oriental China, and three species from Palearctic and Oriental China (Li and Yang 1995; Li and He 2004; Ma et al. 2012, 2018). The unknown male of *C. kaihuanus* Li & Yang, 1995 and the unknown female of *C. tanoi* Tsuneki, 1977 were described from Qinling mountains of Shaanxi Province, China (Ma et al. 2018). *Carinostigmus costatus* Krombein, 1984 and *C. maior* (Maidl, 1925) were reported from Oriental China for the first time (Ma et al. 2012).

The diagnostic characteristics that differentiate *Carinostigmus* from other Pemphredonini genera are: mandible apically tridentate on females and bidentate on males; labrum with different shapes such as triangular, subtriangular, pentagonal or rounded; shallow scapal basin on face; lower frons with inter-antennal tubercle; dense silvery setae absent on clypeus; eyes broadly separated, converging below in male more than female; foveolate, broad or narrow grooves along orbits; occipital carina present, separated from hypostomal carina and complete to midventral line of head; notaulus and omaulus present; episternal sulcus not definite except below omaulus; acetabular carina and sub-omaulus lacking; hypersternaulus foveolate; in female, foretarsus without a rake, hindtibia without a series of posterior spines; stigma large; two submarginal cells; hind wing submedian cell reduced, media diverging well beyond cu-a; petiole longer than twice its diameter; in female, pygidial plate present, oval or U-shaped (Bohart and Menke 1976).

Here we describe three new species from Fujian, Guizhou, Hainan, and Yunnan provinces; and one new record from Yunnan Province of China. A key to Chinese species of *Carinostigmus* is also provided.

Materials and methods

Specimens were collected from Fujian, Guizhou, Hainan and Yunnan Provinces of China. Types and other specimens examined in this study are deposited in the following institutions: Insect Collections of Yunnan Agricultural University, Kunming, Yunnan, China (YNAU); Parasitic Hymenoptera Collection of Zhejiang University, Hangzhou, Zhejiang Province, China (ZJU) and Institute of Zoology, Chinese Academy of Sciences, Beijing, China (CAS).

Specimens were observed with the help of an Olympus stereomicroscope (SZ Series) with an ocular micrometer. The photographs were taken with VHX-5000 and edited by using Adobe Photoshop 8.0. For the terminology we mainly followed Bohart and Menke (1976) and Harris (1979), except the following: inter-antennal tubercle (projection on frontal line Fig. 2b); inner-orbital sulcus (sulcus along inner orbits Fig. 2a); outer-orbital sulcus (sulcus along outer orbits); groove (a long, narrow depression on integument). Measurements and ratio were acquired using an ocular scale on Olympus

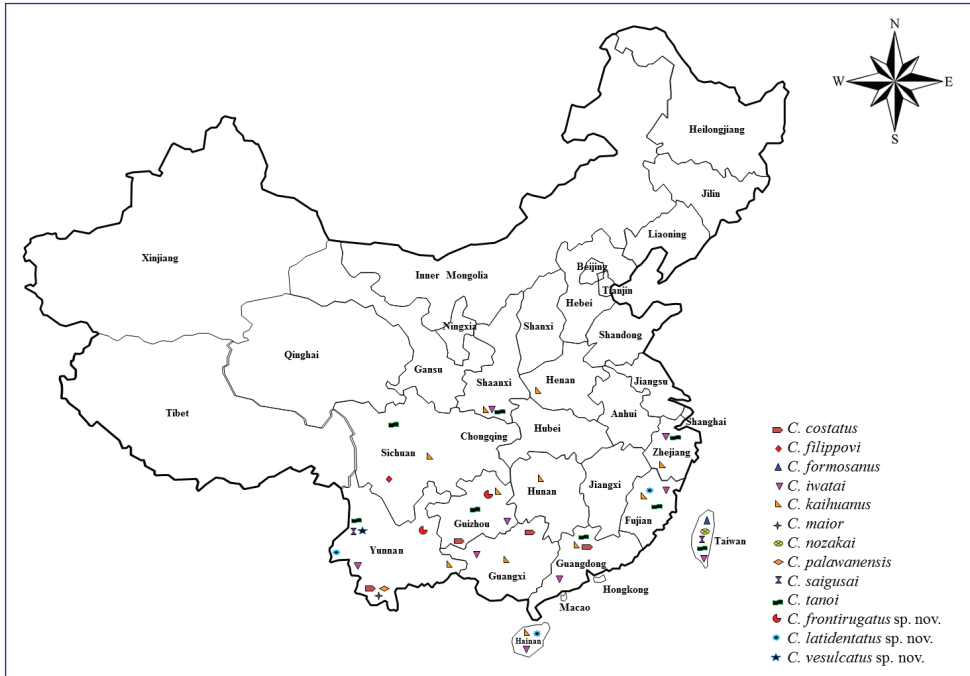


Figure 1. Distribution of *Carinostigmus* from China.

stereo microscope SZX2-TR30 at $2\times$ and $5.4\times$ magnification, respectively. The abbreviations in the text are as follows: BL, body length; HLD, head length in dorsal view (the distance from frons to occipital margin in the middle); HLF, head length in frontal view (the distance from vertex to clypeal margin in the middle); HW, head width (dorsal view); HWmax, head width (dorsal view, maximum); HWmin, head width (dorsal view, minimum); EW, eye width (lateral view, maximum); EWd, eye width (frontal view, maximum); TW, gena width (lateral view, maximum); EL, eye length (lateral view, maximum); POD, postocellar distance (distance between inner margins of hind ocelli); OOD, ocellocular distance (distance between outer margin of hind ocellus and nearest inner orbit); OCD, ocello-occipital distance (distance between posterior margin of hind ocellus and occipital margin, dorsal view); IODc (distance between inner margin of eyes at base of clypeus, frontal view); IODv (distance between inner margin of eyes at base of vertex, dorsal view); IODmin (minimum distance between inner margin of eyes, frontal view); IOW (inner-orbital width); OOW (outer-orbital width); OCW (occipital carina width); AOD (distance from inner eye to antennal socket, frontal view); WAS (width of antennal socket, frontal view); IAD (distance between antennal sockets, frontal view); LS (length of scape); LP (length of pedicel); LFI (length of flagellomere I); WFI (width of flagellomere I); LFII (length of flagellomere II); WFII (width of flagellomere II); LC (length of collar); WC (width of collar); PW, petiole width (dorsal view, in the middle); PL, petiole length (lateral view); WTI, maximum width of metasomal tergum I (dorsal view); LTI, maximum length of metasomal tergum I (dorsal view).

Results

Key to species of the genus *Carinostigmus* Tsuneki from China

Note: Females of *C. nozakai* Tsuneki, and males of *C. frontirugatus* sp. nov. are unknown. OR and PR represent Oriental and Palearctic regions, respectively.

- 1 Ten flagellomeres; abdomen with six exposed segments (Fig. 2f); mandible tridentate apically; female **2**
- Eleven flagellomeres; abdomen with seven exposed segments; mandible bidentate apically; male..... **13**
- 2 Scrobal sulcus narrowed or broad, distinctly foveolate, short or long (Fig. 2d)...**3**
- Scrobal sulcus absent or inconspicuous (Fig. 3g) **8**
- 3 Propodeal posterior surface extensively covered by reticulated ridges well-marked; smooth areas absent..... **4**
- Propodeal posterior surface with median groove, several slender or sturdy longitudinal rugae anteriorly; small or large smooth area medially (Fig. 2i)..... **6**
- 4 Frontal line reaching to anterior ocellus; petiole smooth dorsally and laterally, without striations (Fig. 3c) (OR) ***C. formosanus* (Tsuneki)**
- Frontal line not reaching to anterior ocellus (Fig. 4a, b); weak transversal or longitudinal striations densely on petiole dorsal surface (Fig. 2c), few inconspicuous carina or groove on petiole lateral surface **5**
- 5 Labrum pentagonal (Fig. 2a); inter-antennal tubercle long, equal or more than midocellus diameter (Fig. 2b); admedian and parapsidal lines inconspicuous; pygidial area oval shaped (Fig. 2g) (OR) ***C. maior* (Maidl)**
- Labrum triangular; inter-antennal tubercle shorter than midocellus diameter (Fig. 3b); admedian and parapsidal lines conspicuous; pygidial area U-shaped (Fig. 3h) (OR) ***C. costatus* Krombein**
- 6 Free margin of clypeal lobe deeply emarginated (OR) ***C. palawanensis* (Tsuneki)**
- Free margin of clypeal lobe truncate medially (Fig. 2a) **7**
- 7 Pygidial area punctate throughout (Fig. 2g); omaulus broadened as midtibial width (Fig. 2d); lower gena with coarse punctures; clypeus moderately convex (Fig. 2a); several slender transverse striations anteriorly on scutum (Fig. 2h) (OR)..... ***C. frontirugatus* sp. nov.**
- Pygidial area punctate medially; omaulus narrowed (Fig. 4g); lower gena with fine punctures; clypeus slightly convex; scutum without transverse striations anteriorly (PR and OR) ***C. iwatai* (Tsuneki)**
- 8 Posterior surface of propodeum with a large smooth area medially (Fig. 4k); free margin of clypeal lobe nearly truncate (Fig. 4a) or with four teeth medially (Fig. 3j) **9**
- Posterior surface of propodeum without large smooth area medially (Fig. 2i); free margin of clypeal lobe with three distinct teeth medially **10**

- 9 Labrum wider than long, sub quadrate (Fig. 3a); free margin of clypeal lobe with four teeth, median lobe broadly produced, with two small inconspicuous lateral teeth, slightly reflexed apically, lateral lobe with a strong tooth on each side (Fig. 3j); lower gena with fine punctures medially; lateral surface of propodeum with irregular reticulation posteriorly (Fig. 3g) (OR) ***C. latidentatus* sp. nov.**
- Labrum longer than wide, round toward apex (Fig. 4a); free margin of clypeal lobe sinuous, not forming reflexed teeth (Fig. 4a); lower gena with weak striations; lateral surface of propodeum without reticulation posteriorly (Fig. 4g) (OR) ***C. vesulcatus* sp. nov.**
- 10 Inter-antennal tubercle short, less than midocellus diameter (Figs 3b, 4b) ... **11**
- Inter-antennal tubercle long, equal or more than midocellus diameter (Fig. 2b) **12**
- 11 Upper frons with dense, slender striations, impunctate; vertex impunctate (PR and OR) ***C. filippovi* (Gussakovskij)**
- Upper frons smooth, without striations, with fine punctures; vertex with sparsed, fine punctures (PR and OR) ***C. tanoi* Tsuneki**
- 12 Pronotal collar with sparsed, inconspicuous rugae laterally; scutum dull, with fine punctures; notaulus deeply grooved and foveolate (Fig. 4j), extending to one third of scutum length; inner and outer-orbital sulcus broad (Fig. 2a, b); lower gena with coarse punctures; upper frons with several, fine punctures, frontal longitudinal carina distinct, reaching anterior ocellus (PR and OR) ...
..... ***C. kaihuanus* Li & Yang**
- Pronotal collar smooth, without rugae laterally; scutum shiny, with coarse punctures (Fig. 2e); notaulus inconspicuous, extending to only anterior of scutum length; inner and outer-orbital sulcus narrowed (Fig. 4a); lower gena impunctate; upper frons impunctate, without frontal longitudinal median carina (Fig. 3b) (OR) ***C. saigusai* (Tsuneki)**
- 13 Scrobal sulcus well-marked, short or long, distinctly foveolate (Fig. 2d) **14**
- Scrobal sulcus absent or very weakly impressed (Fig. 3g) **17**
- 14 Scrobal sulcus long; lateral surface of petiole with a groove medially, two distinct lateral carinae or with a groove basally and medially; ocellar triangle area dull, with coarse punctures; free margin of clypeal lobe deeply emarginated medially **15**
- Scrobal sulcus short (Fig. 2d); lateral surface of petiole with a few weak carinae or smooth; ocellar triangle area shiny, with fine punctures; free margin of clypeal lobe slightly emarginated medially **16**
- 15 Labrum pentagonal (Fig. 2a); clypeus moderately convex; inter-antennal tubercle long, equal or more than midocellus diameter (Fig. 2b); occipital carina broad, inconspicuously foveolate; admedian and parapsidal lines inconspicuous; scutellum with inconspicuous rugae posteriorly (OR) ... ***C. maior* (Maidl)**
- Labrum triangular; clypeus flat; inter-antennal tubercle short, less than midocellus diameter (Fig. 3b); occipital carina narrowed, distinctly foveolate (Fig. 3b); admedian and parapsidal lines conspicuous; scutellum with coarse punctures (OR) ***C. costatus* Krombein**

- 16 Vertex behind ocelli dull, impunctate; gena smooth; occipital carina narrowed (Fig. 3b); inner and outer-orbital sulcus narrowed (Fig. 3a, b); pronotal collar smooth; metanotum smooth; petiole lateral surface smooth (OR) *C. formosanus* (Tsuneki)
- Vertex behind ocelli shiny, with fine punctures; gena with several sturdy oblique transverse rugae near mandible area; occipital carina distinctly broad (Fig. 4e); inner and outer-orbital sulcus broad (Fig. 2a, b); pronotal collar with sparsed sturdy rugae; metanotum with dense sturdy longitudinal rugae laterally, smooth medially; petiole lateral with a few weak carinae (PR and OR) *C. iwatai* (Tsuneki)
- 17 Extensive smooth area present on posterior surface of propodeum mesally (Fig. 4k); free margin of clypeal lobe with two triangular lateral teeth (Figs 3d, 4d) **18**
- Extensive smooth area absent on posterior surface of propodeum mesally (Fig. 2i); free margin of clypeal lobe with three distinct teeth **19**
- 18 Labrum wider than long (Fig. 3d); lower gena with fine punctures medially; outer-orbital sulcus narrowed, coarsely foveolate; scutum with coarse punctures (Fig. 3f); parapsidal line conspicuous (Fig. 3f); lateral surface of propodeum with irregular reticulation posteriorly (Fig. 3g) (OR)..... *C. latidentatus* sp. nov.
- Labrum longer than wide (Fig. 4d); lower gena with weak striations; outer-orbital sulcus broad, inconspicuously foveolate; scutum with fine punctures (Fig. 4f); parapsidal line inconspicuous (Fig. 4f); lateral surface of propodeum without reticulation posteriorly (Fig. 4g) (OR) *C. vesulcatus* sp. nov.
- 19 Inter-antennal tubercle long, equal or more than midocellus diameter (Fig. 2b); upper frons frontal carina distinct, not reaching anterior ocellus (Fig. 3b); inner-orbital sulcus broad (Fig. 2a) (PR and OR) *C. kaihuanus* Li & Yang
- Inter-antennal tubercle short, less than midocellus diameter (Fig. 3b); upper frons without frontal carina, or if present, clearly reaching anterior ocellus; inner-orbital sulcus narrowed (Fig. 3a) **20**
- 20 Upper frons with dense, slender striations; vertex impunctate (Fig. 3b); upper frons frontal longitudinal carina distinct anteriorly, reaching to anterior ocellus (PR and OR) *C. filippovi* (Gussakovskij)
- Upper frons without striations; vertex with sparsed fine punctures (Fig. 2b); frontal carina absent on upper frons (Fig. 3b) **21**
- 21 Labrum pentagonal (Fig. 2a), deeply notched at apex; ocellar triangle with fine, sparsed punctures (Fig. 2b); lower gena with weak striations; occipital carina narrowed (Fig. 3b); scutum with coarsely punctuated (Fig. 2e); admedian line inconspicuous; parapsidal line conspicuous (Fig. 2e) (PR and OR) *C. tanoi* Tsuneki
- Labrum rounded, without emargination; ocellar triangle impunctate (Fig. 3b); lower gena smooth; occipital carina broad (Fig. 4e); scutum with fine punctures; admedian line conspicuous; parapsidal line inconspicuous (OR) *C. nozakai* Tsuneki

Taxonomy

Family Crabronidae

Subfamily Pemphredoninae

Genus *Carinostigmus* (Tsuneki, 1954)

Type species. *Stigmus congruus* Walker, 1860; by original designation.

Carinostigmus frontirugatus Bashir & Ma, sp. nov.

<http://zoobank.org/E8811F03-DCDF-4FB7-ACD3-F4F9E3D8196E>

Figs 2, 5a

Type material. *Holotype*: ♀, China: Guizhou: Dabanshui Forest Park, 26°32'N, 106°45'E, 10.VII.2011, No. 201503448, coll. Dongdong Feng (YNAU). *Paratypes*: 1♀ same as holotype except: No. 201503452; 1♀, China: Yunnan: Renhe County, 22°57'N, 104°17'E, 3.X.2016, No. 201605802 (YNAU); 1♀, China: Yunnan: Mengla County: Shangyong: Huiqingzhai, 21°23'N, 101°28'E, 21.V.2005, coll. Peng Wang (YNAU).

Diagnosis. This species is similar to *C. iwatai* (Tsuneki, 1954) in sharing: labrum pentagonal, round toward apex; free margin of clypeal lobe truncate medially (Fig. 2a); inter-antennal tubercle as long as midocellus diameter (Fig. 2b); upper frons with fine puncture; ocellar triangle nearly flat, with fine punctures, sparsely distributed; occipital carina narrowed, not foveolate (Fig. 2b); inner and outer-orbital sulcus broad as flagellomere 1 length (Fig. 2a); admedian line conspicuous (Fig. 2h); notaulus shallowly foveolate; parapsidal line conspicuous (Fig. 2e); mesopleuron with fine punctures, sparsely distributed, hypersternaulus broadened as midtibial width, conspicuously foveolate, scrobal sulcus foveate, short as mid trochanter length (Fig. 2d); propodeum strongly irregular reticulated ridged on propodeal enclosure and side, reticulates broad as Fig. 2i, with shiny interspace, propodeum with a smooth area posterodorsally; propodeum posterior surface with rectangular median groove, reticulate, a small smooth area medially, and irregular reticulation posteriorly (Fig. 2i); petiole side with few weak longitudinal carinae. *Carinostigmus frontirugatus* differs from *C. iwatai* by the following: clypeus moderately convex (Fig. 2a); inter-antennal tubercle distinctly broad at apex (Fig. 2b); median and lower frons rugose (Fig. 2a); upper frons longitudinal carina distinct, reaching anterior ocellus but weak (Fig. 2b); gena with dense, sturdy, oblique transverse rugae; lower gena with coarse punctures densely distributed; pronotal collar strongly elevated medially, lateral angles not so sharp as *C. iwatai* (Fig. 2e); scutum with several slender, transverse striations anteriorly (Fig. 2h); scutellum shiny; omaulus broadened as midtibial width (Fig. 2d); dorsal surface of petiole with dense weak longitudinal striations (Fig. 2c) and pygidial area punctate (Fig. 2g). *Carinostigmus iwatai* (Tsuneki) has following characters: clypeus slightly convex (Tsuneki 1954: fig. 12); inter-antennal tubercle not broad at apex

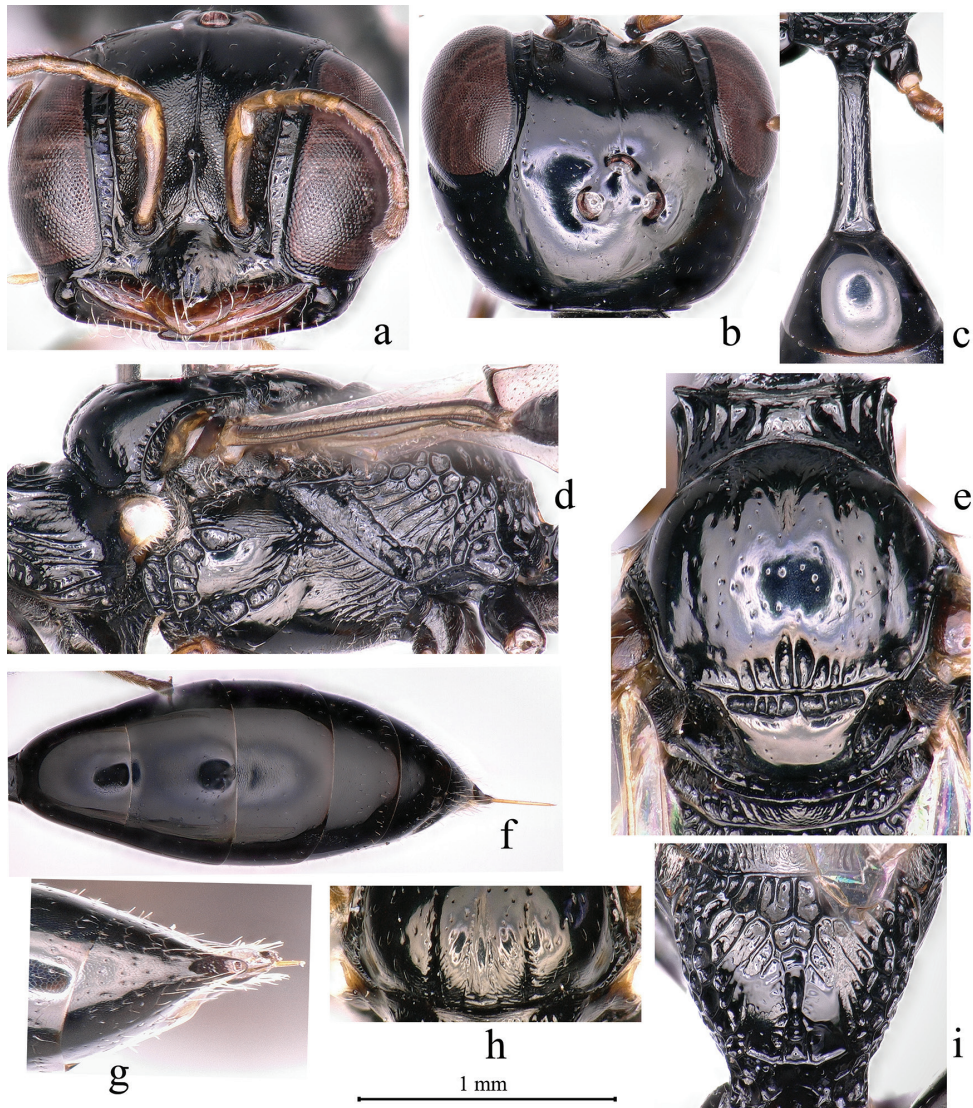


Figure 2. *Carinostigmus frontirugatus* Bashir & Ma, sp. nov. (female) **a** head (frontal view) **b** head (dorsal view) **c** petiole (dorsal view) **d** thorax (lateral view) **e** scutum, scutellum and metanotum (dorsal view) **f** metasoma **g** pygidial plate **h** scutum anterior (dorsal view) **i** propodeum (dorso-posterior view).

(Tsuneki 1954: fig. 13); median and lower frons without rugae (Tsuneki 1954: fig. 12); upper frons longitudinal carina distinct anteriorly, not reaching anterior ocellus (Tsuneki 1954: fig. 12); gena with several sturdy, oblique transverse rugae near mandible area; lower gena with fine, sparsely punctures; pronotal collar not elevated medially, lateral angles sharp (Tsuneki 1954: fig. 10); scutum without transverse striations anteriorly; scutellum dull; omaulus narrowed; dorsal surface of petiole smooth and pygidial area punctate medially.

Description. Female (Figs 2, 5a): Based on holotype, if any variation in paratypes described in square brackets.

Measurements.

BL: 6.2 [6–6.5] mm;

HW:HLD:HLF = 76:50:60;

HW_{max}:HW_{min} = 76:40;

HW:EWd:IOW:EW:OOW:TW:OCW:EL = 75:18:4:25:3:28:1:51;

AOD:WAS:IAD = 6:6:12;

POD:OOD:OCD:IODc:IODv:IODmin = 8:11:21:35:49:35;

LS:LP:LFI:WFI:LFII:WFII = 25:8:8:3:8:3;

LC:WC = 41:8;

PL:PW:LTI:WTI = 50:8:35:30.

Color pattern. Body black with shiny aspect, except the following: mandible medially (reddish brown apically), labrum, palpi, scape, pedicel, fore tibia and tarsus, mid tibia, trochanter and tarsus fulvous; flagellomeres dark brown [flagellomere I–II fulvous]; pronotal lobe whitish; tegula and forewing veins dark brown; hind trochanter reddish brown, tibia apically and tarsus dark brown; setae on margin of clypeus and on mandible pale.

Head. Mandible tridentate apically; setae on mandible sparse, long as pedicel length. Labrum pentagonal, round toward apex (Fig. 2a). Clypeus moderately convex, with coarse punctures, setae on margin of clypeus sparse, long as labrum length, free margin of clypeal lobe truncate medially (Fig. 2a). Median and lower frons rugose laterally, irregularly microstriate mesally, with a sturdy frontal median longitudinal carina, inter-antennal tubercle long, equal to midocellus diameter, distinctly broad at apex (Fig. 2a); upper frons with fine punctures, longitudinal carina distinct, reaching anterior ocellus but feeble (Fig. 2b), ocellar triangle nearly flat, with fine punctures, sparsely distributed (Fig. 2b); vertex behind ocelli shiny [dull], with fine sparsely distributed punctures (Fig. 2b). Gena with dense sturdy transverse rugae, lower gena with coarse punctures. Occipital carina narrow, not foveolate (Fig. 2b); inner-orbital sulcus broad, with inner marginal carina distinct, inconspicuously foveolate (Fig. 2a); outer-orbital sulcus broad, hind marginal carina inconspicuous, inconspicuously foveolate.

Mesosoma. Pronotal collar with sparse, sturdy rugae laterally (Fig. 2d), strongly elevated medially, anterior pronotal ridge strong marked, lateral angles sharp and projected (Fig. 2e). Scutum with coarse [fine] puncture, sparsely distributed, several slender transverse striations anteriorly (Fig. 2h), fovea present on posterior margin (Fig. 2e); admedian line conspicuous, extending to one third of scutum length; notaulus shallowly grooved and foveolate, extending to one third of scutum length (Fig. 2h); parapsidal line conspicuous (Fig. 2e). Scutellum with fine punctures sparsely distributed; metanotum on laterals with sturdy, oblique ridged (Fig. 2e). Mesopleuron with fine punctures, sparsely distributed; omaulus and hypersternaulus broadened as midtibial width, distinctly foveolate; scrobal sulcus short as mid trochanter length, foveate (Fig. 2d). Propodeum strongly irregular reticulated ridged on propodeal enclosure and side, reticulates broad as Fig. 2i and with shiny interspace, smooth area posterodorsally; propodeum posteriorly with rectangular median groove, reticulate, a small smooth area

medially, and irregular reticulation posteriorly (Fig. 2i); propodeal side presenting sparse, sturdy, longitudinal rugae anteriorly, and irregular reticulation posteriorly (Fig. 2d).

Legs. Outer surface of hindtibia without spines.

Metasoma. Petiole nearly cylindrical, slightly bowed, with dense weak rugose, basal and apical petiole width equal (Fig. 2c), lateral with few weak longitudinal carinae [carinae inconspicuous]. Gaster segments with fine sparsed puncture (Fig. 2f). Pygidial area punctate, oval and concave (Fig. 2g).

Male. Unknown

Distribution. China (Guizhou, Yunnan).

Etymology. The name *frontirugatus*, is junction of Latin words: *front* (= face) and *rugatus* (= rugae); referring to rugose on median and lower frons.

***Carinostigmus latidentatus* Bashir & Ma, sp. nov.**

<http://zoobank.org/B4048668-91CD-4E8D-BC1F-9755DA95ABCF>

Figs 3, 5b, c

Type material. Holotype: ♀, China: Yunnan: Jinghong: Menghai: Bulang Mountain, 21°56'N, 100°26'E, 16–IX.14.VII.2018, No. 2019000499, Malaise trap (YNAU).

Paratypes: 2♀♀, same data as holotype except: 25–V.17.IV.2018, No. 2019000009, 20–VIII.16.VII.2018, No. 2019000406; 1♀, China: Yunnan: Jinghong: Menghai: Guanggang Village: Guchalin, 21°56'N, 100°27'E, 27–V.16.IV.2018, No. 2019000082, coll. Malaise trap (YNAU); 1♀, China: Yunnan: Jinghong: Xishuangbanna National Forest Park, 22°01'N, 100°52'E, 31.VII.2003, coll. Qiang Li (ZJU); 1♀, China: Yunnan: Ruili: Mengxiu, 24°04'N, 97°47'E, 2–6.V.1981, No. 813076, coll. Junhua He (ZJU); 1♀, China: Fujian: Yongan County: Tianbaoyan, 25°56'N, 117°23'E, 15–18.VII.2001, No. 20020143, coll. Zaifu Xu (ZJU); 1♀, China: Hainan: Bawangling Mountain, 19°07'N, 109°05'E, 10.VI.2007, No. 200707357, coll. Jingxian Liu (ZJU); 1♀, China: Hainan: Diaoluo Mountain, 18°47'N, 109°52'E, 28.V.2007, No. 200707952, coll. Jingxian Liu (ZJU); 1♂, China: Yunnan: Pingbian: Baihushan, 22°59'N, 103°40'E, 17.VII.2003, 1310–1380 m, coll. Peng Wang (YNAU); 1♂, China: Yunnan: Ruili, 24°01'N, 97°51'E, 2.V.1981, No. 812495, coll. Junhua He (ZJU).

Diagnosis. This species is similar to *C. saigusai* (Tsuneki, 1966) in having the following: labrum broad, wider than long, sub quadrate (Fig. 3j); vertex behind ocelli impunctate (Fig. 3b); gena with several sturdy oblique transverse rugae near mandible area; occipital carina narrowed, distinctly foveolate (Fig. 3b); inner and outer-orbital sulcus narrowed (Fig. 3a); notaulus inconspicuous; scutellum dull, with fine sparsed punctures (Fig. 3f); metanotum densely covered by sturdy longitudinal rugae; omaulus broad as midtibial width, scrobal sulcus absent (Fig. 3g); lateral surface of propodeum with sparsed sturdy or slender oblique longitudinal rugae anteriorly, and irregular reticulation posteriorly (Fig. 3g); petiole dorsal surface nearly cylindrical, slightly bowed (Fig. 3c). Distinguished from *C. saigusai* by setae on mandible short, shorter than pedicel length; clypeus with coarse punctures (Fig. 3a); free margin of clypeal lobe with four teeth, median lobe broadly

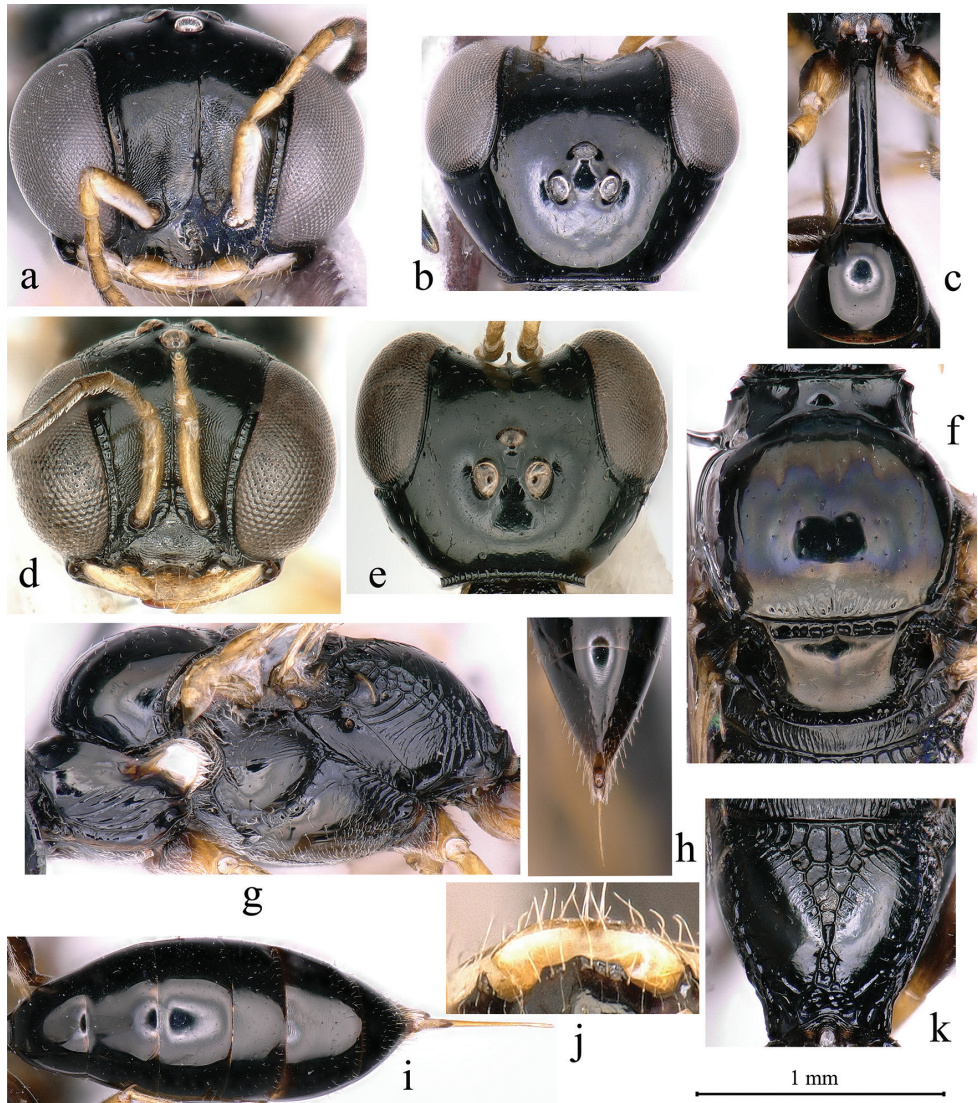


Figure 3. *Carinostigmus latidentatus* Bashir & Ma, sp. nov. (a–c, f–k female d, e male a, d head (frontal view) b, e head (dorsal view) c petiole (dorsal view) f scutum, scutellum and metanotum (dorsal view) g thorax (lateral view) h pygidial plate i metasoma (dorsal view) j free margin of clypeal lobe and labrum k propodeum (dorso-posterior view).

produced, nearly truncate, with two small inconspicuous lateral teeth, slightly reflexed apically (Fig. 3j); median and lower frons dull (Fig. 3a); upper frons with fine punctures, frontal carina distinct anteriorly, not reaching anterior ocellus (Fig. 3b); pronotal collar slightly elevated medially; admedian line inconspicuous; parapsidal line well-marked (Fig. 3f); propodeal enclosure shallowly impressed, triangular; posterior surface of propodeum with triangular median groove, several fairly slender oblique longitudinal rugae

anteriorly, and a large smooth area medially (Fig. 3k). *Carinostigmus saigusai* (Tsuneki) has the following characters: setae on mandible long; clypeus impunctate; free margin of clypeal lobe with three distinct teeth medially (Tsuneki 1966: fig. 25); median and lower frons not dull; upper frons impunctate, without frontal median carina; pronotal collar smooth; admedian line conspicuous; parapsidal line inconspicuous; propodeal enclosure deeply impressed, sub triangular; posterior surface of propodeum with rectangular median groove, and a small smooth area medially (Tsuneki 1966: fig. 27).

Description. Female (Figs 3a–c, f–k, 5b): Based on holotype, if any variation in paratypes described in square brackets.

Measurements.

♀, BL: 5.4 [4.8–5.5] mm;

HW:HLD:HLF = 70:40:55;

HWmax:HWmin = 70:37;

HW:EWd:IOW:EW:OOW:TW:OCW:EL = 70:19:2:21:2:20:1:43;

AOD:WAS:IAD = 3:5:10;

POD:OOD:OCD:IODc:IODv:IODmin = 7:14:18:27:41:27;

LS:LP:LFI:WFI:LFII:WFII = 21:10:9:3:10:3;

LC:WC = 32:6;

PL:PW:LTI:WTI = 48:7:30:34.

♂, BL 4.2–4.7 mm;

HW:HLD:HLF = 62:33:47;

HWmax:HWmin = 62:30;

HW:EWd:IOW:EW:OOW:TW:OCW:EL = 62:17:2:19:2:20:1:41;

AOD:WAS:IAD = 3:5:8;

POD:OOD:OCD:IODc:IODv:IODmin = 5:11:13:23:38:23;

LS:LP:LFI:WFI:LFII:WFII = 19:7:7:2:8:2;

LC:WC = 27:5;

PL:PW:LTI:WTI = 45:6:25:25.

Color pattern. Body black with shiny aspect, except the following: mandible ivory white with yellowish translucent margins (at minus apically), labrum, palpi, scape ventrally, and pronotal lobe ivory white; scape dorsally, pedicel, flagellomeres I–III fulvous (remains progressively dark), and tegula fulvous; forewing veins brown to dark brown; fore coxa extensively, trochanter, tibia, tarsi yellowish to fulvous, rest dark brown; mid coxa extensively, trochanter, base and apex of femur, tibia, tarsi yellowish to fulvous, rest dark brown; hind coxa, trochanter, tarsus yellowish to fulvous, tibia basally ivory, remaining dark brown; pale setae on clypeal margin and on mandible.

Head. Mandible tridentate apically; short setae, shorter than pedicel length on mandible, sparsed. Labrum sub quadrate (Fig. 3j). Clypeus slightly convex [nearly flat], with coarse punctures; setae on margin of clypeus sparse, long (Fig. 3a, j); free margin of clypeal lobe with four teeth, median apical margin of clypeal disk produced, nearly truncate, with two small inconspicuous lateral teeth, slightly reflexed, a strong tooth on apical margin of each lateral lobe (Fig. 3j). Median and lower frons irregularly microstriate, inter-antennal tubercle short, less than midocellus diameter (Fig. 3a); upper frons smooth, with fine punctures, frontal carina distinct on frons, not reaching

to midocellus (Fig. 3b). Ocellar triangle nearly flat, impunctate, vertex behind ocelli impunctate. Gena with several sturdy transverse rugae near mandible area, lower gena with fine punctures medially, sparsely distributed. Occipital carina narrow, foveolate (Fig. 3b). Inner-orbital sulcus narrowed as pedicel width, with inner marginal carina distinct, coarsely foveolate (Fig. 3a); outer-orbital sulcus narrowed as pedicel width, hind marginal carina inconspicuous, inconspicuously foveolate.

Mesosoma. Pronotal collar slightly elevated medially, anterior pronotal ridge strong, lateral angles sharp and projected (Fig. 3f). Scutum with coarse punctures, several slender transverse striations anteriorly, fovea present on scutum posterior margin (Fig. 3f). Admedian line and notaulus inconspicuous [notaulus invisible], extending to only anterior of scutum length, parapsidal line distinctly marked. Scutellum dull, with fine sparsely punctures (Fig. 3f). Metanotum densely covered by sturdy longitudinal rugae. Mesopleuron with sturdy, dense, short longitudinal rugae posteriorly, hypoepimeral area with several slender long longitudinal rugae, omaulus broad as midtibia width, hypersternaulus narrowed as pedicel width, distinctly foveolate, scrobal sulcus absent (Fig. 3g). Propodeal enclosure shallowly impressed, triangular, with sturdy longitudinal rugae, median area reticulate (Fig. 3k); posterior surface of propodeum with triangular median groove, several fairly slender oblique longitudinal rugae anteriorly, a large smooth area medially, and irregular reticulation posteriorly (Fig. 3k); propodeal side presenting sparsely oblique longitudinal rugae anteriorly, and irregular reticulation posteriorly (Fig. 3g).

Legs. Outer surface of hindtibia without spines.

Metasoma. Petiole dorsal surface nearly cylindrical, slightly bowed, basal and apical petiole width equal (Fig. 3c), side smooth. Gaster segments sterna IV–VI with dense fine punctures, remaining nearly impunctate (Fig. 3i). Pygidial area smooth, U-shaped, apex truncate (Fig. 3h).

Male. (Figs 3d, e, 5c). Same as female except labrum fulvous; mandible bidentate apically; labrum notched, with two triangular teeth apically; outer-orbital sulcus with hind marginal carina distinct, coarsely foveolate; flagellomeres without tyloids; admedian line and notaulus conspicuous, extending to half of scutum length; hypersternaulus broad as midtibia width; petiole widened toward apex slightly.

Distribution. China (Yunnan, Fujian, Hainan).

Etymology. The name *latidentatus*, is derived from the Latin words: *lateralis* (= lateral, side) contracted to *lati* and *dentatus* (= toothed, dentate), referring to the strong tooth on the apical margin of the lateral lobe of the clypeus.

***Carinostigmus vesulcatus* Bashir & Ma, sp. nov.**

<http://zoobank.org/0FDD9981-3372-4E78-8C16-BB9D7ECC7353>

Figs 4, 5d, e

Type material. Holotype: ♀, China: Yunnan: Jinghong: Menghai: Bulang Mountain, 21°57'N, 100°27'E, 17–VI.21.V.2018, No. 2019000099, Malaise trap (YNAU).

Paratypes: 2♂♂, China: Yunnan: Dehong: Nabang, 24°26'N, 98°35'E, 15.V.2009, No. 201005191, coll. Jie Zeng, No. 201005205, coll. Manman Wang (YNAU); 1♂,

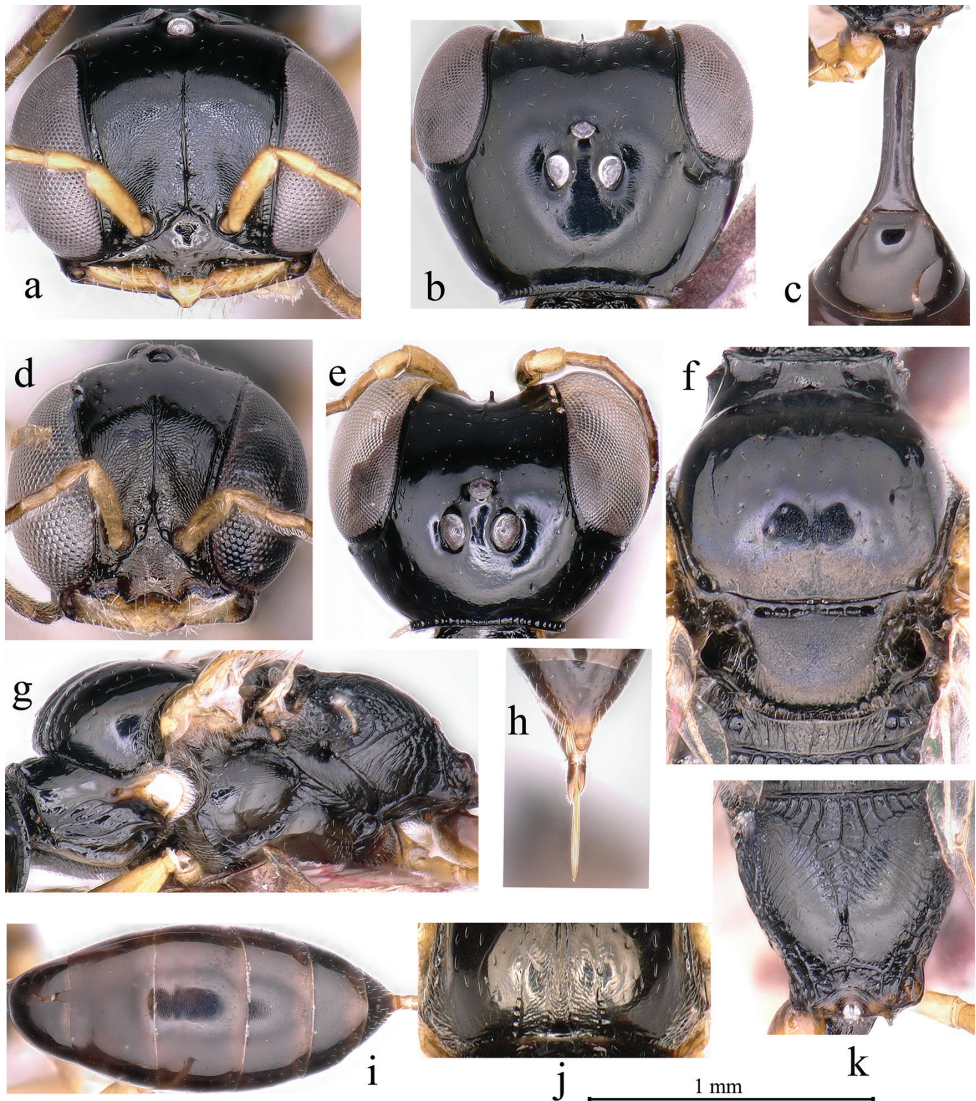


Figure 4. *Carinostigmus vesulcatus* Bashir & Ma, sp. nov. (a–c, f–k female, d, e male): a, d head (frontal view) b, e head (dorsal view) c petiole (dorsal view) f scutum, scutellum and metanotum (dorsal view) g thorax (lateral view) h pygidial plate i metasoma (dorsal view) j scutum anterior k propodeum (dorso-posterior view).

China: Yunnan: Dehong: Yinjiang: Tongbiguan, 24°42'N, 97°55'E, 18.V.2009, No. 201005224, coll. Manman Wang (YNAU); 1♀, China: Yunnan: Nujiang: Fugong: Yueliang Village, 25°49'N, 98°51'E, 27.V.2007, coll. Feng Yuan (CAS); 1♀, China: Yunnan: Kaiyuan: Nandong, 23°40'N, 103°15'E, 16.VII.2003, coll. Qiang Li (YNAU).

Diagnosis. This species resembles *C. congruus* (Walker, 1860) in sharing: median and lower frons microstriate, with a sturdy frontal median longitudinal carina (Fig. 4a); upper frons with fine and coarse punctures, frontal carina distinct anteriorly, not reaching anterior ocellus (Fig. 4b); ocellar triangle flat, gena with several sturdy

oblique transverse rugae medially, lower gena with weak striations; outer-orbital sulcus broad; notaulus deeply grooved (Fig. 4j); propodeal enclosure triangular, with sturdy longitudinal rugae anteriorly, slender dense, longitudinal rugae laterally (Fig. 4k); pygidial area oval shaped (Fig. 4h). It can be differentiated from *C. congruus* by labrum, in female, pentagonal, longer than wide (Fig. 4a), in male, wider as long, deeply emarginated apically forming two rounded lobes (Fig. 4d); clypeus slightly convex; free margin of clypeal lobe nearly truncate medially, teeth inconspicuous (Fig. 4a); inter-antennal tubercle without T-shaped at apex (Fig. 4b); inner-orbital sulcus narrowed, inconspicuously foveolate (Fig. 4a); occipital carina foveolate (Fig. 4b); anterior pronotal ridge strongly marked (Fig. 4f); in female, fovea absent on scutum posterior margin (Fig. 4f); admedian line conspicuous in female, inconspicuous in male; parapsidal line conspicuous, and metanotum with inconspicuous rugae medially (Fig. 4f). *Carinostigmus congruus* (Walker) has the following characters: labrum triangular, broadly rounded at apex; clypeus strongly convex at middle; free margin of clypeal lobe slightly emarginate medially, with two distinct lateral small teeth (Krombein 1984: fig. 9); inter-antennal tubercle with T-shaped at apex (Krombein 1984: fig. 15); inner-orbital sulcus broad, distinctly foveolate (Krombein 1984: fig. 3); occipital carina not foveolate; pronotal collar ridged weakly marked; in female, fovea present on scutum posterior margin; admedian and parapsidal lines inconspicuous, and metanotum smooth medially (Krombein 1984: fig. 39).

Description. Female (Figs 4a–c, f–k, 5d): Based on holotype, if any variation in paratypes described in square brackets.

Measurements.

♀, BL 4.6 [4.5–4.9] mm;

HW:HLD:HLF = 60:38:40;

HWmax:HWmin = 60:31;

HW:EWd:IOW:EW:OOW:TW:OCW:EL = 60:14:1:16:2:22:1:41;

AOD:WAS:IAD = 5:5:10;

POD:OOD:OCD:IODc:IODv:IODmin = 4:12:14:28:36:28;

LS:LP:LFI:WFI:LFII:WFII = 18:7:8:3:8:3;

LC:WC = 25:5;

PL:PW:LTI:WTI = 45:6:30:23.

♂, BL 4–4.6 mm;

HW:HLD:HLF = 65:35:43;

HWmax:HWmin = 65:31;

HW:EWd:IOW:EW:OOW:TW:OCW:EL = 65:18:1:18:2:20:1:40;

AOD:WAS:IAD = 3:3:8;

POD:OOD:OCD:IODc:IODv:IODmin = 4:10:12:20:36:20;

LS:LP:LFI:WFI:LFII:WFII = 20:8:8:2:8:2;

LC:WC = 23:5;

PL:PW:LTI:WTI = 46:6:27:25.

Color pattern. Body black with shiny aspect, except the following: mandible yellowish, apically dark; labrum yellowish with ivory marked medially; palpi pale; scape and pedicel extensively yellowish; flagellomeres I–III yellowish, remaining darker; pronotal lobe ivory

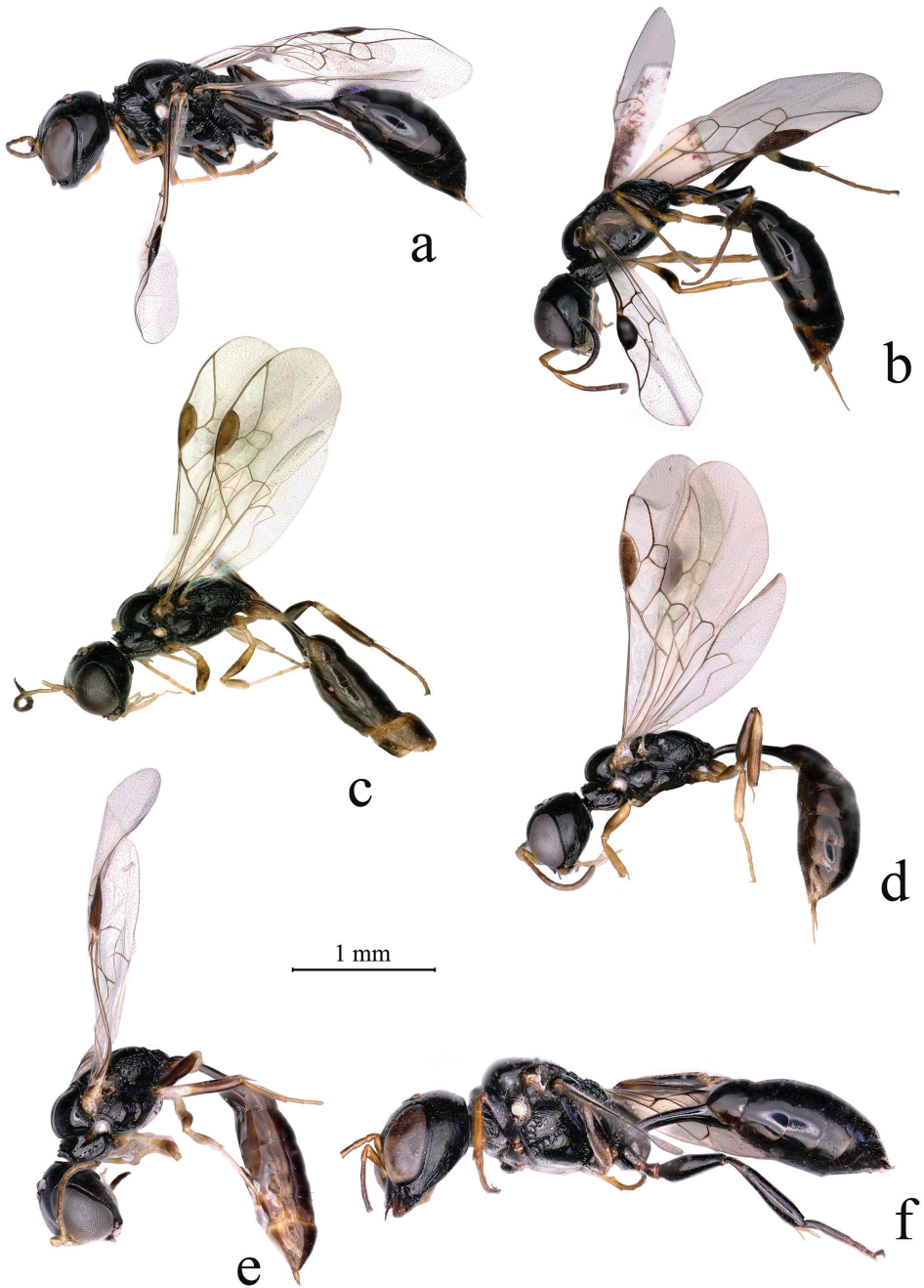


Figure 5. **a** *Carinostigmus frontirugatus* Bashir & Ma, sp. nov., (female) **b, c** *C. latidentatus* Bashir & Ma, sp. nov., (**b** female **c** male) **d, e** *C. vesulcatus* Bashir & Ma, sp. nov., (**d** female **e** male) **f** *C. palawanensis* (Tsuneki, 1976) (female) **a–f** lateral view.

with yellowish spot; tegula fulvous; forewing veins dark brown; legs fulvous except mid and hind femur reddish brown; pale setae on clypeal margin and on mandible.

Head. Mandible tridentate apically; setae on mandible sparsely, long, longer than labrum length. Labrum pentagonal, rounded toward apex (Fig. 4a). Clypeus slightly convex, with coarse punctures; setae on margin of clypeus sparsely, long as labrum length; free margin of clypeal lobe nearly truncate, sinuous, not forming reflexed teeth (Fig. 4a). Median and lower frons microstriate, with a sturdy frontal median longitudinal carina (Fig. 4a), inter-antennal tubercle short, less than midocellus diameter (Fig. 4b); upper frons smooth, with fine and coarse punctures, frontal carina distinct anteriorly, not reaching anterior ocellus (Fig. 4b). Ocellar triangle nearly flat, finely punctate [impunctate]; vertex behind ocelli, finely punctate [impunctate]; gena with several sturdy transverse rugae medially; lower gena with weak striations. Occipital carina broad and foveolate as Fig. 4b; inner-orbital sulcus narrow as flagellomere I width, with inner marginal carina distinct, inconspicuously foveolate (Fig. 4a); outer-orbital sulcus broad as pedicel width, hind marginal carina distinct, inconspicuously foveolate.

Mesosoma. Pronotal collar smooth, strongly elevated mesally, ridged inconspicuously anteriorly, weakly marked, lateral angles blunt (Fig. 4f). Scutum with fine punctures, sparsely distributed, several slender transverse striations anteriorly (Fig. 4j); admedian line conspicuous, extending to one third of scutum length; notaulus deeply grooved and foveolate, extending to only anterior of scutum length (Fig. 4j); parapsidal line inconspicuous (Fig. 4f). Scutellum dull aspect densely micropunctated; metanotum with dense, slender, longitudinal rugae laterally, weak medially (Fig. 4f). Mesopleuron with fine punctures, sparsely distributed; omaulus and hypersternaulus narrowed as pedicel width, inconspicuously foveate [distinctly foveolate]; scrobal sulcus absent (Fig. 4g). Propodeal enclosure shallowly impressed, triangular, with sturdy longitudinal rugae anteriorly, slender dense, longitudinal rugae laterally (Fig. 4k); propodeum posteriorly with oval median groove, slender dense transverse rugae anteriorly, smooth medially (Fig. 4k); propodeal side presenting obliques and regular striae, sparsely distributed (Fig. 4g).

Legs. Outer surface of hindtibia without spines.

Metasoma. Petiole dorsal surface sub quadrate (cross section), basal width narrower than apically (Fig. 4c), side smooth. Gaster segments III–V [IV–VI] with fine sparsely punctures, rest impunctate (Fig. 4i). Pygidial area punctate anteriorly, oval shaped (Fig. 4h).

Male (Figs 4d, e, 5e). Same as female except mandible ivory, reddish brown apically; labrum, scape beneath and pedicel ivory, remaining scape and flagellomeres fulvous; flagellomeres without tyloids; forewing veins brown to dark brown; legs ivory to fulvous; setae on margin of clypeus and on mandible fulvous and short, less than pedicel length; mandible bidentate apically; labrum notched, deeply emarginated at apex; clypeus slightly microstriate, convex, impunctate; gena with several sturdy oblique transverse rugae near eye; fovea present on scutum posterior margin; parapsidal line inconspicuous.

Distribution. China (Yunnan).

Etymology. The name *vesulcatus*, is derived from the Latin words *ve-* (= without) and *sulcatus* (= sulcate), referring to the scrobal sulcus absent.

***Carinostigmus palawanensis* (Tsuneki), 1976, new record for China**

Fig 5f

Specimen examined. 1♀, China: Yunnan: Xishuangbanna: Mengla: Shangyong: Longmen Village, 21°16'N, 101°32'E, 10.IV.2010, 923 m, No. 201000068, coll. Rui Zhang (YNAU).

Description. Female (Fig. 5f).

Head. Mandible tridentate apically. Labrum pentagonal, rounded toward apex (Fig. 2a). Clypeus moderately convex, with coarse punctures (Tsuneki 1976: fig. 124); free margin of clypeal lobe deeply emarginate medially (Tsuneki 1976: fig. 125). Median and lower frons striate (Tsuneki 1976: fig. 122); inter-antennal tubercle short, less than midocellus diameter, distinctly broad at apex (Tsuneki 1976: fig. 122); upper frons with coarse, dense punctures, frontal carina distinct, reaching anterior ocellus but feeble (Tsuneki 1976: fig. 122). Ocellar triangle moderately convex. Gena smooth, rugose ventrally (Tsuneki 1976: fig. 123). Occipital carina narrowed not foveolate, inner and outer-orbital sulcus broad (Tsuneki 1976: fig. 122).

Mesosoma. Pronotal collar smooth, strongly elevated medially, anterior pronotal collar ridged strong, lateral angles sharp and projected (Tsuneki 1976: fig. 126). Scutum with coarse sparsed punctures, slender transverse striations anteriorly, fovea present on scutum posterior margin, admedian line conspicuous, notaulus invisible, parapsidal line inconspicuous (Tsuneki 1976: fig. 126). Scutellum with fine, sparsed punctures, metanotum smooth. Mesopleuron with coarse, sparsed punctures, omaulus narrowed (Fig. 3g), hypersternaulus broad anteriorly, narrow apically, distinctly foveolate, scrobal sulcus short (Fig. 2d). Propodeal enclosure triangular, with sturdy longitudinal rugae; propodeum posterior with several slender oblique longitudinal rugae anteriorly, small smooth area medially, and irregular reticulation posteriorly; propodeum side with sparsed, slender oblique longitudinal rugae anteriorly, and irregular reticulation posteriorly.

Metasoma. Petiole dorsal nearly cylindrical, with dense weak transverse striations, basal and apical petiole width equal, side with weak striations. Gaster segments finely punctate. Pygidial area oval shaped (Fig. 4h).

Distribution. China (Yunnan), Philippines.

Acknowledgements

This study was funded by National Natural Science Foundation of China (31750002, 31760641). The authors extend their appreciation to Dr WJ Pulawski for providing literature. We also would like to thank the reviewers E.M. Khan, M.A. Hassan, L. Kimsey and B.M. Trad for suggestions that helped improve this article.

References

- Bohart RM, Menke AS (1976) Sphecoid wasps of the world, a generic revision. University of California Press, Berkeley, 695 pp. https://archive.org/details/bub_gb_FExMjuRhjpIC
- Gussakovskij VV (1934) Beitrag zur Kenntnis der Pseninen-und Pemphredoninen-Fauna Japans (Hymenoptera, Sphecidae). *Mushi* 7: 79–89.
- Harris RA (1979) A glossary of surface sculpturing. *Occasional Papers in Entomology* 28: 1–31. <https://zenodo.org/record/26215>
- Krombein KV (1984) Biosystematic studies of Ceylonese wasps, XIV: a revision of *Carinostigmus* Tsuneki (Hymenoptera: Sphecoidea: Pemphredonidae). *Smithsonian Contributions to Zoology* 396: 1–37. <https://doi.org/10.5479/si.00810282.396>
- Li Q, He J (2004) Superfamily Sphecoidea. In: He J (Ed.) *Hymenopteran Insect Fauna of Zhejiang*. Science Press, Beijing, 1071–1210.
- Li Q, Yang C (1995) Hymenoptera: Sphecoidea. In: Zhu T (Ed.) *Insects and Macrofungi of Gutianshan, Zhejiang*. Science Technique Press of Zhejiang, 270–273.
- Ma L, Chen XX, Qiang L (2012) The genus *Carinostigmus* Tsuneki (Hymenoptera: Crabronidae) with two newly recorded species from China. *Entomotaxonomia* 34(2): 475–481. http://researcharchive.calacademy.org/research/entomology/Entomology_Resources/Hymenoptera/sphecidae/copies/Ma_Chen_Li_2012.pdf
- Ma L, Li Q, Wang CH, Jiang X, Lu HX (2018) X Sphecoidea. In: Xuexin C (Ed.) *Insect fauna of the Qinling Mountains Hymenoptera*. World Book Publishing House Xi'an Co. Ltd., Xi'an, 823–861. http://researcharchive.calacademy.org/research/entomology/Entomology_Resources/Hymenoptera/sphecidae/copies/Ma_et_al_Insect_fauna_of_the_Qinling_Mountains_2018.pdf
- Maidl F (1925) Fauna sumatrensis (Beitrag Nr. 11). Sphegidae (Hym.). *Entomologische Mitteilungen* 14: 376–390. http://researcharchive.calacademy.org/research/entomology/Entomology_Resources/Hymenoptera/sphecidae/copies/Maidl_1925a.pdf
- Pulawski WJ (2020) *Carinostigmus*: Catalog of Sphecidae. http://researcharchive.calacademy.org/research/entomology/entomology_resources/hymenoptera/sphecidae/genera/Carinostigmus.pdf [accessed 1 June 2020]
- Tsuneki K (1954) The genus *Stigmus* Panzer of Europe and Asia, with description of eight new species (Hymenoptera, Sphecidae). *Memoirs of the Faculty of Liberal Arts, Fukui University, Series II, Natural Science* 3: 1–38. http://researcharchive.calacademy.org/research/entomology/Entomology_Resources/Hymenoptera/sphecidae/copies/Tsuneki_1954a.pdf
- Tsuneki K (1956) A new species of *Stigmus* from Morocco (Hymen., Sphecidae, Pemphredoninae). *Entomologische Berichten* 16: 263–264. http://researcharchive.calacademy.org/research/entomology/Entomology_Resources/Hymenoptera/sphecidae/copies/Tsuneki_1956i.pdf
- Tsuneki K (1966) Contribution to the knowledge of the Pemphredoninae fauna of Formosa and the Ryukyus (Hymenoptera, Sphecidae). *Etizenia* 14: 1–21. http://researcharchive.calacademy.org/research/entomology/Entomology_Resources/Hymenoptera/sphecidae/copies/Tsuneki_1966c.pdf
- Tsuneki K (1974) A contribution to the knowledge of Sphecidae occurring in southeast Asia (Hym.). *Polskie Pismo Entomologiczne* 44: 585–660. http://researcharchive.calacademy.org/research/entomology/Entomology_Resources/Hymenoptera/sphecidae/copies/Tsuneki_1974b.pdf

- Tsuneki K (1976) Sphecoidea taken by the Noona Dan expedition in the Philippine Islands (Insecta, Hymenoptera). *Steenstrupia* 4: 33–120. http://researcharchive.calacademy.org/research/entomology/Entomology_Resources/Hymenoptera/sphecidae/copies/Tsuneki_1976b.pdf
- Tsuneki K (1977) Further notes and descriptions on some Formosan Sphecidae (Hymenoptera). *Special Publications of the Japan Hymenopterists Association* 2: 1–32. http://researcharchive.calacademy.org/research/entomology/Entomology_Resources/Hymenoptera/sphecidae/copies/Tsuneki_1977c.pdf
- Walker F (1860) Characters of some apparently undescribed Ceylon insects. *The Annals and Magazine of Natural History (Third Series)* 5: 304–311. <https://doi.org/10.1080/00222936008697221>

Three new species of *Pseudophanias* Raffray from Japan and Taiwan Island, and synonymy of *Chandleriella* Hlaváč with *Pseudophanias* (Coleoptera, Staphylinidae, Pselaphinae)

Shota Inoue^{1,2}, Shûhei Nomura³, Zi-Wei Yin⁴

1 Entomological Laboratory, Graduate School of Bioresource and Bioenvironmental Sciences, Kyushu University, Fukuoka 819-0395, Japan **2** The Kyushu University Museum, Fukuoka 812-8581, Japan **3** Department of Zoology, National Museum of Nature and Science, 4-1-1, Amakubo, Tsukuba-shi, Ibaraki 305-0005, Japan **4** Laboratory of Systematic Entomology, College of Life Sciences, Shanghai Normal University, 100 Guilin Road, Shanghai 200234, China

Corresponding author: Shota Inoue (pselaphineman@gmail.com)

Academic editor: Jan Klimaszewski | Received 26 April 2020 | Accepted 17 August 2020 | Published 6 November 2020

<http://zoobank.org/861F9C14-6E6D-4222-A41F-FC56F978C2E8>

Citation: Inoue S, Nomura S, Yin Z-W (2020) Three new species of *Pseudophanias* Raffray from Japan and Taiwan Island, and synonymy of *Chandleriella* Hlaváč with *Pseudophanias* (Coleoptera, Staphylinidae, Pselaphinae). ZooKeys 987: 135–156. <https://doi.org/10.3897/zookeys.987.53648>

Abstract

The genus *Pseudophanias* Raffray, 1890 is discovered in Japan and Taiwan Island for the first time, with three new species: *P. yaimensis* Inoue, Nomura & Yin, **sp. nov.**, *P. nakanoi* Inoue, Nomura & Yin, **sp. nov.**, and *P. excavatus* Inoue, Nomura & Yin, **sp. nov.** It is the fifth tmesiphorine genus known from Japan and the first from Taiwan. The genus *Chandleriella* Hlaváč, 2000 is placed as a junior synonym of *Pseudophanias*, resulting in the following new combinations: *P. termitophilus* (Bryant, 1915), **comb. nov.**, and *P. yunnanicus* (Yin, 2019), **comb. nov.** A list of world species, and a key to East and South Asian representatives of *Pseudophanias* is provided.

Keywords

claw morphology, East Asia, identification key, nomenclature, rove beetle, taxonomy, Tmesiphorini

Introduction

The tribe Tmesiphorini Jeannel currently contains 30 extant genera worldwide (Yin et al. 2013a), among them the primarily Oriental genus *Pseudophanias* Raffray, 1890 was established for *P. malaianus* Raffray from Malaysia (Raffray 1890a, b). *Pseudophanias* was initially placed in the tribe Tyrini (Raffray 1905, 1908), then in Phalepsini (Jeannel 1949; Newton and Chandler 1989), and was most recently moved to Tmesiphorini (Chandler 2001). Currently, ten epigeal species are known from the tropical areas in Southeast Asia (Raffray 1890a, b, 1895, 1905), and one cavernicolous species was described from central Nepal (Yin et al. 2015).

Hlaváč (2000) erected a new genus *Chandleriella* Hlaváč for *Lasinus termitophilus* Bryant from Borneo. He correctly recognized *Chandleriella* as a member of Tmesiphorini based on the presence of semi-circular sulci that enclose the antennal bases, but did not compare it to any members of the tribe. A second species of the genus, *C. yunnanica* Yin, was later described from southwestern China (Yin 2019), with two individuals of the type series associated with *Ectomomyrmex* ants.

Specimens of the genus *Chandleriella* have well-developed posterior tarsal claw and an overall elongate body form, whereas those of *Pseudophanias* have a strongly reduced posterior tarsal claw and a stouter body. However, after examining the type species of *Pseudophanias* (by the second author), and a vast collection of undescribed *Pseudophanias-Chandleriella*-like species, transitional states in both claw morphology and habitus were found. Nomura and Idris (2005) already discussed this problem in detail, but no further nomenclatural act was made. Consequently, the two genera cannot be distinguished reliably using current methods. On the other hand, Nomura and Idris (2005) also noted the similarities between *Pseudophanias* and the tribe Hybocephalini, but this relationship needs further investigation.

So far, four tmesiphorine genera have been recognized in Japan: *Saltisedes* Kubota, 1944, *Tmesiphorus* LeConte, 1849, *Tmesiphoromimus* Löbl, 1964, and *Raphitreus* Sharp, 1883 (Shibata et al. 2013; Yin et al. 2013b; Inoue et al. 2020), while none have been found from Taiwan. In this paper, we formally place *Chandleriella*, syn. n., as a junior synonym of *Pseudophanias* and describe three new species from Japan and Taiwan.

Material and methods

The type specimens of *Pseudophanias* species in the Raffray's Collection were examined by the second author at the Muséum National d'Histoire Naturelle, Paris, France (MNHN). The holotypes of *Pseudophanias yaimensis*, *P. nakanoi* and *P. excavatus* are deposited in the National Museum of Nature and Science, Tokyo, Japan (NSMT) and paratypes are deposited in NSMT, and the Kyushu University Museum, Fukuoka, Japan (KUM). Two paratypes of *Pseudophanias yaimensis* are temporarily deposited in the Insect Collection of Shanghai Normal University, Shanghai, China (SNUC), and will be eventually housed in the National Museum of Natural Science, Taichung, Taiwan (NMNS).

The label data of the holotypes are quoted verbatim. A slash (/) was used to separate lines on the same label, and a double slash (//) was used to separate different labels on the same pin.

The specimens were soaked in distilled water overnight, and male genitalia were obtained by removing tergites and sternites VIII–IX. The male genitalia were soaked in cold 10% KOH for about 6 hours, and afterward they were washed in distilled water for 10 minutes. They were subsequently transferred to 50% ethanol for 2–5 minutes and then to 80% ethanol for 2 minutes. Finally, the male genitalia were soaked in 99% ethanol for 10 minutes and were then mounted in Euparal on a 5 × 10 mm micro-cover glass. The micro-cover glass with male genitalia was glued onto a paper card (5 × 7 mm) and pinned under the specimen (Maruyama 2004). The specimens were also examined using a scanning electron microscope (SEM; HITACHI SU-3500) at the Center for Advanced Instrumental and Educational Supports, Faculty of Agriculture, Kyushu University. For the SEM observations, all examined materials were coated with gold by Ion Sputter (Ion sputter; HITACHI MC1000) and examined at 5.00 kV and 30 Pa.

The following abbreviations were applied:

- AL** length of the dorsally visible part of the abdomen along the midline;
- AW** maximum width of the abdomen;
- EL** length of the elytra along the suture;
- EW** maximum width of the elytra;
- HL** length of the head from the anterior clypeal margin to the occipital constriction;
- HW** width of the head across the eyes;
- PL** length of the pronotum along the midline;
- PW** maximum width of the pronotum.

Length of the body (BL) was a combination of HL + PL + EL + AL. All measurements are recorded in millimeters (mm).

Taxonomy

Genus *Pseudophanias* Raffray, 1890

[Japanese name: Tsumugata-arizukamushi]

Pseudophanias Raffray, 1890a: 161. Type species: *Pseudophanias malaianus* Raffray, 1890b: 214 (by subsequent monotypy).

Chandleriella Hlaváč, 2000: 91, syn. nov. Type species: *Lasinus termitophilus* Bryant, 1915: 300 (by original monotypy).

Revised diagnosis. Members of the genus *Pseudophanias* can be distinguished from all other genera of the Tmesiphorini by a combination of the following characteristics: body form strongly stout to markedly elongate; male antennae usually with modified antennomeres 3–10, or 11 alone; greatly reduced maxillary palpi with fusiform

palpomere 4; distinct paratergites on abdomen; tergite IV longest to subequal in size to tergite V; aedeagus usually tuberculate in shape, rarely bulbous.

Distribution. Indonesia, Malaysia, Singapore, China, Japan, Nepal.

Key to *Pseudophanias* of East and South Asia

- 1 Head coarsely punctate (Fig. 11A). Antennae short (ratio of body length to antennal length = 1:<0.5), antennomeres each distinctly transverse, antennomeres 5 to 11 modified to form clasping in male (Fig. 10B, C) (China: Taiwan)..... ***P. excavatus* Inoue, Nomura & Yin, sp. nov.**
- Head finely punctate. Antennae elongate (ratio of body length to antennal length = 1:>0.5), antennomeres each elongate to subquadrate, antennomeres 7, 9, or 11 modified to form various shape in male **2**
- 2 Pronotum with median longitudinal carina (Indonesia, Sumatra) ***P. termitophilus* (Bryant)**
- Pronotum without median longitudinal carina **3**
- 3 Antennomeres each distinctly elongate, male antennomere 7 expanded. Male profemora excavated at bases (Nepal: Pokhara) ***P. spinitarsis* Yin, Coulon & Bekchiev**
- Antennomeres each elongate to subquadrate, male antennomere 7 unmodified. Profemora evenly narrowing at bases in both sex **4**
- 4 Antennomere 9 obliquely expanded laterally, antennomere 11 angularly expanded at lateral margins in male (Fig. 6B). Abdominal tergite IV with long discal carinae (Fig. 7F) (Japan: Ryûkyû, Kyûshû) ***P. nakanoi* Inoue, Nomura & Yin, sp. nov.**
- Antennomere 9 simple, antennomere 11 modified. Abdominal tergite IV with short discal carinae **5**
- 5 Body length 3.50–3.90 mm (female: 3.83–3.85 mm). Antennomere 11 enlarged to form bowl-like structure in male. Pronotum without conical spine (China: Yunnan) ***P. yunnanicus* (Yin)**
- Body length 2.16–2.32 mm (female: 2.20–2.32 mm). Antennomere 11 angulate at anterolateral margins in male (Fig. 2B). Pronotum with conical spine just anterior of median fovea (Fig. 2A) (Japan: Ryûkyû; China: Taiwan) ***P. yaimensis* Inoue, Nomura & Yin, sp. nov.**

***Pseudophanias yaimensis* Inoue, Nomura & Yin, sp. nov.**

<http://zoobank.org/81ADE876-E798-467A-8625-03721012EF1B>

Figs 1–4

[Japanese name: Yaima-tsumugata-arizukamushi]

Type material. *Holotype* (NSMT): ♂, “Japan: [Ryûkyû], Ishigaki- / jima, Takeda-rindô 23 X 2007, Teruaki Ban leg. // HOLOTYPE (red) / ♂, *Pseudophanias yaimensis* sp. nov., / det. Inoue, Nomura & Yin, 2020” **Paratypes:** Japan: 1 ♀, [Ryûkyû], Okinawa

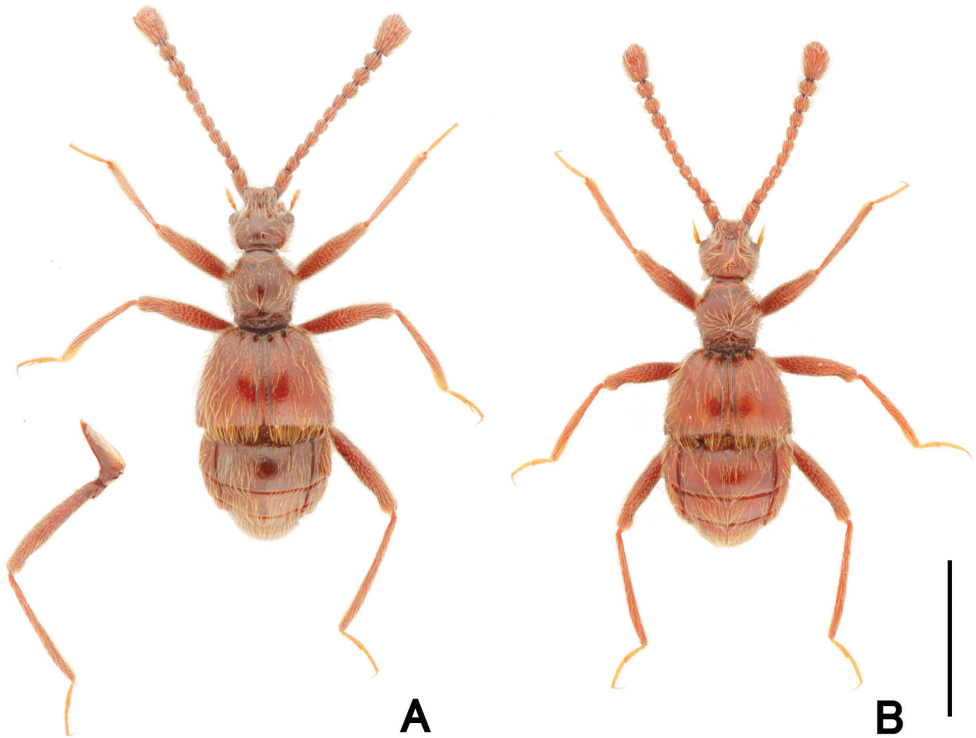


Figure 1. Dorsal habitus of *Pseudophanias yaimensis* **A** male **B** female. Scale bar: 1.0 mm.

ken, Ishigaki-jima Is., Mt. Omoto-dake, 16 VIII 1991, K. Ogata leg. (NSMT); 1 ♂, Ishigaki-jima Is., Mt. Omoto-dake, (FIT), 14–20 V 2002, S. Hori leg. (NSMT); 1 ♂, 1 ♀, China: Taiwan, Taichung Co. (台中县), Guguan (谷关), 1238 m, 24.180691N, 120.944213E, 29 III 2015, local collector, nest of *Nasutitermes parvonasutus* (SNUC). Each paratype pinned with the following label: “PARATYPE (yellow) / ♂ (or ♀), *Pseudophanias yaimensis* sp. nov., / det. Inoue, Nomura & Yin, 2020”.

Diagnosis. *Pseudophanias yaimensis* is most similar to the Sumatran *P. robustus* Raffray, 1904, but can be distinguished by the distinctly smaller body size (3.00–3.20 mm in *P. robustus*), the angulate antennomere 11 at anterolateral margins in the male, the finely punctate head and pronotum, and the shorter discal carinae on tergite IV.

Description. Male (Figs 1A, 2A). Body length 2.16–2.32 mm. Dorsal surface polished and weakly shining, with dense setae. **Head** (Fig. 3A) about as long as wide, HL 0.46 mm, HW 0.42–0.44 mm, same size as pronotum, nearly hexagonal, with dense setae; frontal rostrum with short longitudinal sulcus including large fovea; antennal tubercles prominent, with dense punctures which gradually disappear towards vertex; vertex polished, finely punctate, with pair of foveae; frontal, vertexal foveae glabrous; eyes prominent; postocular margins three times longer than length of eyes. Maxillary palpi (Fig. 3B) symmetrical; palpomere 1 minute; palpomere 2 elongate, narrowed in basal half; palpomere 3 small, widest at apices; palpomere 4 fusiform. **Antennae** (Fig. 2B) elongate, 1.42 mm in length; antennal club formed by apical

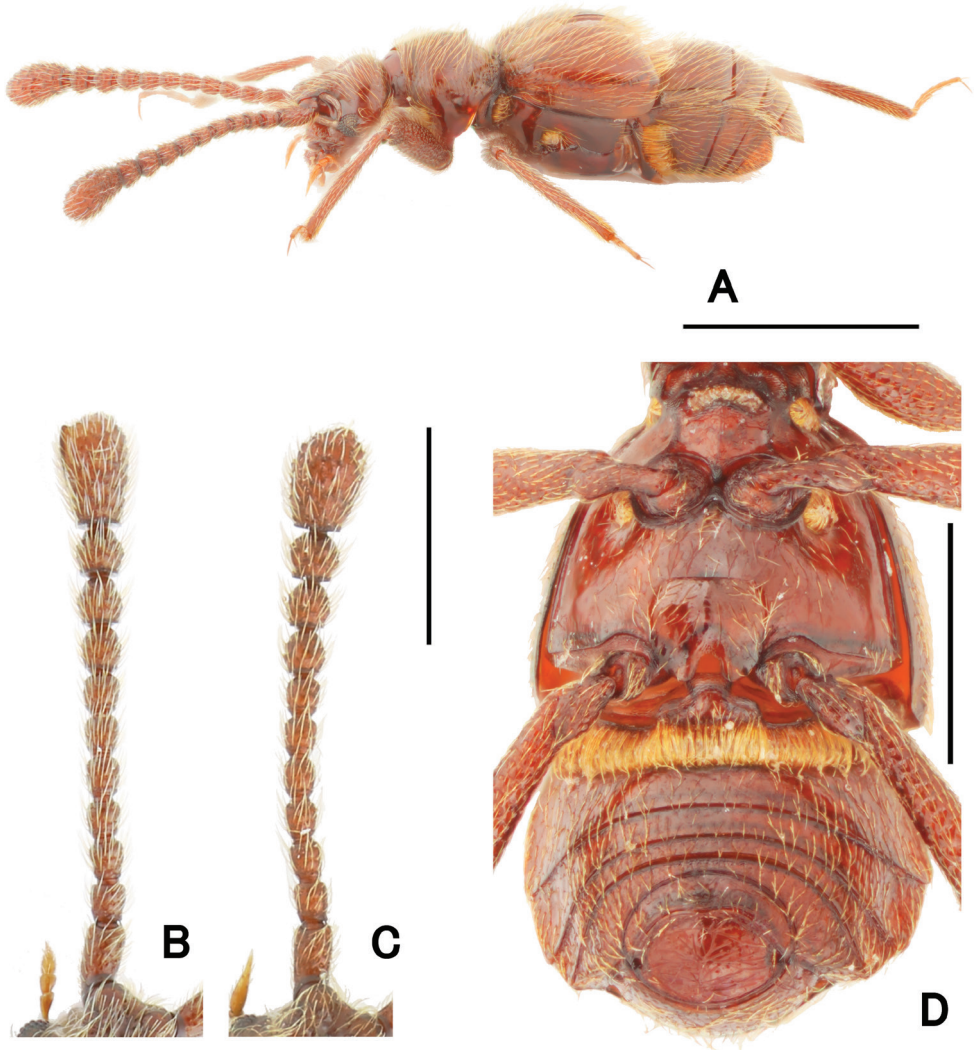


Figure 2. Morphological details of *Pseudophanias yaimensis* **A** habitus in lateral view **B** male antenna **C** female antenna **D** male metaventrite. Scale bars: 1.0 mm (**A**); 0.5 mm (**D**); 0.2 mm (**B**, **C**).

antennomere alone; antennomere 1 thick, elongate, 1.5 times longer than 2; 2 slightly longer than wide; 3–11 successively widened towards apices; 3–7 each slightly elongate; 8–10 quadrate; 11 enlarged, roundly broadened towards apices in inner margin, straightened towards apices in outer margin; each apical half of outer margin distinctly carinate, with angulate spine at anterolateral part. **Pronotum** (Fig. 3C) slightly longer than wide, PL 0.48 mm, PW 0.46 mm; widest at anterior one-third, weakly constricted from widest point towards base, polished, with coarse punctures along posterior margin, with a median and pair of lateral antebasal foveae, with distinct conical spine

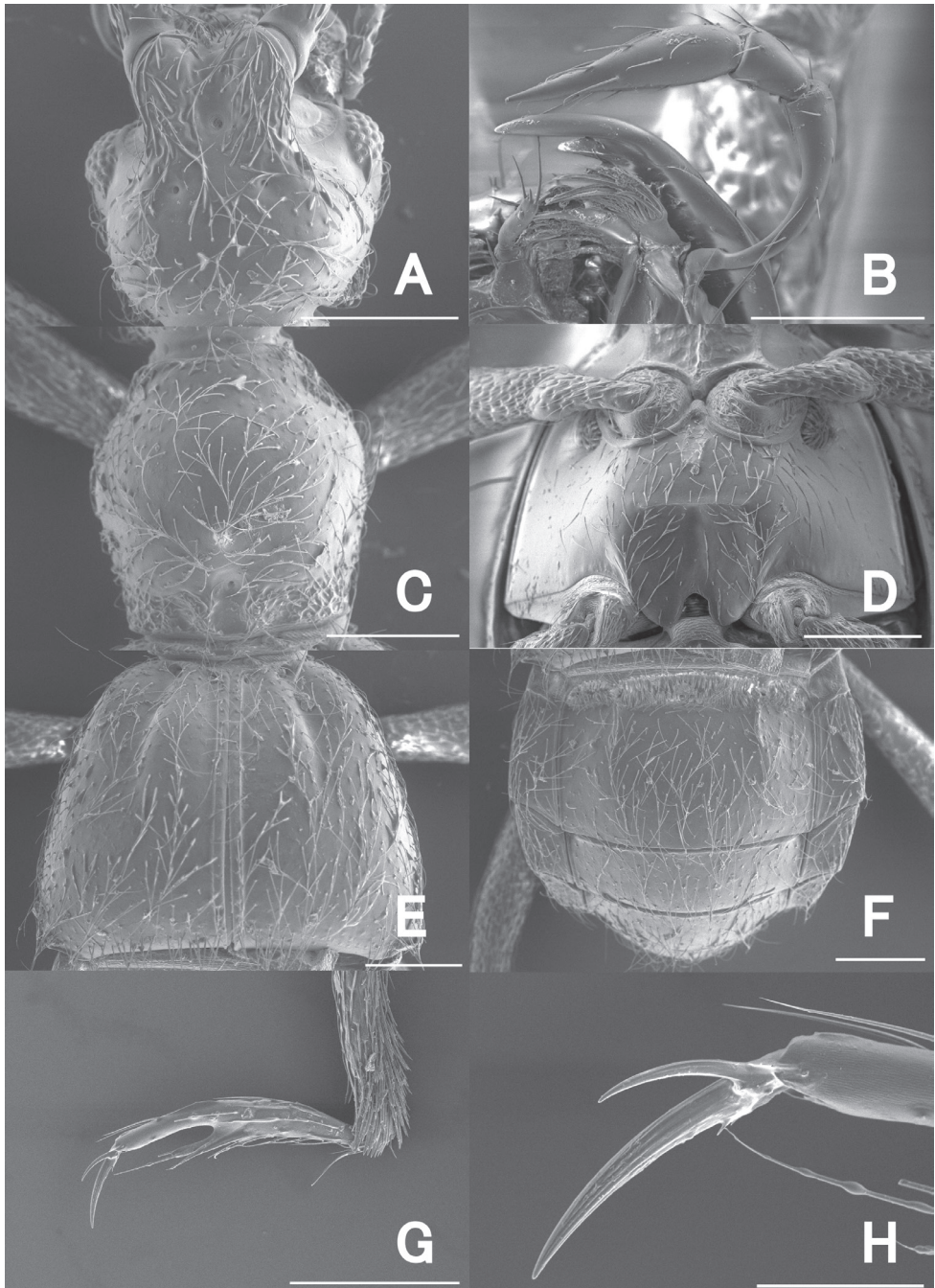


Figure 3. SEM images of *Pseudophanias yaimensis*, male **A** head **B** maxillary palp **C** pronotum **D** metaventricle **E** elytra **F** abdomen **G** mesotarsus **H** mesotarsal claws. Scale bars: 0.2 mm (**A**, **C**–**G**); 0.1 mm (**B**); 0.05 mm (**H**).

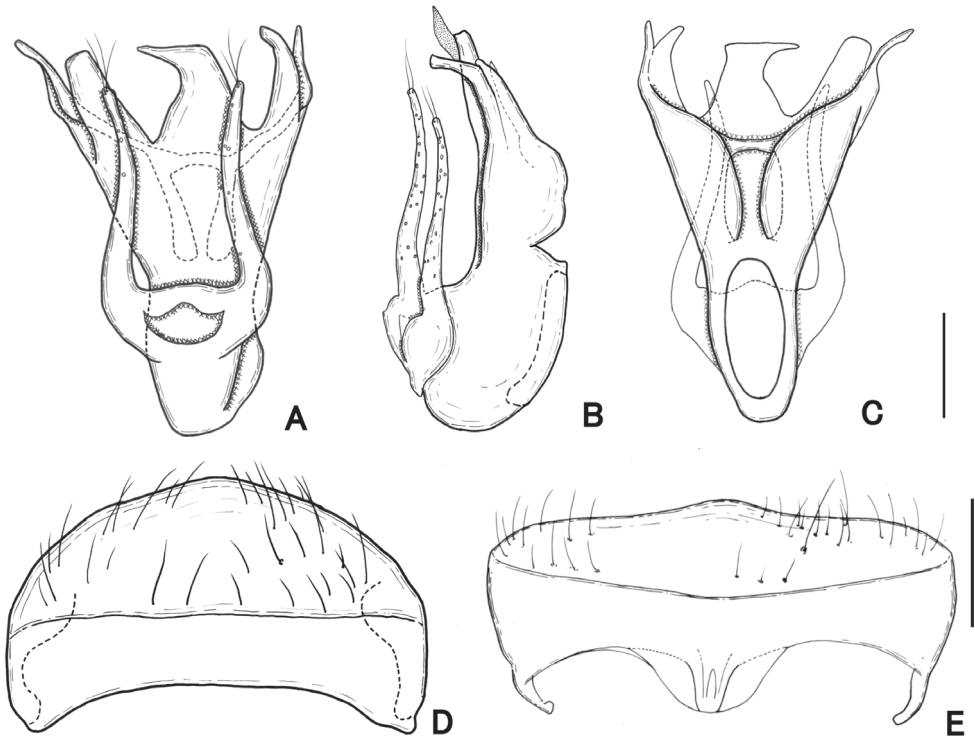


Figure 4. Male genitalia of *Pseudophanias yaimensis* **A** ventral view **B** lateral view **C** dorsal view **D** tergite VIII **E** sternite VIII. Scale bars: 0.1 mm.

just anterior of median fovea. **Metaventricle** (Figs 2D, 3D) finely punctate, moderately convex, but area just above metaventral apex impressed; that impression nearly trapezoidal, half as long as metaventral length, occupying $1/4$ metaventral width; anterior margin of that impression straight, distinct. **Elytra** (Fig. 3E) nearly trapezoidal, widest near posterior $1/4$ much wider than long, EL 0.60–0.62 mm, EW 0.85–0.94 mm; dorsal surface polished, with thin, long setae, finely punctate; each elytron with two basal foveae; discal stria shallow, extending from basal fovea placed middle to posterior half. **Legs**. All legs elongate and slender; femora each broadest near middle; tibiae each slightly broadened to apex, with dense yellow setae at apex; protibiae and mesotibiae nearly straight; metatibiae longest; tarsi each elongate, with tarsomeres 2 about as long as tarsomeres 3; mesotarsi (Fig. 3G) modified, broadest; tarsomeres 3 each with projection of $2/3$ length of entire tarsomere; tarsal claws (Fig. 3H) each asymmetrical; posterior claws thin, short. **Abdomen** (Fig. 3F) wider than long, widest at tergite IV, AL 0.62–0.76 mm, AW 0.85–0.90 mm; tergite IV longest, twice as long as tergite V, with pair of short longitudinal carinae about one-fifth as long as tergal length, with setose depression at base. Tergite and sternite VIII as in Fig. 4D, E. **Aedeagus** (Fig. 4A–C) 0.39–0.40 mm in length, well-sclerotized, asymmetrical; parameres elongate, reaching near apex of median lobe; each paramere with three setae at apex; median lobe

strongly widened towards apex in dorso-ventral view, constricted at median part in lateral view; ventral side of apical part asymmetrical, weakly sclerotized, nearly formed three pronged fork; medioapical part bended laterally; dorsal side of apical part asymmetrical, bifurcate from median part; endophallus indistinct.

Female (Fig. 1B). BL 2.20–2.32 mm; HL 0.40–0.52 mm; HW 0.42–0.45 mm; PL 0.46–0.49 mm; PW 0.44–0.46 mm; EL 0.58–0.63 mm; EW 0.78–0.89 mm; AL 0.70–0.76 mm; AW 0.86–0.90 mm. Antennae (Fig. 2C) with antennomeres 11 unmodified, each ovoid, without carina and angulate spine; eyes smaller than male; mesotarsi without projection.

Etymology. Ishigaki Island, where the type locality of this species was discovered, is a part of the Yaeyama Islands. This specific epithet refers to Yaima which is a local dialect of the Yaeyama Islands.

Distribution. Japan (Ryûkyû: Ishigaki-jima Is.), China (Taiwan).

Biology. Two paratypes from Taiwan were collected with the termite *Nasutitermes parvonasutus* Nawa, 1911. In Japan, one paratype was collected using a Flight Interception Trap (FIT).

Remarks. This species is distributed in Yaeyama-shotô Islands, Japan and Taiwan, China. The two localities are close to each other and shared the same fauna for some insect groups. The two populations show slight difference in the morphology of the aedeagus. The lateral projections of the median lobe of the population of Taiwan are relatively longer and narrower than those of the population of Yaeyama. But the general appearance and especially the male sexual characters are otherwise almost identical. Therefore, we treat such a difference as interspecific variation.

The Taiwanese specimens were collected from a nest of the *Nasutitermes parvonasutus* termite. However, the Japanese specimens were collected from leaf litter samples or by FIT. Some pselaphine species are known to live under the bark and rotten wood with termites. Thus, more information is needed to recognize the possible termitophyly of the new species.

***Pseudophanias nakanoi* Inoue, Nomura & Yin, sp. nov.**

<http://zoobank.org/6782BACF-BBD3-423C-8A48-5EAD6B3645C1>

Figs 5–8

[Japanese name: Nakano-tsumugata-arizukamushi]

Type material. **Holotype** (NSMT): ♂, “屋久島 小楊枝林道, alt. 190 m. / [Yakushima Is.], Japan: / Kagoshima-ken, Kumage-gun, / Yakushima-chô, Koyôji-rindô / 30°17'36"N, 130°25'30"E, / 21 IX 2018, F. Nakano leg. // HOLOTYPE (red) / ♂, *Pseudophanias nakanoi* sp. nov., / det. Inoue, Nomura & Yin, 2020” **Paratype:** Japan: 1 ♀, [Ryûkyû; Tokara-rettô Isls.], Kagoshima-ken, Toshima-mura, Nakano-shima Is, Sato, 7–9 VII 2019, (leaf litter), N. Tsuji leg., with collecting permission of Toshima-mura Village (NSMT). Paratype pinned with the following label: “PARATYPE (yellow) / ♀, *Pseudophanias nakanoi* sp. nov., / det. Inoue, Nomura & Yin, 2020”.

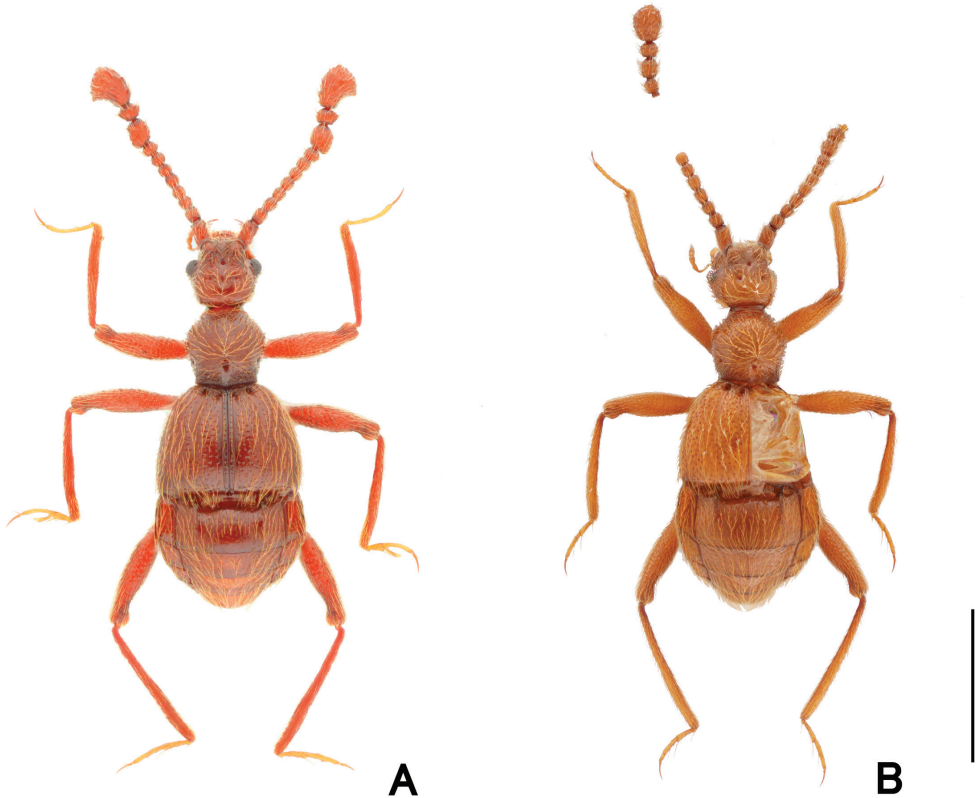


Figure 5. Dorsal habitus of *Pseudophanias nakanoi* **A** male **B** female. Scale bar: 1.0 mm.

Diagnosis. *Pseudophanias nakanoi* is similar to *P. clavatus* Raffray, 1904, but *P. nakanoi* can be distinguished from the latter by its modified antennal clubs, which are formed by three apical antennomeres, and the finely punctate head and pronotum.

Description. Male (Figs 5A, 6A). Body length 2.59 mm. Dorsal surface densely covered with long setae. **Head** (Fig. 7A) as long as wide, HL 0.52 mm, HW 0.52 mm, nearly trapezoidal; frontal rostrum broad, short, strongly sulcate along midline, with large fovea in frontal sulcus; antennal tubercles distinct, with dense punctures which gradually disappear towards vertex; vertex polished, finely punctate, with pair of foveae; frontal, vertexal foveae glabrous; eyes large, weakly prominent; postocular margins two times longer than length of eyes. **Antennae** (Fig. 6B) moderately elongate, 1.36 mm in length; antennal clubs formed by apical three antennomeres; antennomeres 1 thick, elongate, 1.5 times longer than 2; 2 slightly longer than wide; 3–7 nearly moniliform; 8 transverse; 9–11 enlarged, slightly excavated in outer margin; 9 nearly ovoid, each with smooth area on ventral surface; 10 transverse, half as long as 9, each with smooth area on ventral surface; 11 enlarged, widest at apical 1/3, strongly produced outward, roundly broadened to apices in inner margin, each with smooth area on ventral surface. Maxillary palpi (Fig. 7B) symmetrical; palpomeres 1 minute; palpomeres 2 elongate, narrowed in basal

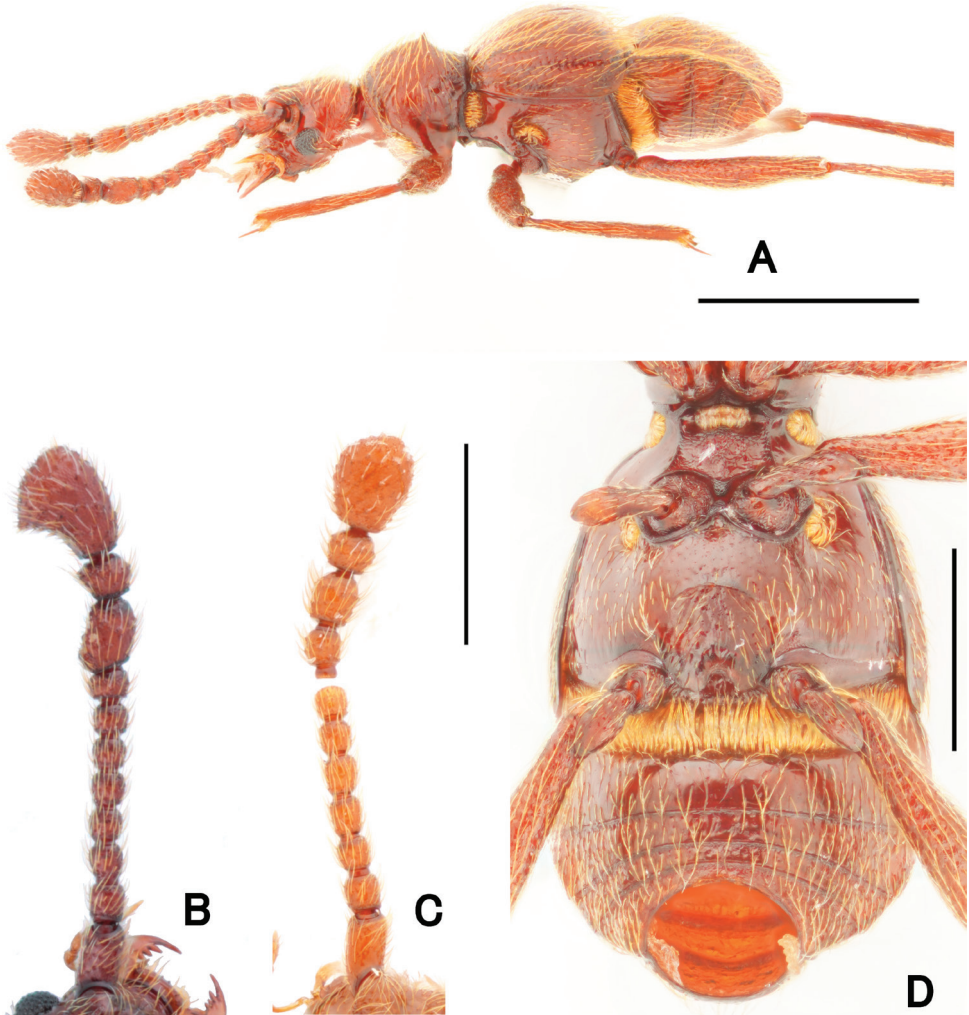


Figure 6. Morphological details of *Pseudophanias nakanoi* **A** habitus in lateral view **B** male antenna **C** female antenna **D** male metaventricle. Scale bars: 1.0 mm (**A**); 0.5 mm (**D**); 0.2 mm (**B, C**).

halves; palpomeres 3 small, widest at apices; palpomeres 4 fusiform. **Pronotum** (Fig. 7C) slightly wider than long, PL 0.53 mm, PW 0.55 mm; widest near anterior 1/3, then narrowed anteriorly, posteriorly, with coarse punctures along posterior margin, with a median and pair of lateral antebasal foveae, with distinct conical spine just anterior of above median fovea. **Metaventricle** (Figs 6D, 7D) finely punctate, moderately convex, but just above metaventral apex roundly impressed; that impression half as long as metaventral length, occupying 1/4 metaventral width; anterior margin of that impression moderately rounded, distinct. **Elytra** (Fig. 7E) nearly subtrapezoidal, widest near posterior 1/4 much wider than long, EL 0.72 mm, EW 0.99 mm, with dense setae, coarsely punctate, each elytron with two basal foveae; discal stria shallow, extending from median fovea to poste-

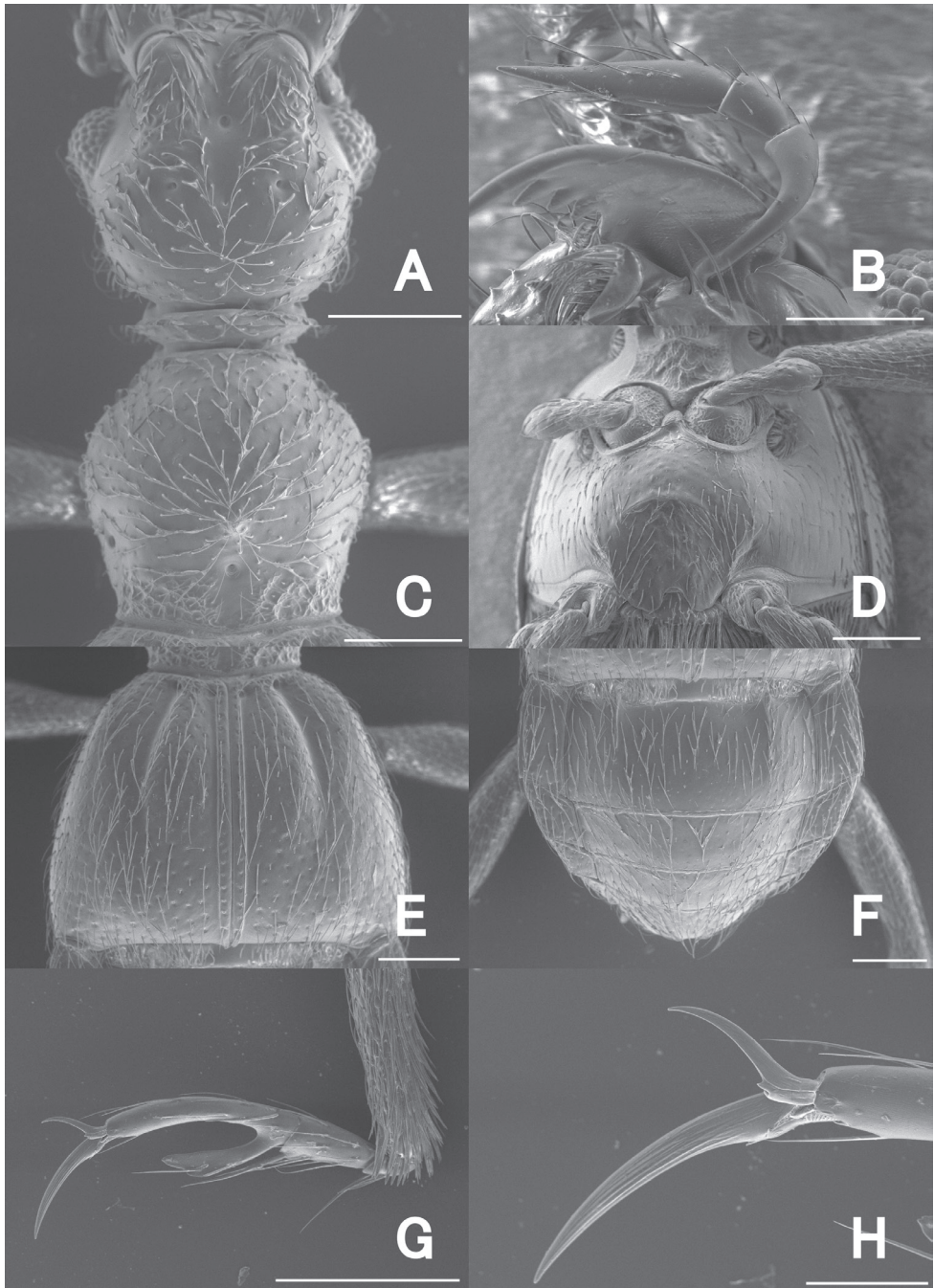


Figure 7. SEM images of *Pseudophanias nakanoi*, male **A** head **B** maxillary palp **C** pronotum **D** metaventricle **E** elytra **F** abdomen **G** mesotarsus **H** mesotarsal claws. Scale bar: 0.2 mm (**A**, **C–G**); 0.1 mm (**B**); 0.05 mm (**H**).

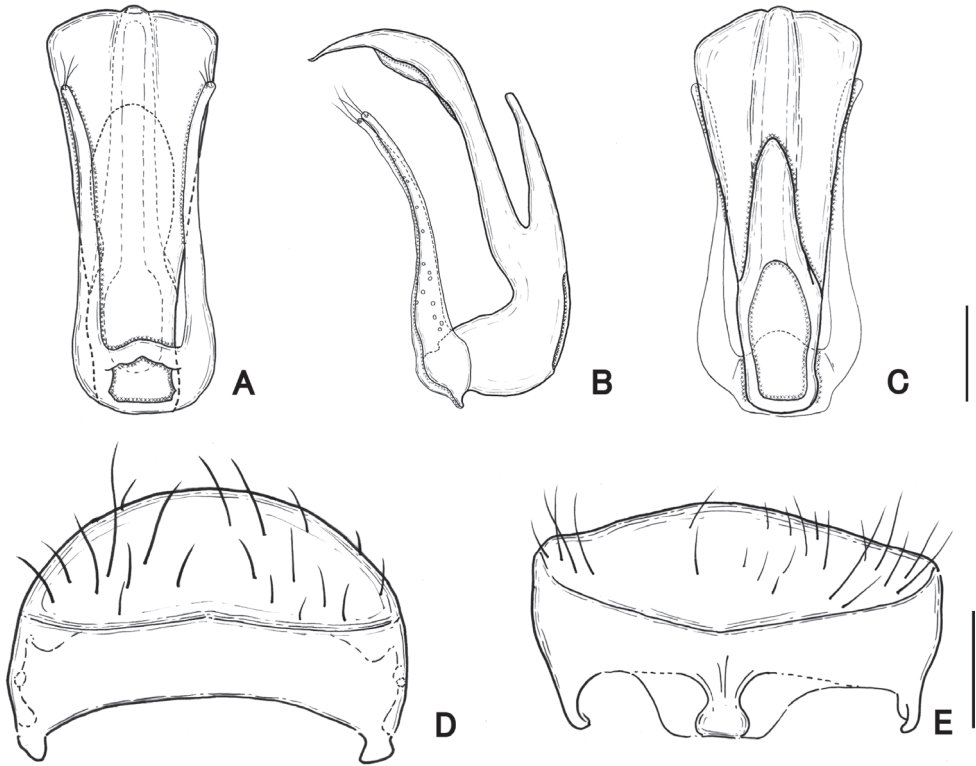


Figure 8. Male genitalia of *Pseudophanias nakanoi* **A** ventral view **B** lateral view **C** dorsal view **D** tergite VIII **E** sternite VIII. Scale bars: 0.1 mm.

rior 1/3. **Legs.** All legs moderately elongate and slender; femora each broadest near middle; tibiae each slightly broadened to apices, with dense yellow setae at apices; protibiae and mesotibiae nearly straight; metatibiae longest; tarsi each elongate, with tarsomeres 2 two-thirds as long as 3; mesotarsi (Fig. 7G) modified, broadest; tarsomeres 3 each with projection of 3/4 length of entire tarsomeres; tarsal claws (Fig. 7H) asymmetrical; anterior claws long; posterior claws thin, short. **Abdomen** (Fig. 7F) wider than long, widest at tergite IV, AL 0.82 mm, AW 1.03 mm; tergite IV longest, twice as long as tergite V, with pair of longitudinal carinae extending to posterior half, with mediobasal setose depression distinct. Tergite and sternite VIII as in Fig. 8D, E. **Aedeagus** (Fig. 8A–C) 0.46 mm in length, well-sclerotized, symmetrical in dorso-ventral view; parameres extremely elongate, reaching near apical fourth, each with three setae at apex; median lobe broad at base, split into ventral and dorsal lobes in lateral view; ventral lobe broadened from base toward apex in dorso-ventral view, curved ventrally and narrowed apically in lateral view; dorsal lobe terminated apical 1/3 of ventral lobe; endophallus indistinct.

Female (Fig. 5B). BL 2.56 mm; HL 0.49 mm; HW 0.52 mm; PL 0.53 mm; PW 0.57 mm; EL 0.73 mm; EW 1.00 mm; AL 0.81 mm; AW 1.03 mm. Antennae

(Fig. 6C) unmodified, nearly moniliform, successively broadened apically; antennomeres 11 largest; eyes smaller than in male; mesotarsi without projection.

Etymology. The new species is named after Mr Fumitaka Nakano, the original collector of the holotype.

Distribution. Japan (Ryûkyû: Tokara-rettô Isls.; Kyûshû: Yakushima Is.)

Biology. The holotype was collected from a dead tree of the family Fagaceae, and the paratype female was collected from leaf litter.

***Pseudophanias excavatus* Inoue, Nomura & Yin, sp. nov.**

<http://zoobank.org/E9C17AEF-CEA2-45DB-A952-52905F0943BE>

Figs 9–13

Type material. Holotype (NSMT): ♂, “Tengshih (1400 m, litter) / Kaosiung Hsien / [M-TAIWAN] / 台湾高雄縣藤枝 / 20–22. iv. 2001, H. Sugaya leg. // HOLOTYPE (red) / ♂, *Pseudophanias excavatus* sp. nov., / det. Inoue, Nomura & Yin, 2020”

Paratypes: (NSMT, KUM, NMNS) 1 ♂, 3 ♀, same data as holotype; 6 ♂, 1 ♀, same data as holotype, but 29–30 IV 2001; 1 ♂, 2 ♀, same data as holotype, but 30 IV 2001. Each paratype pinned with the following label: “PARATYPE (yellow) / ♂ (or ♀), *Pseudophanias excavatus* sp. nov., / det. Inoue, Nomura & Yin, 2020”.

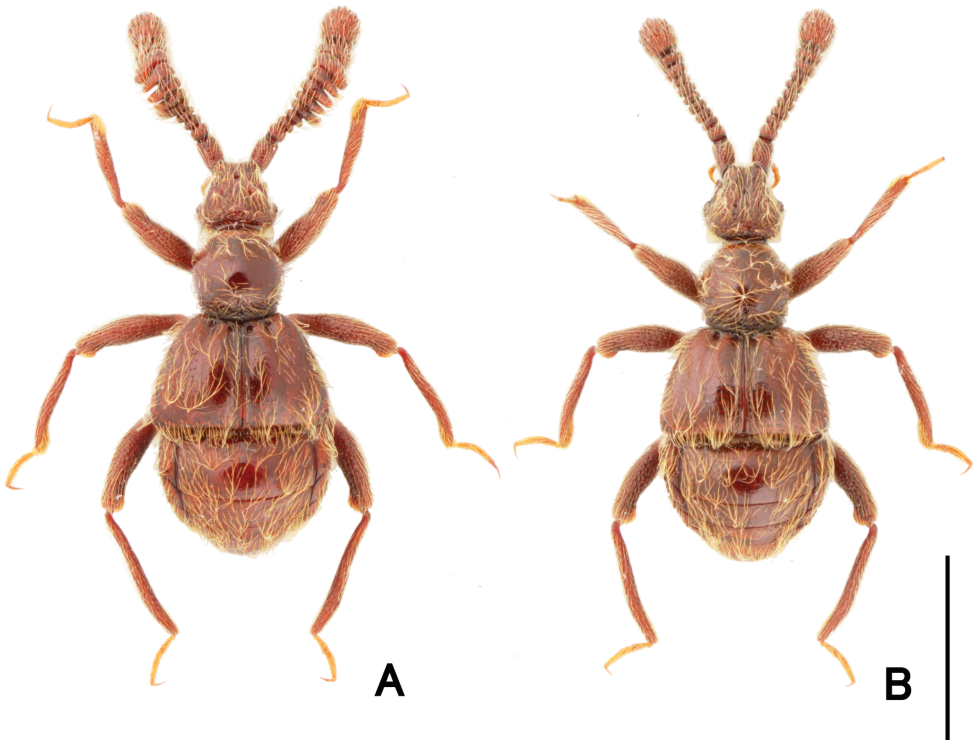


Figure 9. Dorsal habitus of *Pseudophanias excavatus* **A** male **B** female. Scale bar: 1.0 mm.

Diagnosis. This species is readily distinguished from other members of *Pseudophanias* by the clasping formed antennae in the male, frontal sulcus indistinct, and the rounded pronotum.

Description. Male (Figs 9A, 10A). Body length 2.21–2.48 mm. Dorsal surface with dense setae.

Head (Fig. 11A) as long as wide, HL 0.45–0.50 mm, HW 0.43–0.50 mm, densely punctate, with dense, long setae; frontal rostrum broad, with frontal fovea nude; antennal tubercles distinct; vertex flat, with pair of glabrous foveae; eyes prominent, small; occiput with dense setae; postocular margin two times longer than eyes; small areas just posterior to U-shaped setose sulci finely punctate. **Antennae** (Figs 10B, 12A–E)

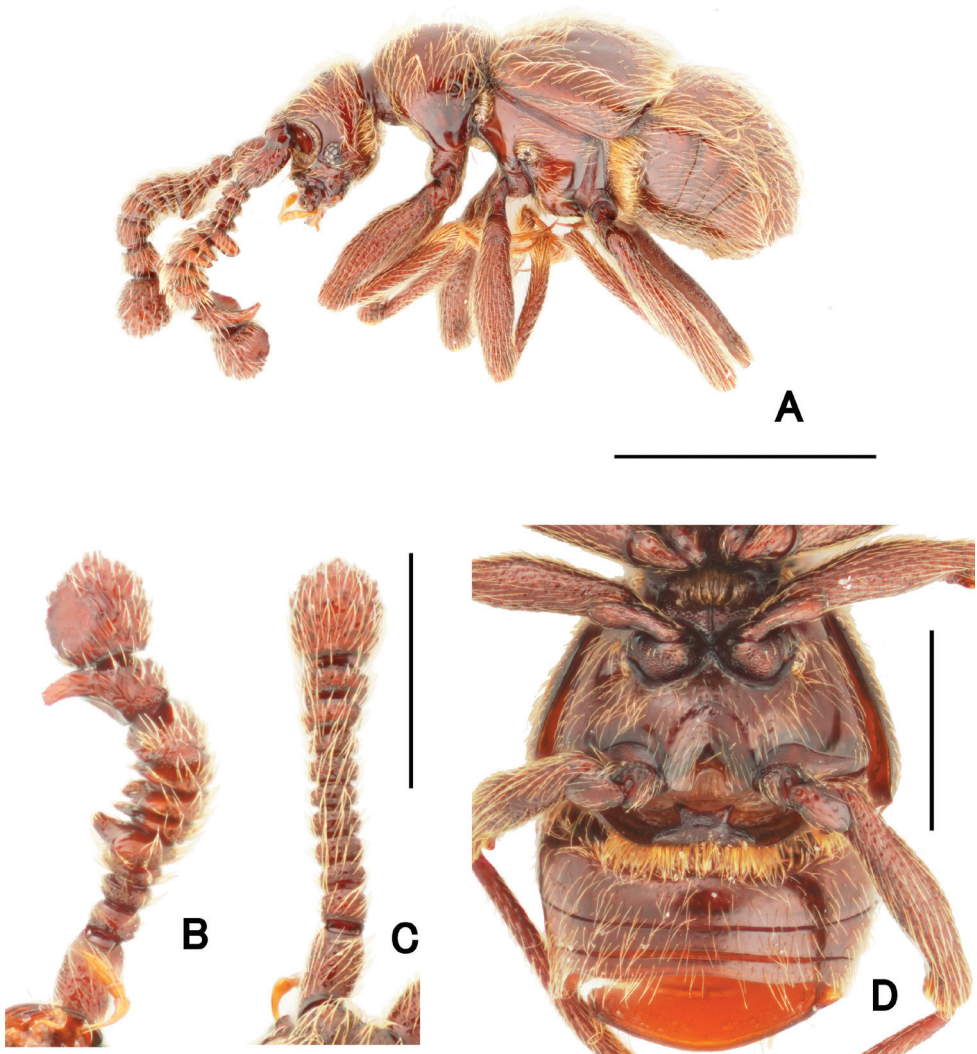


Figure 10. Morphological details of *Pseudophanias excavatus* **A** habitus in lateral view **B** male antenna **C** female antenna **D** male metaventricle. Scale bars: 1.0 mm (**A**); 0.5 mm (**D**); 0.2 mm (**B**, **C**).

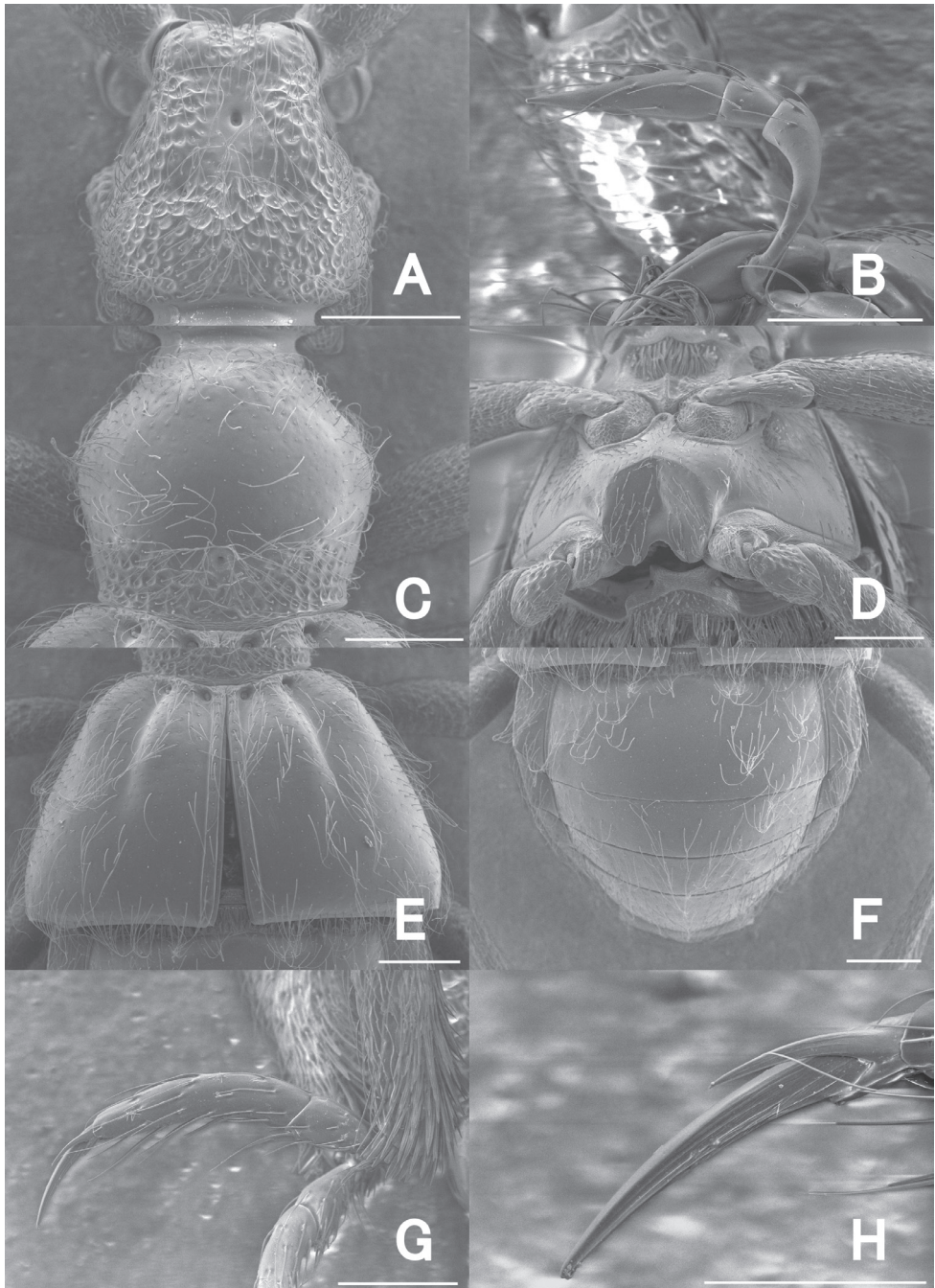


Figure 11. SEM images of *Pseudophanias excavatus*, male **A** head **B** maxillary palp **C** pronotum **D** metaventricle **E** elytra **F** abdomen **G** protarsus **H** protarsal claws. Scale bars: 0.2 mm (**A, C-F**); 0.1 mm (**B, G**); 0.05 mm (**H**).

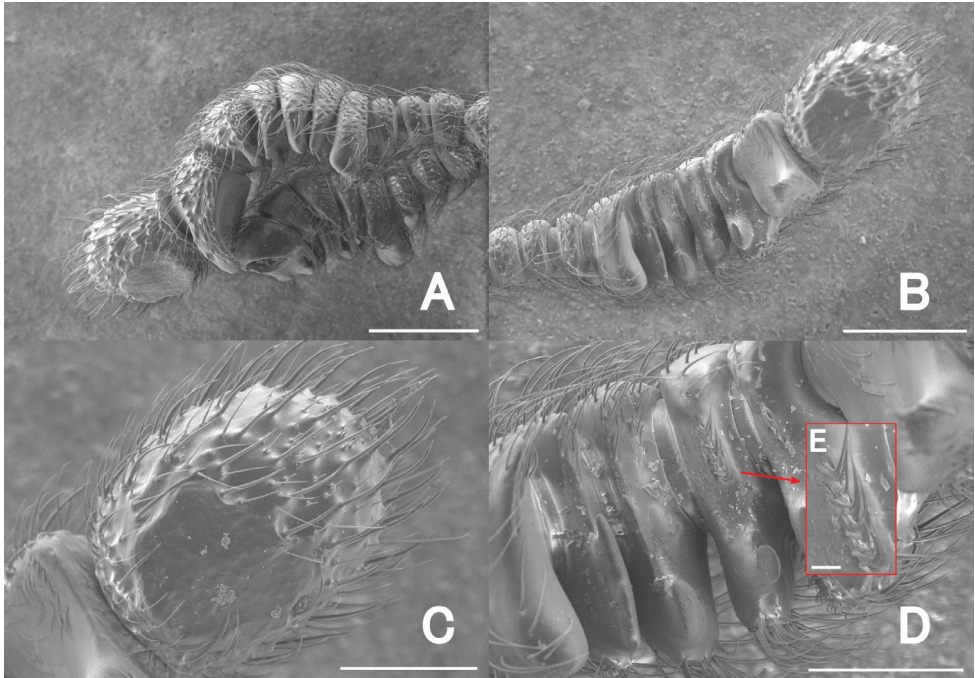


Figure 12. Male antenna of *Pseudophanias excavatus* by SEM images **A** lateral view **B** ventral view **C** antennomere 11 in ventral view **D** antennomeres 5–10 in ventral view **E** special setae on antennomere VIII in ventral view. Scale bars: 0.2 mm (**A, B**); 0.1 mm (**C, D**); 0.01 mm (**E**).

strongly modified, 0.98–1.12 mm in length; antennomeres 1 elongate, as long as 2–4 combined; 2–4 each transverse, successively shorter; 5–11 strongly excavated on ventral side, with tufts of setae on ventral surface, modified to form clasping, each excavated on ventral surface; 5–9 each two times wider than 4, each transverse; 9 longer than 8; 10 as long as 9, asymmetrical; outer side strongly produced ventrally in 9; 11 enlarged, with glabrous areas on ventral side. Maxillary palpi (Fig. 11B) symmetrical; palpomeres 1 minute; palpomeres 2 elongate, narrowed in basal halves; palpomeres 3 small, widest at apices; palpomeres 4 fusiform. **Pronotum** (Fig. 11C) about as long as wide, PL 0.47–0.55 mm, PW 0.50–0.55 mm, broadly rounded, widest at middle, finely punctate on dorsal surface, with a median and pair of lateral antebasal foveae; antebasal area strongly punctate. **Metaventricle** (Figs 10D, 11D) finely punctate, strongly convex, but area just above metaventral apex roundly impressed; that impression $2/3$ as long as metaventral length, occupying $1/4$ metaventral width; anterior margin of that impression sharply rounded, distinct. **Elytra** (Fig. 11E) much wider than long, EL 0.57–0.65 mm, EW 0.90–0.98 mm, trapezoidal, finely punctate, each elytron with two basal foveae; discal stria shallow, extending from basal fovea placed middle to posterior $1/3$. **Legs.** All legs moderately short; each femora broadest near middle; protibiae, mesotibiae with dense yellow setae at apices; protibiae, metatibiae moderately straight;

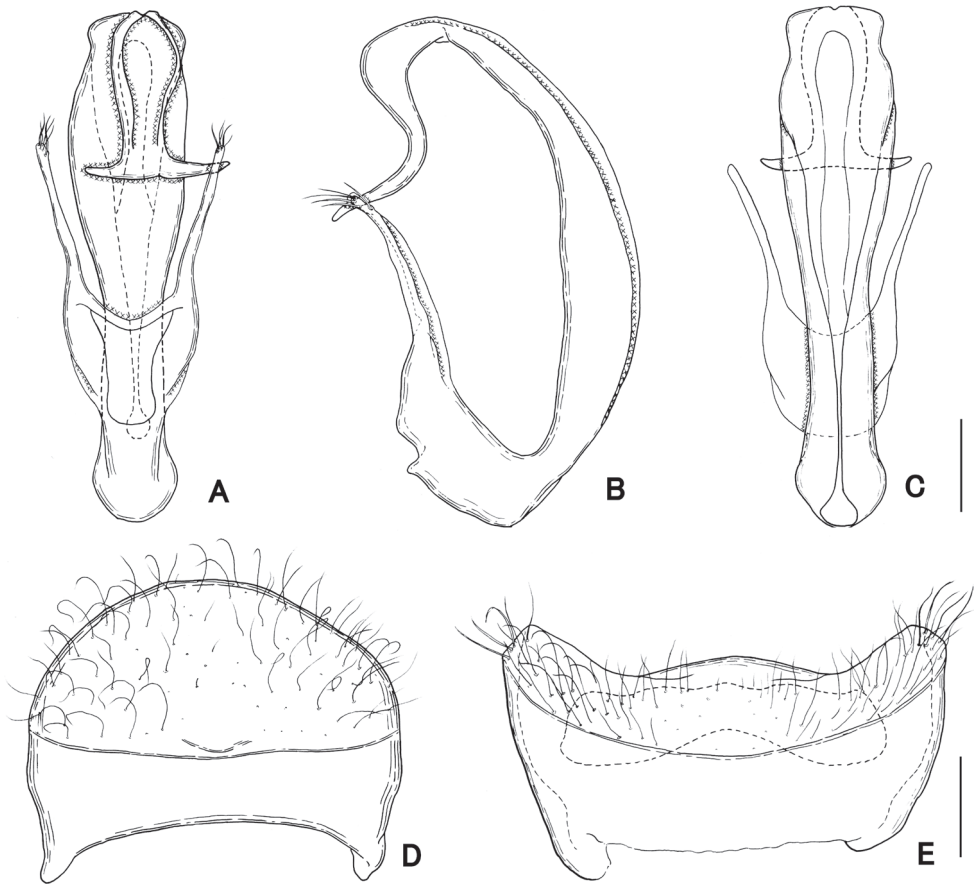


Figure 13. Male genitalia of *Pseudophanias excavatus* **A** ventral view **B** lateral view **C** dorsal view **D** tergite VIII **E** sternite VIII. Scale bars: 0.1 mm.

mesotibiae slightly arcuate at apical fourth; tarsi (Fig. 11G) each with tarsomere 2 half as long as tarsomere 3; tarsal claws (Fig. 11H) asymmetrical; anterior claws long, posterior claws thin, short. **Abdomen** (Fig. 11F) much wider than long, widest at tergite IV, AL 0.64–0.81 mm, AW 0.97–1.05 mm, lacking discal carinae; tergite IV longest, twice as long as V, with setose depression at base. Tergite and sternite VIII as in Fig. 13D, E. **Aedeagus** (Fig. 13A–C) 0.60–0.63 mm in length, well-sclerotized, slightly asymmetrical in dorsal and ventral view, tubular in lateral view; parameres symmetrical, extremely elongate, reaching apical third, each with five setae at apex; median lobe roundly curved, C-shaped in lateral view; apical part widely opened, narrowed towards basal part to connect ovoidal dorsal diaphragm; apical lobe extending downward, curved to form S-shaped in lateral view, widely opened at base, strongly produced laterally at apex; endophallus indistinct.

Female (Fig. 9B). BL 2.21–2.27 mm; HL 0.44–0.48 mm; HW 0.44–0.48 mm; PL 0.47–0.55 mm; PW 0.46–0.51 mm; EL 0.56–0.63 mm; EW 0.90–0.94 mm; AL 0.67–0.70 mm; AW 0.94–0.96 mm. Antennae (Fig. 10C) with antennomeres

11 simple, successively widened towards apices; antennomeres 2–10 each transverse; 11 ovoid, largest. Metaventrite convex, lacking metaventral impression.

Etymology. The specific epithet refers to the strongly excavated antennae in the male of the new species.

Distribution. China (Taiwan).

Biology. This species was collected from leaf litter.

Pseudophanias spinitarsis Yin, Coulon & Bekchiev, 2015

Pseudophanias spinitarsis Yin, Coulon & Bekchiev, 2015: 447.

Diagnosis. This species is readily distinguished from other members of *Pseudophanias* by a combination of the following character states: Body length over 3 mm; antennal club formed by apical 4 antennomeres; antennomeres each distinctly elongate; antennomeres 8 angularly expanded laterally, 9 triangularly expanded in male; pronotal disc with conical spine; profemora concave at basal third, with bunch of thick setae; protarsomeres 2 and 3, and mesotarsomere 2 each spinose; aedeagus symmetrical, with median lobe greatly extended ventrally (Yin, Coulon and Bekchiev 2015).

Pseudophanias yunnanicus (Yin, 2019), **comb. nov.**

Chandleriella yunnanica Yin, 2019: 434.

Diagnosis. This species is readily distinguished from other members of *Pseudophanias* by a combination of the following character states: Body length over 3.50 mm; antennal club formed by antennomere 11 alone; antennomere 11 strongly enlarged and modified to form bowl-like in male; aedeagus symmetric, median lobe tri-lobed at apex; parameres elongate, narrowing from base toward apex, with several long apical setae (Yin 2019).

Discussion

Members of the supertribe Pselaphitae usually have two equal tarsal claws and have posterior claws smaller than the anterior ones in some genera. Some tribes, such as Pselaphini, have singular tarsal claws (Chandler 2001). The tribe Tyrini typically has two tarsal claws equal in size, but a few genera have protarsi with posterior tarsal claws that are reduced in size (Hlaváč and Chandler 2005). The tribe Tmesiphorini has the claw morphology similar to Tyrini (Chandler 2001), but clearly differs in the setose sulci that embrace the antennal bases. The morphology of the claws is frequently used for classification in some genera. However, interspecies differences in tarsal claw morphology have been recognized in the genus *Tmesiphorus* (Inoue et al. 2019). Although the genus *Phalepsus* Westwood of the tribe Phalepsini is distinguished from the other

tribes by its strongly asymmetrical tarsal claws (Raffray 1890a; Jeannel 1949), some species have claws that are nearly subequal in size in *Phalepsus* (Chandler 2001). Therefore, tarsal claw morphology may vary at the species level within a genus in Pselaphitae.

The genus *Chandleriella* was tentatively separated from the genus *Pseudophanias* by a number of external characters (see Introduction). In this study, the three new species we placed in *Pseudophanias* show intermediate and different ratios of posterior and anterior tarsal claws. Additionally, in *Pseudophanias*, many undescribed species are recognized in Southeast Asia, and their posterior tarsal claws are reduced to various degrees in each species (Nomura pers. obs.). Therefore, the genera *Pseudophanias* and *Chandleriella* cannot be separated based on their tarsal claw morphology, and *Chandleriella*, syn. nov., is here synonymized with *Pseudophanias*. The two recognized species of *Chandleriella* are here removed to *Pseudophanias*, resulting in *P. termitophilus* (Bryant, 1915) comb. nov., and *P. yunnanicus* (Yin, 2019) comb. nov.

List of world species

- 1 *Pseudophanias clavatus* Raffray, 1905: 415. Indonesia (Sumatra).
- 2 *Pseudophanias cribricollis* Raffray, 1895: 75. Malaysia (Penang).
- 3 *Pseudophanias elegans* Raffray, 1905: 413. Indonesia (Sumatra).
- 4 *Pseudophanias excavatus* Inoue, Nomura & Yin, sp. nov. China (Taiwan).
- 5 *Pseudophanias heterocerus* Raffray, 1895: 76. Singapore (Seletar).
- 6 *Pseudophanias malaianus* Raffray, 1890b: 214. Malaysia (Penang).
- 7 *Pseudophanias nakanoi* Inoue, Nomura & Yin, sp. nov. Japan (Yakushima Island; Tokara-rettô Islands).
- 8 *Pseudophanias pilosus* Raffray, 1895: 76. Malaysia (Penang).
- 9 *Pseudophanias puberulus* Raffray, 1905: 415. Malaysia (Penang).
- 10 *Pseudophanias punctatus* Raffray, 1905: 414. Singapore.
- 11 *Pseudophanias robustus* Raffray, 1905: 413. Indonesia (Sumatra).
- 12 *Pseudophanias spinitarsis* Yin, Coulon & Bekchiev, 2015: 447. Nepal (Pokhara).
- 13 *Pseudophanias termitophilus* (Bryant, 1915), comb. nov. Indonesia (Sumatra).
= *Lasinus termitophilus* Bryant, 1915: 300.
= *Chandleriella termitophila*; Hlaváč, 2000: 91.
- 14 *Pseudophanias tuberculatus* Raffray, 1905: 414. Indonesia (Sumatra).
- 15 *Pseudophanias yaimensis* Inoue, Nomura & Yin, sp. nov. Japan (Yaeyama Islands), China (Taiwan).
- 16 *Pseudophanias yunnanicus* (Yin, 2019), comb. nov. China (Yunnan).
= *Chandleriella yunnanica* Yin, 2019: 434.

Acknowledgments

We would like to express our sincere thanks to Fumitaka Nakano, Hiroshi Sugaya, Kazuo Ogata, Naomichi Tsuji, Shigehisa Hori, and Teruaki Ban for kindly providing the specimens. Dr Munetoshi Maruyama (KUM) kindly offered invaluable comments

on our previous version of the manuscript. We are very grateful to Dr James Hammond (Natural Resources Canada, Alberta) for his critical reading and invaluable comments on our manuscript. The third author Yin was supported by the National Natural Science Foundation of China (No. 31872965), and the 'Phosphor' Science Foundation, Shanghai Municipal Science and Technology Commission, China (19QA1406600).

References

- Bryant GE (1915) New species of Pselaphidae (group Tyrini). *Entomologist's Monthly Magazine* 51: 297–302. <https://doi.org/10.5962/bhl.part.7791>
- Chandler DS (2001) Biology, morphology and systematics of the ant-like litter beetles of Australia (Coleoptera: Staphylinidae: Pselaphinae). *Memoirs on Entomology, International* 15: 1–560.
- Hlaváč P (2000) Chandleriella, new genus of Tmesiphorini from Borneo (Coleoptera: Staphylinidae: Pselaphinae). *Entomological Problems* 31(1): 91–93.
- Hlaváč P, Chandler DS (2005) World catalogue of the species of Tyrini with a key to the genera (Coleoptera: Staphylinidae: Pselaphinae). *Folia Heyrovskyana* 13: 81–143.
- Inoue S, Maruyama M, Nomura S (2019) Revision of the genus *Tmesiphorus* LeConte, 1849 (Coleoptera: Staphylinidae: Pselaphinae) from Japan. *Zootaxa* 4646(1): 67–86. <https://doi.org/10.11646/zootaxa.4646.1.4>
- Inoue S, Maruyama M, Nomura S (2020) Discovery of *Tmesiphoromimus* Löbl, 1964 (Coleoptera: Staphylinidae: Pselaphinae) from Japan, with description of a new species. *Japanese Journal of Systematic Entomology* 26(1): 87–92.
- Jeannel R (1949) Les Psélaphides de l'Afrique Orientale (Coleoptera). *Mémoires du Muséum National d'Histoire Naturelle, Paris* 29: 1–226.
- Maruyama M (2004) A permanent slide pinned under a specimen. *Elytra* 32(2): 1–276. [http://coleoptera.sakura.ne.jp/Elytra/Elytra32\(2\)2004.pdf](http://coleoptera.sakura.ne.jp/Elytra/Elytra32(2)2004.pdf)
- Newton AF, Chandler DS (1989) World catalog of the genera of Pselaphidae (Coleoptera). *Fieldiana: Zoology, New Series* 53: 1–93.
- Nomura S, Idris AG (2005) Faunistic notes on the Pselaphinae species of the supertribes Goniaceritae, Malaysia and Singapore (Coleoptera: Staphylinidae: Pselaphinae). *Serangga* 10(1–2): 1–36.
- Raffray A (1890a) Étude sur les Psélaphides. V. Tableaux synoptiques. – Notes et synonymie. *Revue d'Entomologie* 9: 81–172.
- Raffray A (1890b) Étude sur les Psélaphides. VI. Diagnoses des espèces nouvelles sur lesquelles sont fondés des genres nouveaux. *Revue d'Entomologie* 9: 193–219.
- Raffray A (1895) Révision des Psélaphides des Iles de Singapore et de Penang. *Revue d'Entomologie* 14: 21–82.
- Raffray A (1905) Genera et catalogue des Psélaphides [continued]. *Annales de la Société Entomologique de France* 73: 401–476. [pls. 1–3]
- Raffray A (1908) Coleoptera. Fam. Pselaphidae. In: Wytzman P (Ed.) *Genera Insectorum*. Fasc. 64. 487 pp. [9 pls.]
- Shibata Y, Maruyama M, Hoshina H, Kishimoto T, Naomi S, Nomura S, Puthz V, Shimada T, Watanabe Y, Yamamoto S (2013) Catalogue of Japanese Staphylinidae (Insecta: Coleoptera). *Bulletin of the Kyushu University Museum* 11: 69–218.

- Yin Z-W (2019) First record of the genus *Chandleriella* Hlaváč (Coleoptera: Staphylinidae: Pselaphinae) from China, with description of a second species. *Zootaxa* 4571(3): 432–438. <https://doi.org/10.11646/zootaxa.4571.3.11>
- Yin Z-W, Coulon G, Bekchiev R (2015) A new species of *Pseudophanias* Raffray from a cave in central Nepal (Coleoptera: Staphylinidae: Pselaphinae). *Zootaxa* 4048(3): 446–450. <https://doi.org/10.11646/zootaxa.4048.3.10>
- Yin Z-W, Coulon G, Li L-Z (2013a) Description of two new species of the genus *Tmesiphodimerus* gen. n. (Coleoptera: Staphylinidae: Pselaphinae) from South Asia. *Zootaxa* 3694(4): 336–342. <https://doi.org/10.11646/zootaxa.3694.4.2>
- Yin Z-W, Nomura S, Chandler DS, Li L-Z (2013b) The genus *Saltisedes* (Coleoptera: Staphylinidae: Pselaphinae): redefinition, synonymic notes, and new species from the Oriental region. *Canadian Entomologist* 145: 1–11. <https://doi.org/10.4039/tce.2012.90>